

**Stochastic Finite Element Modelling of Flow and
Solute Transport in Dual Domain System**

Mohaddeseh Mousavi Nezhad

Ph.D. in Geotechnical Engineering

**University of Exeter
September 2010**



School of Engineering, Computing and Mathematics

**STOCHASTIC FINITE ELEMENT MODELING OF FLOW
AND SOLUTE TRANSPORT IN DUAL DOMAIN SYSTEM**

Submitted by

Mohaddeseh Mousavi Nezhad

to the University of Exeter as a thesis for the degree of
Doctor of Philosophy in Geotechnical Engineering

September 2010

This thesis is available for Library use on the understanding that it is copyright material and that no quotation from the thesis may be published without proper acknowledgement.

I certify that all material in this thesis which is not my own work has been identified and that no material has previously been submitted and approved for the award of a degree by this or any other University.

M. Mousavi Nezhad

ACKNOWLEDGEMENTS

I would like to express my sincere gratitude to Dr Akbar A. Javadi who has been my supervisor since the beginning of my study. He provided me with many helpful suggestions, important advice and constant encouragement.

I also, want to offer my regards and blessings to all of those who supported me in any respect during the completion of this project.

ABSTRACT

Hydrological processes are greatly influenced by the characteristics of the domain through which the process occurs. It is generally accepted that earth materials have extreme variations from point to point in space. Consequently this heterogeneity results in high variation in hydraulic properties of soil. In order to develop a reliable predictive model for transport processes in soil, the effects of this variability must be considered. Soil heterogeneity due to presence of macropores (micro-) and to spatial variability in hydraulic properties (macro-heterogeneity) coexists in the real field conditions. The challenge is to incorporate the effects of both types of soil heterogeneity in simulation models.

This thesis presents development and application of a 2D/3D numerical model for simulation of advection and diffusion-dispersion contaminant transport considering both types of soil heterogeneity. Stochastic finite element approach is used to incorporate the effects of the spatial variability of soil hydraulic properties on contaminant fate. The soil micro heterogeneity effects are modelled with a dual domain concept in which a first order kinetic expression is used to describe the transfer of the solute between the two domains. Also, the capability of the model in 3D simulation of field problems improves the accuracy of the results, since it is possible to avoid the generally applied assumption in 2D simulations.

From comparison of the model results with experimental and analytical results, it is concluded that the model performs well in predicting contaminant fate and the incorporation of the both types of micro- and macro- heterogeneity in the simulation models improves the accuracy of the prediction. Also, capability of the model in evaluation of the concentration variation coefficient as an index of reliability of the model outputs makes it possible to estimate a probable interval (mean concentration minus and plus standard deviation) for the range of oscillations of possible realizations of solute distribution. Moreover, comparison of the results of the proposed method with the results obtained using the Monte Carlo approach yields a pronounced reduction in the computation cost while resulting in virtually the same response variability as the Monte Carlo technique.

LIST OF PUBLICATIONS

The publications listed here were completed during the author's period of registration to the higher degree program.

Book Chapter

- **Mousavi Nezhad, M.** and Javadi, A.A. (2010a). Numerical Modelling of Contaminant Transport in Soils Including the Effect of Chemical Reactions. In "Modelling of Pollutants in Complex Environmental Systems", Chapter 10, G. Hanrahan (Ed.), Volume II, ILM Publications, UK.

Refereed Journals

- **Mousavi Nezhad, M.**, Javadi, A. A. and Abbasi, F. (2010). Stochastic finite element modelling of water flow in variably saturated soils. *International Journal of Numerical and Analytical Methods in Geomechanics*, (accepted, in press).
- **Mousavi Nezhad M.**, Javadi (2010b). Stochastic finite element approach to quantify and reduce uncertainty in pollutant transport modelling. *ASCE Practice Periodical of Hazardous, Toxic, and Radioactive Waste Management*, (accepted).
- **Mousavi Nezhad M.**, Javadi, A. A., AL-Tabbaa, A. and Abbasi, F. (under review). Numerical study of soil heterogeneity effects on contaminant transport in unsaturated soil; model development and validation. *Journal of Hazardous Material*.
- **Mousavi Nezhad M.**, Javadi, (under review). Finite element modelling of contaminant transport considering effects of micro and macro heterogeneity of soil. *Journal of Hydrology*.
- Javadi, A.A., Rezaia, M. and **Mousavi Nezhad M.** (2006). Evaluation of Liquefaction Induced Lateral Displacements using Genetic Programming. *Journal of Computers and Geotechnics*, 33(4-5), pp 222-233.

Refereed Conferences

- **Mousavi Nezhad, M.**, Javadi, A.A. and Rezaia, M. (2010). Stochastic finite element modelling of water flow and solute transport in unsaturated soils - a case study. *International Conference on Computing in Civil and Building Engineering*, Nottingham, UK, 30 June-2 July 2010.
- **Mousavi Nezhad, M.**, Javadi, A.A. (2010). Finite element modelling of biodegradable contaminant transport. *The 2nd National Seminar of Geotechnical problems of irrigation and drainage networks*, Karaj, Iran.

- Rezania, M., Cullen, P., Javadi, A.A. and **Mousavi Nezhad, M.** (2010). Compressive Behavior of Honeycomb Modular Drainage Tanks. The 7th International Conference on Physical Modelling in Geotechnics, Zurich, Switzerland, 28 June-1 July 2010.
- **Mousavi Nezhad, M.**, Javadi, A.A. and Rezania, M. (2009). Stochastic finite element modelling of contaminant transport. The 1st International Symposium on Computational Geomechanics (ComGeo I), 29April -1May 2009, Juan-les-Pins, Cote d'Azur, France.
- **Mousavi Nezhad, M.** and Javadi, A.A. (2009). Finite Element Modelling of Flow and Contaminant Transport in Heterogeneous Soil. The 17th UK National Conference on Computational Mechanics in Engineering, 6-8 April 2009, Nottingham, UK.
- Javadi, A.A., **Mousavi Nezhad, M.**, and Bello-Dambatta, A. (2008). The Effect of Climate Change on Contaminant Transport in Soil, Climate Change Impacts and Adaptation: Dangerous Rates of Change, 22-24 September 2008, Exeter, UK, pp. 147-156.
- Javadi, A.A., Rezania, M. and **Mousavi Nezhad, M.** (2007). A New Approach to Data-Driven Modelling in Civil Engineering. The 1st International Conference on Digital Communications and Computer Applications, 19-22 March, 2007, Amman, Jordan, pp. 17-24.

TABLE OF CONTENTS

Chapter 1. INTRODUCTION	1
1.1 General background.....	1
1.2 Objectives.....	4
1.3 Structure of the thesis.....	5
Chapter 2. LITERATURE REVIEW	7
2.1 Introduction.....	7
2.2 Classical models.....	8
2.2.1 Water flow.....	8
2.2.2 Solute transport.....	12
2.3 Influence of soil texture and structure on hydrological processes.....	20
2.4 Modelling approaches for considering soil heterogeneity.....	25
2.4.1 Dual domain system.....	25
2.4.2 Stochastic approaches.....	30
2.4.2.1 Monte Carol method.....	31
2.4.2.2 Analytical stochastic method.....	37
2.4.2.3 Alternative methods.....	48
Chapter 3. STOCHASTIC FINITE ELEMENT METHOD	49
3.1 Introduction.....	49
3.2 Probability and random variables.....	50
3.3 Stochastic differential equation.....	54
3.4 Finite element method.....	56
3.4.1 Finite element procedure.....	56
3.4.2 General formulation.....	57
3.4.3 Determination of the local element characteristics.....	63
3.4.4 Transformation of the element characteristics.....	63
3.4.5 Assemblage of the global element characteristics.....	63
3.4.6 Imposition of boundary conditions.....	63

3.4.7 Solution.....	64
3.4.7.1 Gaussian elimination and back substitution.....	64
3.5 Finite difference method.....	64
Chapter 4. STOCHASTIC METHODOLOGY	67
4.1 Introduction.....	67
4.2 Classical governing equation for water flow	68
4.3 Large-scale governing equation for water flow in unsaturated soil.....	71
4.4 Calculation of expected values.....	76
4.4.1 Calculation of expected values by spectral method.....	76
4.4.2 Linearized fluctuation equation.....	78
4.4.3 Spectral density function relationships.....	82
4.4.4 Evaluation of $E[h^2]$	85
4.4.5 Evaluation of $E[fh]$	86
4.4.6 Evaluation of $E[ah]$	88
4.4.7 Evaluation of $E[f\partial h/\partial x_i]$	89
4.4.8 Evaluation of $E[a\partial h/\partial x_i]$	90
4.4.9 Evaluation of $E[\gamma h]$	91
4.5 Local governing equation for solute transport.....	93
4.5.1 Advection.....	93
4.5.2 Diffusion.....	93
4.5.3 Mechanical dispersion.....	94
4.5.4 Dual-domain transport model.....	95
4.6 Large-scale governing equation for solute transport.....	97
4.7 Evaluation of concentration variability σ_c^2	103
4.8 Summary and conclusion.....	108
Chapter 5. NUMERICAL SOLUTION	110
5.1 Introduction.....	110
5.2 Finite element formulation for groundwater flow.....	111
5.2.1 Element weighted residual for groundwater flow.....	112
5.2.2 Element effective permeability and capacitance matrixes.....	116
5.2.3 Global effective permeability and capacitance matrixes.....	119

5.2.4 Imposition of boundary condition.....	119
5.3 Finite difference formulation for groundwater flow.....	120
5.4 Hydraulic gradient.....	120
5.5 Groundwater velocity.....	122
5.6 FE formulation for steady-state solute transport.....	122
5.6.1 Element weighted residual for steady-state solute transport.....	124
5.6.2 Element effective advective-dispersive matrix.....	127
5.6.3 Global effective characteristics of domain.....	131
5.7 FE formulation for unsteady-state solute transport.....	132
5.7.1 Element weighted residual for unsteady-state solute transport.....	133
5.7.2 Determination of element effective matrix.....	134
5.7.3 Global effective characteristics of domain.....	135
5.8 Finite difference formulation for transient solute transport.....	136
5.8.1 Single domain solute transport.....	136
5.8.2 Dual domain solute transport.....	136
5.8 Solution procedure.....	138
Chapter 6. NUMERICAL EXAMPLES AND CASE STUDIES	141
6.1 Introduction.....	141
6.2 Numerical examples.....	142
6.2.1 Example 1.....	142
6.2.2 Example 2.....	153
6.2.3 Example 3.....	169
6.2.4 Example 4.....	176
6.2.5 Example 5.....	186
6.3 Case studies.....	192
6.3.1 Case study 1.....	192
6.3.2 Case study 2.....	199
Chapter 7. CONCLUSIONS AND RECOMMENDATIONS	212
7.1 Concluding remarks.....	212
7.2 Recommendations for future work.....	216
REFERENCES	217

LIST OF FIGURES

Figure 2.1	Typical cross section of soil.....	21
Figure 2.2	Steady-state gravimetric water content profile, along the 95% confidence interval Butter, et al. (1989).....	22
Figure 2.3	Permeability space series from laboratory test, by Bakr (1976).....	23
Figure 2.4	Porosity space series from laboratory test, by Bakr (1976).....	23
Figure 2.5	General schematic of dual-domain flow system	26
Figure 2.6	Schematic illustration of Monte Carlo method concept (Yeh 1992).....	32
Figure 3.1	(a) Linear triangular element with global coordinates (b), linear tetrahedral element with global coordinates.....	58
Figure 4.1	Transport mechanisms: mobile and immobile phases (AL-Najjar 2006).....	96
Figure 4.2	Coordinate system xz corresponds to the mean flow direction and coordinate system $x'z'$ corresponds to mean hydraulic conductivity (Mantoglou 1984).....	100
Figure 5.1	General structure of developed model.....	139
Figure 6.1	(a) 1-D horizontal groundwater seepage with the boundary conditions, (b) Finite element mesh with linear triangle element.....	143
Figure 6.2	Pressure head distribution through the bar for various times (mesh B: symbols, mesh A: solid lines).....	144
Figure 6.3	Pressure head distribution through the bar for various times (analytical: symbols, numerical: solid lines, t: time).....	147
Figure 6.4	Water content distribution through the bar for various times (analytical: symbols, numerical: solid lines, t: time).....	147
Figure 6.5	(a) 1-D vertical groundwater flow with the boundary conditions, (b) Finite element mesh with linear triangle element.....	148
Figure 6.6	Pressure head distribution through the column for various times (symbols: analytical, solid lines: numerical results, t: time (hr)).....	152
Figure 6.7	Moisture content distribution through the column for various times (symbols: analytical, solid lines: numerical results, t: time (hr)).....	152
Figure 6.8	(a) Dimensions of the lysimeter used for the experiment and (b) the FE mesh showing boundary conditions.....	154
Figure 6.9	Position of wetting front vs. time for Stochastic, deterministic and experimental approaches.....	157
Figure 6.10	Position of wetting front vs. time for Stochastic, deterministic approaches.....	157

Figure 6.11	Volumetric water content (predicted by deterministic approach vs. the observed values).....	159
Figure 6.12	Volumetric water content (predicted by stochastic approach vs. observed).....	159
Figure 6.13	Pressure head distribution through the lysimeter for the stochastic and deterministic models (from 100 hrs until 1200 hrs).....	161
Figure 6.14	Volumetric water content distribution through the lysimeter from stochastic and deterministic approach every 100 hours (from 00 hrs until 1200 hrs).....	164
Figure 6.15	Pressure head variance through the lysimeter for various time.....	167
Figure 6.16	Mean pressure head distribution +/- standard deviation vs. depth 600 hours after irrigation (SD: Standard deviation, H: Mean pressure head).....	167
Figure 6.17	Mean pressure head distribution +/- standard deviation vs. depth 1200 hours after irrigation (SD: Standard deviation, H: Mean pressure head).....	168
Figure 6.18	(a) Dimensions of the simulated soil column for steady-state flow and solute transport (b) the FE mesh showing boundary conditions.....	169
Figure 6.19	(a) Mean solute concentration vs. time obtained from MCM and SFEM, (b) σ_c^2 vs. time, (c) normalized mean solute concentration vs. depth after 23 days, (d) normalized solute concentration vs. depth after 39 days, normalized solute concentration vs. depth for different times..	172
Figure 6.20	Solute concentration vs. time obtained for different values of σ_f	173
Figure 6.21	Solute concentration vs. depth obtained for different values of σ_f	174
Figure 6.22	Solute concentration vs. depth obtained from the stochastic and deterministic finite element models after a) 10 days, b) 30 days and c) 50 days.....	175
Figure 6.23	Dimensions of the simulated 3D hypothetical solute transport problem. (a) Plan, (b) Cross section.....	176
Figure 6.24	Solute concentration vs. x direction obtained from analytical and deterministic finite element methods (y=2 and z= 2.5 m).....	179
Figure 6.25	Solute concentrations (mg/l) at y= 2 m obtained from DFE method at different times.....	180
Figure 6.26	Solute concentrations (mg/l) at y= 2 m obtained from SFE method $\sigma_f^2 = 0.2$ at different times.....	181
Figure 6.27	Solute concentrations (mg/l) at y= 2 m obtained from SFE method $\sigma_f^2 = 0.5$ at different times.....	183
Figure 6.28	Deviation of solute concentration (mg/l) at y= 2 m	184
Figure 6.29	Problem definition	186
Figure 6.30	Relative solute concentration vs. time	188

Figure 6.31 Relative solute concentration vs. depth, for different value of ζ after 83 and 139 h	189
Figure 6.32 Solute concentration vs. depth	191
Figure 6.33 Solute concentration vs. depth	191
Figure 6.34 Plan of site.....	194
Figure 6.35 Finite element mesh.....	196
Figure 6.36 Comparison between measured data and the results of SFEM and DFEM.....	197
Figure 6.37 Comparison between SFEM and DFEM predictions	198
Figure 6.38 Solute concentration vs. length at Sep 2004 obtained for different values of σ_f^2	198
Figure 6.39 Plan view of the furrow irrigation field experiments, not to scale, (Abbasi, et al., 2004).	200
Figure 6.40 Position of neuron probe access tubes at different locations in the furrow cross-section. Numbers relate to access tubes installed in two different rows; the first row includes tubes 2 and 4 along the sides and the second row includes tubes 1, 3 and 5 (Abbasi, et al., 2004).....	200
Figure 6.41 Water boundary conditions used for numerical modelling.....	202
Figure 6.42 Measured and predicted (using stochastic finite element and HYDRUS2-D models) soil water contents for the inlet and outlet sites (measured: symbols, simultaneous: solid black lines, two-step: dashed lines, stochastic finite element: solid red lines).....	204
Figure 6.43 Measured and predicted (using stochastic finite element and HYDRUS2-D models) bromide concentration for the inlet and outlet sites (measured: symbols, simultaneous: solid black lines, two-step: dashed lines, stochastic finite element: solid red lines).....	205
Figure 6.44 Solute concentration (mg/l) after 2hours from the start of the first irrigation using (a) deterministic (b) stochastic method.....	207
Figure 6.45 Solute concentration (mg/l) after 2days from the start of the first irrigation using (a) deterministic (b) stochastic method.....	208
Figure 6.46 Solute concentrations (mg/l) after 5 days from the start of the first irrigation using (a) deterministic (b) stochastic method.....	209
Figure 6.47 Bromide concentration ($*10^{-3}$ mg/l) at (a) t=2 hours, (b) 2 days and (c) 5 days after the start of first irrigation.....	211

LIST OF TABLES

Table 6.1	Value of parameters used in horizontal groundwater flow example.....	143
Table 6.2	Value of parameters for vertical groundwater flow example.....	149
Table 6.3	Values of parameters for example problem (Polmann et al., 1990).....	153
Table 6.4	Value of parameters for steady-state groundwater flow and solute transport example.....	170
Table 6.5	Values of parameters used for 3D solute transport example.....	177
Table 6.6	Contaminated plume dimensions for different value for correlation scale.....	185
Table 6.7	Values of input parameters used for simulation of the experiments A and B.....	187
Table 6.8	Analysis of contaminants in aquifer (January 2003) (Data provided by Exeter Environmental Services).....	195
Table 6.9	Model parameters used in the FEM analysis.....	196
Table 6.10	Parameter values used for the numerical simulations.....	201

LIST OF SYMBOLS

A	mean value of scaling parameter
A_{ij}	tensors of macrodispersion coefficient
$A^{(e)}$	area of element
C	specific water capacity
\hat{C}	effective soil moisture capacity
D	dynamic dispersion transport coefficient
D_a	effective diffusion coefficient at the interface of two regions
D_m	molecular diffusion coefficient
E	total energy
F	mean value of natural logarithm of saturated hydraulic conductivity
$F_x(x)$	cumulative probability distribution function
H	mean capillary tension head
J	mean hydraulic gradient
K_a	hydraulic conductivity at or near the surface of high permeable region
\hat{K}	effective hydraulic conductivity
K	hydraulic conductivity
K_s	saturated hydraulic conductivity
M_w	mass of water
N_i	interpolation function
Q	Sink/source of water
R	retardation coefficient
R_{cc}	covariance of concentration
S	cross-spectral density function
$V^{(e)}$	volume of element
$w^{(e)}$	element's weighting function
a	fluctuations of pore size distribution parameter
c	solute concentration
c'	fluctuations of solute concentration

f	fluctuations of natural logarithm of saturated hydraulic conductivity
g	gravitational acceleration
h	fluctuations of capillary tension head
h_w	hydraulic head
\vec{k}	wave number vector
n	soil porosity
q	water specific discharge
q'	fluctuations of water specific discharge
r	characteristic radius or half-wide of the matrix structure
t	time
u_w	pore water pressure
w_h	relative volumetric proportion of the HK pores
z	vertical coordinate
dZ	random Fourier-Stieltjes amplitude
α	pore size distribution parameter
α_L	local longitudinal dispersivity
α_s	first-order solute mass transfer coefficient
α_T	local transversal dispersivity
α_w	first-order water transfer coefficient
β	dimensionless coefficient depending on the geometry of aggregates
χ	first order reaction rate coefficient
Δt	time increment
ϕ	angle between mean flow direction and z direction in normal Cartesian coordinate system
Γ	element boundary
Γ_s	transfer term for solute exchange between the two pore systems
Γ_w	transfer term for water exchange between the two pore systems
γ	fluctuations of soil specific moisture capacity
γ_w	corrective empirical coefficient
λ	correlation scale of random parameters
v	groundwater velocity
Θ	mean value of volumetric water content
θ_g	gravimetric water content
θ	volumetric water content

ρ_w	density of water
σ_a^2	variance of α
σ_f^2	variance of $\ln K_s$
σ_h^2	variance of capillary tension head
σ_λ^2	variance of λ
Ω	domain region governed by Equation
ψ	capillary tension head
ζ	rate coefficient of the mass transfer between mobile and immobile domains

CHAPTER 1

INTRODUCTION

1.1 General background

The movement of contaminant through soils to the groundwater is a major cause of degradation of water resources. Management of lands as a non-renewable resource, itself, is a crucial requirement for sustainability. Contaminated land management and selection of appropriate and efficient remedial technologies are strongly dependent on the accuracy of predictive models for simulation of flow and solute transport in the soil, and require the understanding of real mechanisms that occur in field conditions. Recent studies have shown that the current models and methods are not capable of adequately describing the leaching of contaminants through soils; they often underestimate the risk of groundwater contamination by surface-applied contaminants and overestimate the concentration of resident solutes (Stagnitti et al. 2001). Therefore for development of an appropriate model for simulation of groundwater flow and contaminant transport with high accuracy, at least the following two issues should be addressed:

- i) Selection of comprehensive mathematical models describing physical and chemical mechanisms involved in the processes.
- ii) Solution of the model for complex problems subjected to different geometry and boundary conditions.

Transport mechanisms such as advection and dispersion in aquifers are functions of formation of soil porous matrix, properties of solid and aqueous phases and the interaction between these two phases. Therefore, water flow and contaminant transport are significantly influenced by the uncertainty and inherent heterogeneity which exists in the structure and texture of the soil. Analysis of the data obtained from laboratory experiments using morphological techniques (Bouma 1991; Lu et al. 1994; Vanderborght et al. 1997; Wang et al. 2006), and from site hydrological properties investigations and field scale experiments (Bakr, 1976; Sundicky 1986) imply spatial variability of the hydrologic properties of soil and its high influence on the flow and solute transport. The results of these investigations show that the field soils exhibit two different types of spatial heterogeneity which often also coexist; one is referred to as macro-heterogeneity which is due to as spatial variability in the macroscopic properties of soil, and another is referred to micro-heterogeneity of the soil which is heterogeneity due to spatial distribution of macropores. In principle, both spatial variability in soil hydraulic properties and structure-induced heterogeneity can contribute to the initiation of preferential pathways.

For simplicity the classical mathematical governing equations for water flow and contaminant transport have been developed assuming that the soil is a homogeneous medium. Accordingly, the parameters which are present in the classical governing equations and associated with transport mechanisms are defined with average determined values through the whole aquifer. However, in reality these parameters are subject to uncertainty due to variability in soil porosity and porous matrix. The importance of the consideration of physical heterogeneity in modelling transport phenomena has been highlighted in the literature (Kabala and Sposito 1991 and Burr et al. 1994). Therefore, spatial variability and randomness of the hydrological parameters involved in the flow and contaminant transport should be incorporated in the mathematical flow and contaminant transport governing equations.

The source of randomness in physical realizations of the majority of stochastic problems is related to either an inherent irregularity in the phenomena being observed and impossibility of exhaustive deterministic description (such as the kinetic theory of gas), or a generalized lack of knowledge about the processes involved. Uncertainty in modelling the flow and contaminant transport phenomena in soils is related to the second category of random sources. The level of uncertainty associated to this class of

problems can usually be reduced by recording more observations of the process. Hydraulic properties of soils are uniquely defined at a given spatial location within a medium. It is however impractical to measure them at all points or even at a relatively large number of points. From a finite number of observations, these properties may be modelled as random variables or with a higher level of sophistication, as random processes with the actual medium properties considered as a particular realization of these processes. As a result, the governing equations for flow and solute transport are considered as differential equations with random parameters. The solution of partial differential equations with random parameters is the main impetus of this study.

Following the successful application of the Monte Carlo method (MCM), in simulation of random processes in various engineering fields, researchers have been encouraged to use the potential of MCM in solution of the stochastic differential equations (SDEs) governing the flow and contaminant transport. However, as a computational algorithm, MCMs have their own drawbacks. These methods rely on repeated random sampling to compute their results. Because of their reliance on repeated computation of random numbers, which can be a very time consuming procedure, they are not efficient simulation techniques especially for aquifers with large dimensions. Also, because of statistical nature of these methods, they do not provide conceptual understanding of the effects of soil heterogeneity on transport mechanisms, which is necessary for planning proper and efficient remediation techniques. Analytical methods are another approach to deal with random processes and provide a closed form equation presenting the relationship between randomness in hydraulic parameters of soil. With respect to the physical and conceptual understandings, although analytical stochastic methods are more useful than MCMs, the effectiveness of these methods is limited to the simulation of simple problems, as they are unable to simulate complicated systems with complex geometry and boundary conditions.

Thus, the development of a stochastic finite element (SFE) based model as an analytical-numerical method which can overcome the shortcomings of analytical and non-efficient MCMs would be of great advantage. The methodology used for the development of SFE, takes advantage of both analytical and numerical techniques. It involves the following two steps:

- i) Incorporation of spatial variabilities of hydraulic and transport parameters in the classical governing equations and development of tractable stochastic

differential equations (SDEs) representing structured and feasible relationships between the variations of soil hydrological and transport parameters using analytical stochastic methods.

- ii) Solution of the developed SDEs, using finite element (FE) technique as an efficient and versatile numerical approach.

Macropores (micro-heterogeneity) cause high-permeable zones in different parts of aquifers. Flow and solute transport in extremely heterogeneous porous media with macropores are conceptualized as a dual-domain system. Based on this system, the aquifer is divided into two distinct transport regions. The region with macropores is considered as a second domain with high permeability next to the less permeable region.

In spite of the efforts made for the incorporation of soil heterogeneity in the simulation of contaminant transport models, none of the existing models have included the effects of both types of soil heterogeneity. They have either included the effects of micro-heterogeneity or macro-heterogeneity. The purpose of this work is to develop an analytical-numerical model, which considers the potential impacts of both micro-and macro-heterogeneity, through implementation of SFE method on the mathematical model of contaminant transport in a dual-domain system.

1.2 Objectives

The stochastic finite element methodology is a theory which has been developed and tested for the evaluation of probability measures of the occurrence of random processes. Further investigations of the methodology showed its great performance in other scientific and engineering fields. Motivated by the capabilities of SFE, the objectives of this work are

- The full description and development of SFE methodology for simulation of groundwater flow and contaminant transport problem, and incorporation of the spatial variability of soil hydraulic properties into the model.

- Development of a 2-D and 3-D computer model, based on SFE methodology, to find the numerical solution for flow and contaminant transport problems with complex geometry and boundary conditions, and investigation of the technical aspects involved in algebraic equations used for evaluation of the statistical moments of outputs.
- Incorporation of the effects of immobile water in the computer code in order to consider the effects of macropores on the flow and transport phenomena.
- Validation of the proposed SFE model through 5 illustrative flow and contaminant transport examples by comparing the results for different scenarios to those obtained by deterministic approaches, other stochastic approaches and experimental data.
- Verifying the applicability of the model to field scale problems subjected to all the variety of complex boundary conditions through application of the model on the field-scale case-studies.
- Numerical investigation of the effects of soil heterogeneity on advection and dispersion mechanisms, and adsorption of the solute mass to the soil matrix using sensitivity analysis on relevant parameters.

1.3 Structure of the thesis

With the above objectives, this thesis is organised in 7 chapters. The main text of each chapter is intentionally kept as short as possible in favour of easy reading and is written to include only the fundamental concepts and the new ideas.

In chapter 2, a literature review of the efforts that have been made on different methods developed and used for incorporating the effects of soil heterogeneity in prediction of flow and transport processes, is provided. This chapter begins with the review of several works which have been done to prove the importance of considering the effects of soil heterogeneity in modelling flow and transport processes, followed by an overview of main published works related to different modelling techniques used to incorporate uncertainty in this field. Different methods used at each work are studied and the merits and deficiencies of each work are discussed in detail.

Chapter 3 gives an insight into the general concept of SFE method. The mathematical representations and concepts used in this work are discussed briefly, and the analytical stochastic method used in development of SDEs is illustrated. Following this, the general concepts of FE method for discretization of the SDEs in time and space domains are discussed.

In chapter 4, the governing equations that have been used for the development of the model are presented and the stochastic methodology which is implemented in the classical governing equations for flow and solute transport is described.

In chapter 5, SDEs developed and presented in the previous chapter are discretized in space and time domains using finite element and finite difference (FD) methods, respectively.

Chapter 6 is one of the main chapters of this thesis, in which the SFE model is validated through some examples and the applicability of this model is tested through the simulation of some complex case studies.

Finally in chapter 7, the main conclusion of the thesis and the recommendations for further research are presented.

CHAPTER 2

LITERATURE REVIEW

2.1 Introduction

Contaminant and chemical sources are usually located in unsaturated zones or they come from the soil surface area to the unsaturated area and pass through it to reach the saturated zone. The various processes occurring within this region, therefore, play a major role in determining both the quality and quantity of water recharging into the saturated zone and may cause subsurface and groundwater contamination. Management of groundwater and contaminated lands as a non-renewable resource will be a crucial requirement for sustainability and needs accrue predictions of contaminant fate and solute transport in subsurface. As a result, many efforts have been made in recent years to investigate the subsurface hydrological processes, and different models have been developed for simulation of flow and transport in soils.

This chapter is mainly dedicated to a discussion of various approaches used for modelling of water flow and contaminant transport in saturated and unsaturated soils.

After a brief description of the classical approach for simulating water flow and solute transport in porous media, issues related to classical approaches for the modelling of these phenomena are highlighted. It is concluded that the simplified classical models of the water flow (Richards' equation) and solute transport are not able to describe flow and transport in heterogeneous soils (Stagnitti et al. 2001). The chapter also contains a comprehensive discussion of alternative modelling approaches, which make it possible to describe the flow and transport processes in heterogeneous soils with higher accuracy at local and field scales. As weight of heterogeneity increases, modelling approaches evolve from a purely deterministic description to a stochastic analysis. They vary from the multi-porosity models to the stochastic-continuum models.

2.2 Classical models

2.2.1 Water flow

The water flux in soils is commonly described using Darcy's law. Through a series of experiments, Darcy (1856) found that the water discharge rate into a specified volume of soil is linearly proportional to the hydraulic head gradient through the volume. Darcy's law was developed with respect to a saturated porous medium. His experimental results were used by Buckingham (1907) to study steady-state flow in unsaturated soils. Darcy' law has also been applied to the flow of water through an unsaturated soil (Childs and Collis-George, 1950). The well-established Richard's equation which is the Darcy's equation embedded in the mass conservation equation is the commonly used mathematical model for water flow in unsaturated soils.

A major characteristic of flow in the unsaturated zone is the dependency of hydraulic conductivity of the medium on the level of saturation, which generally becomes a strong nonlinear function for many soil types (Gunduz, 2004). In addition to the complexity of Richards' equation, the complexity of constitutive relationships that link the degree of saturation to capillary pressure and hydraulic conductivity further complicates the governing equations and their numerical solutions. Richards' equation is originally based on the capillary pressure. Numerous researchers have developed various

modified forms by changing the dependent variable of the equation. Over the years, three different forms of Richards' equation have been widely adopted (AL-Najjar, 2006); there are: (i) Pressure head-based equation, (ii) Moisture content-based equation, (iii) Mixed form of the equation with both the pressure head and the water content explicitly appearing as dependent variables of the equation.

The original pressure-head based equation is applicable to all levels of saturation in the porous medium. It performs in a superior way under saturated conditions when some of the other forms fail to properly represent the flow conditions (Huang et al., 1996). This behaviour is mostly related to the fact that the pressure head is a continuous function, both in saturated and unsaturated media under heterogeneous soil profiles. Unfortunately, the pressure head-based equation does not perform as well as the water content based equation under significantly dry conditions (Huang et al., 1996). In particular, under conditions of infiltration to a very dry soil, the pressure-based form develops large balance errors due to the highly nonlinear nature of the specific moisture capacity and notably underestimates the infiltration depth. Regardless of the limitations associated with it, the original form of the equation has been tried extensively in solving both the unsaturated zone and variably saturated-unsaturated zone flow problems (Pan et al., 1996; Romano et al., 1998; Williams et al., 2000).

To alleviate the problems associated with the pressure head-based form of the governing equation, water content based form was proposed as an alternative formulation of the unsaturated zone flow. This formulation is found to be superior in terms of mass conservation, particularly in the discrete approximations of its numerical solution such as finite element (FE) and finite difference (FD) methods (Hills et al., 1989; Gottardi and Venutelli, 1993; Pan and Wierenga, 1997). Moreover, the hydraulic functions are less nonlinear when expressed in terms of moisture content rather than capillary head, particularly when modelling infiltration into a relatively dry medium (Williams et al., 2000). However, the water content-based form of the equation is also limited in application to variably saturated and unsaturated flow since it is not able to properly simulate the saturated conditions. When the flow domain gets locally or completely saturated, the equation degenerates since the time rate of change of the moisture content

becomes zero (Celia et al., 1990). In addition, using moisture content as the dependent variable introduces problems of continuity in the domain since it is not a state variable which is always continuous in space regardless of the soil non-homogeneities. To overcome the difficulties associated with both the pressure-based and the moisture content-based forms of Richards' equation, a so-called mixed-form has been proposed, which uses both the moisture content and the pressure head as the dependent variables. Celia et al., (1990) solved Richard's equation using a method that employs the mixed form of the equations to guarantee mass conservation. The method has been shown to be robust and accurate, but requires a fine spatial and temporal discretization and so is fairly computationally demanding (Binning, 1994). The mixed form has both the superior mass conservation characteristics of the moisture content-based equation as well as the unlimited applicability to both saturated and unsaturated regions of flow that the pressure-based equation offers. In this regard, the numerical solution of the mixed form has found wide applicability in the last decade and many researchers used this form to model the flow in variably saturated-unsaturated media (e.g. Tocci et al., 1997; Miller et al., 1998; Williams and Miller, 1999; Zhang and Ewen, 2000; Zhang et al, 2002). Apart from these standard forms of the equations, some researchers did not directly use these three forms of the governing equation but rather applied certain transformation functions to smooth the strong non-linearity of the constitutive functions (e.g. Pan and Wierenga, 1997; Williams and Miller, 1999; Williams et al., 2000). Even though these transformation techniques provide some relief to the problems associated with the numerical solution, they did not find wide applicability mainly due to the fact that they are only an approximation to the original equation and lack any underlying physical theory (AL-Najjar, 2006).

Regardless of the form of Richards' equation, one needs to supplement the governing equation with the auxiliary equations to complete the mathematical representation of moisture movement in the unsaturated zone. Therefore, researchers developed numerous empirical formulas to describe the relationship between capillary pressure head and soil moisture as well as capillary pressure head and hydraulic conductivity. The most commonly used relationships were proposed by Brooks and Corey (1964), Mualem (1976) and Van Genuchten (1980). It is important to note that the original

forms of these relations did not consider the phenomenon of hysteresis, and pressure head was considered to be a single valued function of the moisture content.

Many approaches to solve the unsaturated flow equations have been suggested in the literature. A number of analytical solutions have been developed for transient infiltration under various boundary conditions (e.g. Philip and Knight, 1991 and Van Genuchten, 1980). Unsaturated drainage of a uniformly wet soil was solved by Sisson et al., (1980) for gravitational flow, whereas more complicated solutions for drainage with capillary suction was derived by Warrick et al., (1990) and Philip (1992).

Analytical solutions can only be obtained for these equations under certain assumptions. This makes their applicability very limited. However, if the assumptions and limitations of these solutions are properly understood, analytical models can be powerful diagnostic tools that can give great insight into the situations where they are used. This is exemplified by the model of Johnson and Perrott (1991) which combines a simple user interface with an analytical model of air flow to create a tool for the initial evaluation of a venting scheme. There are many other analytical models of water flow in the unsaturated zone. They include the numerous solutions like those presented by Milly (1988) and Sander et al. (1988).

The extreme variability and complexity of geological materials, dry initial conditions, varying boundary conditions and the strong nonlinearity between the pressure head and moisture content as well as the pressure head and hydraulic conductivity make the solution of Richards' equation quite a challenge, particularly within acceptable limits of accuracy and computational effort. Since analytical solutions are only possible when these nonlinear relationships are linearised and simplified (Tracy, 1995), numerical techniques are the only available method of solution. Specific applications of numerical models include analysis of complex systems (complex in terms of geology, hydrology, geometry, and boundary conditions), quantifying groundwater mechanisms and processes occurring at a site, and assessing long term impacts due to natural and human induced stresses. Numerical models have been used in several groundwater studies. In numerical solution of Richards' equation, the spatial discretisation is commonly

performed by FD or FE method (e.g. Celia et al., 1990; Hong et al., 1994; Rathfelder and Abriola, 1994; Pan et al., 1996; Huang et al., 1996; Miller et al., 1998; Van Dam and Feddes, 2000; Zhang and Ewen, 2000; Zhang et al., 2002).

2.2.2 Solute transport

Numerous human activities utilize subsurface as a receptor of various contaminants, which include hazardous waste landfills, ponds and lagoons bearing industrial or domestic wastewater, and on land applications of treated or partially treated domestic and industrial wastewater. These activities have always resulted in release of various pollutants into the subsurface and, consequently, to the nearby environment including groundwater resources. Thus, in recent years, some research has been directed specifically towards establishing better knowledge of what governs the transport of contaminants in the subsurface environment (AL-Najjar, 2006).

The transport of non-reactive solutes in a porous medium takes place through two processes; (1) solute advection defined as the average solute particle velocity, and (2) the solute dispersion. The average solute particle velocity defines the centroid of the solute plume at a given time or the average arrival time of solutes at a given depth. Solute transport was considered only in a very limited way in early groundwater investigations. The generally applied method of analysis was advective calculation. Further research regarding the problem of transport in porous media, especially in the groundwater engineering field, showed that the average fluid velocity did not describe the actual motion of individual solute particles, and that advective calculation could therefore never give a full description of solute movement. Statistical theories of hydrodynamic dispersion were developed by De Josselin de Jong (1958) and Saffman (1959) which addressed the difference between advectively calculated movement and observed movement. A number of laboratory and theoretical investigations of dispersion were completed of which those of Day (1956) and Rifai et al., (1956) were of particular significance. The solute dispersion quantifies the dispersion of the solute plume around the centroid at a certain time. In porous media, solute dispersion is caused by two mechanisms: (1) molecular diffusion and (2) hydrodynamic dispersion.

Hydrodynamic dispersion is explained by the tortuous nature of the convective stream lines resulting from microscopic fluctuations of the advection velocity. When the scale of the macroscopic transport process is much larger than the scale of the microscopic velocity fluctuations, the effect of these fluctuations on the macroscopic solute transport can be modelled as a Fickian, gradient-type process, similar to molecular diffusion. The theory of advective-dispersive transport continued to develop, particularly in the contributions of Bear (1961) and Bachmat (1967). Using the continuum approach and the macroscopic mass conservation, classical advective-dispersive solute transport equation was developed.

Advances in solute transport simulation have necessarily depended on advances in flow simulation. Many analytical (e.g., Govindaraju et al., 1996) and numerical (e.g., Bear, et al., 1993; Istok, 1989; Nwaogazie, 1986; Gunduz, 2004) models developed for simulation of solute transport in saturated zones are based on assumption of steady-state flow. Marshall et al., (2000) concluded that steady models can adequately predict solute movement in regions with small temporal variations of the flow rate, but are inaccurate under highly transient flow (Russo et al., 1994). Empirical and conceptual models developed for saturated flow conditions, such as that developed by Bear (1972), have not been easily adapted to the unsaturated case. Solute transport models are coupled to the water flow models in order to simulate the transient solute transport. Also, as mentioned earlier, since pollution from the surface and subsurface pollution sources pass through the unsaturated zones to reach the groundwater, simulation of solute transport in unsaturated area plays a significant role in the prediction of groundwater pollution risk. So, in the literature of recent years there has been a profusion of studies of the transport equations in the unsaturated zone. The impetus for this rapid development has been the strict regulatory stance on groundwater pollution (Gee et al., 1991). Therefore, research on contamination in the unsaturated zone has become more important and the studies for developing reliable predictive models have been increased. Each model has different features that tailor the model to the particular application for which it was designed. The models use a variety of solution techniques. These include: analytical solutions, FD, FE, particle tracking and Eulerian Lagrangian methods. Islas and Illangasekare, (1992) and Barry et al., (1993) developed analytical solutions for

simulation of water movement and solute transport in unsaturated zones. Smiles et al., (1978) developed a quasi-analytical solution for non-reactive solute flow during unsteady horizontal infiltration under constant concentration boundary conditions which has been discussed by Watson and Jones, (1981) particularly in relation to assessing the performance of the solute model.

Lessoff and Indelman (2004) presented an analytical model of solute transport by unsteady unsaturated gravitational infiltration. The solution was developed for gravitational flow and advective transport was applied to two scenarios of solute applications encountered in the applications: a finite pulse of solute dissolved in irrigation water and an instantaneous pulse broadcast onto the soil surface.

Analytical models are typically used in restrictive settings such as for modelling transport in experimental column studies (Shoemaker et al., 1990, Jury et al., 1983) to test the accuracy of numerical approximations to the equations (e.g., Yeh et al., 1993). In these settings the exact solution of the governing equations is not possible. However, for more complex geometries and boundary conditions, numerical solutions must be sought.

FD techniques are the simplest of the numerical techniques to apply and there are a large number of models using this solution technique. Weeks et al., (1982), were some of the first to use a numerical model to study transport in the unsaturated zone. The FD models range from the simple one dimensional model of Rosenbloom et al., (1993), through to the comprehensive model of Sleep and Sykes (1993). The FD models have usually used forward (explicit) time stepping. Benson et al., (1993) and Sleep and Sykes (1993), presented a summary of the arguments for the different forms of temporal discretization. The implicit method is less computationally expensive than the explicit method. The implicit time stepping scheme is unconditionally stable, so that large time steps can be taken. However, large time steps may not be advantageous in an implicit scheme as the truncation error increases with time step size leading to a loss of accuracy in the solution. In contrast, the explicit methods do have a limitation on the time step

size, so that small time steps must be taken. Accuracy of an explicit scheme increases with increasing time step size.

FE method is another common numerical approach to solve the transport equations. The Galerkin FE method was applied by Mendoza and Frind (1990) and Culver et al., (1991). The solutions obtained by the method are prone to oscillations. Awadallah et al., (1997), demonstrated a horizontal contaminant transport model through unsaturated soil analytically and experimentally. The water and solute transport equations were solved using the Boltzmann transformation, to convert the partial differential equations to ordinary differential equations. Karkuri and Molenkamp (1997) analyzed the advection-dispersion of non-reactive pollutant movement through a layered porous medium domain under the effect of transient groundwater flow. The governing partial differential equations of the groundwater flow and advection-dispersion of pollutant together with their integral formulations were based on Galerkin's method and Green's theorem. Li et al., (1999), presented a numerical FE model to simulate miscible contaminant transport through unsaturated soils to account for the influence of multiple non-equilibrium sources on the contaminant transport.

Hazardous waste disposal is increasingly one of the most serious problems confronting health and the environment. The movement of chemicals through the soil to the groundwater represents a degradation of these resources. In many cases, serious human and stock health implications are associated with this form of pollution. The chemicals of interest mainly include nutrients, pesticides, salts, and industrial wastes (Stagnitti, et al. 2001). Chemical effects in solute transport simulation have continued to evolve although numerous difficulties still limit this aspect of the technology. Ahuja and Lehman (1983) and Snyder and Woolhiser (1985) presented the earliest works in this area. They presented a set of experimental data that indicated a more detailed description of chemical transport in soil and water was needed. Rubin and James (1973) provided an early example of a transport model with equilibrium controlled reactions. Rubin (1983), described the mathematical requirements for simulation of several classes of reaction, and noted the computational difficulties presented by various systems. At the same time, extensive research has been done on the biodegradation of

organic chemicals in the subsurface, leading to methods of approximating some biodegradation effects in transport calculation. The knowledge about the mechanism that dominates the transport of hydrophobic organic chemicals is essential for the understanding of pollution processes. Gillham and Cherry (1982) reviewed some of the existing mathematical models for the well established transport processes in saturated soils, including molecular diffusion, mechanical dispersion, and some types of chemical interactions such as sorption, precipitation, decomposition and oxidation-reduction. In many investigations of the contaminant migration in groundwater, reactive contaminants rather than unreactive ones are the focus of the concern.

Biodegradation which is a bacterial mediate chemical reaction has been paid considerable attention by geochemical researchers, because of the important role that this type of chemical reactions plays in alleviation of geo-environmental pollutions. Three different conceptual frameworks were assumed to describe bacteria growth through the biodegradation and chemical utilization including biofilms, microcolonies and Monod kinetics (Chen, 1994). Baveye and Valocchi (1989) evaluated the mathematical models developed that founded on each of these conceptual assumptions. The biofilm concept is discussed in the works of Rittmann et al. (1980), Bouwer and McCarty, (1984) and Characklis, (1990). Molz et al., (1986) explained the microcolony concept of bacterial growth. Based on this assumption, the bacteria do not grow in continuous fixed films, but in small discrete units of 10 to 100 bacterial per colony attached to particle surfaces. Concepts of biofilm and microcolonies, focus on mechanisms taking place at the pore scale and have not been aimed at modelling large-scale transport problems. The most extensively used expression for describing the biodegradation process in chemical transport modelling in large-scale is the one based on the concept of Monod kinetics.

MacQuarrie, et al., (1990) developed a FE model for simulation of biodegradable solute transport in steady-state condition using dual Monod kinetic model, and the effects of microbial growth and electron acceptor limitation (Oxygen) were considered in this model. The accuracy and reliability of this model were proved by means of the simulation of a laboratory column experiment and good agreement was observed

between the simulated and experimental measured results. Availability of electron acceptor, usually Oxygen, plays an important role in occurrence of biodegradation of organic contaminants. Limitation of supply of Oxygen in biodegradation process was investigated through an experimental technique presented by Huang et al., (2003). They, also, used numerical codes MT3D/RT3D developed by Clement et al., (1998) which is for simulating multi-species reactive transport in soils to simulate their experiments.

With non-dimensionalization of contaminant transport governing equation coupled with Monod kinetic model, Brusseau et al, (1999) studied some factors controlling the amount and speed of the biodegradation through the contaminant transport process.

Liang et al., (2002) studied the transport mechanism of hydrophobic organic chemicals and the energy change in a soil/solvent system. A soil leaching column chromatographic experiment at an environmental temperature range of 20–40C was carried out; it was found that the transport process quickens with the increase of column temperature. Arsene (2000) presented the migration assessment of (^3H ^{14}C and ^{241}AM) in unsaturated soils which constitute the emplacement medium for the disposal of conditioned wastes. Gao et al., (2001) presented a model for simulating the transport of chemically reactive components in conjunction with energy transport in saturated and unsaturated groundwater systems. McGrail, (2001) developed a numerically based simulator to assist in the interpretation of complex laboratory experiments examining transport processes of chemical and biological contaminants subject to nonlinear adsorption or source terms. The governing equations for the problem were solved by the method of FD including any combination of three boundary conditions.

In spite of numerous mathematical models that have been developed to simulate the migration of pollutants in soils, still most of the models simulate either geochemical processes (e.g., Engesgaard and Kip, 1992; Walter et al., 1994) or biological transformations (Kindred and Celia, 1989; Clement et al., 1996) in soils. Relatively few models include the interaction between biodegradation and inorganic geochemical reactions in soils (Zysset et al., 1994; Prommer et al., 1999). Modelling geochemical

interactions between organic biodegradation and inorganic species is a current research topic.

Smith et al., (1992), developed a non-equilibrium sorption dispersion-advection model that involves a convolution integral of the product of the rate of change of concentration and a time dependent sorption coefficient, and Kohn et al., (1998) presented a numerical study of contaminant migration in saturated porous media by using a finite difference method for this purpose. The advection-diffusion equation describes the evolution of contaminant plumes in a vertical cross section of an aquifer. At the same time, Dawson (1998) studied the numerical approximation of a nonlinear diffusion equation arising in contaminant transport. The equation is characterized by advection, diffusion, and adsorption assuming the adsorption term is modelled by a Freundlich isotherm.

Remesikova (2005) introduced an efficient operator splitting scheme for solving two dimensional convection-diffusion problems with adsorption. He particularly, considered a practical problem of soil parameters identification using dual-well tests by using a general mathematical model including advection, mechanical dispersion and molecular diffusion and adsorption in both equilibrium and non-equilibrium modes. However, due to the transformation, the linear or non-linear transport problem was reduced to one dimensional and solved in an analytical form. The dispersion part was solved using standard finite volume method.

Kacur et al., (2003), discussed the numerical approximation schemes for the solution of contaminant transport with adsorption. Their method was based on time stepping and operator splitting for the transport with adsorption and diffusion. The nonlinear diffusion was solved using a finite volume method and by Newton's type of linearization.

Most of the studies for evaluation and investigation of chemical reactions were concentrated on the problems in saturated area. Thomas et al., (1995) described a model of the hydro-thermo-mechanical behaviour of unsaturated soil, developed in the context of high level nuclear waste disposal. Then, Thomas and He (1997) developed a mass

transport model for a multi-component solution system which includes coupled pore water, pore air and contaminant transport in unsaturated soils. A numerical solution of the governing differential equations was achieved using FE method as a spatial discretisation technique coupled with a FD recurrence relationship to describe transient behaviour. Thomas and Ferguson (1999) presented a fully coupled heat and mass transfer numerical model describing the migration of a contaminant gas through unsaturated porous medium. The model treats the migration of liquid water, air, and heat and contaminant gas separately with independent system variables of capillary potential, temperature, pore air pressure and concentration of the contaminant gas.

Kuechler and Noack, (2002) investigated the transport of reacting solutes through the unsaturated zone by presenting and discussing the results of numerical calculations dealing with the flow of water, the chemical reaction at the water mineral interface and the transport of chemical species caused by such flows. The source of the water flow through the soil was solely the rainfall. The water motion was calculated for two different soil classes and for typical annual precipitation. The transport of chemical species was described by a set of partial differential equations, and the chemical processes, under the assumption of equilibrium, were described by a set of nonlinear algebraic equations. A description of chemical transport in the unsaturated zone is important for the management of potential hazardous chemicals in the ecosystem. Water flow is much more intricate in the unsaturated zone than in the saturated zone, besides the high heterogeneity of the unsaturated soil.

Javadi and AL-Najjar (2007) developed a coupled 2-D numerical model to simulate chemical reactions through contaminant transport in unsaturated soils. In this model, FE and FD techniques were combined for simulation of the flow of air and water and transient chemical solutes. The model is capable of simulating various phenomena governing miscible contaminant transport in soils. Linear first-order model was used for estimation of chemical reaction rate and the model was used for simulation of a laboratory-scale experiment. Comparison of the numerical results with experimental measurements showed robustness of the model for simulation of these processes. This work was followed by Mousavi Nezhad and Javadi, (2010), for considering the effect of

chemical reaction using non-linear Monod kinetic model for biodegradation and the results obtained using non-linear Monod kinetic biodegradation compared with those obtained by first-order linear model. It was concluded that the non-linear model simulates the chemical fate with higher accuracy than the linear one.

2.3 Influence of soil texture and structure on hydrological processes

Soil texture is a soil property used to describe the relative proportion of different grain sizes of mineral particles in a soil. The textural class of a soil is determined by the percentage of sand, silt, and clay. Soils can be classified as one of four major textural classes: (i) sands; (ii) silts; (iii) loams; and (iv) clays (Smith and Smith, 1998). Soil structure refers to the arrangement of the solid parts of the soil and of the pore space located between them. In essence, soil structure is a physical condition of soil and is the product of processes that aggregate, cement, compact or unconsolidate soil or of other processes of soil material formation caused by human activities or natural atmospheric condition such as climatically-driven physical processes, shrinking-swelling, freezing-thawing, and other physico-chemical processes. Also, biological processes exert a particularly strong influence on the formation of structure in surface horizons. Depending on the various processes and their intensity that constitute the formation of soil at different locations, soil formation and structure vary with space either in vertical or horizontal direction. Figure 2.1 is a cross section of a soil which clearly shows high variability in formation of soil.



Figure 2.1 Typical cross section of soil.

From mid 60's until mid 80's, much research was carried out to investigate the effects of soil heterogeneity on water flow and solute transport in soils. White, (1985) reviewed the research work which has been done, in order to investigate the effects of macroporosity on steady-state and unsteady-state flow conditions and solute distribution through either externally applied solutes or indigenous solutes such as nitrate and salts. It has been concluded that macropores can greatly decrease the time taken for dissolved and suspended matter applied to the surface to reach subsurface drains or groundwater and the convective-dispersive theory of solute transport has limitations in predicting the distribution of solutes and their appearance in the drainage from soils with macropores.

Published experimental data clearly indicate random spatial variability in soil hydraulic characteristics of soil. Figure (2.2) shows the gravimetric water content (θ_g) as a function of depth measured in intervals of 0.15-0.45 m obtained from a field scale experimental study on a dimension of 0.64 ha carried out by Butters, et al. (1989). Spatial variability of gravitational water content can be seen clearly in this figure.

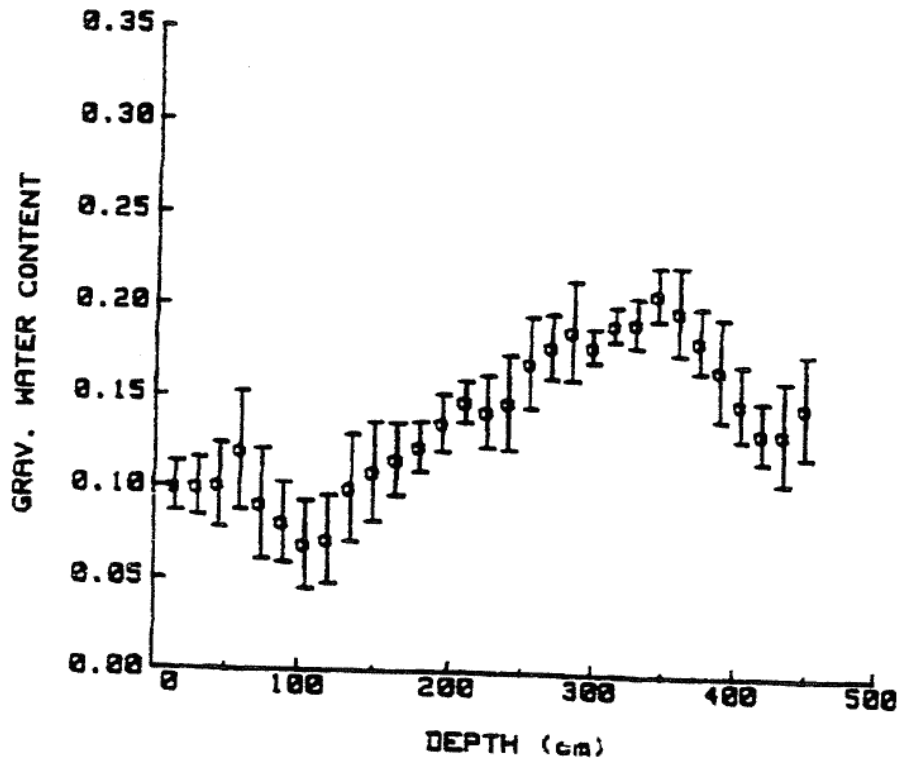


Figure 2.2 Steady-state gravimetric water content profile, along the 95% confidence interval Butter, et al. (1989).

Also, in this experiment, transport of bromide as a non-reactive chemical at steady state condition was studied. Many samples were taken from different locations in depth and lateral places of area and lateral variability of solute transport was concluded based on some breakthrough curves presenting minimum and maximum arrival time of solute at each depth at different sites. The large variability in transport was evidenced by the very rapid solute breakthrough at some sites, in contrast to the late arrival and slow passage of solute at others.

Quantitative observations obtained from laboratory tests of core samples obtained by Bakr (1976) imply spatial variability of the hydrologic properties of soil. Laboratory results of this work, presented in Figures 2.3 and 2.4, show the extreme variability of porosity and permeability of soil in space domain.

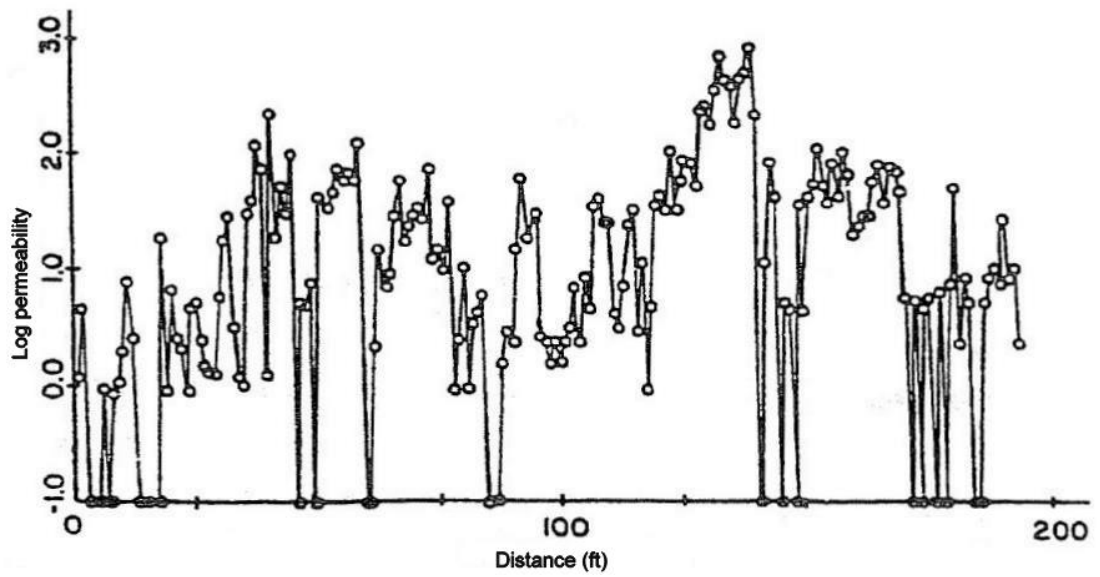


Figure 2.3 Permeability space series from laboratory test, by Bakr (1976).

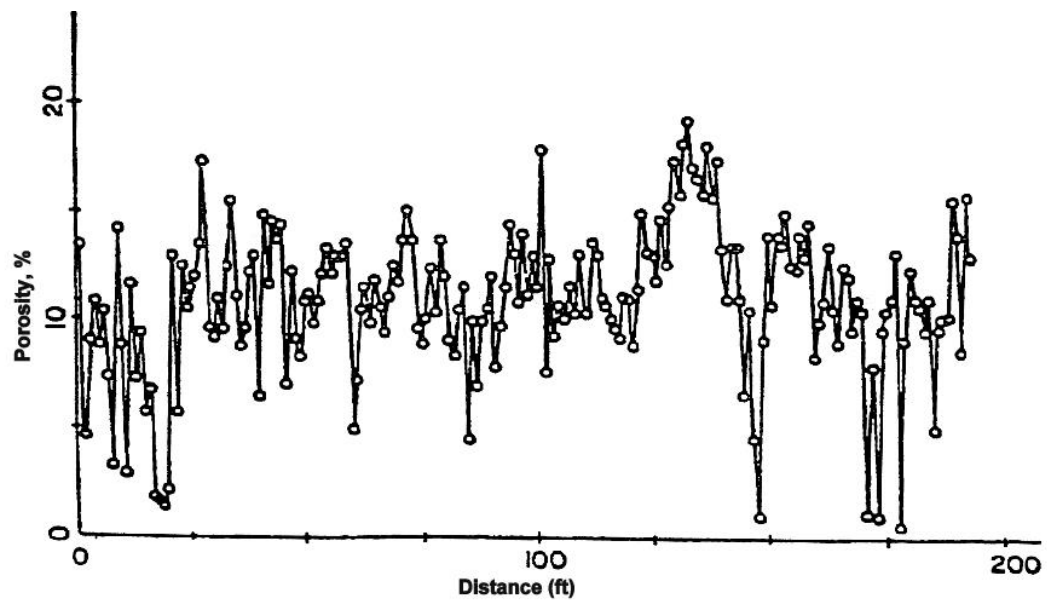


Figure 2.4 Porosity space series from laboratory test, by Bakr (1976).

Sundicky (1986) carried out a long-term tracer test in the Borden aquifer. Spatial variability of hydraulic conductivity in a heterogeneous media was investigated by the results of this experiment. Dagan (1988) discussed the fact that the dispersion of solutes by groundwater is governed by large-scale spatial heterogeneity of natural formations. He concluded that the proper setting for relating transport to aquifer properties is the stochastic one.

Also, some morphological techniques such as study of thin soil sections under microscope, analysis of two or three dimensional image of soils and dye experiments were used in order to investigate the macropore patterns and measure soil pore size distribution (Bouma 1981). Although detailed description of these techniques is beyond this work, the results obtained from these methods show strong variability in soil pores in terms of size, shape, arrangement and continuity. Since, soil pores provide pathways for flow and solute transport, these processes are influenced by variability in the formation of soil voids and pores. Foregoing techniques have been used widely in the literature (Bouma 1991; Lu et al. 1994; Wildenschild et al. 1994; Vanderborght et al. 1997; Wang et al. 2006) in order to investigate the effects of soil formation and heterogeneity on flow and solute transport.

The results of these investigations have shown that the field soils exhibit different types of spatial heterogeneity, such as soil spatial variability and soil structure, which often also coexist. Within the concept of soil heterogeneity, spatial variability relates to the spatial distribution of macroscopic model parameters, such as the hydraulic conductivity, while in structured soils microscale effects sometimes become so dominant that they affect macroscopic scale flow process. In principle, both spatial variability in soil hydraulic properties and structure-induced heterogeneity can contribute to the initiation of preferential pathways (Vogel, 2000). An appropriate model for flow and solute transport must consider all mechanisms governing these phenomena and must describe the structure and texture of soil as surrounding area of the process. So, classical equations which do not consider heterogeneity of domain are not appropriate for accurate modelling of foregoing processes. Essential need for having

accurate and reliable models has led researchers to put a lot of effort in order to consider profound effects of natural heterogeneity of soil in hydraulic processes.

One way to account for the large spatial variability of the hydraulic properties of soils could be to measure the actual three-dimensional distribution of hydraulic conductivity in complete detail of the field site, and these data can then be applied to a numerical model able to capture all of the effects of the variability. Unfortunately, this approach is impractical for two reasons:

- It is a computationally intensive approach.
- The measurement program required to determine the detailed distribution of the hydraulic conductivity would be totally unworkable.

Therefore, some alternative methods using some simplifications have been proposed for this purpose.

2.4 Modelling approaches for considering soil heterogeneity

2.4.1 Dual domain system

Macropores cause high-permeable zones in different parts of aquifers. Flow and solute transport in extremely heterogeneous porous media with macropores are conceptualized as a dual- domain (dual-permeability or dual-porosity) system. Based on this system, the aquifer is divided into two distinct transport regions. The region with macropores is considered as a second domain with high permeability (HK) next to the less permeable (LK) region. Water flow and solute transport in dual-permeability models are described using separate flow and transport equations for each region which are coupled together with an exchange term accounting for the mass transfer of water and/or solutes between the regions (Gerke and van Genuchten, 1996; Gerke and van Genuchten, 1993a). Figure 2.5 shows the general schematic of dual-domain flow system.

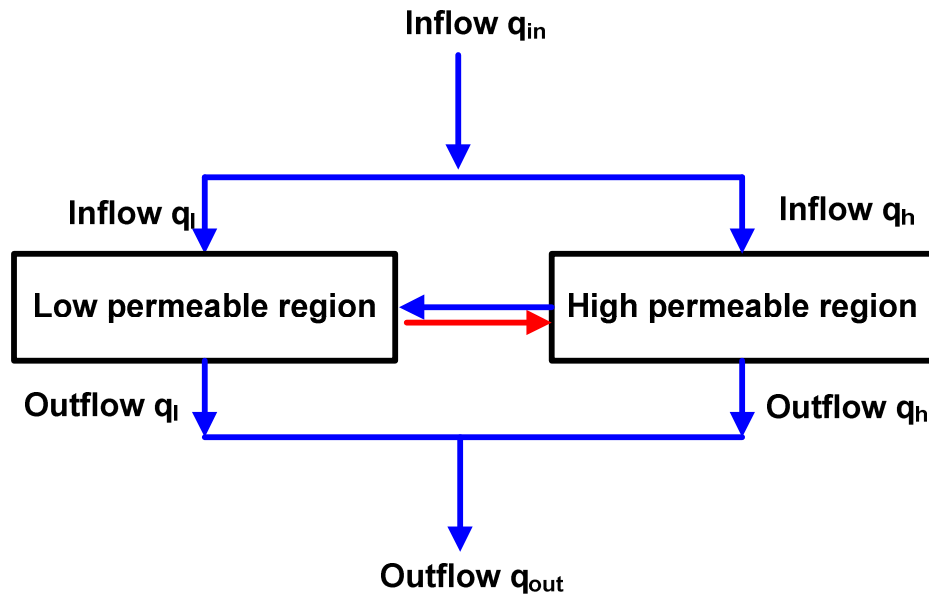


Figure 2.5 General schematic of dual-domain flow system.

Flow of water in the two regions of the dual-domain system is described by two coupled Richard's equation as (Gerke and van Genuchten, 1993a)

$$C_h \frac{\partial H_h}{\partial t} = \nabla \cdot (K_h \nabla H_h) + \nabla \cdot (K_h \nabla z) - \frac{\Gamma_w}{w_h} \quad (2.1)$$

$$C_l \frac{\partial H_l}{\partial t} = \nabla \cdot (K_l \nabla H_l) + \nabla \cdot (K_l \nabla z) - \frac{\Gamma_w}{w_l} \quad (2.2)$$

where, H is capillary tension head [L], K is hydraulic conductivity [L][T]⁻¹, C is the specific water capacity [L]⁻¹, z is the vertical coordinate taken positive upward [L], t is time [T] and Γ_w is the transfer term for water exchange between the two pore systems [T]⁻¹. The exchange of water between the two regions is based on their relative saturation S_e differences or pressure head H differences; w_h is the relative volumetric proportion of the HK pores, $w_l = 1 - w_h$ and subscripts l and h denote the characteristics of low permeability and high permeability regions, respectively.

Solute transport in dual domain system is predominantly advective through the zones of high hydraulic conductivity and is largely diffusive in zones of low hydraulic

conductivity filled with immobile or relatively stagnant water. The early arrival of solute may be attributed to preferential flow of water through the larger channels of the wetted pore space (large channels and wetted regions between finer pores in an aggregated soil) whereas, the water in the finer pores is more stagnant and does not contribute to solute transport, except for diffusion exchange. Solute transport equations in dual-domain system models are given as (Gerke and van Genuchten, 1993a)

$$\frac{\partial(\theta_h R_h c_h)}{\partial t} = \nabla \cdot (\theta_h D_h \nabla c_h) - \nabla \cdot (q_h c_h) - \chi_h \theta_h c_h - \frac{\Gamma_s}{w_h} \quad (2.3)$$

$$\frac{\partial(\theta_l R_l c_l)}{\partial t} = \nabla \cdot (\theta_l D_l \nabla c_l) - \nabla \cdot (q_l c_l) - \chi_l \theta_l c_l + \frac{\Gamma_s}{w_l} \quad (2.4)$$

where, θ is volumetric water content, R is retardation coefficient, D is dynamic dispersion transport coefficient $[L][T]^{-1}$, c is solute concentration $[M][L]^{-3}$, χ is the first order reaction rate coefficient $[T]^{-1}$, q is water specific discharge $[L][T]^{-1}$, Γ_s is the transfer term for solute exchange between the two pore systems $[M][L]^{-3}[T]^{-1}$.

Dual-domain solute transport mode is coupled with dual-domain water flow model in order to predict solute fate in macroporous soils under transient flow condition. Crucial components of these types of models are transfer terms. Gerke and van Genuchten (1993a) developed a model for water flow and solute transport in unsaturated soils assuming that all properties of the bulk medium are composed of two local properties, one associated with the fracture and one with the pore matrix, and the exchange of water between two regions is assumed to be proportional to the pressure head difference between the two regions as

$$\Gamma_w = \alpha_w (H_f - H_m) \quad (2.5)$$

$$\alpha_w = \gamma_w \frac{\beta}{r^2} K_a \quad (2.6)$$

where, α_w is the first-order water transfer coefficient $[\text{L}]^{-1}[\text{T}]^{-1}$, r is the characteristic radius or half-wide of the matrix structure $[\text{L}]$, β is the dimensionless coefficient depending on the geometry of aggregates, K_a the hydraulic conductivity at or near the surface of high permeable region $[\text{L}][\text{T}]^{-1}$ and γ_w is a corrective empirical coefficient.

Also, Gerke and van Genuchten (1993b) obtained the following general expressions for the solute transfer coefficient.

$$\Gamma_s = \pm \Gamma_w c_h + \alpha_s w_l \theta_l (c_h - c_l) \quad (2.7)$$

$$\alpha_s = \frac{\beta}{r^2} D_a \quad (2.8)$$

where α_s is the first-order solute mass transfer coefficient $[\text{T}]^{-1}$ and D_a is the effective diffusion coefficient $[\text{L}]^2[\text{T}]^{-1}$ at the interface of two regions.

Jarvis et al. (1991a) investigated the need to consider a dual-domain system for modelling of flow and solute transport in macroporous soils. They used two different models one based on assumption of single-domain system and another based on dual-domain system for simulation of the same problem of water flow and solute transport. Also, in this work, a set of sensitivity analysis was carried out with respect to parameters of exchange terms related to the size distribution of aggregates and the geometry of flow paths. The results of sensitivity analysis showed dependency of flow and solute transport on the structure of soil. Jarvis et al. (1991b) continued this work and they used the above model for simulation of chloride transport in soil samples under field conditions. Their results showed that the macropores constituted the dominant flow pathway (about 80% of the total water outflow) and diffusive exchange of chloride between the two flow domains caused a significant fluctuation in the amount of solute leaching.

Saxena et al. (1994) compared the results obtained from simulating non-reactive solute transport through undisturbed soil samples with the observed experimental results. They used a model which could be performed in both single and dual-domains. Their results

showed that the dual domain model can improve the approximation of solute transport compared with classical convective-dispersive model.

Sun et al. (1999) extended the code so-called RT3D developed by Clement et al. (1998) to a dual-domain model in order to investigate the effect of heterogeneity resulting from the presence of HK/LK conditions on bioremediation rate. The reaction between hydrocarbon and Oxygen, catalyzed by the biomass was expressed by dual-substrate Monod expression. The mathematical model embedded into this modified code was based on the two-media approach with diffusive exchange between them and in the water occupying LK region, the advection was assumed to be negligible. Both aqueous and solid microbes were considered in the HK sub-domain. The aqueous microbes are transported like a solute in the HK sub-domain. Only attached biomass was considered in the LK sub-domain. Results obtained from simulation of a hypothetical case-study suggest that the biodegradation process is significantly slower in the LK subsystem than in the HK domain. Since hydrocarbon and oxygen are transported faster in the HK domain than in the LK one, the microbes grow faster in the contamination period and mediate more rapid contaminant degradation during the pure biodegradation period. On the other hand, the concentration of microbes in the LK system changes slowly. It takes a long time to contaminate the LK system; it also takes a long time to clean it by natural biodegradation. The results obtained from dual-domain model were compared against those determined by using a single-domain model and it was concluded that biodegradation efficiency is overestimated in the LK system and under-estimated in the HK domain, when a single porosity model is used to describe the HK/LK system.

Vogel et al. (2000), simulated flow and solute transport under an irrigation furrow using a 2-D model developed by Gerke and van Genuchten (1993a). They considered 5 different scenarios including: a single domain with uniformly distributed soil hydraulic properties (SU), a single domain with randomly generated hydraulic conductivities (SR), a two-domain system with uniformly distributed hydraulic properties (DU), a two-domain system consisting of a uniform matrix and a fracture domain having randomly generated hydraulic conductivities (DRF), and a two-domain system with a uniform fracture domain but a randomized matrix domain (DRM). The results obtained from

scenario SR, showed that the hydraulic connection between the furrows and the water table and consequently, the solute concentration front movement were established much faster than the scenario SU. Different results were obtained for the scenario DU. In this case, water flow in the fracture domain reached steady state relatively soon, while the water content in the matrix domain was increasing only relatively slowly, predominantly through the absorption of water from the fractures. Also, as expected, solute transport rates were significantly higher in the fracture than in the matrix pore system. Simulation results obtained from scenario DRF showed the most heterogeneous distributions, especially for the solute concentration. As compared to DU, the water content in the fracture domain increased much faster. The randomization apparently provides high-flux pathways for both water and the dissolved solute. The DRM scenario results were quite similar to those obtained from DU. The pressure head profile in the matrix system still exhibited a somewhat distinctive preferential flow pattern. However, the matrix pressure head distributions did not greatly affect solute displacement in the matrix domain.

Comparison of results obtained from different scenarios, demonstrated the importance of considering macroheterogeneity of soils due to variability of soil hydraulic parameters such as permeability and the usefulness of combining dual-permeability features with a model that considers spatially distributed hydraulic properties. However, their results have not been compared with observed distributions under field conditions in order to find the proper scenario for this case and randomization of macroscale parameters.

2.4.2 Stochastic approaches

Simulation of processes with random variation in one or more inputs can be treated by stochastic approaches. In these approaches, random variables and consequently the output are defined in a probabilistic framework by statistical moments like mean and variance rather than using a certain constant value. Distributions of potential results which are derived from a stochastic approach reflect the random variation in the input(s). In the stochastic approach, the continuous models are the most common way of describing heterogeneity. These models focus on soil property or parametric variability

to describe the local variations of certain parameters (hydraulic conductivity, porosity, dispersivity, etc.). These types of models are frequently used in the field of subsurface hydrology which is main focus of this work. The main objective of these approaches is to derive the stochastic properties of flow and solute transport variables (i.e., pressure head, water content, water flux, solute concentration, solute flux) from the stochastic properties (i.e., mean, variance and spatial correlation structure) of hydrological parameters of soil.

2.4.2.1 Monte Carlo method

Monte-Carlo approach is a powerful technique for considering uncertainties in a system. In general, Monte Carlo method consists of two procedures (i) generation of sample realizations for input parameters from a given probability distribution, $P(X)$, to represent the uncertainty present in the process. (ii) Estimation of expectations of functions under this distribution by solving the classical continuum governing equations for each realization of random fields whether numerically or analytically and statistical analysis of the outputs (MacKay, 1998). The procedure of the method is simple. It assumes that the probability distribution of the parameter (e.g., hydraulic conductivity) and its covariance function are available from measured field data. However the probability distribution function and covariance function do not provide information about the parameter value at a particular point in space. In order to obtain the spatial distribution of the parameter values, many possible realizations of parameter values that conform to the assumed probability distribution and the covariance function are generated by using a random number generator with special techniques. The assumptions of the probability density function of the model parameters or joint probability density function for a number of parameters in the model are based on some field tests and/or laboratory tests. Each realization of the parameter values is subsequently input to classical governing equations of the procedure of interest which are then solved by standard numerical or analytical methods. In most cases, numerical methods are used. Thus, a solution is obtained for each realization of the input parameters. If there are N realizations of input parameters used for simulation, then N realization of output are obtained from solving the governing equations (Shinozuka,

1972; Mantoglou and Wilson, 1982). It is then, possible to analyse the statistical moments of output. The principle of the method is illustrated in Figure 2.6.

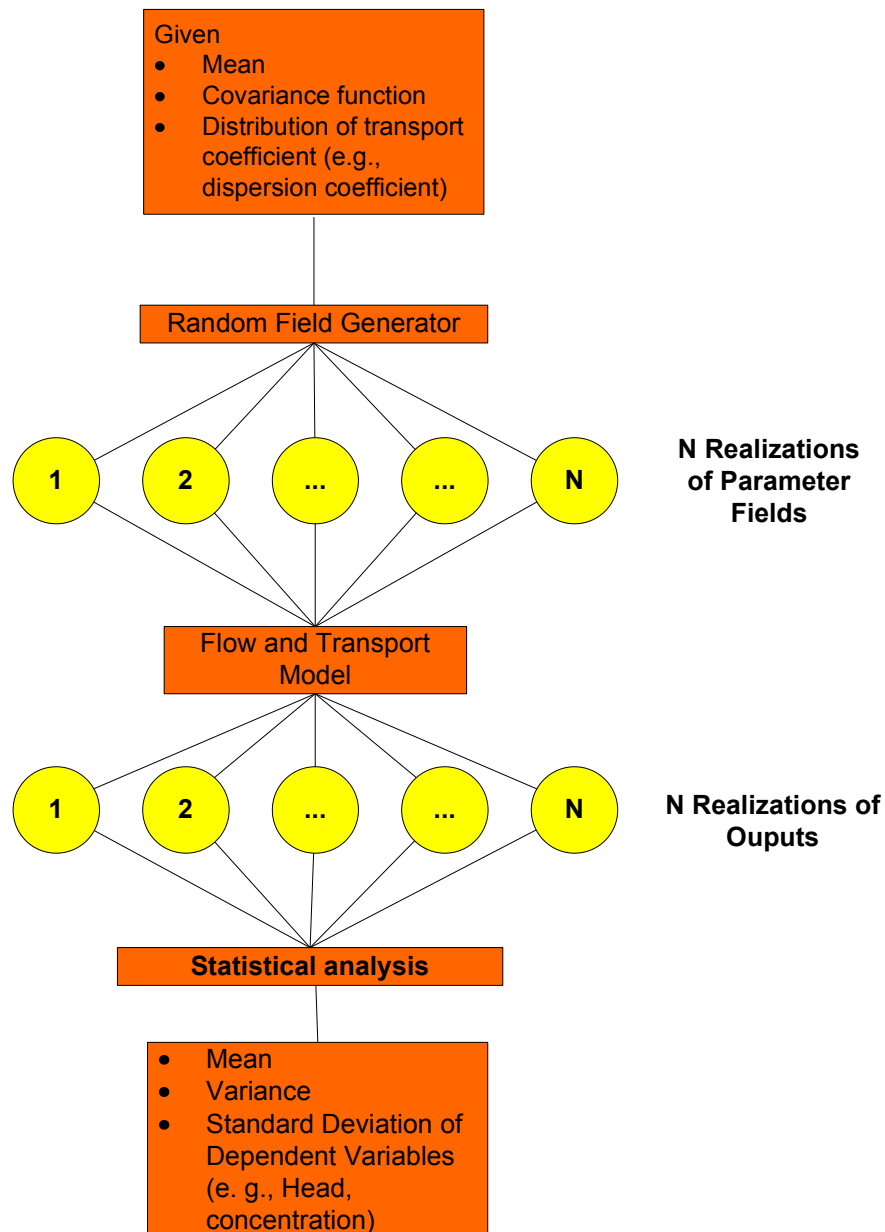


Figure 2.6 Schematic illustration of Monte Carlo method concept (Yeh 1992).

Sample generation of random fields plays a fundamental role in results accuracy and efficiency of stochastic Monte Carlo method. There are different techniques to generate realizations for the random parameters based on random field variables type in terms of their spatial correlation. The simplest case of a random field variable is an orthogonal random field variable, which consists of random univariate samples at each location.

This can be implemented easily with any efficient random number generator. However, a particular challenge arises when the random variables are dependent and they are (spatially) correlated and defined through a joint or multivariate distribution. Hydrological random parameters contributing in the flow and solute transport are spatially correlated. Not only do the generated random fields have to converge in the mean to the desired ensemble mean and variance (and any higher order moments if appropriate), they also have to converge in the mean to the desired correlation structure.

Anderson and Shapiro (1983) used Monte Carlo approach to study steady-state one-dimensional flow. A drawback of this work is that flow is generally three dimensional and transient, thus the conclusions based on a steady and one-dimensional theory may be unrealistic.

Harter and Yeh (1998) used MCM for simulation of steady-state water flow. They explained the ability of the stochastic numerical models for simulation of steady-state water flow in the aquifers with complex geometry. Hassan, et al. (1998a) studied the effects of soil heterogeneity on water flow and solute transport using Monte-Carlo method in two-dimensional synthetic conductivity fields. The flow problem was solved via a FD scheme, and a random walk approach was employed to solve the transport equation for a conservative tracer. The model was tested for mass conservation and convergence of computed statistics and found to yield accurate results. Following this, Hassan et al. (1998b) used Monte Carlo method for flow and transport in two-dimensional random conductivity, porosity, and geochemistry fields to explore the influence of their spatial variability on flow and transport processes for both conservative and reactive chemicals. For conservative transport, the results showed that when the porosity is correlated to the hydraulic conductivity (which may be expected in geologic formations); the dispersion process is significantly affected. Positive cross correlation between the porosity and the conductivity decreases dispersion, while a negative correlation tends to increase dispersion in the longitudinal direction. For reactive transport in physically and chemically heterogeneous media, the geochemical variability alone yields results that are significantly different than when both

geochemistry and porosity are random space variables correlated to the conductivity field.

Bruggeman, et al. (1999) developed a FE model for simulating flow and solute transport in soils with macropores. The model simulates preferential movement of water and solutes and uses Monte Carlo simulation to represent the stochastic processes inherent to the soil-water system. The model was applied to a field case-study for the evaluation of the developed model. The field application suggested that the model underestimated the fast leaching of water and solutes from the root zone. However, the computed results were substantially better than the results obtained when no preferential flow component was included in the model.

To take full advantage of the field data, the input sample generation can be conditioned on the information known about the particular points in space, where measurements were taken. Conditional simulation is a special kind of Monte Carlo simulation technique. The realizations generated by conditional methods are a subset of generated unconditional realizations. The conditional subset consists of all those samples in the unconditional set that preserves the known data at the measured locations. Then, the realizations of the hydraulic parameter value which do not agree with data at sample locations are simply eliminated. It is expected that the variance of output from the conditional simulation is smaller than that from the Monte Carlo simulation (Davis 1987; Clifton and Neuman 1982; Gelhar and Axness 1983).

Conditional simulations with the turning bands method were one of the first stochastic methods in hydrologic applications (Delhomme 1979). Abdou and Flury (2004) used MCM to simulate flow and solute transport through heterogeneous soils. The main objective of this work was numerical study of (i) the effect of the lower boundary conditions in two-dimensional heterogeneous soils under transient-flow conditions, and (ii) the effect of spatially structured hydraulic properties on water flow and solute transport. So, they simulated water flow and solute transport in hypothetical domains with two different lower boundary conditions; free drainage boundary condition and semi finite boundary condition. Also, three different soil structures were investigated in this work; isotropic, horizontal and vertical layered structures. Turning band technique

was used for generation of random fields (i.e., hydraulic properties) which represent spatial heterogeneity of soils. Water flow and transport equations were solved numerically with the finite element code CHAIN_2D developed by Simunek and van Genuchten (1994). They concluded that the effect of lower boundary condition on the water flow and solute transport is more pronounced in the case of soil with vertical structure. The results showed that in the vertical soil structures, water was moving faster and with larger amounts in some regions and under the effects of lower boundary condition solute leaching is retarded for the case with free drainage boundary condition.

The principal advantage of the Turning band method is that it reduces the generation of a two- or three-dimensional, random, spatially correlated process to the generation of one-dimensional, correlated line processes. The reduction in dimensionality is made possible by the fact that the transformation from a 3- or 2-dimensional covariance function into an equivalent one-dimensional covariance function can be uniquely defined (Matheron, 1973; Mantoglou and Wilson, 1982). After determining the equivalent 1-dimensional covariance, a one-dimensional, multivariate process $Y(x)$ can be generated along a finite line by using an appropriate autoregressive or other proper algorithms.

Fu and Gómez-Hernández (2008), used Markov chain Monte Carlo (MCMC) theory to develop an algorithm for generation of proper realizations of soil hydrologic parameters representing uncertainty of hydrologic properties of soils in simulation of flow and solute transport. When generation of realizations directly from desired conditional probability distribution function (cpdf) of random parameters is impossible, a Markov chain of realizations can be built that will converge to a series drawn from this cpdf. According to Markov chain theory, a chain of realizations can be built using an appropriate transition kernel that, eventually, will converge to a series of random drawings from a pre-specified probability distribution function (pdf). Each member of the chain is conditional to the previous member and its value is determined through the transition kernel as a function of the previous chain member value. The transition kernel is a probability distribution function, much simpler to draw the realizations from than the target probability distribution function. The two problems faced in any MCMC implementation are which transition kernel to use, and how long it will take for the

chain to converge (Fu and Gómez-Hernández, 2009). Details of methods for finding a proper transition kernel is beyond the scope of this work and can be found in MacKay (1998).

Gotovac, et al. (2009) used MCM to obtain reliable flow and travel time statistics in highly heterogeneous porous media. They simulated a 2-D steady, linear and unidirectional flow in highly heterogeneous domain with $\ln K$ variance up to 8. Since each Monte-Carlo step presents a potentially serious source of errors, especially for highly heterogeneous aquifers in this study, strict accuracy and convergence analysis was performed in order to define which resolution level for all flow and transport variables is needed to obtain reliable flow and travel time statistics. Based on numerical experiments, they concluded that a high resolution level is needed to accurately solve the flow equation due to the large variability in hydraulic properties.

Coppola, et al. (2009) investigated the impact of heterogeneity of hydraulic properties of a structured soil on various soil water flow processes with different top boundary conditions (evaporation and infiltration). Using a numerical solution of the Richards' equation in a stochastic framework, the ensemble characteristics and flow dynamics were studied for drying and wetting processes observed during a time interval of ten days under a series of relatively intense rainfall events. The results of their predictions were compared to mean water contents measured over time in several sites at field scale. The contribution of the variability of soil structural parameters was studied on the variance of the water contents obtained as the main output of the stochastic simulations. The contribution of each parameter depends on the sensitivity of the model to the parameters and on the flow process being observed. They concluded that the contribution of the retention parameters to uncertainty increases during drainage processes while the opposite occurs with the hydraulic conductivity parameters.

MCM is a powerful tool in simulating stochastic phenomena while few assumptions are required and it is very easy to understand. The main disadvantage of the MCM is its computational effort. The probability density function or the histogram of the input parameters must be known. A large number of realizations are necessary in order to get

a meaningful statistical analysis. A conceptual disadvantage of the MCM is that it provides no theoretical insight into physical phenomena. Also, for highly nonlinear stochastic differential equations, there is no guarantee that Monte Carlo simulations have converged to the exact (ensemble) solution after some large number of realizations. Also, there are no well-established computational criteria to predict the number of realizations required to achieve the desired accuracy. This becomes especially critical in assessing higher order moments or the probability distribution of state variables of interest (Yeh, 1992).

2.4.2.2 Analytical stochastic method

The analytical stochastic method provides an approach which explicitly incorporates the effects of natural heterogeneity of soil in simulation and prediction of large-scale behaviour of both the flow and solute transport. During the last three decades rapid developments have been made in the theoretical research treating groundwater flow and solute transport in an analytical probabilistic framework. Among the different methods, perturbation and spectral methods are the mostly used in this field. Based on these methods, soil heterogeneity is represented by considering hydraulic parameters as random spatial variables and the resulting predictions are represented through probability distributions or/and in terms of their statistical moments.

Based on the principle of Perturbation method, the input parameter X and the output variable Y can be expressed in a power series (usually Taylor series) expansion as,

$$X = X_0 + \iota X_1 + \iota^2 X_2 \dots \quad (2.9)$$

$$Y = Y_0 + \iota Y_1 + \iota^2 Y_2 + \dots \quad (2.10)$$

where, ι is a small parameter (smaller than unity). These expressions are incorporated into the differential equations of the system to get a set of equations in terms of zero and higher-order expressions of the factor ι . The equation that is in terms of zero ι corresponds to the mean value of parameter or variable. This equation in terms of first-

order of ϵ corresponds to the perturbation of the parameter and variable. In practice only two or three terms of series are usually evaluated. It is very important to notice that the accuracy of perturbation methods is related to the magnitude of the truncation error and then they are most applicable to problems with relatively small variance (Connel 1995).

Analytical perturbation method was used by Chang and Kemblowski (1994) for investigation of the statistical behaviour of both one and three dimensional unsaturated flow in heterogeneous porous media in steady-state condition. Also, Liedl (1994) developed a stochastic model for water flow in unsaturated soils for transient conditions using perturbation theory and simulated vertical infiltration process into a dry sandy loam. The simulation results obtained from this model were compared with the result obtained with Monte Carlo method for this case. Comparison showed excellent agreement between the results obtained from these two different techniques while computer time was reduced by more than 90% for stochastic perturbation method.

Another type of analytical method is spectral method which was used for the study of the spatial variation of the stochastic parameters as random fields. In this method, random fields are characterized by mean and perturbation values and theoretical spatial covariance in real space. Statistical characteristics of random parameters in real space are transferred to spectral domain. Then statistical relationships between input parameters themselves and their relationships with output variables are evaluated using spectral representations and their spectral density function. Therefore, this method has the advantage that it provides a physical understanding through development of closed form equations presenting an explicit relationship between statistical characteristics of the input parameters and system response. More description of this technique is found in chapter 4 of this thesis.

One of the distinctive features of stochastic analytical methods is that through this method, a set of structured stochastic governing equations are developed that specify the relation between statistical moments of inputs and output parameters. This feature makes the analytical method efficient in terms of time and computational cost, since the

statistical properties of the model outputs can be obtained through the solution of developed stochastic governing equations rather than statistical computations of the results of classical conventional governing equations for different possible realization of the input parameters. Encouraged by the attractive features of the analytical methods, after exploration of the potential of these methods for incorporation of random variability of input parameters into classical governing equations of flow and transport; a large number of analytical stochastic models have been developed. In the following a detailed review of major published studies on the analytical based stochastic models for flow and solute transport is presented.

Bakr et al. (1978) applied a combination of perturbation and spectral method to the classical Richard's equation and developed two stochastic models; one for one-dimensional and another for three-dimensional water flow in unsaturated soil. The comparison of the models developed shows that the variance of hydraulic head for the case of three-dimensional flow is about 5% of that in the case of one-dimensional flow. This indicates that significant errors could be introduced if a one-dimensional analysis is used to study the effects of random variability of soil hydraulic properties which are three-dimensional in reality on water flow process. They investigated the influence of the inherent spatial variability of aquifer properties on water flow in steady-state condition. They represented the hydraulic conductivity parameter as a spatial stochastic process and developed a mathematical relationship between the pressure head variance and the log hydraulic conductivity. The relationship obtained in this work shows strong dependence of the head variance on correlation length of log hydraulic conductivity field. This demonstrates the essential role of spatial statistical structure in such phenomena. However, the models developed in this work were not applied to a real example or case-study which is necessary to ascertain them as reliable models to be used for practical situations.

Dagan (1979) used perturbation method together with bounds method to consider the effects of soil heterogeneity in the groundwater contamination problem. The bounds method establishes upper and lower bounds of the random variable (e.g. effective conductivity) of a heterogeneous material when the only information available is the

frequency distribution of the variable. These bounds are widely separated for materials of high variability, and a self-consistent model which provides an estimate of the average conductivity is subsequently adopted. The advantages of this method are (i) providing simple estimates of statistical flow properties with no restrictions imposed on the permeability variance, (ii) relying heavily on physical models which facilitate understanding of the phenomena. The main limitation of this method is that it is assumed the average properties of the material vary slowly in space and time.

Dagan (1982) studied the spread of a solute in formations of random two-and three-dimensional structures for transport of solute in large heterogeneous porous media. He proposed an approximate analytical approach and applied it to simple cases in order to verify its applicability. The fundamental case of uniform average flow through an unbounded formation and of release of small solute body as initial condition was investigated. It was explained that in a homogeneous aquifer the centre of gravity of the solute body transforms uniformly and solute spread is governed by pore scale dispersion. In a heterogeneous aquifer this is no longer the case since streamlines become tortuous even if the flow is uniform in the average. In his paper, the various possible paths of solute body were determined in probabilistic terms and subsequently the distribution of the expectation and variance of concentration in space and time were evaluated.

Dagan (1990) studied transport of solute in heterogeneous soils. It was assumed that the advection is the only mechanism of solute transport and local dispersion is negligible. It was shown that soil heterogeneity causes solute to disperse with higher rate in porous media.

Yeh et al. (1985a), developed a mean equation describing large-scale behaviour of water flow using stochastic first-order perturbation approach and spectral representation techniques. Also general equations were derived relating capillary pressure head variations in terms of mean capillary pressure head field. The model was developed only for the case of one-dimension vertical infiltration in steady-state condition. Also, the model was valid when the scale of heterogeneity is much smaller than the overall

scale of the problem. It was assumed that hydrological properties of soil are statistically isotropic i.e., the variation of the related parameters in every direction is the same. However in real conditions these parameters can be statistically anisotropic. Therefore following this work, Yeh et al., (1985b), studied the effect of statistical anisotropy of hydraulic properties on head variance and effective hydraulic conductivity considering two different cases. In the first case, the saturated hydraulic conductivity was assumed to be statistically variable and the pore size distribution parameter (α) constant. The results from this study showed that the pressure head variance in a steady state infiltration in an anisotropic medium depends on the statistical parameters of the media and the mean hydraulic gradient while in the case of isotropic assumption, it was shown that the variance depends on mean capillary pressure head. They considered another case in which both saturated hydraulic conductivity and parameter α were considered to be stochastic processes. The results for this case showed that the head variance could be significantly larger depending on the magnitude of the mean capillary pressure, especially for the soil with a larger variance of the parameter α . It was concluded that in order to apply the result of the stochastic analysis to a field situation, it was necessary to invoke the ergodic hypothesis. The ergodic hypothesis implies that the scale of the problem under consideration has to be many times larger than the correlation scale of the input process. In this way, equivalence between ensemble average and space average can be achieved.

Yeh et al. (1985c) applied their previous results to a field situation where relatively large amounts of soil hydrologic data were collected so that the stochastic results could be tested. The theory developed earlier indicated that the capillary head variance increases with its mean value. This means that the variance becomes large as the soil becomes dryer. It was also found that the effective unsaturated hydraulic conductivity depends on the mean gradient, the orientation of stratification, and the correlation scales, and its anisotropy varies substantially when the mean capillary pressure changes if the variance of the parameter α is large. The results also showed that the horizontal unsaturated hydraulic conductivity of a stratified soil formation could be several orders of magnitude greater than the vertical saturated hydraulic conductivity and the vertical conductivity decreases considerably as mean capillary pressure increases. As the soil

becomes drier, horizontal hydraulic conductivity becomes more important than the vertical conductivity causing the migration of water in the horizontal direction.

Gelhar and Axness (1983) presented an analytical stochastic theory for evaluation of dispersion due to complex flow in a large-scale transport problem which is called macrodispersion. The developed theory was used to study the solute transport mechanisms in two specific aquifers. They showed that dispersivities predicted from the stochastic theory are consistent with the results of controlled field experiments and numerical simulations. Also, they concluded that inclusion of three-dimensionality is important in analyzing the macroscopic dispersion process and important features are lost when the flow is considered to be two-dimensional. However, the proposed theory was applied only to the steady state flow and transport equations and transient condition was not considered which is common situation in real problems.

Later on, Gelhar (1986) investigated the applicability of above theory on field-scale problems through comparing some results obtained of this method with those obtained by Monte-Carlo method. The importance of finding the appropriate value for correlation scale and variation of hydraulic conductivity for specific aquifer was illustrated. Also range of values for correlation scale and perturbation for different aquifers was presented.

Following exploration of strong capability and potential of spectral method in incorporation of the effects of spatial variability of random hydraulic parameters in transport phenomena, this probabilistic framework was used by Mantoglou and Gelhar (1987a) for modelling of large-scale transient unsaturated flow systems. In this work, effects of sinks/sources of water such as vapour flow were ignored. The most important advantage of this method is that the effective parameters of the large-scale model depend on only a few parameters describing the statistics of local variability (i.e., mean, variances, and correlation lengths) rather than the actual local soil properties which are infinite. However, the general stochastic theory developed requires evaluation of several three-dimensional integrals. These integrals are generally very complex and are not analytically tractable.

Mantoglou and Gelhar (1987b) solved the above mentioned integrals for stratified soil. Field observations show that natural soil formations are often stratified. The hydrologic properties of stratified soil formations can be visualized as realizations of three-dimensional, statistically anisotropic random fields, with the correlation lengths in the directions parallel to stratification being significantly larger than the correlation length in the direction perpendicular to stratification. They presented analytically tractable expressions for capillary tension head variance, mean soil moisture content, and effective specific soil moisture capacity of transient unsaturated flow in soils. Consequently, they tried to make these equations simpler through implementation of some constraints related to some specific cases of wetting or drying condition. They considered the conditions that in which the random parameters and variables are correlated or uncorrelated and developed some simple and transparent relationships between capillary tension head variance, mean soil moisture content and effective specific soil moisture capacity with statistical parameters of hydraulic properties of soil. The attractive feature of these expressions is that they provide a conceptual understanding of the effects of variability and type of distribution of input parameters on statistical values of output.

Mantoglou and Gelhar (1987c) simplified the general stochastic equations derived in Mantoglou and Gelhar (1987a) and presented a set of generic expressions for evaluation of the effective hydraulic conductivities for the soils with stratified formation. However, these simple expressions are valid at particular range of soil property. They showed that effective hydraulic conductivities show significant hysteresis and are anisotropic with the degree of anisotropy depending on the mean flow condition (wetting and drying). Such hysteresis and anisotropy are produced by the spatial variability of the hydraulic soil properties rather than hysteresis or anisotropy of the local parameters.

Vomvoris and Gelhar (1990) used spectrally based perturbation approach to evaluate the concentration fluctuations for a steady-state flow field in a three-dimensional statistically homogeneous and anisotropic aquifer. The theoretical model developed in this work, was used for numerical study of the effects variance of saturated hydraulic conductivity and concentration gradient on the variance of solute concentration. They

concluded that increase of both the variance of saturated hydraulic conductivity and solute concentration gradient causes increase in variance of solute concentration. In spite of very good numerical results obtained from the mathematical model developed in this work, it has a complex structure that limits the application of this model since the model can not be easily solved with analytical techniques.

Van Kooten, (1994) used analytical perturbation technique for developing a model to predict mean travelling time and rate of contaminant movement in the confined aquifer. The effects of linear non-equilibrium sorption and first-order decay were taken into account in this model. He developed asymptotic expression for two different 2D flow patterns including flow parallel to the boundary of domain and flow toward pumping wells. The performance of the model developed in this work depends on the ratio of the advection and dispersion. Accuracy of prediction increases as the ratio of advection and dispersion increases.

Kapoor and Gelhar (1994a) studied the movement of contaminants and concentration fluctuations in heterogeneous porous media. They focused on the transport mechanisms that occur in the saturated zone and considered the groundwater velocity as a spatially variable instead of considering a uniform mean velocity. It was concluded that the variability in concentrations in this condition is more than when only local dispersion is considered in uniform velocity. Also, they showed that the mean and variance of concentration field undergo a translation with the mean velocity field and the rate of creation of fluctuations increases with the mean concentration gradient and it decreases with an increase in the plume scale.

Kapoor and Gelhar (1994b) presented an analytical solution to the equation for concentration variance developed in Kapoor and Gelhar (1994a) for a special case of multi-dimensional finite-size impulse input. The coefficient of variation that was estimated from a bromide tracer test data was compared with their theoretical predictions. The coefficient of variation of the concentration was defined as the standard deviation of concentration divided by its mean in this work. Both theoretical and experimental results showed that the coefficient of variation of concentration decreases

with time. Also, they noticed that the regions in which the coefficient of variation is small were the regions for which the mean concentration was a good predictor of the actual concentration levels in a sample realization of a hydraulic conductivity field.

Russo (1993) used stochastic method for modelling transport coupled with flow in unsaturated zone. He combined the Lagrangian formulation developed by Dagan (1984) for modelling of solute transport with stochastic theory developed with Yeh et al. (1985a, b) for steady-state water flow. Therefore, the statistical moments of solute transport were related to hydrological properties of the heterogeneous unsaturated soils. Then, through a numerical investigation, they showed that solute spread increases as water saturation decreases.

Russo (1995a, b) developed a model based on Lagrangian-stochastic method for transient solute transport in vados-zone. He evaluated a macrodispersion coefficient for the saturated case and applied this coefficient for the unsaturated case with employing the assumption that for a given mean capillary pressure head, water saturation is a deterministic constant and log conductivity is a multivariate normal, stationary random space function. The proposed approach is applicable to vados zone flow and transport as long as, the scale of heterogeneity in the direction of the mean flow is smaller than approximately one tenth of the characteristic length of unsaturated flow. Effects of water saturation on solute transport, was investigated. He concluded that for a soil with a specific formation, the magnitude of macrodispersion in unsaturated flow is larger than that in saturated flow, and increases as water saturation decreases.

Yang et al. (1996) derived an analytical solution of macrodispersivity for adsorbing solute transported in physically and chemically heterogeneous unsaturated soils under the condition of gravity dominated flow and expressed as a function of statistical properties of the unsaturated soil and chemical heterogeneities. The unsaturated hydraulic conductivity and water content were treated as spatial random functions. The chemical adsorption, described as linear equilibrium isotherm, and the adsorption coefficient were represented as a spatial random function.

Miralles-Wilhelm and Gelhar (1996) carried out a stochastic analysis of transient characteristics of sorption at field scale and showed that sorption macro-kinetics arises as a result of physical and chemical heterogeneities of aquifer. They developed an analytical expression for the time evaluation of the field scale retardation factor and longitudinal macrodispersivity for a reactive solute. They presented a stochastic analysis of solute transport and first-order decay for the case of spatially varying porous media (hydraulic conductivity), flow (groundwater velocity), and decay rate.

Miralles-Wilhelm et al. (1997) developed a three-dimensional analytical model to quantify the process of oxygen-limited biodegradation as it occurs at field scales. The model incorporated the effects of chemical and microbiological heterogeneities inherent to the biodegradation process in a stochastic analysis of coupled transport equations for a system consisting of a contaminant and an oxidizing agent (oxygen) in heterogeneous and anisotropic aquifers. Natural aquifer variability, equilibrium linear sorption and Monod-type kinetics for the microbial population constitute the sources of these heterogeneities. Their results showed that in oxygen-limited biodegradation, the presence of heterogeneities has strong effects on the longitudinal macrodispersivities for contaminant and the dissolved oxygen. But this model does not consider the effects interaction between oxygen and hydrocarbon concentration fluctuations. Following this, Kemblowski et al. (1997) developed a methodology to obtain a clear understanding of mixing-limited biodegradation processes in heterogeneous geologic formations. They showed that, their model and particularly the effective biodegradation rate, depend strongly on the cross correlation between the oxygen and hydrocarbon concentration fluctuations.

Xin and Zhang (1998) presented a close form solution for a one-dimensional transport model coupled with biodegradation in heterogeneous porous media. The model consists of two reaction-advection equations for nutrient and pollution and a rate equation for biomass. The hydrodynamic dispersion was ignored. Uncertainty and spatial variability in geochemical and biological parameters were not considered and spatial variability of porosity was considered as the only source of randomness in process. Statistics of degradation fronts were studied via representations in terms of the travel time

probability density function and travelling front profiles. In all above studies, it was assumed biomass does not move in the domain.

Miralles-Wilheim et al. (2000) expanded the model presented in Miralles-Wilheim et al. (1997) in order to consider transient microbial dynamics. Comparing their results in this paper with Miralles-Wilheim et al. (1997) assuming an established active biomass at steady state, shows that, the effects of transient microbial growth dynamics on the effective retardation factor and macrodispersivities are minor, while modest effects are produced in the effective decay rate. Advantages of this model are that it capture the most important large-scale system characteristics and has few effective parameters which are identifiable from a realistic data set. However, solution of this stochastic partial differential equation needs to a proper numerical method due to complex nature of these equations.

Zhang and Brusseau (2004) used a stochastic approach to study the effects of uncertainty in dissolution and sorption/desorption rate due to soil heterogeneity on transport of immiscible organic liquid constituents in water-saturated porous media. In this approach a probability density function was used to describe a continuous distribution of sorption domains and associated rate coefficients. The initial dissolution rate coefficient and the sorption/desorption rate coefficient were considered as random parameters and Log-normal probability density functions were used to describe their distributions. They concluded that both heterogeneous rate-limited sorption/desorption and heterogeneous rate-limited dissolution can significantly increase the time required to elute immiscible-liquid constituents from a contaminated porous medium.

Chaudhuri and Sekhar (2005) used a stochastic analytical method similar to that of Gelhar and Axness (1983) in order to evaluate coefficient of macrodispersivity in three-dimensional heterogeneous porous media. Both hydraulic conductivity and local dispersion coefficient were considered as random variables, while, in the mathematical model developed by Gelhar and Axness (1983), local dispersion coefficient was considered as deterministic parameter.

From study of the documents presented in this section, it can be concluded that the analytical stochastic approaches can be used to provide valuable insight about the effects of soil heterogeneity on the behaviour of large-scale unsaturated flow and solute transport in soils. However, these approaches are not capable of simulating complicated problems; particularly problems related to aquifers with the complex boundary conditions. In the case of simulating particular domains of an aquifer, numerical approaches are more appropriate than analytical methods. Therefore, the combination of analytical methods, for incorporating the uncertainty present in the problem, with numerical techniques, for simulating the complex geometry and boundary conditions of the aquifer, can be used to overcome the limitations of analytical approaches and to take advantage of both analytical and numerical methods.

2.4.2.3 Alternative methods

Polmann et al. (1991) used FD technique to solve the analytical-based partial differential equations developed by Mantoglou and Gelhar (1987a, b, c) for modelling of transient water flow through unsaturated soils. The results obtained from their mean flow method were compared with those obtained using turning band method (Ababou, 1988 and Ababou and Gelhar, 1988). Good agreement between the results of these two different methods indicates that, the assumptions and simplifications applied for the development of mean flow equations from the spectral based method are not critical in simulating of water flow. However, in this work, the effects of the spatial gradient of mean capillary tension head in evaluation of hydraulic conductivity were ignored. The same problem was solved by Aguirre and Haghighi (2002) using a numerical FE technique and they obtained different results from those gained by Polmann et al. (1991). In this work, the effects of the spatial gradient of mean capillary tension were considered. Following this, Aguirre and Haghighi (2003) worked on further development of their model and tried to consider heterogeneity in their FE model. However their model had the shortcomings of not considering some of the critical mechanisms affecting the fate of solute, such as chemical reaction and molecular diffusion. Additional drawback of their model could also be that it could not be applied to some practical problems, because it lacks having a versatile top boundary condition and considering the effects of atmospheric evaporation.

CHAPTER 3

STOCHASTIC FINITE ELEMENT METHOD

3.1 Introduction

From a geo-environmental perspective, the most common stochastic problem involves one or more differential equations with random coefficients. These coefficients represent the properties of the system under investigation. They can be thought of as random variables or more accurately and with an increasing level of complexity, as random processes with a specified probability structure. Mathematically the problem can be formulated as

$$\Lambda u = f \tag{3.1}$$

where Λ is a stochastic differential operator, u is the random response, and f is the possibly random excitation.

The problem in dealing with stochastic equations is two-fold. Firstly, the random properties of the system must be modelled adequately as random variables or processes, with a realistic probability distribution. A good treatment of this modelling phase is presented by Gelhar and Axness (1983), Gelhar (1993) and Russo et al. (1994). Secondly, the resulting differential equation must be solved and response quantities of interest obtained, usually as determined by their second order statistics. The solutions to most of such differential equations are too complex for analytical methods and are commonly obtained using approximate numerical techniques.

The problems dealt with in this study involve concepts of mathematics and probability. It is both necessary and instructive to introduce the mathematical concepts which are used in the sequel. So the primary focus of this chapter is on stochastic processes and random fields that provide the tools needed to represent the continuous variation of parameters in space. Then, it is explained that how stochastic spectral method is applied to mathematical models of stochastic processes to obtain the related stochastic differential equations (SDEs). Finally, a description of finite element and finite difference procedures for finding numerical solution of resulted stochastic partial differential equations is presented.

3.2 Probability and random variables

A random variable X is defined in terms of its cumulative probability distribution function (cdf) as

$$F_x(x) = P[X \leq x] \quad (3.2)$$

which denotes the probability that the random variable X is less than some specified value x . In this section, Capital letters are used to denote random quantities and lowercase letters to identify deterministic numerical values. In an applied sense, probability is usually thought of as the relative frequency of occurrence, expressed as

$$P[X \leq x] = \frac{\text{number of occurrence with } X \leq x}{\text{total number of occurrences}} \quad (3.3)$$

The cdf is a non-decreasing function, ranging from 0 to 1 as X goes from $-\infty$ to ∞ . For a continuous random variable the probability density function (pdf) is

$$f_x(x) = \frac{dF}{dx} \quad (3.4)$$

which can be expressed in terms of the probability that x is in some small interval δx

$$f_x(x) \delta x = P[x < X < x + \delta x] \quad (3.5)$$

By integrating Equation (3.4),

$$F_x(x) = \int_{-\infty}^x f_x(u) du \quad (3.6)$$

which the area under probability density function is 1 ($F_x(\infty) = 1$).

Random variables are often characterized by their moments; for example, the expected value, or mean of X is found by taking the first moment

$$\mu_x = E[X] \equiv \int_{-\infty}^{\infty} x f_x(x) dx \quad (3.7)$$

which is a measure of central tendency of random variable. The second moment about the mean, the variance, is

$$\sigma_x^2 = E[(X - \mu_x)^2] \equiv \int_{-\infty}^{\infty} (x - \mu_x)^2 f(x) dx \quad (3.8)$$

When more than one random variable is analysed it is necessary to consider how the variables are interrelated probabilistically. For example, if X_1 and X_2 are two random variables, then their joint distribution function is

$$F(x_1, x_2) = P[X_1 \leq x_1 \text{ and } X_2 \leq x_2] \quad (3.9)$$

and the joint probability density function is

$$f(x_1, x_2) = \frac{\partial^2 F(x_1, x_2)}{\partial x_1 \partial x_2} \quad (3.10)$$

For continuous random variables, the conditional probability density function of X_1 , given $X_2=x_2$, is defined by

$$f(x_1 | x_2) = \frac{f(x_1, x_2)}{\int_{-\infty}^{\infty} f(x_1, x_2) dx_1} = \frac{f(x_1, x_2)}{f_2(x_2)} \quad (3.11)$$

where $f_2(x_2)$ denotes the marginal probability density function of X_2 defined as

$$f_2(x_2) = \int_{-\infty}^{\infty} f(x_1, x_2) dx_1 \quad (3.12)$$

The covariance function of a stochastic process as function of time, $X(t_1)$ and $X(t_2)$, is

$$\text{cov}(t_1, t_2) = E\left[\left(X(t_1) - \mu(t_1)\right)\left(X(t_2) - \mu(t_2)\right)\right] = R(\tau) \quad (3.13)$$

When $t_1=t_2$, Equation (3.13) gives the variance the process. The covariance function is a measure of the degree of linear relationship between $X(t_1)$ and $X(t_2)$.

If a process is stationary, it is virtually always possible to describe the process in terms of a kind of Fourier representation. A stationary process is one in which the probabilistic descriptions become independent of origin of independent variable (time or space). Consider a zero-mean stationary process, $X(t)$; then, the spectral representation of the process is

$$X(t) = \int_{-\infty}^{\infty} e^{ik\bar{t}} dZ(\bar{k}) \quad (3.14)$$

where, \vec{k} represents wave number vector. This is a Fourier-Stieltjes integral in which Z is a stochastic process having the properties that

$$\begin{aligned} E\left[dZ(\vec{k})\right] &= 0 \\ E\left[dZ(\vec{k}_1)dZ^*(\vec{k}_2)\right] &= 0; \quad \vec{k}_1 \neq \vec{k}_2 \\ E\left[dZ(\vec{k}_1)dZ^*(\vec{k}_2)\right] &= S(\vec{k})d\vec{k}; \quad \vec{k}_1 \neq \vec{k}_2 = k \end{aligned} \quad (3.15)$$

where, Z^* is conjugate of Z and S is spectral density function of random process Z .

In this work, the spectral representation theorem is accepted as a well-established mathematical theorem and the concept and details of this theorem can be found in Priestley (1981) and Lumley and Panofsky (1964).

For a zero-mean stationary stochastic process $X(t)$, the covariance function can be written as (Lumley and Panofsky, 1964)

$$\begin{aligned} R(\tau) &= E\left[X(t+\tau)X^*(t)\right] \\ &= E\left[\int_{-\infty}^{\infty} e^{i\vec{k}(\bar{t}+\bar{\tau})}dZ(\vec{k})\int_{-\infty}^{\infty} e^{-i\vec{k}'\bar{t}}dZ^*(\vec{k}')\right] \\ &= \int_{-\infty}^{\infty}\int_{-\infty}^{\infty} e^{i[(\vec{k}-\vec{k}')\bar{t}+\vec{k}\bar{\tau}]}E\left[dZ(\vec{k})dZ^*(\vec{k}')\right] \end{aligned} \quad (3.16)$$

The first line on the right side of Equation (3.16) results because X is real, so that it is equal to its complex conjugate. The second line is simply a substitution of the representation in Equation (3.14). The third line follows from the interchange of the order of expectation and integration, noting that the exponential terms are deterministic. When X is stationary process, its covariance function must be independent of t , as a result, the term involving t and the last line of Equation (3.16) must cancel out as a result of the integration. This can be expressed as (Lumley and Panofsky, 1964)

$$E\left[dZ(\vec{k})dZ^*(\vec{k}')\right] = S(\vec{k})\delta(\vec{k}'-\vec{k})d\vec{k}d\vec{k}' \quad (3.17)$$

where δ is a Dirac delta function. The covariance function in Equation (3.16) then reduces to

$$R(\tau) = \int_{-\infty}^{\infty} e^{i\vec{k}\tau} S(\vec{k}) d\vec{k} \quad (3.18)$$

which shows covariance function can be written as the inverse Fourier transform of the spectrum. The corresponding transform relationship for the spectrum is then

$$S(\vec{k}) = \frac{1}{2\pi} \int_{-\infty}^{\infty} e^{-i\vec{k}\tau} R(\tau) d\tau \quad (3.19)$$

Equations (3.18) and (3.19) are classical results for stationary stochastic processes that show that the covariance and spectrum contain essentially equivalent information. These mathematical relationships are used for solution of stochastic partial differential equations using spectral method that is explained briefly in the following section in general case and in chapter 4 in the case of flow and solute transport.

3.3 Stochastic differential equation

In order to illustrate the approach that has been used to treat SDEs, consider a simple SDE of the form

$$\frac{dX}{dt} = -AX + Y \quad (3.20)$$

If A is a constant, then this is a stochastic differential equation with a random non-homogeneous part. The second-moment solution of this equation can be approached by expressing X and Y as their expected values plus a zero-mean perturbation, that is,

$$\begin{aligned} X &= \bar{X} + x; & E[X] &= \bar{X}; & E[x] &= 0 \\ Y &= \bar{Y} + y; & E[Y] &= \bar{Y}; & Y[y] &= 0 \end{aligned} \quad (3.21)$$

By using this decompositions in Equation (3.9),

$$\frac{d\bar{X}}{dt} + \frac{dx}{dt} = -A\bar{X} - Ax + \bar{Y} + y \quad (3.22)$$

and by taking the expected value of this equation, the equation describing the mean becomes

$$\frac{d\bar{X}}{dt} = -A\bar{X} + \bar{Y} \quad (3.23)$$

and when the mean equation is subtracted from Equation (3.22), it results in the following equation for the zero-mean perturbations:

$$\frac{dx}{dt} + Ax = y \quad (3.24)$$

Note that no approximations have been introduced in order to decompose the problem into this form involving differential equations for the mean and perturbation.

The perturbation equation, considers, first, the possibility of a stationary solution for X, given that Y is stationary process. Then, using the spectral representation for x and y,

$$\int_{-\infty}^{\infty} e^{ik\tau} \left[ikdZ_x + AdZ_x - dZ_y \right] = 0 \quad (3.25)$$

Then, by the uniqueness of the spectral representation, it follows that (Gelhar 1993)

$$dZ_x = \frac{dZ_y}{(A + ik)} \quad (3.26)$$

and multiplying dZ_x by its complex conjugate, it follows that the spectra of x and y are related by

$$S_{xx}(k) = \frac{S_{yy}(k)}{(A^2 + k^2)} \quad (3.27)$$

where, S_{xx} and S_{yy} are the spectral density functions of x and y respectively.

The perturbation equation is treated analytically to develop a set of algebraic equations for evaluation of variance of response variables. The mean equation can be solved directly as a deterministic ordinary differential equation, given the expected value of Y . Finite element method can be used to solve the mean equation.

3.4 Finite element method

The finite element method is a numerical analysis technique for obtaining approximate solutions to a wide variety of engineering problems (Huebner et al. 2001). This method was designed to study stresses in airframe structures and then adapted to a wider field of mechanics. Finite elements are used to solve a complex problem by dividing the problem into smaller problems and solving them separately. Thus this method looks at a model as made up of small inter-connected sub-regions or elements. The idea of the finite element method is that a “solution region” i.e., a model can be analysed or approximated by replacing the region with a finite number of distinct elements. These elements can then be placed in different ways to make up complex problems.

3.4.1 Finite element procedure

In general the solution procedure for a continuum problem using the finite element method involves the following basic steps (Cheung et al. 1996):

- i) Discretising the problem domain into a number of sub-regions known as finite elements. The field variables are assigned at the nodes of each element with the nodal values of these field variables being the unknown parameters of the problem.
- ii) Selection of element interpolation functions to represent variation of the field variables over the element.
- iii) Evaluation of individual element properties. This involves approximating the governing differential equations using a simpler system of algebraic

equations over the element domain. The approximation is commonly achieved using either variational techniques or weighted residual approaches. Galerkin's weighted residual approach is adopted in this research for its simplicity and accuracy.

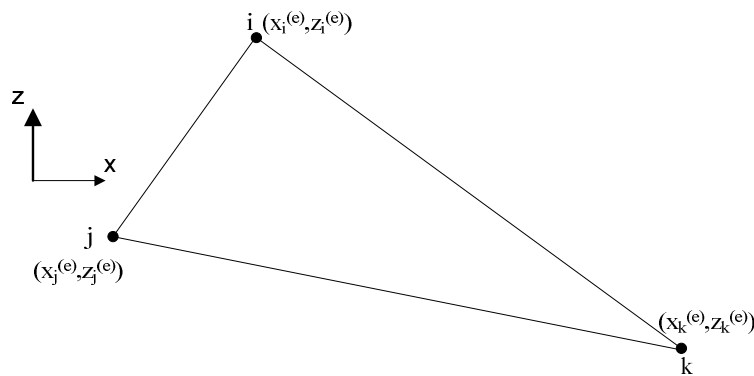
- iv) Formation of elements stiffness matrix.
- v) Assembling the element properties to obtain the system equations that will represent the overall system.
- vi) Imposing boundary conditions to modify the global system of equations using the known values of the nodal variables at the continuum boundary.
- vii) Solving the system of equations for the unknown nodal variables using conventional numerical analysis techniques.
- viii) Finally, further computations to evaluate second-order moment of system response and additional important parameters such as mean soil water content and other physically meaningful quantities from the computed nodal variables and element properties.

3.4.2 General formulation

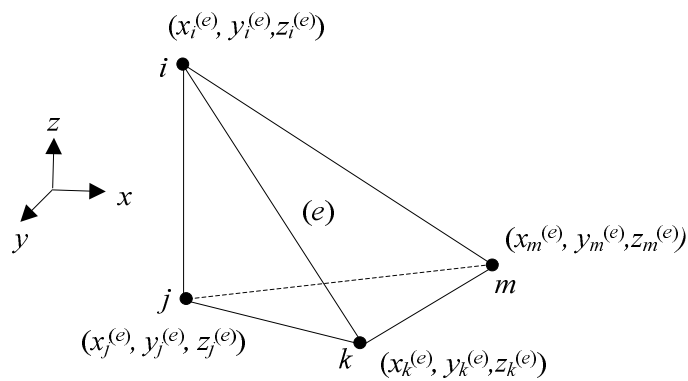
Basics of FE Formulation

The basic idea behind the finite element method is to divide the structure, body or region being analysed into a suitable number of elements with associated nodes and to choose the most appropriate element type to model most closely the actual physical behaviour. The number of elements used and their variation in size and type within a given region are primarily matters of engineering judgment. These elements may be one, two or three dimensional. Discretisation results in the specification of the finite element mesh and involves two distinct but related tasks: nodes definitions and elements definitions. The nodes are always numbered consecutively from one to the total number of nodes present. The nodal numbering pattern has a strong influence on execution time in a computer program (for large problems). Usually the nodes are numbered in such a way so as to minimise the bandwidth of the assemblage matrix. Node definition completes when the coordinates of each of the nodes are also specified. The element numbering scheme is completely arbitrary. To define the elements, one needs to number them consecutively from one to the maximum number of the elements present.

The nodes associated with each element must be specified. In addition, the material property data to be used for each element should be specified (Stasa 1985). The choice of appropriate element for a particular problem is one of the major tasks that must be carried out by analyst. However, the elements must be small enough to give usable results and yet large enough to reduce computational effort. Small elements are generally desirable where the results are changing rapidly, such as where changes in geometry occur; large elements can be used where results are relatively constant (Daryl 2002). Figure 3.1 shows three-node triangular element and four-node tetrahedral element with their nodal coordinate, which have been used in the developed FE programs for this work.



(a)



(b)

Figure 3.1 (a) Linear triangular element with global coordinates, (b) linear tetrahedral element with global coordinates.

For the finite element procedure a set of so called shape functions has to be considered so that they exclusively define the state of unknown variable of the problem within each element in terms of its nodal values. The shape functions for a typical three-node element are given as (Stasa 1985)

$$N_i^{(e)}(x, z) = \frac{1}{2A^{(e)}}(a_i + b_i x + c_i z) \quad (3.28)$$

$$N_j^{(e)}(x, z) = \frac{1}{2A^{(e)}}(a_j + b_j x + c_j z) \quad (3.29)$$

$$N_k^{(e)}(x, z) = \frac{1}{2A^{(e)}}(a_k + b_k x + c_k z) \quad (3.30)$$

where

$$\begin{aligned} a_i &= x_j^{(e)} z_k^{(e)} - x_k^{(e)} z_j^{(e)} & a_j &= x_k^{(e)} z_i^{(e)} - x_i^{(e)} z_k^{(e)} & a_k &= x_i^{(e)} z_j^{(e)} - x_j^{(e)} z_i^{(e)} \\ b_i &= z_j^{(e)} - z_k^{(e)} & b_j &= z_k^{(e)} - z_i^{(e)} & b_k &= z_i^{(e)} - z_j^{(e)} \\ c_i &= x_k^{(e)} - x_j^{(e)} & c_j &= x_i^{(e)} - x_k^{(e)} & c_k &= x_j^{(e)} - x_i^{(e)} \end{aligned} \quad (3.31)$$

and $A^{(e)}$ is the area of the element which is evaluated as

$$A^{(e)} = \frac{1}{2} \begin{vmatrix} 1 & x_i^{(e)} & z_i^{(e)} \\ 1 & x_j^{(e)} & z_j^{(e)} \\ 1 & x_k^{(e)} & z_k^{(e)} \end{vmatrix} \quad (3.32)$$

The derivatives of the interpolation functions are

$$\begin{aligned} \frac{\partial N_i^{(e)}}{\partial x} &= \frac{b_i}{2A^{(e)}} & \frac{\partial N_j^{(e)}}{\partial x} &= \frac{b_j}{2A^{(e)}} & \frac{\partial N_k^{(e)}}{\partial x} &= \frac{b_k}{2A^{(e)}} \\ \frac{\partial N_i^{(e)}}{\partial z} &= \frac{c_i}{2A^{(e)}} & \frac{\partial N_j^{(e)}}{\partial z} &= \frac{c_j}{2A^{(e)}} & \frac{\partial N_k^{(e)}}{\partial z} &= \frac{c_k}{2A^{(e)}} \end{aligned} \quad (3.33)$$

The shape functions for a typical tetrahedral four-node element are given as (Stasa 1985)

$$N_i^{(e)}(x, y, z) = m_{11} + m_{21}x + m_{31}y + m_{41}z \quad (3.34)$$

$$N_j^{(e)}(x, y, z) = m_{12} + m_{22}x + m_{32}y + m_{42}z \quad (3.35)$$

$$N_k^{(e)}(x, y, z) = m_{13} + m_{23}x + m_{33}y + m_{43}z \quad (3.36)$$

$$N_m^{(e)}(x, y, z) = m_{14} + m_{24}x + m_{34}y + m_{44}z \quad (3.37)$$

where

$$\begin{aligned} m_{11} &= \frac{1}{6V} \det \begin{bmatrix} x_j & y_j & z_j \\ x_k & y_k & z_k \\ x_m & y_m & z_m \end{bmatrix} & m_{21} &= -\frac{1}{6V} \det \begin{bmatrix} 1 & y_j & z_j \\ 1 & y_k & z_k \\ 1 & y_m & z_m \end{bmatrix} \\ m_{31} &= \frac{1}{6V} \det \begin{bmatrix} 1 & x_j & z_j \\ 1 & x_k & z_k \\ 1 & x_m & z_m \end{bmatrix} & m_{41} &= -\frac{1}{6V} \det \begin{bmatrix} 1 & x_j & y_j \\ 1 & x_k & y_k \\ 1 & x_m & y_m \end{bmatrix} \end{aligned} \quad (3.38)$$

and so forth. $V^{(e)}$ is the volume of the tetrahedron which is evaluated as

$$V^{(e)} = \frac{1}{6} \begin{vmatrix} 1 & x_i^{(e)} & y_i^{(e)} & z_i^{(e)} \\ 1 & x_j^{(e)} & y_j^{(e)} & z_j^{(e)} \\ 1 & x_k^{(e)} & y_k^{(e)} & z_k^{(e)} \\ 1 & x_m^{(e)} & y_m^{(e)} & z_m^{(e)} \end{vmatrix} \quad (3.39)$$

The unknown variable of the problem, x , at any point within an element can be approximated in terms of their nodal values.

$$\{x\} = [N]\{x\}_{nodal} \quad (3.40)$$

The approximation of the unknown of the problem by Equation (3.40) makes it possible to formulate the equilibrium equation for each element which can then be used to describe the characteristic of the element such as element's hydrological behaviour. The element characteristic matrices extracted by formulation of the equilibrium equation over each linear triangular element can be readily computed using the following integration formula (Stasa, 1984)

$$\int_{A^{(e)}} \left(N_i^{(e)}\right)^a \left(N_j^{(e)}\right)^b \left(N_k^{(e)}\right)^c dA = \frac{a!b!c!}{(a+b+c+2)!} 2A^{(e)} \quad (3.41)$$

and it can be computed over each linear tetrahedral element using the following integration formula (Stasa, 1984)

$$\int_{V^{(e)}} \left(N_i^{(e)}\right)^a \left(N_j^{(e)}\right)^b \left(N_k^{(e)}\right)^c \left(N_m^{(e)}\right)^d dV = \frac{a!b!c!d!}{(a+b+c+d+3)!} 6V^{(e)} \quad (3.42)$$

A single governing equation with only one independent variable can be considered as:

$$f[T(x)] = 0 \quad \text{in} \quad \Omega \quad (3.43)$$

where,

T : the function sought, which is function of only x .

Ω : the domain region governed by Equation (3.43).

In addition, the boundary conditions can be specified in the form:

$$\begin{aligned} g_1[T(x)] &= 0 & \text{in} & \Gamma_1 \\ g_2[T(x)] &= 0 & \text{in} & \Gamma_2 \end{aligned} \quad (3.44)$$

where, Γ_1 , Γ_2 , include only those parts of Ω that are on the boundary. An approximation solution to Equation (3.43) with boundary conditions (3.44) can be presented as an approximate function T' :

$$T' = T'(x; c_1, c_2, \dots, c_n) = \sum_{i=1}^n c_i N_i(x) \quad (3.45)$$

which, has one or more unknown parameters c_1, c_2, \dots, c_n and that satisfies the boundary conditions given by Equation (3.44) exactly. The major requirement placed on the trial functions is that they should be admissible functions: that is, the trial functions are continuous over the domain of interest and satisfy the boundary conditions exactly. In addition, the trial functions should be selected to satisfy the physics of the

problem in general sense (Hutton 2004). If this approximation solution T' is substituted into Equation (3.43) for $T(x)$, it should not be surprising that it will not necessarily satisfy this equation exactly; there may be some residual error $R(x; c_1, c_2, \dots, c_n)$. Therefore it can be written as follows:

$$f[T'(x; c_1, c_2, \dots, c_n)] = R(x; c_1, c_2, \dots, c_n) \quad (3.46)$$

The method of weighted residual requires that the parameters $(x; c_1, c_2, \dots, c_n)$, be determined by satisfying:

$$\int_{\Omega} w_i(x) R(x; c_1, c_2, \dots, c_n) dx = 0 \quad i = 1, 2, \dots, n \quad (3.47)$$

where, the function $w_i(x)$ are the n arbitrary weighting functions. The method of weighted residuals is useful for developing the element equations and allows the finite element method to be applied directly to any differential equation (Daryl 2002). However, there are four particular methods which can be used. These are:

1. Point collocation.
2. Subdomain collocation.
3. Least squares.
4. Galerkin.

Galerkin's method is most widely used in finite element analysis (Stasa 1985). The success of the Galerkin finite element method is largely due to the best approximation result (Brooks and Hughes 1982). In the Galerkin weighted residual method, the trial functions $N_i(x)$ themselves are used as weighting functions or:

$$w_i(x) = N_i(x) \quad (3.48)$$

So that Equation (3.47) then becomes:

$$\int_{\Omega} N_i(x) R(x, c_1, c_2, \dots, c_n) dx = 0 \quad \text{for } i = 1 \text{ to } n \quad (3.49)$$

Because there is one trial function for each unknown parameter, Equation (3.49) generates n such equations that, when solved, yield the values of the unknown parameters, c_1, c_2, \dots, c_n . Obviously, the values obtained for the c_i 's are dependent on the choice of trial functions. In this work, Galerkin method has been used in conjunction with the finite element model

3.4.3 Determination of the local element characteristics

Element characteristics mean the element stiffness matrices and nodal unknown vectors. The word "local" refers to the fact that the element characteristics are derived in a local reference system, which usually change from element to element and are determined numerically for each element. The element characteristics, the local stiffness matrices and nodal unknown vectors may be determined numerically for each element (Stasa 1985).

3.4.4 Transformation of the element characteristics

The element characteristics are transformed from the local coordinate system to the global system. The transformation of the local element characteristics needs to be performed only when the unknown parameter function is a vector such as the (nodal) pore water pressure, and then only when the local coordinate system is used (Stasa 1985).

3.4.5 Assemblage of the global element characteristics

The global element stiffness matrices and global element nodal force vectors must be assembled to form the assemblage element stiffness matrix and nodal unknown vector to find the properties of the overall system modelled by the network of elements. The matrix equations for the system have the same form as the equations for an individual element except that they contain many more terms because they include all nodes. The unknown parameters functions have the same value at any given node regardless of the element containing (Stasa 1985).

3.4.6 Imposition of the boundary conditions

The boundary conditions of the problem must be considered to modify the system of equations and prepare them for the solution phase. At this stage, known nodal values of the dependent variables are imposed (Huebner et al. 2001).

3.4.7 Solution

The assembly process gives a set of simultaneous equations that must be solved to obtain the unknown nodal values of the problem. For engineering applications of the finite element formulation, the material behaviour can be assumed to be linear or nonlinear depending on the material parameters used in the assembly of stiffness matrix. For each case the solution may be obtained by any of the methods suitable to a system of algebraic equations.

In linear finite element analysis, one of the most popular methods to solve the system of algebraic equations is direct Gauss elimination method. However for nonlinear problems a direct solution of the system of equations is generally impossible and an iterative scheme must be adopted (Owen and Hinton 1980).

3.4.7.1 Gaussian elimination and back substitution

Gaussian elimination is the name given to a well known method of solving simultaneous equations by successively eliminating unknowns. In this work, Gaussian elimination and back substitution method of solution has been used to find the final values of unknown nodal vectors for linear problems; it has also been used to solve the system of equations at every iteration, for nonlinear problems. The general concept of Gaussian elimination and back substitution can be found in Chandrupatla and Belegundu (1991) and Klaus (1996).

3.5 Finite difference method

In this work, both the finite element and finite difference methods are used to solve a time dependent contaminant transport problem. The Finite difference method is another numerical technique frequently used to obtain approximate solutions of problems governed by differential equations. The finite difference method is based on the definition of the derivative of a function $f(t)$ that is:

$$\frac{df(t)}{dt} = \lim_{\Delta t \rightarrow 0} \frac{f(t + \Delta t) - f(t)}{\Delta t} \quad (3.50)$$

where, t is the independent variable. In the finite difference method, as implied by its name, derivatives are calculated by an equation like Equation (3.50) using small, but finite values of Δt . So an approximation to the first derivative is obtained by omitting the limiting process (Neylon 1994).

$$\frac{df(t)}{dt} \approx \frac{f(t + \Delta t) - f(t)}{\Delta t} \quad (3.51)$$

A differential equation such as:

$$\frac{df(t)}{dt} + x = 0 \quad 0 \leq t \leq 1 \quad (3.52)$$

is expressed as:

$$\frac{f(t + \Delta t) - f(t)}{\Delta t} + x = 0 \quad (3.53)$$

In the finite difference method, Equation (3.53) can be written as:

$$f(t + \Delta t) = f(t) - x(\Delta t) \quad (3.54)$$

The solution of a first order differential equation contains one constant of integration. The constant of integration must be determined such that one condition (a boundary condition or an initial condition) is satisfied. If it is assumed that the specified condition is $t_0 = A = \text{constant}$ and an integration step Δt is chosen to be a small constant value (the integration step is not required to be constant) therefore it can be written as:

$$t_{i+1} = t_i + \Delta t \quad i = 0, n \quad (3.55)$$

where, n is the total number of steps required to cover the domain. Equation (3.54) is then:

$$f_{i+1} = f_i + x_i(\Delta t) \quad f_o = A \quad i = 0, n \quad (3.56)$$

The above equation is known as a recurrence relation and provides an approximation to the values of unknown function $f(t)$ at a number of discrete points in the domain of the problem (Hutton 2004). In the finite difference method, approximations such as that presented by Equation (3.56) are applied to differential equation at each grid point, with Δt being the time increment (in this study). This results in an equation for each node, involving the approximation to the solution variables at all nodes. Approximation presented by Equation (3.51) is known as a forward difference. Other finite difference approximations are the backward difference

$$\frac{df(t)}{dt} \approx \frac{f(t) - f(t - \Delta t)}{\Delta t} \quad (3.57)$$

and the central difference

$$\frac{df(t)}{dt} \approx \frac{f(t + \Delta t) - f(t - \Delta t)}{2\Delta t} \quad (3.58)$$

In fact, one somewhat practical way to assess the accuracy of the solution is to compare the results for two different steps and if the results for the two different steps are within some acceptable tolerance, a good approximation to the true solution has been obtained. The error in the approximation (i.e., Equations 3.53, 3.54, 3.55) is termed the truncation error. An expression for this is calculated by performing a Taylor series expansion on the $f(t + \Delta t)$ term about t (Neylon 1994).

CHAPTER 4

STOCHASTIC METHODOLOGY

4.1 Introduction

Choosing an appropriate model is essential in simulation of water flow and solute transport in soils. The model must comprehensively describe physical and chemical behaviours of the system. Also, it must represent all different characteristics of the system. Hence, water flow and solute transport models in the soil must include all mechanisms of flow, and consider heterogeneity of the structure and formation of soils.

In this chapter, the classical mathematical models for water flow and solute transport in unsaturated soils are presented. These classical equations include the mechanisms of flow and solute transport, and they are applicable to local scale processes in which variations of hydraulic parameters are negligible. Variations of hydraulic parameters due to heterogeneous nature of soil are incorporated in these models using analytical

stochastic methodology, and then related large-scale mathematical models are developed. Hydraulic conductivity, moisture retention parameters and macrodispersion coefficient are defined as effective coefficients in the large-scale models. Finally, spectral method used to evaluate these effective coefficients and the variance of water pressure head and solute concentration is explained.

4.2 Classical governing equation for water flow

The driving potential for flow of water is related to three primary components of energy, namely gravitational, pressure, and velocity. Total energy of an arbitrary point A, in the water phase, for flow of water is written as (Fredlund and Rahardjo, 1993)

$$E = M_w g z + \frac{M_w u_w}{\rho_w} + \frac{M_w v_w^2}{2} \quad (4.1)$$

where E is total energy at point A [M] [L]²[T]⁻², M_w is mass of water at point A [M], g is gravitational acceleration [L][T]⁻², z is elevation of point A above an arbitrary datum [L], u_w is pore water pressure at point A [M][L]⁻¹[T]⁻², ρ_w is density of water [M][L]⁻³, and v_w is the velocity of water at point A [L][T]⁻¹.

In Equation (4.1), the term $M_w g z$ is the gravitational energy, $\frac{M_w u_w}{\rho_w}$ is the component of energy due to the water pressure at point A and $\frac{M_w v_w^2}{2}$ is the part of energy due to the velocity of water at the point A.

Total hydraulic head at a certain point is defined as the total driving energy per unit weight of water at that point. Therefore, total head can be obtained through dividing Equation (4.1) by the weight of water ($M_w g$) at the point under consideration as

$$h_w = z + \frac{u_w}{\rho_w g} + \frac{v_w^2}{2g} \quad (4.2)$$

where h_w is the hydraulic head or total head [L].

Since the velocity head in the soil is negligible in comparison with the gravitational and pressure heads, the expression for the hydraulic head at any point in the soil mass can be presented as

$$h_w = z + \frac{u_w}{\rho_w g} \quad (4.3)$$

It is the gradient of hydraulic head that causes flow in soil. Darcy (1856) postulated the following equation to express the rate of water flow through a mass of soil

$$q_i = K(\psi) \frac{\partial(\psi + z)}{\partial x_i} \quad (4.4)$$

where q_i is the specific discharge in direction i [L][T]⁻¹, ψ is the capillary tension head [L], K is the unsaturated hydraulic conductivity [L][T]⁻¹.

Darcy's equation is mainly applicable for saturated soils. However Equation (4.4) is used for soils in unsaturated condition as well. Fredlund and Rahardjo (1993) investigated the validity and applicability of Darcy's equation in unsaturated soils, based on the findings of Childs (1969) and experimental results presented by Childs and Collis-George, (1950).

The conservation of mass law for the soil moisture leads to the governing partial differential equation for water movement in unsaturated medium presented as Equation (4.5). In derivation of Equation (4.5), it has been assumed that the soil matrix is rigid (i.e., incompressible) and sink-source terms have been ignored.

$$-\frac{\partial \theta}{\partial t} = \frac{\partial q_i}{\partial x_i} \quad i = 1, 2, 3 \quad (4.5)$$

where θ is the soil volumetric moisture content and x_1, x_2, x_3 are coordinates in a Cartesian system.

Substituting Equation (4.4) into Equation (4.5) yields the unsaturated flow equation as

$$-\frac{\partial \theta}{\partial t} = \frac{\partial}{\partial x_i} \left[K(\psi) \frac{\partial (\psi + z)}{\partial x_i} \right] \quad (4.6)$$

Equation (4.6) is applicable to small-scale problems in which the spatial variability is negligible.

The coefficient of permeability which is a function of volume-mass properties of the soil is obtained at each point of the domain under consideration based on parameters such as degree of saturation or matric suction. Different functional forms have been proposed for coefficient of permeability relationships in unsaturated soils. Gardner (1958) has proposed the following simple parameterization for the coefficient of permeability

$$\ln K(\psi) = \ln K_s - \alpha \psi \quad (4.7)$$

where K_s is saturated hydraulic conductivity $[L][T]^{-1}$, and α is a scaling parameter $[L]^{-1}$, equals to the slope of curve of $\ln K(\psi)$ versus ψ .

The coefficient of permeability with respect to water phase is a measure of the space available for water to flow through the soil. The coefficient of permeability depends on the properties of the fluid and the properties of the porous medium. Different types of fluid (e.g., water and oil) or different types of soil (e.g., sand and clay) produce different values for the coefficient of permeability. Also, water flow is controlled by soil moisture capacity coefficient. This coefficient is the slope of retention curve of the soil.

The soil moisture retention curve presents relationship between soil moisture content and the capillary tension head. This curve is a characteristic for different types of soil. This can be used to predict soil water storage capability. The water holding capacity of any soil is due to the porosity and the nature of the bonding in the soil. Then spatial variability of soil type and consequently spatial variability of soil characteristic in natural soil cause significant variation in the coefficients of permeability and moisture capacity. These result in non-applicability of Equation (4.6) for large-scale problems and consequently show essential need to incorporate the effects of these variations in the related governing equation. In the following section, the method which has been proposed by Mantoglou and Gelhar (1987a), for incorporating variability in hydraulic properties of soil into governing equation of water flow in a stochastic framework, will be explained.

4.3 Large-scale governing equation for water flow

Basic hydraulic parameters of soil (i.e., K_s , α and soil specific moisture capacity C) vary randomly in space domain. These parameters can be defined by stochastic representations. They are considered as realizations of random fields. Realization is the profile of random variable through dimension where it varies. This dimension could be time or space. It is assumed that these random fields are three-dimensional, spatially cross-correlated, and are composed of two components, mean and fluctuations

$$\ln K_s = F + f \quad (4.8)$$

$$\alpha = A + a \quad (4.9)$$

$$C = \Gamma + \gamma \quad (4.10)$$

The first terms on right hand-side of Equations (4.8), (4.9) and (4.10) are assumed to be deterministic, while the second terms are three-dimensional zero mean second-order stationary random fields. A stationary random field is one in which the probabilistic

descriptions become independent of time origin and they are invariant under shifts of the time origin. These random variables are inputs of governing partial differential equation of flow. Classical differential equation with random parameters, coefficients, boundaries and initial values is called stochastic differential equation (SDE). The output of a SDE (here, ψ), is random. Therefore it is possible to express ψ as

$$\psi = H + h \quad (4.11)$$

where, H is the mean of ψ and h is fluctuations around the mean. The basic assumptions are: (i) the fluctuations f, a, γ and h are relatively small, and (ii) the scale of variations of the mean values F, A, Γ and H is much larger than the scale of variations of the fluctuations f, a, γ and h .

The large-scale model of transient unsaturated flow is obtained by averaging the small-scale governing equation over the ensemble of possible realizations of the stochastic processes f, a and γ . Therefore, expected value of small-scale equation with respect to fluctuations is calculated. Taking the expected value of Equation (4.6) with respect to f, a , and γ , yields

$$-\frac{\partial\{E[\theta]\}}{\partial t} = \frac{\partial}{\partial x_i} \left\{ E \left[K \frac{\partial(\psi + z)}{\partial x_i} \right] \right\} \quad (4.12)$$

Substituting Equations (4.8), (4.9) and (4.11) into Equation (4.7) yields,

$$K = K_m \exp(f - Ah - Ha - ah) \quad (4.13)$$

where

$$K_m = e^F e^{-AH} = K_G e^{-AH} \quad (4.14)$$

and substituting Equation (4.11) into the term related to spatial rate of head pressure yields

$$\frac{\partial(\psi + z)}{\partial x_i} = \frac{\partial(H + h + z)}{\partial x_i} = J_i + \frac{\partial h}{\partial x_i} \quad (4.15)$$

where $J_i = \partial(H + z)/\partial x_i$ is the mean hydraulic gradient in the direction x_i . Using Equations (4.4), (4.13) and (4.15), the expected value in the right-hand side of Equation (4.12) can be written as follows

$$E[q_i] = K_m E \left[\exp(f - Ah - Ha - ah) \left(J_i + \frac{\partial h}{\partial x_i} \right) \right] \quad (4.16)$$

In order to expand the exponential terms, Taylor series can be used as

$$\exp(f - Ah - Ha - ah) = 1 + (f - Ah - Ha - ah) + \frac{1}{2}(f - Ah - Ha - ah)^2 + \dots \quad (4.17)$$

As it is assumed that fluctuations are small, the third- and higher-order terms can be neglected. Substituting Equation (4.17) into Equation (4.16) yields

$$E[q_i] = K_m \left\{ J_i \left[1 - E(ah) + \frac{1}{2} E[(f - Ah - Ha)^2] \right] + E \left[(f - Ah - Ha) \frac{\partial h}{\partial x_i} \right] \right\} \quad (4.18)$$

where expected values due to fluctuations of third- or higher-order terms have been neglected. Effective hydraulic conductivity is defined as having the following property Mantoglou and Gelhar (1987a)

$$E[q_i] = \hat{K}_{ij} J_i \quad i=1,2,3 \quad \text{no sum on } i \quad (4.19)$$

This definition of effective hydraulic conductivity helps to express the mean flow Equation (4.12) in a form similar to the small-scale governing Equation (4.6). Incorporating Equation (4.18) into Equation (4.19) gives

$$\hat{K}_{ij} = K_m \left[1 - E(ah) + \frac{\sigma_\varepsilon^2}{2} + \frac{\tau_i}{J_i} \right] \quad i=1, 2, 3 \quad (4.20)$$

where

$$\begin{aligned} \sigma_\varepsilon^2 &= E \left[(f - Ah - Ha)^2 \right] \\ &= \sigma_f^2 + A^2 E[h^2] + H^2 \sigma_a^2 - 2A E[fh] - 2H E[fa] + 2AH E[ah] \end{aligned} \quad (4.21)$$

$$\tau_i = E \left[(f - Ah - Ha) \frac{\partial h}{\partial x_i} \right] = E \left[f \frac{\partial h}{\partial x_i} \right] - H E \left[a \frac{\partial h}{\partial x_i} \right] \quad (4.22)$$

where, σ_f^2 is the variance of $\ln K_s$ and σ_a^2 is variance of α .

It is assumed that terms inside the parenthesis in Equation (4.20) are essentially the first two terms of a Taylor series expansion of an exponential term. By converting these terms to the exponential term, Equation (4.20) gives

$$\hat{K}_{ij} = K_M \exp \left(\frac{\sigma_\varepsilon^2}{2} + \frac{\tau_i}{J_i} \right) \quad \text{no sum on } i \quad (4.23)$$

where $K_M = K_m \exp\{-E[ah]\}$.

Equation (4.23) calculates the effective hydraulic conductivity for large scale flow governing equation.

Now left-hand side of Equation (4.12) is examined. The expected value $E[\theta]$ represents the mean soil moisture content $\Theta = E[\theta]$. For small fluctuations, h , it holds Mantoglou and Gelhar (1987b)

$$\theta = \theta(\psi) \approx \theta(H) - Ch \quad (4.24)$$

where

$$C = -\left. \frac{\partial \theta}{\partial \psi} \right|_{\psi=H} \quad (4.25)$$

Substituting Equations (4.10) and (4.11) into Equation (4.24) and taking the expected value yields

$$\Theta = E[\theta(H)] - E[\gamma h] \quad (4.26)$$

The effective specific moisture capacity is defined by Mantoglou and Gelhar (1987b)

$$\hat{C} = -\partial \Theta / \partial H = -\frac{\partial [E[\theta(H)] - E[\gamma h]]}{\partial H} \quad (4.27)$$

where $E[\theta(H)]$ is assumed to be a known characteristic of spatial variability of $\theta(H)$. Substituting Equations (4.19) into Equation (4.12) and using Equations (4.26) and (4.27) yield large-scale governing equation for flow in unsaturated soils as

$$\frac{\partial \Theta}{\partial t} = -\hat{C} \frac{\partial H}{\partial t} = \frac{\partial}{\partial x_i} \left(\hat{K}_{ij} \frac{\partial (H + z)}{\partial x_i} \right) \quad (4.28)$$

4.4 Calculation of expected values

Equation (4.28) presents large-scale governing equation of water flow in soil. This equation is in the similar form of the related small-scale governing equation. The effective moisture capacity and effective hydraulic conductivity coefficients (i.e, \hat{C} and \hat{K}) are calculated by Equations (4.27) and (4.23), respectively. Then according to Equations (4.21), (4.22), (4.23) and (4.27), evaluation of the effective hydraulic conductivity, mean soil moisture content Θ and the effective specific moisture capacity \hat{C} has now been reduced to the evaluation of the expected values $E[\gamma h]$, $E[h^2]$, $E[fh]$, $E[ah]$, $E[f \partial h / \partial x_i]$ and $E[a \partial h / \partial x_i]$.

4.4.1 Calculation of expected values by spectral method

The foregoing expected values are evaluated using spectral analysis. The following spectral representation properties are used in this analysis. Two cross-correlated stationary random fields $u(\vec{x})$ and $v(\vec{x})$ can be expressed in the spectral domain as (Gelhar 1993)

$$\begin{aligned} u(\vec{x}) &= \iiint_{-\infty}^{\infty} \exp(i\vec{k} \cdot \vec{x}) dZ_u(\vec{k}) \\ v(\vec{x}) &= \iiint_{-\infty}^{\infty} \exp(i\vec{k} \cdot \vec{x}) dZ_v(\vec{k}) \end{aligned} \quad (4.29)$$

where, $\vec{k} = (k_1, k_2, k_3)$ is the wave number vector, $\vec{x} = (x_1, x_2, x_3)$ is the position vector.

The cross-spectral density function of u and v , called $S_{uv}(\vec{k})$ is given by (Lumley and Panofsky, 1964)

$$\begin{aligned} E \left[dZ_u(\vec{k}_1) dZ_v^*(\vec{k}_2) \right] &= S_{uv}(\vec{k}) d\vec{k}; \quad \text{if } \vec{k}_1 = \vec{k}_2 = \vec{k} \\ &0 \quad ; \quad \text{otherwise} \end{aligned} \quad (4.30)$$

where $dZ_u(\vec{k})$ and $dZ_v(\vec{k})$ are random Fourier-Stieltjes amplitudes of $u(\vec{x})$ and $v(\vec{x})$ respectively. Z is a complex-value and asterisk (*) denotes complex conjugate of complex number. The expected value of $u(\vec{x})$ and $v(\vec{x})$ can be represented as function of the cross-spectral density function $S_{uv}(\vec{k})$

$$E[uv] = E \left[\int \int \int_{-\infty}^{\infty} \exp(i\vec{k}\vec{x}) dZ_u(\vec{k}) \int \int \int_{-\infty}^{\infty} \exp(-i\vec{k}\vec{x}) dZ_v^*(\vec{k}) \right] = \int \int \int_{-\infty}^{\infty} S_{uv}(\vec{k}) d\vec{k} \quad (4.31)$$

In this way, the following expected values are evaluated as (Mantoglou and Gelhar 1987a)

$$E[h^2] = \sigma_h^2 = \int \int \int_{-\infty}^{\infty} S_{hh}(\vec{k}) d\vec{k} \quad (4.32)$$

$$E[fh] = E[hf] = \int \int \int_{-\infty}^{\infty} S_{hf}(\vec{k}) d\vec{k} \quad (4.33)$$

$$E[ah] = E[ha] = \int \int \int_{-\infty}^{\infty} S_{ha}(\vec{k}) d\vec{k} \quad (4.34)$$

$$E[\gamma h] = \int \int \int_{-\infty}^{\infty} S_{h\gamma}(\vec{k}) d\vec{k} \quad (4.35)$$

$$E \left[f \frac{\partial h}{\partial x_i} \right] = E \left[\frac{\partial h}{\partial x_i} f \right] = \int \int \int_{-\infty}^{\infty} (ik_i) S_{hf}(\vec{k}) d\vec{k} \quad (4.36)$$

$$E \left[a \frac{\partial h}{\partial x_i} \right] = \int \int \int_{-\infty}^{\infty} (ik_i) S_{ha}(\vec{k}) d(\vec{k}) \quad (4.37)$$

Then evaluation of these expected values has been reduced to the evaluation of cross spectral density functions emerged in Equations (4.32) to (4.37). In Section (4.4.2), a

linearized perturbation partial differential equation is extracted. This equation presents a relation between capillary tension head fluctuations and soil properties fluctuations. This equation is used to evaluate the cross spectral density function relationships of fluctuations of soil properties.

4.4.2 Linearized fluctuation equation

A linearized perturbation equation relating the capillary tension head fluctuations h to the soil property fluctuations f , a , and γ is derived using the local flow equation. Substituting Equation (4.7) and (4.25) into the Equation (4.6) and expanding derivatives yield

$$\frac{C}{K_s} \exp(\alpha\psi) \frac{\partial \psi}{\partial t} = \frac{\partial(\ln K_s - \alpha\psi)}{\partial x_i} \frac{\partial(\psi + z)}{\partial x_i} + \nabla^2 \psi \quad (4.38)$$

Substituting Equations (4.9) and (4.11) into the left-hand side of Equation (4.38) yields

$$\begin{aligned} L &= \frac{C}{K_s} \exp(\alpha\psi) \frac{\partial \psi}{\partial t} \\ &= (\Gamma + \gamma) \exp(AH - F) \exp(Ah + Ha - f - ah) \frac{\partial(H + h)}{\partial t} \end{aligned} \quad (4.39)$$

where, L represents the left-hand side of equation (4.38).

The second exponential term in Equation (4.39) is expanded using a Taylor series representation

$$\begin{aligned} \exp(Ah + Ha - f + ah) &= 1 + (Ah + Ha - f + ah) + \\ &\quad \frac{1}{2} (Ah + Ha - f + ah)^2 + \dots \end{aligned} \quad (4.40)$$

Rewriting gives

$$\exp(Ah + Ha - f + ah) = 1 + Ah + Ha - f + ah + T_H \quad (4.41)$$

where, T_H contains second- and higher-order terms. Substituting Equation (4.41) into Equation (4.39) yields

$$\begin{aligned} L = & \exp(AH - F) \left(\Gamma \frac{\partial H}{\partial t} + A\Gamma + H\Gamma a - \Gamma f + \gamma \right) \frac{\partial H}{\partial t} + \\ & \Gamma \frac{\partial h}{\partial t} + (\Gamma ah + A\gamma h + H\gamma a - \gamma f + \gamma ah) \frac{\partial H}{\partial t} + \\ & (A\Gamma h + H\Gamma a - \Gamma f + \Gamma ah + \gamma + A\gamma h + H\gamma a - \gamma f + \gamma ah) \frac{\partial h}{\partial t} + \\ & T_H (\Gamma + \gamma) \frac{\partial (H + h)}{\partial t} \end{aligned} \quad (4.42)$$

Rewriting Equation (4.42) gives

$$L = L_0 + L_1 + L_H \quad (4.43)$$

where L_0 is independent of the fluctuations (zero-order term)

$$L_0 = \exp(AH - F) \left(\Gamma \frac{\partial H}{\partial t} \right) \quad (4.44)$$

L_1 is linear in the fluctuations (first-order terms)

$$L_1 = (A\Gamma h + H\Gamma a - \Gamma f + \gamma) \frac{\partial H}{\partial t} + \Gamma \frac{\partial h}{\partial t} \quad (4.45)$$

and L_H contains the remaining second and higher-order terms.

Substituting Equations (4.8), (4.9), (4.10) and (4.11) in the first component of the first term in right-hand side of Equation (4.38) yields

$$\begin{aligned}
\frac{\partial(\ln K_s - \alpha\psi)}{\partial x_i} &= \frac{\partial(\ln K_s - AH - Ah - Ha - ah)}{\partial x_i} \\
&= \frac{\partial f}{\partial x_i} - A \frac{\partial H}{\partial x_i} - A \frac{\partial h}{\partial x_i} - a \frac{\partial h}{\partial x_i} - H \frac{\partial a}{\partial x_i} - \frac{\partial(ah)}{\partial x_i}
\end{aligned} \tag{4.46}$$

The terms $\partial F/\partial x_i$ and $\partial A/\partial x_i$ are negligible because the spatial variation of F and A is assumed to be very slow. Substituting Equations (4.8), (4.9), (4.10), and (4.11) in the right-hand side of Equation (4.38) yields

$$\begin{aligned}
R &= \frac{\partial(\ln K_s - \alpha\psi)}{\partial x_i} \frac{\partial(\psi + z)}{\partial x_i} + \nabla^2 \psi = \left(-J_i A \frac{\partial H}{\partial x_i} + \nabla^2 H \right) + \\
&\quad \left(J_i \frac{\partial f}{\partial x_i} - J_i A \frac{\partial h}{\partial x_i} - J_i \frac{\partial H}{\partial x_i} a - J_i H \frac{\partial a}{\partial x_i} - A \frac{\partial H}{\partial x_i} \frac{\partial h}{\partial x_i} + \nabla^2 h \right) + \\
&\quad \left(-J_i \frac{\partial(ah)}{\partial x_i} + \frac{\partial f}{\partial x_i} \frac{\partial h}{\partial x_i} - A \left(\frac{\partial h}{\partial x_i} \right)^2 - \frac{\partial H}{\partial x_i} a \frac{\partial h}{\partial x_i} - H \frac{\partial a}{\partial x_i} \frac{\partial h}{\partial x_i} - \frac{\partial(ah)}{\partial x_i} \frac{\partial h}{\partial x_i} \right)
\end{aligned} \tag{4.47}$$

Rewriting equation (4.47) gives

$$R = R_0 + R_1 + R_H \tag{4.48}$$

where R_0 is independent of the fluctuations (zero-order terms)

$$R_0 = -J_i A \frac{\partial H}{\partial x_i} + \nabla^2 H \tag{4.49}$$

R_1 is linear in the fluctuations (first-order terms)

$$R_1 = J_i \frac{\partial f}{\partial x_i} - J_i A \frac{\partial h}{\partial x_i} - J_i \frac{\partial H}{\partial x_i} a - J_i H \frac{\partial a}{\partial x_i} - A \frac{\partial H}{\partial x_i} \frac{\partial h}{\partial x_i} + \nabla^2 h \tag{4.50}$$

R_H contains the remaining second and higher-order terms.

Rewriting Equation (4.38) using Equations (4.43) and (4.48) gives

$$L_0 + L_1 + L_H = R_0 + R_1 + R_H \quad (4.51)$$

Taking the expected value of Equation (4.51) with respect to f , a , γ and remembering that the expected value of the linear term is zero, yields

$$L_0 + E[L_H] = R_0 + E[R_H] \quad (4.52)$$

Subtracting (4.52) from (4.51) produces

$$L_1 + L_H - E[L_H] = R_1 + R_H - E[R_H] \quad (4.53)$$

Assuming that fluctuations f , α , γ and h are small, the higher order terms can be approximated by their expected values; $L_H \approx E[L_H]$ and $R_H \approx E[R_H]$ (Mantoglou and Gelhar 1987a). Substituting these in Equation (4.53) and rewriting it yields

$$L_1 = R_1 \quad (4.54)$$

Then, according to the Equations (4.45) and (4.50), Equation (4.54) is rewritten as

$$\begin{aligned} \exp(AH - F) \left((A\Gamma h + H\Gamma a - \Gamma f + \gamma) \frac{\partial H}{\partial t} + \Gamma \frac{\partial h}{\partial t} \right) = \\ J_i \frac{\partial f}{\partial x_i} - J_i A \frac{\partial h}{\partial x_i} - J_i \frac{\partial H}{\partial x_i} a - J_i H \frac{\partial a}{\partial x_i} - A \frac{\partial H}{\partial x_i} \frac{\partial h}{\partial x_i} + \nabla^2 h \end{aligned} \quad (4.55)$$

Defining two new terms

$$G = \frac{1}{K_m} \frac{\partial H}{\partial t} \quad (4.56)$$

and

$$L_i = J_i + \frac{\partial H}{\partial x_i}, \quad (4.57)$$

substituting Equations (4.56) and (4.57) into Equation (4.55) and rearranging yields

$$\begin{aligned} \frac{\partial h}{\partial t} + \frac{K_m}{\Gamma} \left(-\nabla^2 h + A\Gamma G h + AL_i \frac{\partial h}{\partial x_i} \right) = \\ \frac{K_m}{\Gamma} \left[\left(J_i \frac{\partial f}{\partial x_i} + \Gamma G f \right) - \left(J_i H \frac{\partial a}{\partial x_i} + ba \right) - G\gamma \right] \end{aligned} \quad (4.58)$$

where

$$b = J_i \frac{\partial H}{\partial x_i} + H\Gamma G \quad (4.59)$$

4.4.3 Spectral density functions relationships

Spectral method is used to solve the fluctuation equation (i.e., Equation 4.58). This equation is written in the spectral domain and general solution of the resulted equation is obtained in the spectral domain as (Mantoglou and Gelhar, 1987a)

$$y(k, t) = dZ_h(k, t) = W_f(k, t) dZ_f(k) + W_a(k, t) dZ_a(k) + W_\gamma(k, t) dZ_\gamma(k) \quad (4.60)$$

where

$$W_\beta(k, t) = \left[\int_0^t g_\beta(\tau) \exp\left(\int_0^\tau g_1(s) ds\right) \right] \exp\left(-\int_0^t g_1(s) ds\right) \quad (4.61)$$

$$g_1(t) = \frac{K_m}{\Gamma} (k_1^2 + k_2^2 + k_3^2 + A\Gamma G + iAL_i k_i) \quad (4.62)$$

$$g(t) = \frac{K_m}{\Gamma} \left[(iJ_i k_i + \Gamma G) dZ_f - \left(iHJ_i k_i + J_i \frac{\partial H}{\partial x_i} + H\Gamma G \right) dZ_a - G dZ_\gamma \right] \quad (4.63)$$

where, $\beta = f, \alpha$, or γ , In transient case functions g_l and g depend on t since the mean flow properties H , etc., depend on t .

The solution is a linear function relating spectral amplitudes of capillary tension head to spectral amplitudes of soil properties fluctuations. Using Equations (4.60) and (4.30)

$S_{hh}(k)$ is evaluated as (Mantoglou and Gelhar, 1987a)

$$\begin{aligned} S_{hh}(k)dk &= E \left[\left(W_f dZ_f + W_a dZ_a + W_\gamma dZ_\gamma \right) \left(W_f dZ_f + W_a dZ_a + W_\gamma dZ_\gamma \right)^* \right] \\ &= \left(|W_f|^2 S_{ff} + |W_a|^2 S_{aa} + |W_\gamma|^2 S_{\gamma\gamma} + W_f W_a^* S_{fa} + W_f W_\gamma^* S_{f\gamma} + \right. \\ &\quad \left. W_a W_f^* S_{af} + W_a W_\gamma^* S_{a\gamma} + W_\gamma W_f^* S_{\gamma f} + W_\gamma W_a^* S_{\gamma a} \right) dk \end{aligned} \quad (4.64)$$

Equation (4.64) determines cross-spectral density function S_{hh} as function of those of soil properties f, γ and a , which are known in the problems. Also, by defining

$$\varepsilon^2 = \frac{\sigma_a^2}{\sigma_f^2} \quad (4.65)$$

and

$$\eta^2 = \frac{\sigma_\gamma^2}{\sigma_f^2} \quad (4.66)$$

the relationships between the spectral density functions of f, a and γ are written as (Mantoglou 1984)

if f, a and γ are uncorrelated

$$S_{aa} = \varepsilon^2 S_{ff} \quad (4.67)$$

$$S_{\gamma\gamma} = \eta^2 S_{ff} \quad (4.68)$$

$$S_{fa} = 0 \quad (4.69)$$

$$S_{a\gamma} = 0 \quad (4.70)$$

$$S_{\gamma f} = 0 \quad (4.71)$$

if f, a and γ are correlated

$$S_{aa} = \varepsilon^2 S_{ff} \quad (4.72)$$

$$S_{\gamma\gamma} = \eta^2 S_{ff} \quad (4.73)$$

$$S_{fa} = \xi S_{ff} \quad (4.74)$$

$$S_{a\gamma} = \xi \eta S_{ff} \quad (4.75)$$

$$S_{\gamma f} = \eta S_{ff} \quad (4.76)$$

From Equations (4.67) to (4.76), the following relationship can be derived

$$S_{uv}(\vec{k}) = \mu S_{ff}(\vec{k}) \quad \mu = \xi^2, \eta^2, 0, 0, 0, \xi^2, \eta^2, \xi, \xi\eta, \eta \quad (4.77)$$

Cross spectral density functions in Equations (4.32) to (4.37) are substituted by their related equivalence as function of S_{ff} through Equations (4.67) to (4.76). After these substitutions, evaluation of integrals in Equations (4.32) to (4.37) is still very complicated. But, they can be evaluated in some certain cases. Mantoglou and Gelhar

(1987b, 1987c), evaluated them for stratified soil. They assumed soils are stratified which is an acceptable assumption for soil structure in real condition. Their resulted equations have been employed in this work. A summary of the results in the case of a stratified soil is presented here.

4.4.4 Evaluation of $E[h^2]$

$$E[h^2] = \sigma_h^2 = 2 \frac{\sigma_f^2 \lambda_1}{\pi} I_1 \quad (4.78)$$

where, λ is correlation scale of random parameters [L].

and

$$I_1 = \int_0^\infty \frac{a_1 k_1^2 + a_2}{k_1^4 + a_3 k_1^2 + a_4} \frac{1}{1 + a_5 k_1^2} dk_1 \quad (4.79)$$

where

$$a_3 = 2A\Gamma G + A^2 L_1^2 \quad (4.80)$$

$$a_4 = A^2 \Gamma^2 G^2 \quad (4.81)$$

$$a_5 = \lambda_1^2 \quad (4.82)$$

and if f, a and γ are uncorrelated

$$a_1 = (1 + \xi^2 H^2) + J_1^2 \quad (4.83)$$

$$a_2 = (\Gamma^2 + \eta^2) G^2 + \xi^2 b \quad (4.84)$$

if f, a and γ are fully correlated

$$a_1 = (1 - \xi^2 H^2) J_1^2 \quad (4.85)$$

$$a_2 = (\Gamma G - \xi b - \eta G) \quad (4.86)$$

where

$$b = J_i \frac{\partial H}{\partial x_i} + H \Gamma G \quad (4.87)$$

Defining $\Delta = a_3^2 - 4a_4 = A^2 L_1^2 + 4A \Gamma G$.

If $\Delta > 0$, evaluating the integral in Equation (4.79) and substituting in Equation (4.78) gives (Mantoglou and Gelhar, 1985)

$$\sigma_h^2 = \sigma_f^2 \lambda_1 \left[\frac{a_1 \sqrt{a_4} + a_1 a_4 a_5 - \sqrt{a_4} a_2 a_5 + a_2 - a_2 a_3 a_5}{A \Gamma G (1 + a_4 a_5^2 - a_3 a_5) \sqrt{4(A \Gamma G) + A^2 L_1^2}} - a_5 \frac{a_1 - a_2 a_5}{(1 + a_4 a_5^2 - a_3 a_5) \lambda_1} \right] \quad (4.88)$$

and if $\Delta < 0$

$$\sigma_h^2 = \sigma_f^2 \lambda_1 \left[\frac{-a_1 \sqrt{a_4} - a_1 a_4 a_5 + \sqrt{a_4} a_2 a_5 - a_2 + a_2 a_3 a_5}{A \Gamma G (1 + a_4 a_5^2 - a_3 a_5) (A L_1)} - a_5 \frac{a_1 - a_2 a_5}{(1 + a_4 a_5^2 - a_3 a_5) \lambda_1} \right] \quad (4.89)$$

4.4.5 Evaluation of $E[fh]$

$$E[fh] = 2 \frac{\sigma_f^2 \lambda_1}{\pi} I_1 \quad (4.90)$$

The integral is given by Equation (4.79). The terms a_3, a_4, a_5 are given by Equations (4.80), (4.81) and (4.82) and a_1, a_2 are different for each case, as follows

if f, a and γ are uncorrelated

$$a_1 = \Gamma G + AL_1 J_1 \quad (4.91)$$

$$a_2 = A\Gamma^2 G^2 \quad (4.92)$$

if f, a and γ are fully correlated

$$a_1 = \Gamma G - \xi \left(J_i \frac{\partial H}{\partial x_i} + H\Gamma G \right) - \eta G + AL_1 J_1 (1 - \xi H) \quad (4.93)$$

$$a_2 = \left(\Gamma G - \xi \left(J_i \frac{\partial H}{\partial x_i} + H\Gamma G \right) - \eta G \right) A\Gamma G \quad (4.94)$$

The result for the integral I_1 depends if $\Delta = a_3^2 - 4a_4 = A^2 L_1^2 + 4A\Gamma G$ is a negative or a positive value.

Evaluating the integral in Equation (4.79) and substituting in Equation (4.90) gives (Mantoglou and Gelhar, 1985)

For $\Delta > 0$,

$$E[fh] = \sigma_f^2 \lambda_1 \left[\frac{a_1 \sqrt{a_4} + a_1 a_4 a_5 - \sqrt{a_4} a_2 a_5 + a_2 - a_2 a_3 a_5}{A\Gamma G (1 + a_4 a_5^2 - a_3 a_5) \sqrt{4(A\Gamma G) + A^2 L_1^2}} - a_5 \frac{a_1 - a_2 a_5}{(1 + a_4 a_5^2 - a_3 a_5) \lambda_1} \right] \quad (4.95)$$

and if $\Delta < 0$

$$E[fh] = \sigma_f^2 \lambda_1 \left[\frac{-a_1 \sqrt{a_4} - a_1 a_4 a_5 + \sqrt{a_4} a_2 a_5 - a_2 + a_2 a_3 a_5}{A\Gamma G (1 + a_4 a_5^2 - a_3 a_5) (AL_1)} - a_5 \frac{a_1 - a_2 a_5}{(1 + a_4 a_5^2 - a_3 a_5) \lambda_1} \right] \quad (4.96)$$

4.4.6 Evaluation of $E[ah]$

$$E[ah] = 2 \frac{\sigma_f^2 \lambda_1}{\pi} I_1 \quad (4.97)$$

The integral I_1 is given by Equation (4.79). Substituting Equation (4.79) in Equation (4.97) gives (Mantoglou and Gelhar, 1985)

For $\Delta > 0$

$$E[ah] = \sigma_f^2 \lambda_1 \left[\frac{a_1 \sqrt{a_4} + a_1 a_4 a_5 - \sqrt{a_4} a_2 a_5 + a_2 - a_2 a_3 a_5}{A\Gamma G (1 + a_4 a_5^2 - a_3 a_5) \sqrt{4(A\Gamma G) + A^2 L_1^2}} - a_5 \frac{a_1 - a_2 a_5}{(1 + a_4 a_5^2 - a_3 a_5) \lambda_1} \right] \quad (4.98)$$

and if $\Delta < 0$

$$E[ah] = \sigma_f^2 \lambda_1 \left[\frac{-a_1 \sqrt{a_4} - a_1 a_4 a_5 + \sqrt{a_4} a_2 a_5 - a_2 + a_2 a_3 a_5}{A\Gamma G (1 + a_4 a_5^2 - a_3 a_5) (AL_1)} - a_5 \frac{a_1 - a_2 a_5}{(1 + a_4 a_5^2 - a_3 a_5) \lambda_1} \right] \quad (4.99)$$

The terms a_3, a_4, a_5 are given by Equations (4.80), (4.81) and (4.82), and a_1, a_2 are as follows

if f, a and γ are uncorrelated

$$a_1 = -\xi^2 (b + AL_1 J_1 H) \quad (4.100)$$

$$a_2 = -\xi^2 b A\Gamma G \quad (4.101)$$

if f, a and γ are fully correlated

$$a_1 = \xi [b + AL_1 J_1 (1 - \xi H)] \quad (4.102)$$

$$a_2 = \xi b A \Gamma G \quad (4.103)$$

4.4.7 Evaluation of $E[f \partial h / \partial x_i]$

$$E[f \partial h / \partial x_i] = 2 \frac{\sigma_f^2 \lambda_1}{\pi} I_2 \quad (4.104)$$

where

$$I_2 = \int_0^\infty \frac{(a_1 k_1^2 + a_2) k_1^2}{k_1^4 + a_3 k_1^2 + a_4} \frac{1}{1 + a_5 k_1^2} dk_1 \quad (4.105)$$

Substituting Equation (4.105) in Equation (4.104) gives (Mantoglou and Gelhar, 1985)

For $\Delta > 0$

$$E\left[f \frac{\partial h}{\partial x_1}\right] = \sigma_f^2 \lambda_1 \left[\frac{a_2 \sqrt{a_4} + a_2 a_4 a_5 + \sqrt{a_4} a_1 a_4 a_5 + a_1 a_3 \sqrt{a_4} - a_1 a_4}{A \Gamma G (1 + a_4 a_5^2 - a_3 a_5) \sqrt{4(A \Gamma G) + A^2 L_1^2}} + \frac{a_1 - a_2 a_5}{(1 + a_4 a_5^2 - a_3 a_5) \lambda_1} \right] \quad (4.106)$$

and if $\Delta < 0$

$$E\left[f \frac{\partial h}{\partial x_1}\right] = \sigma_f^2 \lambda_1 \left[\frac{-a_2 \sqrt{a_4} - a_2 a_4 a_5 - \sqrt{a_4} a_1 a_4 a_5 + a_1 a_3 \sqrt{a_4} + a_1 a_4}{A \Gamma G (1 + a_4 a_5^2 - a_3 a_5) (A L_1)} + \frac{a_1 - a_2 a_5}{(1 + a_4 a_5^2 - a_3 a_5) \lambda_1} \right] \quad (4.107)$$

The terms a_3, a_4, a_5 are given by Equations (4.80), (4.81) and (4.82) and a_1, a_2 are as follows

$$a_1 = -J_1 \quad (4.108)$$

$$a_2 = A\Gamma G(L_1 - J_1) \quad (4.109)$$

if f, a and γ are fully correlated

$$a_1 = (-J_1)(1 - \xi H) \quad (4.110)$$

$$a_2 = -[A\Gamma G(1 - \xi H)J_1 - AL_1 b_1] \quad (4.111)$$

For $i=2, 3$,

$$E\left[f \frac{\partial h}{\partial x_i}\right] = 0 \quad (4.112)$$

4.4.8 Evaluation of $E[a\partial h/\partial x_i]$

$$E[a\partial h/\partial x_i] = 2 \frac{\sigma_f^2 \lambda_1}{\pi} I_2 \quad (4.113)$$

Substituting Equation (4.105) in Equation (4.113) gives (Mantoglou and Gelhar, 1985)

For $\Delta > 0$

$$E\left[a \frac{\partial h}{\partial x_1}\right] = \sigma_f^2 \lambda_1 \left[\frac{a_2 \sqrt{a_4} + a_2 a_4 a_5 + \sqrt{a_4} a_1 a_4 a_5 + a_1 a_3 \sqrt{a_4} - a_1 a_4}{A\Gamma G(1 + a_4 a_5^2 - a_3 a_5) \sqrt{4(A\Gamma G) + A^2 L_1^2}} + \frac{a_1 - a_2 a_5}{(1 + a_4 a_5^2 - a_3 a_5) \lambda_1} \right] \quad (4.114)$$

and if $\Delta < 0$

$$E \left[a \frac{\partial h}{\partial x_1} \right] = \sigma_f^2 \lambda_1 \left[\frac{-a_2 \sqrt{a_4} - a_2 a_4 a_5 - \sqrt{a_4} a_1 a_4 a_5 + a_1 a_3 \sqrt{a_4} + a_1 a_4}{A\Gamma G(1 + a_4 a_5^2 - a_3 a_5)(AL_1)} + \frac{a_1 - a_2 a_5}{(1 + a_4 a_5^2 - a_3 a_5) \lambda_1} \right] \quad (4.115)$$

The terms a_3, a_4, a_5 are given by Equations (4.80), (4.81) and (4.82) and a_1, a_2 are as follows

if f, a and γ are uncorrelated

$$a_1 = J_1 \xi^2 H \quad (4.116)$$

$$a_2 = \xi^2 (H J_1 A\Gamma G - AL_1 b) \quad (4.117)$$

if f, a and γ are fully correlated

$$a_1 = (-\xi J_1)(1 - \xi H) \quad (4.118)$$

$$a_2 = -\xi [A\Gamma G(1 - \xi H) J_1 - AL_1 b_1] \quad (4.119)$$

For $i=2, 3$

$$E \left[a \frac{\partial h}{\partial x_i} \right] = 0 \quad (4.120)$$

4.4.9 Evaluation of $E[\gamma h]$

$$E[\gamma h] = 2 \frac{\sigma_f^2 \lambda_1}{\pi} I_1 \quad (4.121)$$

The terms a_3, a_4, a_5 are given by Equations (4.80), (4.81) and (4.82) and a_1, a_2 are as follows:

if f, a and γ are uncorrelated

$$a_1 = -\eta^2 G \quad (4.122)$$

$$a_2 = -\eta^2 A \Gamma G^2 \quad (4.123)$$

if f, a and γ are fully correlated

$$a_1 = \eta \left(\Gamma G - \xi \left(J_i \frac{\partial H}{\partial x_i} + H \Gamma G \right) - \eta G + A L_1 J_1 (1 - \xi H) \right) \quad (4.124)$$

$$a_2 = \eta \left(\Gamma G - \xi \left(J_i \frac{\partial H}{\partial x_i} + H \Gamma G \right) - \eta G \right) A \Gamma G \quad (4.125)$$

Substituting Equation (4.79) in Equation (4.121) gives (Mantoglou and Gelhar, 1985)

For $\Delta > 0$

$$E[\gamma h] = \sigma_f^2 \lambda_1 \left[\frac{a_1 \sqrt{a_4} + a_1 a_4 a_5 - \sqrt{a_4} a_2 a_5 + a_2 - a_2 a_3 a_5}{A \Gamma G (1 + a_4 a_5^2 - a_3 a_5) \sqrt{4(A \Gamma G) + A^2 L_1^2}} + a_5 \frac{a_1 - a_2 a_5}{(1 + a_4 a_5^2 - a_3 a_5) \lambda_1} \right] \quad (4.126)$$

and if $\Delta < 0$

$$E[\gamma h] = \sigma_f^2 \lambda_1 \left[\frac{-a_1 \sqrt{a_4} - a_1 a_4 a_5 + \sqrt{a_4} a_2 a_5 - a_2 + a_2 a_3 a_5}{A \Gamma G (1 + a_4 a_5^2 - a_3 a_5) (A L_1)} + a_5 \frac{a_1 - a_2 a_5}{(1 + a_4 a_5^2 - a_3 a_5) \lambda_1} \right] \quad (4.127)$$

4.5 Local governing equation for solute transport

The transport of solute in soil is carried out by advection, dispersion and diffusion mechanisms. In what follows, these mechanisms are briefly described and the associated mathematical models are presented.

4.5.1 Advection

Advection is the transport of material caused by the net flow of the fluid in which the material is suspended. Whenever a fluid is in motion, all contaminants in the flowing fluid, including both molecules and particles, are advected along with the fluid (Nazaroff and Alvarez-Cohen, 2001). The rate of contaminant transport that occurs by advection, in a rigid domain, is given by the product of contaminant concentration c and the component of groundwater specific discharge q . For three-dimensional case, the rate of contaminant transport due to advection is (Javadi and AL-Najjar, 2007).

$$F_{x,advection} = q_x c \quad (4.128)$$

$$F_{y,advection} = q_y c \quad (4.129)$$

$$F_{z,advection} = q_z c \quad (4.130)$$

where, $F_{x,advection}$, $F_{y,advection}$ and $F_{z,advection}$ are advection fluxes in x , y and z directions respectively $[M][L]^{-2}[T]^{-1}$, q_x , q_y , and q_z are groundwater specific discharge in x , y and z directions, respectively $[L][T]^{-1}$ and c is the solute concentration $[M][L]^{-3}$.

4.5.2 Diffusion

The process by which contaminants are transported by the random thermal motion of contaminant molecules is called diffusion (Yong et al., 1992). The rate of contaminant transport that occurs by diffusion is given by Fick's law. The equations for evaluation of components of diffusive flux are expressed as (Javadi and AL-Najjar, 2007)

$$F_{x,diffusion} = -D_m \frac{\partial c}{\partial x} \quad (4.131)$$

$$F_{y, diffusion} = -D_m \frac{\partial c}{\partial y} \quad (4.132)$$

$$F_{z, diffusion} = -D_m \frac{\partial c}{\partial z} \quad (4.133)$$

where, $F_{x, diffusion}$, $F_{y, diffusion}$ and $F_{z, diffusion}$ are diffusion fluxes in x , y and z directions respectively $[M][L]^{-2}[T]^{-1}$, and D_m is the molecular diffusion coefficient in the porous medium $[M]^2[T]^{-1}$.

4.5.3 Mechanical dispersion

Mechanical dispersion is a mixing or spreading process caused by small scale fluctuations in groundwater velocity along the tortuous flow paths within individual pores (Zheng and Bennett 2002). The rate of contaminant transport by mechanical dispersion is given by (Javadi and AL-Najjar, 2007)

$$F_{x, dispersion} = -D_{xx} \frac{\partial c}{\partial x} - D_{xy} \frac{\partial c}{\partial y} - D_{xz} \frac{\partial c}{\partial z} \quad (4.134)$$

$$F_{y, dispersion} = -D_{yx} \frac{\partial c}{\partial x} - D_{yy} \frac{\partial c}{\partial y} - D_{yz} \frac{\partial c}{\partial z} \quad (4.135)$$

$$F_{z, dispersion} = -D_{zx} \frac{\partial c}{\partial x} - D_{zy} \frac{\partial c}{\partial y} - D_{zz} \frac{\partial c}{\partial z} \quad (4.136)$$

where, $F_{x, dispersion}$, $F_{y, dispersion}$ and $F_{z, dispersion}$ $[M][L]^2[T]^{-1}$ are dispersion fluxes in x , y and z directions, respectively and D_{xx} , D_{xy} , D_{xz} , D_{yx} , D_{yy} , D_{yz} , D_{zx} , D_{zy} and D_{zz} are the tensor of coefficients of dispersivity $[L][T]^{-1}$.

Based on mass balance law, solute concentration governing equation is given as

$$n \frac{\partial(c)}{\partial t} = \nabla F_{advection} - \nabla F_{dispersion-diffusion} + F \quad (4.137)$$

where, n is porosity, $\nabla F_{advection}$ and $\nabla F_{dispersion-diffusion}$ are concentration change due to movement of solute by advection and diffusion-dispersion mechanisms respectively in the specified area and time duration, and F represents the solute sink-source terms.

Substituting Equations (4.128) to (4.136) into the Equation (4.137) leads to (Javadi et al., 2006)

$$n \frac{\partial(c)}{\partial t} = -\frac{\partial(cq_i)}{\partial x_i} + \frac{\partial}{\partial x_i} \left[E_{ij} \frac{\partial c}{\partial x_j} \right] + F \quad i = x, y, z \quad (4.138)$$

where, E_{ij} is local Bulk dispersion equal to nD_{ij} (D_{ij} is dispersion coefficient including dispersion and molecular diffusion).

In the transport Equation (4.138), the left-hand side term describes the change of contaminant mass in time. In the right-hand side, the first term represents the movement of contaminant due to advection and the second term represents the effects of dispersion and diffusion.

In the steady-state condition when the change in solute concentration with time is zero, local solute transport equation becomes

$$-\frac{\partial(cq_i)}{\partial x_i} + \frac{\partial}{\partial x_i} \left[E_{ij} \frac{\partial c}{\partial x_j} \right] + F = 0 \quad i = x, y, z \quad (4.139)$$

4.5.4 Dual-domain transport model

Immobile or stagnant water regions may exist within the porous medium due to the water occupying dead-end macropores, or local zones with very low permeability. In unsaturated flow this may also occur in pendular rings of drained pores as can be seen in Figure 4.1. So, for the area subjected to this structural form, the contaminant transport system can be viewed in terms of a dual-domain model, which divides the aquifer into two distinct transport domains, termed mobile and immobile domains.

Immobile or stagnant water regions may exist within the porous medium due to the water occupying dead-end macropores, or local zones with very low permeability. In unsaturated flow this may also occur in pendular rings of drained pores as can be seen in Figure 4.1. So, for the area subjected to this structural form, the contaminant transport system can be viewed in terms of a dual-domain model, which divides the aquifer into two distinct transport domains, termed mobile and immobile domains.

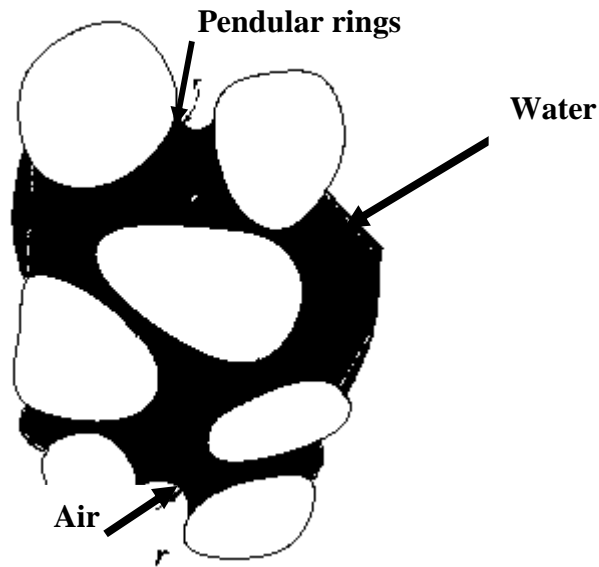


Figure 4.1 Transport mechanisms: mobile and immobile phases (AL-Najjar 2006).

Transport is predominantly advective in the mobile domain but largely diffusive in the immobile domain. The early arrival of solute may be attributed to preferential flow of water through the larger channels of the wetted pore space (large channels and wetted regions between finer pores in an aggregated soil) whereas, the water in the finer pores is more stagnant and does not contribute to solute transport, except for diffusion exchange. In the mobile region, solute is transported by an advection-dispersion process whereas, in the immobile region, a rate-limited diffusion process exchanges solute with the mobile region. It is common to assume that neither hydrodynamic dispersion nor advection of a pollutant can take place in a body of immobile water. However, there is a pollutant exchange process between immobile and mobile water responsible for the transport. The governing equation for solute transport in dual-domain soil is

where, subscripts m and im represent the characteristics of mobile and immobile domains, and ζ is the rate coefficient of the mass transfer between mobile and immobile domains $[\text{T}]^{-1}$ modelled as a first-order, reversible kinetic reaction.

In above equations groundwater specific discharge q as a function of hydraulic conductivity varies randomly in spatial domain. The effect of this spatial variability is profound in the case of large scale problems and causes unsuitability of local-scale governing equations for simulation of large scale problems. An appropriate model for solute transport can be found by incorporation of the effect of this spatial variability in the related governing equations. In the following section, the stochastic method proposed by Gelhar (1986) and Vomvoris and Gelhar (1990) for incorporating spatial variability of hydraulic properties of soil into the classical Equations (4.138) and (4.139) is explained.

4.6 Large-scale governing equation for solute transport

Local specific discharge, q , has been considered as random parameter in the model, and as a result the output of the model, (i.e., the solute concentration, c) is a random variable. These parameters can be defined by stochastic representations. They are considered as realizations of random fields. It is assumed that these random fields are three-dimensional, spatially cross-correlated, and they are composed of two components, mean and fluctuations

$$q_i = \bar{q}_i + q'_i \quad i = x, y, z \quad (4.142)$$

$$c = \bar{c} + c' \quad (4.143)$$

The first terms in the right hand-side of Equations (4.142) and (4.143) are assumed to be deterministic, while the second terms are three-dimensional zero mean second-order stationary random fields.

$$c = \bar{c} + c' \quad (4.143)$$

The first terms in the right hand-side of Equations (4.142) and (4.143) are assumed to be deterministic, while the second terms are three-dimensional zero mean second-order stationary random fields.

The basic assumptions are: (i) the fluctuations q' and c' are relatively small, and (ii) the scale of variations of the mean values \bar{q} and \bar{c} is much larger than the scale of variations of the fluctuations q' and c' .

The large-scale model of steady-state solute transport is obtained by averaging the local-scale governing equation over the ensemble of possible realizations of the stochastic processes, q' . In this way, expected value of small-scale equation with respect to fluctuations is calculated. Taking the expected value of Equation (4.138) with respect to q' , yields

$$n \frac{\partial E[c]}{\partial t} = - \frac{\partial E[cq_i]}{\partial x_i} + \frac{\partial}{\partial x_i} \left[E_{ij} \frac{\partial E[c]}{\partial x_j} \right] + F \quad i = x, z \quad (4.144)$$

Substituting Equations (4.142) and (4.143) into Equation (4.144), the first term on the right-hand side of this equation (i.e., $E[(cq_i)]$) can be rewritten as

$$E[(q_i c)] = E[(\bar{q}_i + q')(\bar{c} + c')] = \bar{c} \bar{q}_i + E[q'_i c'] \quad (4.145)$$

In Equation (4.145), $\bar{c} \bar{q}_i$ represents the advective flux and $E[q'_i c']$ represents macro-dispersive flux. Macro-dispersive flux is a dispersive flux due to spatial variation of groundwater discharge in large-scale problems.

In this work, it is assumed that dispersion is Fickian. Fick's law postulates that dispersive flux goes from region of high concentration to region of low concentration,

$$D_{yy} = \alpha_T q \quad (4.147)$$

$$D_{zz} = \alpha_T q \quad (4.148)$$

$$D_{xz} = 0 \quad (4.149)$$

$$D_{zx} = 0 \quad (4.150)$$

$$D_{xy} = 0 \quad (4.151)$$

$$D_{yx} = 0 \quad (4.152)$$

$$D_{yz} = 0 \quad (4.153)$$

$$D_{zy} = 0 \quad (4.154)$$

where α_L and α_T are the local longitudinal and transversal dispersivities, respectively, and q is a mean specific discharge equal to

$$q = \sqrt{\hat{k}_{xx} J'_1 + \hat{k}_{zz} J'_2} \quad (4.155)$$

where \hat{k}_{xx} and \hat{k}_{zz} are effective hydraulic conductivities in x and z directions, respectively, given by Equation (4.23) and J'_1 and J'_2 are mean gradients in directions x' and z' given by Equation (4.15).

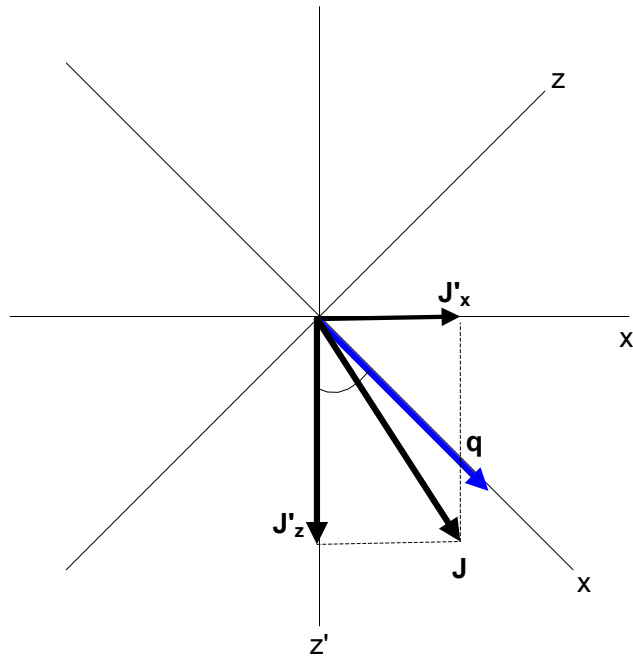


Figure 4.2 Coordinate system xz corresponds to the mean flow direction and coordinate system $x'z'$ corresponds to mean hydraulic conductivity (Mantoglou 1984).

Also, based on Fick's law, macro-dispersive flux can be written as

$$E[(c'q'_i)] = -\hat{E}_{ij} \frac{\partial \bar{c}}{\partial x_j} \quad (4.156)$$

where \hat{E}_{ij} is the effective bulk macrodispersion coefficient tensor. By defining a macrodispersion tensor as

$$A_{ij} = \frac{\hat{E}_{ij}}{q} \quad (4.157)$$

Equation (4.156) can be written as

$$E[c'q'_i] = -A_{ij} q \frac{\partial \bar{c}}{\partial x_j} \quad (4.158)$$

and substituting Equations (4.158) and (4.145) into Equation (4.144) and rearranging, yields

$$n \frac{\partial \bar{c}}{\partial t} = \frac{\partial}{\partial x_i} \left[(E_{ij} + A_{ij}q) \frac{\partial \bar{c}}{\partial x_j} \right] - \frac{\partial (\bar{c} \bar{q}_i)}{\partial x_i} \quad (4.159)$$

Equation (4.159) is the relationship for large-scale unsteady-state solute transport problem. In steady-state condition in which concentration in a certain point is constant along the time, the first term in the Equation (4.159) is equal to zero (i.e., $\frac{\partial \bar{c}}{\partial t} = 0$).

Therefore, the large-scale solute transport governing equation for steady-state condition can be presented as

$$\frac{\partial (\bar{c} \bar{q}_i)}{\partial x_i} = \frac{\partial}{\partial x_i} \left[(E_{ij} + A_{ij}q) \frac{\partial \bar{c}}{\partial x_j} \right] \quad (4.160)$$

Comparing Equations (4.159) and (4.160) to the related local transport Equations (4.138) and (4.139), it is noticed that they have a similar form. The term $E_{ij} + A_{ij}q$ is the total large-scale dispersion coefficient. The difference between local-scale and large-scale dispersivity is the effective Bulk macrodispersion ($A_{ij}q$). This difference is due to the variations in the groundwater specific discharge (q_i) or equivalent groundwater seepage, ($\frac{q_i}{n}$).

In this work, the following expressions developed by Mantoglou (1984) are used for evaluation of macrodispersivities (A_{ij}). Two assumptions were considered in order to get the following analytical expression: (i) the soil is assumed to be horizontally stratified, and (ii) the lateral head gradients are considered to be small.

$$A_{xx} = \frac{\sigma_f^2 \lambda_x \lambda_z}{\pi \gamma^2 b} (T_{22} + 2\xi^2 T_{23} + \xi^4 T_{33}) \quad (4.161)$$

$$A_{yy} = \frac{\sigma_f^2 \lambda_x \lambda_y J_y^2}{\pi \gamma^2 o J_x^2} (\xi^4 T_{33}) \quad (4.162)$$

$$A_{zz} = \frac{\sigma_f^2 \lambda_x \lambda_z J_z^2}{\pi \gamma^2 o J_x^2} (\xi^4 T_{23}) \quad (4.163)$$

$$A_{zx} = A_{xz} = \frac{\sigma_f^2 \lambda_x \lambda_z J_z}{\pi \gamma^2 o J_x} \xi^2 (T_{23} + \xi^2 T_{33}) \quad (4.164)$$

$$A_{xy} = A_{yx} = A_{yz} = A_{zy} = 0 \quad (4.165)$$

where

$$\gamma^2 = \frac{q^2}{K_m^2 J_x^2 \beta^2} \quad (4.166)$$

$$o = \sqrt{\lambda_x^2 (\sin \phi)^2 + \lambda_z^2 (\cos \phi)^2} \quad (4.167)$$

$$\xi^2 = \frac{\lambda_x^2}{\lambda_z^2} (\sin \phi)^2 + (\cos \phi)^2 \quad (4.168)$$

where $\phi = \arctg \left(\frac{\hat{k}_{zz} J_{z'}}{\hat{k}_{xx} J_{x'}} \right)$ defines direction of the axes x and z with respect to axes x'

and y' (see Figure 4.2).

If f and a are uncorrelated, then

$$\beta^2 = 1 + \xi^2 H \quad (4.169)$$

If f and a are perfectly correlated, then

$$\beta^2 = 1 - \xi H \quad (4.170)$$

and

$$J_x = J'_x \cos \phi + J'_z \sin \phi \quad (4.171)$$

$$J_z = -J'_x \sin \phi + J'_z \cos \phi \quad (4.172)$$

T_{22} , T_{23} and T_{33} are evaluated by the following integrals

$$T_{22} = 4 \int_0^{\pi/2} \frac{1}{8(a^2 - c^2)} \left[\pi - \frac{8c^2}{a^2 - c^2} \ln \left(\frac{c^2}{a^2} \right) \right] (\cos \phi)^4 d\phi \quad (4.173)$$

$$T_{23} = 2 \int_0^{\pi/2} \frac{c^2}{a^2(a^2 - 2c^2)} \left[\frac{\ln \left(\frac{c^2}{a^2} \right)}{a^2 - c^2} - \frac{c^2 \pi}{4} \right] \left[1 - 2(\sin \phi)^2 (\cos \phi)^2 \right] d\phi \quad (4.174)$$

$$T_{33} = 4 \int_0^{\pi/2} \frac{1}{8(a^2 - c^2)} \left[\pi - \frac{8c^2}{a^2 - c^2} \ln \left(\frac{c^2}{a^2} \right) \right] (\sin \phi)^4 d\phi \quad (4.175)$$

where

$$a^2 = (\cos \phi)^2 + (\sin \phi)^2 \quad (4.176)$$

and

$$c^2 = A^2 L_z^2 b^2 (\cos \phi)^2 \quad (4.177)$$

4.7 Evaluation of concentration variability σ_c^2

In this section, the concentration variance is evaluated as

$$\sigma_c^2 = R_{cc}(0) \quad (4.178)$$

where σ_c^2 is the solute concentration variance and R_{cc} is the covariance of concentration if $\zeta = 0$. The relationship between variance and covariance has been explained in Chapter 3. The covariance function for solute concentration is presented as

$$R_{cc}(\zeta) = \int_{-\infty}^{\infty} e^{ik\zeta} S_{cc}(k) dk \quad (4.179)$$

According to Equation (4.179), evaluation of the covariance of solute concentration is reduced to evaluation of spectrum of solute concentration. Assuming the spectrum of hydraulic conductivity is known, the spectrum of solute concentration is evaluated using its relationship with the spectrum of hydraulic conductivity. Linear solute perturbation equation is used for this purpose. The linear fluctuation equation relates the concentration fluctuations to the specific discharge fluctuations and is obtained by subtracting Equation (4.159) from Equation (4.138) as

$$\frac{\partial c'}{\partial t} + q'_i \frac{\partial \bar{c}}{\partial x_i} + \bar{q}_i \frac{\partial c'}{\partial x_i} - \frac{\partial}{\partial x_i} E_{ij} \frac{\partial c'}{\partial x_j} = E \left[q'_i \frac{\partial c'}{\partial x_i} \right] - q'_i \frac{\partial c'}{\partial x_i} \cong 0 \quad (4.180)$$

Equation (4.180) is solved using spectral method. Using Equation (4.29), the concentration and specific discharge, pressure head and natural logarithm of the saturated hydraulic conductivity perturbations can be written as

$$c' = \int \int \int_{-\infty}^{\infty} \exp(i\vec{k} \cdot \vec{x}) dZ_c(\vec{k}) \quad (4.181)$$

$$q'_i = \int \int \int_{-\infty}^{\infty} \exp(i\vec{k} \cdot \vec{x}) dZ_{q_i}(\vec{k}) \quad (4.182)$$

$$h = \int \int \int_{-\infty}^{\infty} \exp(i\vec{k} \cdot \vec{x}) dZ_h(\vec{k}) \quad (4.183)$$

$$f = \int \int \int_{-\infty}^{\infty} \exp(i\vec{k} \cdot \vec{x}) dZ_f(\vec{k}) \quad (4.184)$$

where \vec{k} is the wave number vector, and \vec{x} is the position vector.

Substituting Equations (4.181) and (4.182) into Equation (4.180) leads to

$$G_i dZ_{q_i} = G_j dZ_{q_j} = \left(E_{ij} k^2 - i \vec{k} \vec{q}_i \right) dZ_c \quad (4.185)$$

where, $k^2 = k_1^2 + k_2^2 + k_3^2$.

Multiplying both sides of Equation (4.185), once by complex conjugate Fourier amplitude $dZ_{q_j}^*$ and another time by dZ_c^* and taking the mean values, and using the spectral relationship presented at Equation (4.30), lead to

$$G_j S_{q_i q_j} = \left(E_{ij} k^2 - i \vec{k} \vec{q}_i \right) S_{c q_j} \quad (4.186)$$

and

$$G_i S_{c q_i} = \left(E_{ij} k^2 - i \vec{k} \vec{q}_i \right) S_{cc} \quad (4.187)$$

where

$$G_i = - \frac{\partial \bar{c}}{\partial x_i} \quad (4.188)$$

Substituting Equation (4.187) into Equation (4.186) yields

$$\frac{G_i G_j S_{q_i q_j}(\vec{k})}{\left(E_{ij} k^2 - i \vec{k} \vec{q}_i \right)^2} = S_{cc}(\vec{k}) \quad (4.189)$$

where, $S_{cc}(k)$ is the spectrum of the concentration perturbation. $S_{q_j q_i}(k)$ is the spectrum of the specific discharge along the x_i and x_j . Also, the relationship between $S_{q_j q_i}(k)$ and $S_{ff}(k)$, the spectrum of the hydraulic conductivity, is determined

using Darcy's equation (Gelhar and Axness 1983). Darcy's equation with locally isotropic hydraulic conductivity, is written as

$$q_i = -K \frac{\partial \psi}{\partial x_i} \quad (4.190)$$

Substituting Equations (4.8) and (4.11) into Equation (4.190) and using Taylor expansion yields

$$q_i = -e^F e^f \frac{\partial(H+h)}{\partial x_i} = -e^F \left(1 + f + \frac{f^2}{2} + \dots \right) \left(\frac{\partial H}{\partial x_i} + \frac{\partial h}{\partial x_i} \right) \quad (4.191)$$

Assuming small perturbations and dropping products of perturbed quantities, the mean removed form of Equation (4.191) is

$$\begin{aligned} q_i' &= -e^F e^f \frac{\partial(H+h)}{\partial x_i} \\ &= -e^F \left(f \frac{\partial H}{\partial x_i} + \frac{\partial h}{\partial x_i} \right) \end{aligned} \quad (4.192)$$

and using spectral representations for h and q_i'

$$dZ_{q_i} = e^F (J_i dZ_f - ik_i dZ_h) \quad (4.193)$$

Perturbed flow equation is given as (Bakr et al., 1978)

$$\frac{\partial^2 h}{\partial x_i^2} = J_i \frac{\partial f}{\partial x_i} \quad (4.194)$$

Substituting spectral representations for h and f (i.e., Equations (4.183) and (4.184)), into Equation (4.194) yields

$$dZ_h = \frac{-iJ_i k_i dZ_f}{k^2} \quad (4.195)$$

Combining Equations (4.193) and (4.195), produces the following relationship between complex Fourier amplitudes of specific discharge and hydraulic conductivity perturbations

$$dZ_{q_i} = e^F \left(J_i - \frac{J_j k_i k_j}{k^2} \right) dZ_f \quad (4.196)$$

With similar procedure used for producing relationship between the spectrum of solute concentration and the spectrum of the specific discharge, (i.e., producing Equation (4.189) from Equation (4.185)), the relationship between spectrum of specific discharge and spectrum of hydraulic conductivity is obtained from Equation (4.196) and spectral representations presented at Equations (4.30) and (4.31) as

$$S_{q_i}(k) = K_l^2 J_m J_n \left(\delta_{jm} - \frac{k_j k_m}{k^2} \right) \left(\delta_{jn} - \frac{k_i k_n}{k^2} \right) S_{ff}(k) \quad (4.197)$$

Note that summation over m and n is implied.

Substituting Equations (4.197), (4.189) and (4.179), into Equation (4.178) and taking $\xi = 0$ produces the following equation for evaluation of solute concentration variance (Vomvoris and Gelhar 1990).

$$\begin{aligned} \sigma_c^2 &= \int_{-\infty}^{\infty} S_{cc}(k) dk \\ &= \int_{-\infty}^{\infty} \left(\frac{G_i G_j K_l^2 J_m J_n \left(\delta_{jm} - \frac{k_j k_m}{k^2} \right) \left(\delta_{jn} - \frac{k_i k_n}{k^2} \right) S_{ff}(k)}{(E_{ij} k^2 - ik\bar{q}_i)} \right) dk \end{aligned} \quad (4.198)$$

The integration presented in Equation (4.198) was solved analytically by Vomvoris and Gelhar (1990). Their resulted equations are used in this work for evaluation of solute concentration. The equations is presented bellow

$$\sigma_c^2 = T_{ii}(\rho_1, \rho_2, \varepsilon, \nu) \sigma_f^2 \lambda_3 G_i^2 \quad (4.199)$$

where,

$$T_{xx} = \frac{1}{\gamma^2} \frac{2}{3} \frac{1}{\nu \varepsilon} \frac{1}{\rho_1} \frac{1}{\rho_2} \quad (4.200)$$

$$T_{yy} = T_{zz} = \frac{1}{\gamma^2} \frac{1}{6} \left[\frac{1}{2\rho_1^2} + \frac{1}{R^2} + \left(\frac{1}{2} + \frac{1}{R^2} \right) \frac{1}{R} \ln \frac{R+2R^2}{R-2R^2} \right] \quad (4.201)$$

$$\text{and } \rho_1 = \frac{\lambda_z}{\lambda_x}, \rho_2 = \frac{\lambda_z}{\lambda_y}, \varepsilon = \frac{\alpha_L}{\lambda_z}, \nu = \frac{\alpha_T}{\alpha_L}, R^2 = 1 - \rho_1^2.$$

4.8 Summary and conclusion

In order to develop a reliable model for water flow and solute transport it is essential to consider the effects of spatial variability of soil formation on water seepage rate in soils and its frequent effects on solute transport. Based on the literature (Polmann et al., 1990 and Mantoglou and Gelhar, 1987), spectral approach is known as appropriate method for dealing with random processes (in order to incorporate spatial variability of random parameters existed in the processes into the related governing equations). This approach has been selected in this work. The procedure of implementation of spectral method to the classical governing equations for development of large-scale mean governing equations for these processes were described in this chapter.

The large-scale partial differential governing equations include some terms which are called effective parameters. These effective parameters are produced by fluctuations of random hydraulic parameters due to natural heterogeneity of soils. Perturbation equations for flow and solute transport are used in order to evaluate these effective parameters. They were also employed to evaluate flow and concentration variances. Perturbation partial differential equations were developed by removing mean flow and transport partial differential equations from the classical governing partial differential equations. Analytical spectral method used for solving the perturbation equations and

developing algebraic equations for evaluation of effective parameters was described. In the developed algebraic equations, some complex integrals appear that could not be solved by simple analytical methods. However, these integrals have been solved using some assumptions which are consistent with real field condition by Mantoglou and his co-workers (Mantoglou and Gelhar, 1987a, 1987b, 1987c and Mantoglou, 1984). These solutions were used in this work.

The resulting stochastic partial and algebraic equations predict large-scale flow and solute transport characteristics rather than local details of flow. The advantage of the resulted equations is that they depend on few parameters describing the statistics of local variability (i.e., mean, variance, correlation lengths) which are finite rather than depending to the actual soil properties which are infinite. The formation of these equations which show the relationship between mean flow and perturbation characteristics with statistic of local variability provides a better understanding of the probabilistic nature of this process and effects of present uncertainty in soil properties on relevant phenomena.

As the large-scale models representations were discussed in partial differential equation form, they can be evaluated by numerical techniques. In the next chapter (Chapter 5), numerical finite element and finite difference techniques that have been used to solve these stochastic partial differential equations are discussed in detail (see Figure 5.1).

CHAPTER 5

NUMERICAL SOLUTION

5.1 Introduction

The transport of pollutants in the unsaturated zone is modelled using two sets of equations. The first set of equations describes the groundwater flow through the problem domain. These equations include a stochastic partial differential relationship expressing temporal variability of mean capillary tension head through the domain and mathematical algebraic equations for evaluation of important parameters such as effective hydraulic conductivity, second-order moment (variance) of capillary tension head, mean hydraulic gradient and mean groundwater velocity. The second set of equations describes the ways that the fluid phase transports a miscible contaminant that include a stochastic partial differential equation expressing movement of solute through the domain with time and algebraic equations for evaluation of important parameters such as effective diffusion of the area and second-order moment of solute concentration through the domain.

The solutions of these equations are too complex for analytical methods; however they can be obtained using approximate numerical methods. In the model developed in this work, the governing equations of these procedures are solved using a finite element

method in the space domain and a finite difference scheme in the time domain. In this chapter, the procedure for generating finite element formulations for the prescribed governing differential equations and implementation of a finite difference scheme on them are presented. Possible various types of boundary conditions influencing on hydrologic procedures and commonly present to contaminated lands and aquifers are discussed.

5.2 Finite element formulation for groundwater flow

In this section, finite element formulations are derived for stochastic mathematical model of unsteady-state (transient) groundwater flow in unsaturated soil. The stochastic partial differential equation for unsteady-state groundwater flow through an unsaturated soil is

$$\frac{\partial \Theta}{\partial t} = -\hat{C} \frac{\partial H}{\partial t} = -\frac{\partial}{\partial x_i} \left[\hat{K}_{ij} \frac{\partial (H+z)}{\partial x_i} \right] \quad i = x, y, z \quad (5.1)$$

The three-dimensional form of equation (5.1) is

$$\hat{C} \frac{\partial H}{\partial t} = \frac{\partial}{\partial x} \left[\hat{K}_x \frac{\partial H}{\partial x} \right] + \frac{\partial}{\partial y} \left[\hat{K}_y \frac{\partial H}{\partial y} \right] + \frac{\partial}{\partial z} \left[\hat{K}_z \left(\frac{\partial H}{\partial z} + 1 \right) \right] \quad (5.2)$$

Mean capillary tension head is the unknown variable of the equation. An approximate solution of this variable is defined in terms of its nodal values and associated nodal shape function as

$$\hat{H}(x, y, z, t) = \sum_{i=1}^n N_i(x, y, z) H_i(t) \quad (5.3)$$

where $\hat{H}(x, y, z, t)$ is the approximated value of capillary tension head at any location of the problem, N_i is the interpolation function at node i , H_i is the mean capillary tension head value at node i , and n is the number of nodes in the element.

When the approximate solution for hydraulic head is substituted into the equation (5.2), the equation is not satisfied exactly. Then

$$\frac{\partial}{\partial x} \left[\hat{K}_x \frac{\partial \hat{H}}{\partial x} \right] + \frac{\partial}{\partial y} \left[\hat{K}_y \frac{\partial \hat{H}}{\partial y} \right] + \frac{\partial}{\partial z} \left[\hat{K}_z \left(\frac{\partial \hat{H}}{\partial z} + 1 \right) \right] - \hat{C} \frac{\partial \hat{H}}{\partial t} = R \neq 0 \quad (5.4)$$

where R is the residual or error due to the approximate solution. The residual at each point in the problem domain is a measure of the degree to which the head does not satisfy the governing equation. Based on the philosophy behind the weighted residual method, the weighted average of residuals at nodes over the solution domain is forced to be zero.

$$\iiint_{\Omega} \left(\frac{\partial}{\partial x} \left[\hat{K}_x \frac{\partial \hat{H}}{\partial x} \right] + \frac{\partial}{\partial y} \left[\hat{K}_y \frac{\partial \hat{H}}{\partial y} \right] + \frac{\partial}{\partial z} \left[\hat{K}_z \left(\frac{\partial \hat{H}}{\partial z} + 1 \right) \right] - \hat{C} \frac{\partial \hat{H}}{\partial t} \right) d\Omega = 0 \quad (5.5)$$

After some mathematical manipulation this equation leads to a system of algebraic equations to solve the governing differential equation of transient water flow and work out its unknown variable (mean capillary tension head) approximately. According to the basic theory behind the finite element method Equation (5.5) is formulated for each finite number of distinct elements that together they form the problem domain. The system of algebraic equations is generated by summation of element equations over the domain. Generation of these algebraic formulations is carried out through four steps including: (i) determination of contribution of elements in weighted residual (ii) determination of element characteristics, (iii) summation of element residual formulation over the problem domain and (iv) employing the weighted residual method. In the following sections these four steps are discussed in details.

5.2.1 Element weighted residual for groundwater flow

Equation (5.3) is used to approximate the capillary tension head over an element. In this case, parameter n, is the number of nodes in each element. Then, the contribution of every element, e, to the residual at node i, to which the element is connected, is obtained by substituting the approximated capillary tension head of each element.

$$\begin{aligned}
\{R^{(e)}\} = & - \int_{V^{(e)}} W_i^{(e)} \left\{ \frac{\partial}{\partial x} \left[\hat{K}_x^{(e)} \frac{\partial \hat{H}^{(e)}}{\partial x} \right] + \frac{\partial}{\partial y} \left[\hat{K}_y^{(e)} \frac{\partial \hat{H}^{(e)}}{\partial y} \right] + \frac{\partial}{\partial z} \left[\hat{K}_z^{(e)} \left(\frac{\partial \hat{H}^{(e)}}{\partial z} + 1 \right) \right] \right. \\
& \left. - \hat{C}^{(e)} \frac{\partial \hat{H}^{(e)}}{\partial t} \right\} dV = - \int_{V^{(e)}} W_i^{(e)} \left\{ \frac{\partial}{\partial x} \left[\hat{K}_x^{(e)} \frac{\partial \hat{H}^{(e)}}{\partial x} \right] + \frac{\partial}{\partial y} \left[\hat{K}_y^{(e)} \frac{\partial \hat{H}^{(e)}}{\partial y} \right] \right. \\
& \left. + \frac{\partial}{\partial z} \hat{K}_z^{(e)} \left(\frac{\partial \hat{H}^{(e)}}{\partial z} \right) + \frac{\partial \hat{K}_z^{(e)}}{\partial z} - \hat{C}^{(e)} \frac{\partial \hat{H}^{(e)}}{\partial t} \right\} dV
\end{aligned} \tag{5.6}$$

where $w_i^{(e)}$ is the element's weighting function for node i and the limits of the integration are chosen to represent the area of element e .

In this work, Galerkin's method is employed; therefore, the weighting function for each node in the element is taken as the element's interpolation function for that node (i.e., $W_i^{(e)} = N_i^{(e)}$). Then, Equation (5.6) is written as

$$\begin{aligned}
\{R^{(e)}\} = & - \int_{V^{(e)}} N_i^{(e)} \left\{ \frac{\partial}{\partial x} \left[\hat{K}_x^{(e)} \frac{\partial \hat{H}^{(e)}}{\partial x} \right] + \frac{\partial}{\partial y} \left[\hat{K}_y^{(e)} \frac{\partial \hat{H}^{(e)}}{\partial y} \right] \right. \\
& \left. + \frac{\partial}{\partial z} \left[\hat{K}_z^{(e)} \left(\frac{\partial \hat{H}^{(e)}}{\partial z} + 1 \right) \right] - \hat{C}^{(e)} \frac{\partial \hat{H}^{(e)}}{\partial t} \right\} dV \\
= & N_i^{(e)} \left\{ \frac{\partial}{\partial x} \left[\hat{K}_x^{(e)} \frac{\partial \hat{H}^{(e)}}{\partial x} \right] + \frac{\partial}{\partial y} \left[\hat{K}_y^{(e)} \frac{\partial \hat{H}^{(e)}}{\partial y} \right] \right. \\
& \left. - \int_{V^{(e)}} + \frac{\partial}{\partial z} \left[\hat{K}_z^{(e)} \frac{\partial \hat{H}^{(e)}}{\partial z} \right] + \frac{\partial \hat{K}_z^{(e)}}{\partial z} - \hat{C}^{(e)} \frac{\partial \hat{H}^{(e)}}{\partial t} \right\} dV
\end{aligned} \tag{5.7}$$

Because the approximate solution is a linear function of x , y and z , $\frac{\partial^2 \hat{H}}{\partial x^2}$, $\frac{\partial^2 \hat{H}}{\partial y^2}$ and

$\frac{\partial^2 \hat{H}}{\partial z^2}$ are not defined. However, the approximate solution does have a continuous first

derivative; therefore, Equation (5.7) can be evaluated if it is rewritten in terms of $\frac{\partial \hat{H}}{\partial x}$,

$\frac{\partial \hat{H}}{\partial y}$ and $\frac{\partial \hat{H}}{\partial z}$.

Using integration by parts to the second order derivate terms of Equation (5.7) yields

$$\begin{aligned}
& - \int_{V^{(e)}} N_i^{(e)} \left\{ \frac{\partial}{\partial x} \left[\hat{K}_x^{(e)} \left(\frac{\partial \hat{H}^{(e)}}{\partial x} \right) \right] + \frac{\partial}{\partial y} \left[\hat{K}_y^{(e)} \left(\frac{\partial \hat{H}^{(e)}}{\partial y} \right) \right] + \frac{\partial}{\partial z} \left[\hat{K}_z^{(e)} \frac{\partial \hat{H}^{(e)}}{\partial z} \right] \right\} dV = \\
& \int_{V^{(e)}} \left\{ -\hat{K}_x^{(e)} \frac{\partial}{\partial x} \left(N_i^{(e)} \frac{\partial \hat{H}^{(e)}}{\partial x} \right) - \hat{K}_y^{(e)} \frac{\partial}{\partial y} \left(N_i^{(e)} \frac{\partial \hat{H}^{(e)}}{\partial y} \right) - \hat{K}_z^{(e)} \frac{\partial}{\partial z} \left(N_i^{(e)} \frac{\partial \hat{H}^{(e)}}{\partial z} \right) + \right. \\
& \left. \hat{K}_x^{(e)} \frac{\partial N_i^{(e)}}{\partial x} \left(\frac{\partial \hat{H}^{(e)}}{\partial x} \right) + \hat{K}_y^{(e)} \frac{\partial N_i^{(e)}}{\partial y} \left(\frac{\partial \hat{H}^{(e)}}{\partial y} \right) + \hat{K}_z^{(e)} \frac{\partial N_i^{(e)}}{\partial z} \left(\frac{\partial \hat{H}^{(e)}}{\partial z} \right) \right\} dV \quad (5.8)
\end{aligned}$$

Green's Theorem is applied to the second-order derivative terms of Equation (5.8); therefore,

$$\begin{aligned}
& - \int_{V^{(e)}} \left\{ \hat{K}_x^{(e)} \frac{\partial}{\partial x} \left[N_i^{(e)} \left(\frac{\partial H^{(e)}}{\partial x} \right) \right] + \hat{K}_y^{(e)} \frac{\partial}{\partial y} \left[N_i^{(e)} \left(\frac{\partial H^{(e)}}{\partial y} \right) \right] + \hat{K}_z^{(e)} \frac{\partial}{\partial z} \left[N_i^{(e)} \frac{\partial H^{(e)}}{\partial z} \right] \right\} dV = \\
& - \int_{\Gamma_{yz}} N_i^{(e)} \hat{K}_x^{(e)} \frac{\partial H^{(e)}}{\partial x} dydz - \int_{\Gamma_{xz}} N_i^{(e)} \hat{K}_y^{(e)} \frac{\partial H^{(e)}}{\partial y} dx dz - \int_{\Gamma_{xy}} N_i^{(e)} \hat{K}_z^{(e)} \frac{\partial H^{(e)}}{\partial z} dx dy \quad (5.9)
\end{aligned}$$

where, Γ_{yz} , Γ_{xz} and Γ_{xy} are projections of element boundary surface on the plans yz , xz and xy respectively.

Equation (5.9) represents the groundwater flow across the element's surface. Thereafter, this term is denoted by $Q_i^{(e)}$, or

$$Q_i^{(e)} = - \int_{\Gamma_{yz}} N_i^{(e)} \hat{K}_x^{(e)} \frac{\partial H^{(e)}}{\partial x} dydz - \int_{\Gamma_{xz}} N_i^{(e)} \hat{K}_y^{(e)} \frac{\partial H^{(e)}}{\partial y} dx dz - \int_{\Gamma_{xy}} N_i^{(e)} \hat{K}_z^{(e)} \frac{\partial H^{(e)}}{\partial z} dx dy \quad (5.10)$$

$Q_i^{(e)}$ is zero for the internal elements and is defined as boundary condition for the elements that are on the boundary of domain.

Then, substituting the Equations (5.8), (5.9), (5.10) into the residual equation yields

$$\begin{aligned} \{R^{(e)}\} = & -Q_i^{(e)} + \int_{V^{(e)}} \left\{ \hat{K}_x^{(e)} \frac{\partial N_i^{(e)}}{\partial x} \left(\frac{\partial \hat{H}^{(e)}}{\partial x} \right) + \hat{K}_y^{(e)} \frac{\partial N_i^{(e)}}{\partial y} \left(\frac{\partial \hat{H}^{(e)}}{\partial y} \right) \right. \\ & \left. + \hat{K}_z^{(e)} \frac{\partial N_i^{(e)}}{\partial z} \left(\frac{\partial \hat{H}^{(e)}}{\partial z} \right) \right\} dV - \int_{V^{(e)}} N_i^{(e)} \frac{\partial \hat{K}_z^{(e)}}{\partial z} dV + \int_{V^{(e)}} N_i^{(e)} \hat{C}^{(e)} \frac{\partial \hat{H}^{(e)}}{\partial t} dV \end{aligned} \quad (5.11)$$

Over each element, the following variables are approximated by polynomial shape functions relating them to their nodal values:

$$\hat{H}^{(e)} = [N_i^{(e)}] \{H_i^{(e)}\} \quad (5.12)$$

$$\frac{\partial \hat{H}^{(e)}}{\partial t} = [N_i^{(e)}] \{\dot{H}_i^{(e)}\} \quad (5.13)$$

If equivalent set of approximated capillary tension head and time derivative of the approximated capillary tension head are substituted into the Equation (5.11), the residual equation can be written as

$$\begin{aligned} \{R^{(e)}\} = & \int_{V^{(e)}} \left\{ \left(\frac{\partial N_i^{(e)}}{\partial x} \hat{K}_x^{(e)} \frac{\partial N_i^{(e)}}{\partial x} + \frac{\partial N_i^{(e)}}{\partial y} \hat{K}_y^{(e)} \frac{\partial N_i^{(e)}}{\partial y} + \frac{\partial N_i^{(e)}}{\partial z} \hat{K}_z^{(e)} \frac{\partial N_i^{(e)}}{\partial z} \right) \{H_i^{(e)}\} \right\} dV \\ & + \int_{V^{(e)}} N_i^{(e)} \hat{C}^{(e)} N_i^{(e)} \{\dot{H}_i^{(e)}\} dV - \int_{V^{(e)}} N_i^{(e)} \frac{\partial \hat{K}_z^{(e)}}{\partial z} dV - Q_i^{(e)} \end{aligned} \quad (5.14)$$

Equation (5.14) is written in the matrix form as

$$\{R^{(e)}\} = [\hat{p}^{(e)}] \{\dot{H}_i^{(e)}\} + [\hat{K}^{(e)}] \{H_i^{(e)}\} - \{F_i^{(e)}\} \quad (5.15)$$

where $[\hat{p}^{(e)}]$ is the effective capacitance matrix which is equal to

$$[p^{(e)}] = \int_{V^{(e)}} [N_i^{(e)}] \{\hat{C}^{(e)}\} [N_i^{(e)}] dV \quad (5.16)$$

$[\hat{K}^{(e)}]$ is the effective permeability matrix which is equal to

$$\begin{aligned}
[\hat{K}^{(e)}] = \int_{V^{(e)}} & \left(\frac{\partial [N_i^{(e)}]}{\partial x} \{ \hat{K}_x^{(e)} \} \frac{\partial [N_i^{(e)}]^T}{\partial x} + \frac{\partial [N_i^{(e)}]}{\partial y} \{ \hat{K}_y^{(e)} \} \frac{\partial [N_i^{(e)}]^T}{\partial y} \right. \\
& \left. + \frac{\partial [N_i^{(e)}]}{\partial z} \{ \hat{K}_z^{(e)} \} \frac{\partial [N_i^{(e)}]^T}{\partial z} \right) dV
\end{aligned} \tag{5.17}$$

and $\{F_i^{(e)}\}$ is the force vector which include gravitational force and Neumann boundary condition

$$[F_i^{(e)}] = \int_A [N_i^{(e)}]^T \frac{\partial \{ \hat{K}_z^{(e)} \}}{\partial z} dA + Q_i^{(e)} \tag{5.18}$$

Evaluation of the effective permeability and effective capacitance matrices and force vector necessitates the determination of the interpolation function for each node of every element. In the following section, the type of element and related interpolation functions that have been used in this work are described.

5.2.2 Element effective permeability and capacitance matrices

Linear triangular 3-node element and linear tetrahedral 4-node element are used in this work. They are the commonly used two-dimensional and three-dimensional elements. The interpolations for this type of elements were presented in the chapter 3. The element matrices for linear triangular and tetrahedral elements can be readily computed using equations (3.41) and (3.42) respectively.

Two-dimensional element matrix

The element effective conductivity matrix for the two dimensional problems is written in an expanded matrix form as

$$\left[\hat{K}^{(e)} \right] = \iint_{A^{(e)}} \begin{bmatrix} \frac{\partial N_1^{(e)}}{\partial x} & \frac{\partial N_1^{(e)}}{\partial z} \\ \vdots & \vdots \\ \frac{\partial N_n^{(e)}}{\partial x} & \frac{\partial N_n^{(e)}}{\partial z} \end{bmatrix} \begin{bmatrix} \hat{K}_x^{(e)} & 0 \\ 0 & \hat{K}_z^{(e)} \end{bmatrix} \begin{bmatrix} \frac{\partial N_1^{(e)}}{\partial x} & \dots & \frac{\partial N_n^{(e)}}{\partial x} \\ \frac{\partial N_1^{(e)}}{\partial z} & \dots & \frac{\partial N_n^{(e)}}{\partial z} \end{bmatrix} dx dy \quad (5.19)$$

where, n is number of nodes per element.

Then, using the interpolation functions and Equation (3.41) the first array of the effective conductivity matrix for each element can be evaluated as

$$\begin{aligned} \left[\hat{K}^{(e)} \right] &= \iint_{A^{(e)}} \frac{\partial N_1^{(e)}}{\partial x} \hat{K}_x^{(e)} \frac{\partial N_1^{(e)}}{\partial x} dx dz + \iint_{A^{(e)}} \frac{\partial N_1^{(e)}}{\partial z} \hat{K}_z^{(e)} \frac{\partial N_1^{(e)}}{\partial z} dx dz \\ &= \frac{b_i^2}{4A^{(e)}} \hat{K}_x^{(e)} + \frac{c_i^2}{4A^{(e)}} \hat{K}_z^{(e)} \end{aligned} \quad (5.20)$$

Other arrays of the matrix can be evaluated in a similar way. The final result is

$$\left[\hat{K}^{(e)} \right] = \frac{\hat{K}_x^{(e)}}{4A^{(e)}} \begin{bmatrix} b_i^2 & b_i b_j & b_i b_k \\ b_j b_i & b_j^2 & b_j b_k \\ b_k b_i & b_k b_j & b_k^2 \end{bmatrix} + \frac{\hat{K}_z^{(e)}}{4A^{(e)}} \begin{bmatrix} c_i^2 & c_i c_j & c_i c_k \\ c_j c_i & c_j^2 & c_j c_k \\ c_k c_i & c_k c_j & c_k^2 \end{bmatrix} \quad (5.21)$$

A similar procedure can be used to compute the effective capacitance matrix. The result is

$$\left[\hat{p}^{(e)} \right] = \frac{\hat{C}^{(e)} A^{(e)}}{12} \begin{bmatrix} 2 & 1 & 1 \\ 1 & 2 & 1 \\ 1 & 1 & 2 \end{bmatrix} \quad (5.22)$$

Three-dimensional element matrix

The element effective conductivity matrix for three dimensional problems is written in an expanded matrix form as

$$[\hat{K}^{(e)}] = \int \int \int_{V^{(e)}} \begin{bmatrix} \frac{\partial N_1^{(e)}}{\partial x} & \frac{\partial N_1^{(e)}}{\partial y} & \frac{\partial N_1^{(e)}}{\partial z} \\ \vdots & \vdots & \vdots \\ \frac{\partial N_n^{(e)}}{\partial x} & \frac{\partial N_n^{(e)}}{\partial y} & \frac{\partial N_n^{(e)}}{\partial z} \end{bmatrix} \begin{bmatrix} \hat{K}_x^{(e)} & 0 & 0 \\ 0 & \hat{K}_y^{(e)} & 0 \\ 0 & 0 & \hat{K}_z^{(e)} \end{bmatrix} \begin{bmatrix} \frac{\partial N_1^{(e)}}{\partial x} \dots \frac{\partial N_n^{(e)}}{\partial x} \\ \frac{\partial N_1^{(e)}}{\partial y} \dots \frac{\partial N_n^{(e)}}{\partial y} \\ \frac{\partial N_1^{(e)}}{\partial z} \dots \frac{\partial N_n^{(e)}}{\partial z} \end{bmatrix} dx dy dz \quad (5.23)$$

Using the interpolation functions and Equation (3.42) the first array of the effective conductivity matrix for each element can be evaluated as

$$\begin{aligned} [\hat{K}^{(e)}] &= \int \int \int_{V^{(e)}} \frac{\partial N_1^{(e)}}{\partial x} \hat{K}_x^{(e)} \frac{\partial N_1^{(e)}}{\partial x} dx dy dz + \int \int \int_{V^{(e)}} \frac{\partial N_1^{(e)}}{\partial z} \hat{K}_z^{(e)} \frac{\partial N_1^{(e)}}{\partial z} dx dy dz \\ &+ \int \int \int_{V^{(e)}} \frac{\partial N_1^{(e)}}{\partial y} \hat{K}_y^{(e)} \frac{\partial N_1^{(e)}}{\partial y} dx dy dz \end{aligned} \quad (5.24)$$

and so on for each array of the matrix. The final result is

$$\begin{aligned} [\hat{K}^{(e)}] &= \frac{\hat{K}_x^{(e)}}{6V^{(e)}} \begin{bmatrix} m_{ji}m_{ji} & m_{ji}m_{jj} & m_{ji}m_{jk} \\ m_{jj}m_{ji} & m_{jj}m_{jj} & m_{jj}m_{jk} \\ m_{jk}m_{ji} & m_{jk}m_{jj} & m_{jk}m_{jk} \\ m_{jm}m_{ji} & m_{jm}m_{jj} & m_{jm}m_{jk} \end{bmatrix} + \\ &\frac{\hat{K}_y^{(e)}}{6V^{(e)}} \begin{bmatrix} m_{ki}m_{ki} & m_{ki}m_{kj} & m_{ki}m_{kk} \\ m_{kj}m_{ki} & m_{kj}m_{kj} & m_{kj}m_{kk} \\ m_{kk}m_{ki} & m_{kk}m_{kj} & m_{kk}m_{kk} \\ m_{km}m_{ki} & m_{km}m_{kj} & m_{km}m_{kk} \end{bmatrix} + \\ &\frac{\hat{K}_z^{(e)}}{6V^{(e)}} \begin{bmatrix} m_{mi}m_{ki} & m_{mi}m_{kj} & m_{mi}m_{kk} \\ m_{mj}m_{ki} & m_{mj}m_{kj} & m_{mj}m_{kk} \\ m_{mk}m_{ki} & m_{mk}m_{kj} & m_{mk}m_{kk} \\ m_{mm}m_{ki} & m_{mm}m_{kj} & m_{mm}m_{kk} \end{bmatrix} \end{aligned} \quad (5.25)$$

A similar procedure can be used to compute the effective capacitance matrix. The result is

$$[\hat{P}^{(e)}] = \frac{\hat{C}^{(e)}V^{(e)}}{20} \begin{bmatrix} 2 & 1 & 1 & 1 \\ 1 & 2 & 1 & 1 \\ 1 & 1 & 2 & 1 \\ 1 & 1 & 1 & 2 \end{bmatrix} \quad (5.26)$$

5.2.3 Global effective permeability and capacitance matrices

Summing up the weighted residuals of elements over the domain and minimising them to zero yield

$$\sum_e \left(\int_{V^{(e)}} \left\{ \left(\frac{\partial N_i^{(e)}}{\partial x} \hat{K}_x^{(e)} \frac{\partial N_i^{(e)}}{\partial x} + \frac{\partial N_i^{(e)}}{\partial z} \hat{K}_y^{(e)} \frac{\partial N_i^{(e)}}{\partial z} \right) \{H_i^{(e)}\} + N_i^{(e)} \hat{C}^{(e)} N_i^{(e)} \{ \dot{H}_i^{(e)} \} - N_i^{(e)} \frac{\partial \hat{K}_x^{(e)}}{\partial x} \right\} dV - Q_i^{(e)} \right) = 0 \quad (5.27)$$

Equation (5.27) can be written in the matrix form as

$$\sum_e \left[[\hat{p}^{(e)}] \{ \dot{H}_i^{(e)} \} + [\hat{K}^{(e)}] \{ H_i^{(e)} \} - \{ F_i^{(e)} \} \right] = 0 \quad (5.28)$$

Thus, the general finite element formulation for groundwater flow is

$$[\hat{p}] \{ \dot{H} \} + [\hat{K}] \{ H \} - \{ F \} = \{ 0 \} \quad (5.29)$$

where $[\hat{p}]$ is the global effective capacitance matrix and $[\hat{K}]$ is the global effective permeability matrix over the problem domain.

5.2.4 Imposition of the boundary conditions

The boundary conditions of the problem can be as specified flow (Neumann boundary conditions) or specified head (Dirichlet boundary conditions). Dirichlet boundary conditions are directly introduced in the final system of equations.

$$H(x, y, z, t)_\Gamma = H_\Gamma \quad (5.30)$$

Neumann boundary conditions are imposed by the global Force vector $\{F\}$. The force vector term is associated with gravitational force and water flow flux $Q_i^{(e)}$. For the adjacent elements on the interior of the mesh $Q_i^{(e)}$ will have opposite signs cancelling the contribution of this term for the two elements for the node(s) they share. But, for the elements on the exterior of the mesh this term will be used to represent specific rates of groundwater flow as

$$q(x, y, z, t)_{\Gamma} = q_n \quad (3.31)$$

5.3 Finite difference formulation for groundwater flow

Numerical evaluation of transient equation is completed using time discretisation of effective matrices in time domain. Applying the finite difference approach to the equation yields the final form of the equation system for evaluation of pressure heads in the problem domain as

$$\left([\hat{P}] + \Delta t [\hat{K}] \right) \{H\}_{t+\Delta t} = [\hat{P}] \{H\}_t + \Delta t \{F\}_{t+\Delta t} \quad (5.32)$$

where, subscript t and $t + \Delta t$ represent time level and Δt is time increment.

5.4 Hydraulic gradient

In this section, vertical and horizontal hydraulic gradients for the triangular element are evaluated. According to the shape function approximation, the partial derivative of hydraulic head with respect to the x direction is given by

$$\frac{\partial H}{\partial x} = \sum_{i=1}^N H_i \frac{\partial N_i}{\partial x} \quad (5.33)$$

Spatial derivatives of interpolation functions can be written with respect to the area coordinates of the element as

$$\frac{\partial N_i}{\partial x} = \left(\frac{\partial N_i}{\partial L_1} \frac{\partial L_1}{\partial x} + \frac{\partial N_i}{\partial L_2} \frac{\partial L_2}{\partial x} + \frac{\partial N_i}{\partial L_3} \frac{\partial L_3}{\partial x} \right) \quad (5.34)$$

$$\frac{\partial L_3}{\partial x} = -\frac{\partial L_1}{\partial x} - \frac{\partial L_2}{\partial x} \quad (5.35)$$

$$\frac{\partial L_1}{\partial x} = (z_3 - z_2) / 2A \quad (5.36)$$

$$\frac{\partial L_2}{\partial x} = (z_3 - z_1) / 2A \quad (5.37)$$

Substituting Equations (5.35) to (5.37) into the Equation (5.34) yields

$$\begin{aligned} \left(\frac{\partial H}{\partial x} \right)^{(e)} &= \sum_{i=1}^n H_i \left[\left(\frac{\partial N_i}{\partial L_1} - \frac{\partial N_i}{\partial L_3} \right) \frac{\partial L_1}{\partial x} + \left(\frac{\partial N_i}{\partial L_2} - \frac{\partial N_i}{\partial L_3} \right) \frac{\partial L_2}{\partial x} \right] \\ &= H_1 \left[\left(\frac{\partial N_1}{\partial L_1} - \frac{\partial N_1}{\partial L_3} \right) \frac{\partial L_1}{\partial x} + \left(\frac{\partial N_1}{\partial L_2} - \frac{\partial N_1}{\partial L_3} \right) \frac{\partial L_2}{\partial x} \right] \\ &\quad + H_2 \left[\left(\frac{\partial N_2}{\partial L_1} - \frac{\partial N_2}{\partial L_3} \right) \frac{\partial L_1}{\partial x} + \left(\frac{\partial N_2}{\partial L_2} - \frac{\partial N_2}{\partial L_3} \right) \frac{\partial L_2}{\partial x} \right] \\ &\quad + H_3 \left[\left(\frac{\partial N_3}{\partial L_1} - \frac{\partial N_3}{\partial L_3} \right) \frac{\partial L_1}{\partial x} + \left(\frac{\partial N_3}{\partial L_2} - \frac{\partial N_3}{\partial L_3} \right) \frac{\partial L_2}{\partial x} \right] \\ &= [H_1 - H_3] \frac{\partial L_1}{\partial x} + [H_2 - H_3] \frac{\partial L_2}{\partial x} \\ &= [H_1 - H_3] \left(\frac{z_2 - z_3}{2A^{(e)}} \right) + [H_2 - H_3] \left(\frac{z_3 - z_1}{2A^{(e)}} \right) \end{aligned} \quad (5.38)$$

Following a similar procedure, the vertical hydraulic gradient is evaluated as

$$\begin{aligned} \left(\frac{\partial H}{\partial z} \right)^{(e)} &= [H_1 - H_3] \frac{\partial L_1}{\partial z} + [H_2 - H_3] \frac{\partial L_2}{\partial z} \\ &= [H_1 - H_3] \left(\frac{x_3 - x_2}{2A^{(e)}} \right) + [H_2 - H_3] \left(\frac{x_1 - x_3}{2A^{(e)}} \right) \end{aligned} \quad (5.39)$$

5.5 Groundwater velocity

The parameters appearing in the contaminant transport equation include groundwater velocity and the coefficient of dispersion. Also the coefficient of dispersion is a function of velocity. This implies that the groundwater velocity is a crucial variable in contaminant transport modelling in an aquifer. The water flow velocity is calculated based on the hydraulic gradient and hydraulic conductivity. The mathematical equation for the estimation of water flow velocity in porous media is based on Darcy's law

$$v_i = -\frac{K_i}{n} \frac{\partial H}{\partial x_i} \quad i = x, y, z \quad (5.40)$$

Therefore, groundwater velocity for each element in the problem domain is evaluated by substituting the effective hydraulic conductivity and hydraulic gradient of each element in Darcy's equation as

$$v_x = -\frac{\hat{K}_x^{(e)}}{n} \left[[H_1 - H_3] \left(\frac{z_2 - z_3}{2A^{(e)}} \right) + [H_2 - H_3] \left(\frac{z_3 - z_1}{2A^{(e)}} \right) \right] \quad (5.41)$$

$$v_z = -\frac{\hat{K}_z^{(e)}}{n} \left[[H_1 - H_3] \left(\frac{x_3 - x_2}{2A^{(e)}} \right) + [H_2 - H_3] \left(\frac{x_1 - x_3}{2A^{(e)}} \right) \right] \quad (5.42)$$

5.6 FE formulation for steady-state solute transport

The stochastic partial differential equation for steady-state solute transport through an unsaturated soil is

$$\frac{\partial(\bar{c}q_i)}{\partial x_i} = \frac{\partial}{\partial x_i} \left[\hat{D}_{ij} \frac{\partial \bar{c}}{\partial x_j} \right] \quad (5.43)$$

where $\hat{D}_{ij} = E_{ij} + A_{ij}q$.

The three-dimensional form of the Equation (5.43) is

$$\begin{aligned} \left(\frac{\partial(\bar{q}_x \bar{c})}{\partial x} + \frac{\partial(\bar{q}_y \bar{c})}{\partial y} + \frac{\partial(\bar{q}_z \bar{c})}{\partial z} \right) &= \frac{\partial}{\partial x} \left[\hat{D}_{xx} \frac{\partial \bar{c}}{\partial x} + \hat{D}_{xy} \frac{\partial \bar{c}}{\partial y} + \hat{D}_{xz} \frac{\partial \bar{c}}{\partial z} \right] \\ &+ \frac{\partial}{\partial y} \left[\hat{D}_{yx} \frac{\partial \bar{c}}{\partial x} + \hat{D}_{yy} \frac{\partial \bar{c}}{\partial y} + \hat{D}_{yz} \frac{\partial \bar{c}}{\partial z} \right] \\ &+ \frac{\partial}{\partial z} \left[\hat{D}_{zx} \frac{\partial \bar{c}}{\partial x} + \hat{D}_{zy} \frac{\partial \bar{c}}{\partial y} + \hat{D}_{zz} \frac{\partial \bar{c}}{\partial z} \right] \end{aligned} \quad (5.44)$$

Mean solute concentration is the unknown variable of the Equation (5.44). A procedure similar to the one used for the flow, is employed for extracting finite element equation for solute transport. An approximate solution of this variable is defined in terms of its nodal values and associated nodal shape functions as

$$\hat{c}(x, y, z, t) = \sum_{i=1}^n N_i(x, y, z) \bar{c}_i(t) \quad (5.45)$$

where $\hat{c}(x, y, z, t)$ is the approximated value of solute concentration at any location of the problem, N_i is the interpolation function at node i , \bar{c}_i is the mean solute concentration value at node i , and n is the number of nodes in the mesh. The approximated value does not exactly satisfy Equation (5.44). Based on the weighting residual method, weighted average of residuals at nodes, produced by substituting approximated solution into Equation (5.44) over the solution domain is forced to be zero. Then,

$$\begin{aligned} \iiint_{\Omega} -w_i \left(\frac{\partial(\bar{q}_x \hat{c})}{\partial x} + \frac{\partial(\bar{q}_y \hat{c})}{\partial y} + \frac{\partial(\bar{q}_z \hat{c})}{\partial z} \right. \\ \left. + \frac{\partial}{\partial x} \left[\hat{D}_{xx} \frac{\partial \hat{c}}{\partial x} + \hat{D}_{xy} \frac{\partial \hat{c}}{\partial y} + \hat{D}_{xz} \frac{\partial \hat{c}}{\partial z} \right] \right. \\ \left. + \frac{\partial}{\partial y} \left[\hat{D}_{yy} \frac{\partial \hat{c}}{\partial x} + \hat{D}_{yx} \frac{\partial \hat{c}}{\partial y} + \hat{D}_{yz} \frac{\partial \hat{c}}{\partial z} \right] \right. \\ \left. + \frac{\partial}{\partial z} \left[\hat{D}_{zx} \frac{\partial \hat{c}}{\partial x} + \hat{D}_{zy} \frac{\partial \hat{c}}{\partial y} + \hat{D}_{zz} \frac{\partial \hat{c}}{\partial z} \right] \right) d\Omega = 0 \end{aligned} \quad (5.46)$$

5.6.1 Element weighted residual for steady-state solute transport

The contribution of any element, e , to the residual at node i to which the element is jointed is acquired by substituting the approximated mean solute concentration and other related hydraulic parameters of each element into the Equation (5.46).

$$\begin{aligned}
 R^{(e)} = & - \int_{V^{(e)}} W_i^{(e)} \left\{ - \left[\frac{\partial(\bar{q}_x^{(e)} \hat{c})}{\partial x} + \frac{\partial(\bar{q}_y^{(e)} \hat{c})}{\partial y} + \frac{\partial(\bar{q}_z^{(e)} \hat{c})}{\partial z} \right] \right. \\
 & - \frac{\partial}{\partial x} \left(\hat{D}_{xx}^{(e)} \frac{\partial \hat{c}}{\partial x} + \hat{D}_{xy}^{(e)} \frac{\partial \hat{c}}{\partial y} + \hat{D}_{xz}^{(e)} \frac{\partial \hat{c}}{\partial z} \right) \\
 & - \frac{\partial}{\partial y} \left(\hat{D}_{yx}^{(e)} \frac{\partial \hat{c}}{\partial x} + \hat{D}_{yy}^{(e)} \frac{\partial \hat{c}}{\partial y} + \hat{D}_{yz}^{(e)} \frac{\partial \hat{c}}{\partial z} \right) \\
 & \left. - \frac{\partial}{\partial z} \left(\hat{D}_{zx}^{(e)} \frac{\partial \hat{c}}{\partial x} + \hat{D}_{zy}^{(e)} \frac{\partial \hat{c}}{\partial y} + \hat{D}_{zz}^{(e)} \frac{\partial \hat{c}}{\partial z} \right) \right\} dV
 \end{aligned} \tag{5.47}$$

Using Galerkin's method, Equation (5.47) can be written as

$$\begin{aligned}
 R^{(e)} = & - \int_{V^{(e)}} N_i^{(e)} \left\{ - \left[\frac{\partial(\bar{q}_x^{(e)} \hat{c})}{\partial x} + \frac{\partial(\bar{q}_y^{(e)} \hat{c})}{\partial y} + \frac{\partial(\bar{q}_z^{(e)} \hat{c})}{\partial z} \right] \right. \\
 & - \frac{\partial}{\partial x} \left(\hat{D}_{xx}^{(e)} \frac{\partial \hat{c}}{\partial x} + \hat{D}_{xy}^{(e)} \frac{\partial \hat{c}}{\partial y} + \hat{D}_{xz}^{(e)} \frac{\partial \hat{c}}{\partial z} \right) \\
 & - \frac{\partial}{\partial y} \left(\hat{D}_{yx}^{(e)} \frac{\partial \hat{c}}{\partial x} + \hat{D}_{yy}^{(e)} \frac{\partial \hat{c}}{\partial y} + \hat{D}_{yz}^{(e)} \frac{\partial \hat{c}}{\partial z} \right) \\
 & \left. - \frac{\partial}{\partial z} \left(\hat{D}_{zx}^{(e)} \frac{\partial \hat{c}}{\partial x} + \hat{D}_{zy}^{(e)} \frac{\partial \hat{c}}{\partial y} + \hat{D}_{zz}^{(e)} \frac{\partial \hat{c}}{\partial z} \right) \right\} dV
 \end{aligned} \tag{5.48}$$

Because of linearity of solute concentration with respect to x , y or z , $\frac{\partial^2 \hat{c}}{\partial x^2}$, $\frac{\partial^2 \hat{c}}{\partial y^2}$ and

$\frac{\partial^2 \hat{c}}{\partial z^2}$ are not defined. However, the approximate solution does have a continuous first

derivative; therefore Equation (5.48) can be evaluated if it is rewritten in terms of $\frac{\partial \hat{c}}{\partial x}$,

$\frac{\partial \hat{c}}{\partial y}$ and $\frac{\partial \hat{c}}{\partial z}$.

By integration by parts, the second-order derivative terms can be written as

$$\begin{aligned}
& - \int_{V^{(e)}} N_i^{(e)} \left\{ \frac{\partial}{\partial x} \left[\hat{D}_{xx}^{(e)} \frac{\partial \hat{c}}{\partial x} \right] + \frac{\partial}{\partial x} \left[\hat{D}_{xy}^{(e)} \frac{\partial \hat{c}}{\partial y} \right] + \frac{\partial}{\partial x} \left[\hat{D}_{xz}^{(e)} \frac{\partial \hat{c}}{\partial z} \right] \right. \\
& \quad + \frac{\partial}{\partial y} \left[\hat{D}_{yx}^{(e)} \frac{\partial \hat{c}}{\partial x} \right] + \frac{\partial}{\partial y} \left[\hat{D}_{yy}^{(e)} \frac{\partial \hat{c}}{\partial y} \right] + \frac{\partial}{\partial y} \left[\hat{D}_{yz}^{(e)} \frac{\partial \hat{c}}{\partial z} \right] \\
& \quad \left. + \frac{\partial}{\partial z} \left[\hat{D}_{zx}^{(e)} \frac{\partial \hat{c}}{\partial x} \right] + \frac{\partial}{\partial z} \left[\hat{D}_{zy}^{(e)} \frac{\partial \hat{c}}{\partial y} \right] + \frac{\partial}{\partial z} \left[\hat{D}_{zz}^{(e)} \frac{\partial \hat{c}}{\partial z} \right] \right\} dV = \\
& - \int_{V^{(e)}} \left\{ \hat{D}_{xx}^{(e)} \left(\frac{\partial N_i^{(e)}}{\partial x} \right) \frac{\partial \hat{c}}{\partial x} - \hat{D}_{xx}^{(e)} \frac{\partial}{\partial x} \left(N_i^{(e)} \frac{\partial \hat{c}}{\partial x} \right) + \right. \\
& \quad \hat{D}_{xy}^{(e)} \left(\frac{\partial N_i^{(e)}}{\partial x} \right) \frac{\partial \hat{c}}{\partial y} - \hat{D}_{xy}^{(e)} \frac{\partial}{\partial x} \left(N_i^{(e)} \frac{\partial \hat{c}}{\partial y} \right) + \\
& \quad \hat{D}_{xz}^{(e)} \left(\frac{\partial N_i^{(e)}}{\partial x} \right) \frac{\partial \hat{c}}{\partial z} - \hat{D}_{xz}^{(e)} \frac{\partial}{\partial x} \left(N_i^{(e)} \frac{\partial \hat{c}}{\partial z} \right) + \\
& \quad \hat{D}_{yx}^{(e)} \left(\frac{\partial N_i^{(e)}}{\partial y} \right) \frac{\partial \hat{c}}{\partial x} - \hat{D}_{yx}^{(e)} \frac{\partial}{\partial y} \left(N_i^{(e)} \frac{\partial \hat{c}}{\partial x} \right) + \\
& \quad \hat{D}_{yy}^{(e)} \left(\frac{\partial N_i^{(e)}}{\partial y} \right) \frac{\partial \hat{c}}{\partial y} - \hat{D}_{yy}^{(e)} \frac{\partial}{\partial y} \left(N_i^{(e)} \frac{\partial \hat{c}}{\partial y} \right) + \\
& \quad \hat{D}_{yz}^{(e)} \left(\frac{\partial N_i^{(e)}}{\partial y} \right) \frac{\partial \hat{c}}{\partial z} - \hat{D}_{yz}^{(e)} \frac{\partial}{\partial y} \left(N_i^{(e)} \frac{\partial \hat{c}}{\partial z} \right) + \\
& \quad \hat{D}_{zx}^{(e)} \left(\frac{\partial N_i^{(e)}}{\partial z} \right) \frac{\partial \hat{c}}{\partial x} - \hat{D}_{zx}^{(e)} \frac{\partial}{\partial z} \left(N_i^{(e)} \frac{\partial \hat{c}}{\partial x} \right) + \\
& \quad \hat{D}_{zy}^{(e)} \left(\frac{\partial N_i^{(e)}}{\partial z} \right) \frac{\partial \hat{c}}{\partial y} - \hat{D}_{zy}^{(e)} \frac{\partial}{\partial z} \left(N_i^{(e)} \frac{\partial \hat{c}}{\partial y} \right) + \\
& \quad \left. \hat{D}_{zz}^{(e)} \left(\frac{\partial N_i^{(e)}}{\partial z} \right) \frac{\partial \hat{c}}{\partial z} - \hat{D}_{zz}^{(e)} \frac{\partial}{\partial z} \left(N_i^{(e)} \frac{\partial \hat{c}}{\partial z} \right) \right\} dV =
\end{aligned} \tag{5.49}$$

Applying Green's theorem to Equation (5.49) and substituting the resulted equation into the residual Equation (5.48), yields

$$\begin{aligned}
 R^{(e)} = - \int_{V^{(e)}} & \left\{ -N_i^{(e)} \left(\frac{\partial (\bar{q}_x^{(e)} \hat{c})}{\partial x} \right) - N_i^{(e)} \left(\frac{\partial (\bar{q}_y^{(e)} \hat{c})}{\partial y} \right) - N_i^{(e)} \left(\frac{\partial (\bar{q}_z^{(e)} \hat{c})}{\partial z} \right) + \right. \\
 & \hat{D}_{xx}^{(e)} \left(\frac{\partial N_i^{(e)}}{\partial x} \right) \frac{\partial \hat{c}}{\partial x} + \hat{D}_{xy}^{(e)} \left(\frac{\partial N_i^{(e)}}{\partial x} \right) \frac{\partial \hat{c}}{\partial y} + \hat{D}_{xz}^{(e)} \left(\frac{\partial N_i^{(e)}}{\partial x} \right) \frac{\partial \hat{c}}{\partial z} + \\
 & \hat{D}_{yx}^{(e)} \left(\frac{\partial N_i^{(e)}}{\partial y} \right) \frac{\partial \hat{c}}{\partial x} + \hat{D}_{yy}^{(e)} \left(\frac{\partial N_i^{(e)}}{\partial y} \right) \frac{\partial \hat{c}}{\partial y} + \hat{D}_{yz}^{(e)} \left(\frac{\partial N_i^{(e)}}{\partial y} \right) \frac{\partial \hat{c}}{\partial z} + \\
 & \left. \hat{D}_{zx}^{(e)} \left(\frac{\partial N_i^{(e)}}{\partial z} \right) \frac{\partial \hat{c}}{\partial x} + \hat{D}_{zy}^{(e)} \left(\frac{\partial N_i^{(e)}}{\partial z} \right) \frac{\partial \hat{c}}{\partial y} + \hat{D}_{zz}^{(e)} \left(\frac{\partial N_i^{(e)}}{\partial z} \right) \frac{\partial \hat{c}}{\partial z} \right\} dV - f_i^{(e)}
 \end{aligned} \tag{5.50}$$

where,

$$\begin{aligned}
 f_i^{(e)} = & \int_{\Gamma_{yz}} \left(N_i^{(e)} (-\hat{D}_{xx}^{(e)}) \frac{\partial \hat{c}}{\partial x} + N_i^{(e)} (-\hat{D}_{xy}^{(e)}) \frac{\partial \hat{c}}{\partial y} + N_i^{(e)} (-\hat{D}_{xz}^{(e)}) \frac{\partial \hat{c}}{\partial z} \right) dydz \\
 & + \int_{\Gamma_{xz}} \left(N_i^{(e)} (-\hat{D}_{yx}^{(e)}) \frac{\partial \hat{c}}{\partial x} + N_i^{(e)} (-\hat{D}_{yy}^{(e)}) \frac{\partial \hat{c}}{\partial y} + N_i^{(e)} (-\hat{D}_{yz}^{(e)}) \frac{\partial \hat{c}}{\partial z} \right) dx dz \\
 & + \int_{\Gamma_{yx}} \left(N_i^{(e)} (-\hat{D}_{zx}^{(e)}) \frac{\partial \hat{c}}{\partial x} + N_i^{(e)} (-\hat{D}_{zy}^{(e)}) \frac{\partial \hat{c}}{\partial y} + N_i^{(e)} (-\hat{D}_{zz}^{(e)}) \frac{\partial \hat{c}}{\partial z} \right) dy dx
 \end{aligned} \tag{5.51}$$

Equation (5.51) represent the solute sink/source across the element's surface. This term in equation (5.50) is equal to zero for the internal elements and applied as solute flux for the boundary elements.

Over each element, the element mean solute concentration is approximated by polynomial shape functions relating it to its nodal values as

$$\hat{c}^{(e)} = [N_i^{(e)}] \{ \bar{c}_i \} \tag{5.52}$$

Substituting Equation (5.52) into the Equation (5.50), yields

$$\begin{aligned}
R^{(e)} = - \int_{V^{(e)}} \left\{ \left[N_i^{(e)} \right] \bar{q}_x^{(e)} \frac{\partial [N_i^{(e)}]}{\partial x} + [N_i^{(e)}] \bar{q}_y^{(e)} \frac{\partial [N_i^{(e)}]}{\partial y} + [N_i^{(e)}] \bar{q}_z^{(e)} \frac{\partial [N_i^{(e)}]}{\partial z} + \right. \\
\left. \left(\frac{\partial [N_i^{(e)}]}{\partial x} \right) \hat{D}_{xx}^{(e)} \frac{\partial [N_i^{(e)}]}{\partial x} + \frac{\partial [N_i^{(e)}]}{\partial x} \hat{D}_{xy}^{(e)} \frac{\partial [N_i^{(e)}]}{\partial y} + \frac{\partial [N_i^{(e)}]}{\partial x} \hat{D}_{xz}^{(e)} \frac{\partial [N_i^{(e)}]}{\partial z} \right. \\
\left. \frac{\partial [N_i^{(e)}]}{\partial y} \hat{D}_{yx}^{(e)} \frac{\partial [N_i^{(e)}]}{\partial x} + \left(\frac{\partial [N_i^{(e)}]}{\partial y} \right) \hat{D}_{yy}^{(e)} \frac{\partial [N_i^{(e)}]}{\partial y} + \frac{\partial [N_i^{(e)}]}{\partial y} \hat{D}_{yz}^{(e)} \frac{\partial [N_i^{(e)}]}{\partial z} \right. \\
\left. \frac{\partial [N_i^{(e)}]}{\partial z} \hat{D}_{zx}^{(e)} \frac{\partial [N_i^{(e)}]}{\partial x} + \frac{\partial [N_i^{(e)}]}{\partial z} \hat{D}_{zy}^{(e)} \frac{\partial [N_i^{(e)}]}{\partial y} + \frac{\partial [N_i^{(e)}]}{\partial z} \hat{D}_{zz}^{(e)} \frac{\partial [N_i^{(e)}]}{\partial z} \right) \{ \bar{c}_i \} \Big\} dV \\
- f_i^{(e)}
\end{aligned} \tag{5.53}$$

Equation (5.53) is written in the matrix form as

$$\{ R^{(e)} \} = [\hat{D}^{(e)}] \{ \bar{c} \} - \{ f^{(e)} \} \tag{5.54}$$

where $[\hat{D}^{(e)}]$ is the effective advective-dispersive matrix which is equal to

$$\begin{aligned}
[\hat{D}^{(e)}] = - \int_{V^{(e)}} \left\{ \left[N_i^{(e)} \right] \bar{q}_x^{(e)} \frac{\partial [N_i^{(e)}]}{\partial x} + [N_i^{(e)}] \bar{q}_y^{(e)} \frac{\partial [N_i^{(e)}]}{\partial y} + [N_i^{(e)}] \bar{q}_z^{(e)} \frac{\partial [N_i^{(e)}]}{\partial z} + \right. \\
\frac{\partial [N_i^{(e)}]}{\partial x} \hat{D}_{xx}^{(e)} \frac{\partial [N_i^{(e)}]}{\partial x} + \frac{\partial [N_i^{(e)}]}{\partial x} \hat{D}_{xy}^{(e)} \frac{\partial [N_i^{(e)}]}{\partial y} + \frac{\partial [N_i^{(e)}]}{\partial x} \hat{D}_{xz}^{(e)} \frac{\partial [N_i^{(e)}]}{\partial z} + \\
\frac{\partial [N_i^{(e)}]}{\partial y} \hat{D}_{yy}^{(e)} \frac{\partial [N_i^{(e)}]}{\partial x} + \frac{\partial [N_i^{(e)}]}{\partial y} \hat{D}_{yx}^{(e)} \frac{\partial [N_i^{(e)}]}{\partial y} + \frac{\partial [N_i^{(e)}]}{\partial y} \hat{D}_{yz}^{(e)} \frac{\partial [N_i^{(e)}]}{\partial z} + \\
\left. \frac{\partial [N_i^{(e)}]}{\partial z} \hat{D}_{zx}^{(e)} \frac{\partial [N_i^{(e)}]}{\partial x} + \frac{\partial [N_i^{(e)}]}{\partial z} \hat{D}_{zy}^{(e)} \frac{\partial [N_i^{(e)}]}{\partial y} + \frac{\partial [N_i^{(e)}]}{\partial z} \hat{D}_{zz}^{(e)} \frac{\partial [N_i^{(e)}]}{\partial z} \right\} dV
\end{aligned} \tag{5.55}$$

5.6.2 Element effective advective-dispersive matrix

Two-dimensional element matrix

The element effective advective-dispersive matrix for two dimensional problems is written in the expanded form as

$$\begin{aligned}
\left[\hat{D}^{(e)} \right] = & - \iint_{A^{(e)}} \left\{ \begin{array}{c} \left[\begin{array}{cc} \frac{\partial N_1^{(e)}}{\partial x} & \frac{\partial N_1^{(e)}}{\partial z} \\ \vdots & \vdots \\ \frac{\partial N_n^{(e)}}{\partial x} & \frac{\partial N_n^{(e)}}{\partial z} \end{array} \right] \left[\begin{array}{cc} \hat{D}_{xx}^{(e)} & \hat{D}_{xz}^{(e)} \\ \hat{D}_{zx}^{(e)} & \hat{D}_{zz}^{(e)} \end{array} \right] \left[\begin{array}{cc} \frac{\partial N_1^{(e)}}{\partial x} \dots \frac{\partial N_n^{(e)}}{\partial x} \\ \frac{\partial N_1^{(e)}}{\partial z} \dots \frac{\partial N_n^{(e)}}{\partial z} \end{array} \right] \\ + \\ \left[\begin{array}{cc} N_1^{(e)} & N_1^{(e)} \\ \vdots & \vdots \\ N_n^{(e)} & N_n^{(e)} \end{array} \right] \left[\begin{array}{cc} \hat{q}_{xx}^{(e)} & 0 \\ 0 & \hat{q}_{zz}^{(e)} \end{array} \right] \left[\begin{array}{cc} \frac{\partial N_1^{(e)}}{\partial x} \dots \frac{\partial N_n^{(e)}}{\partial x} \\ \frac{\partial N_1^{(e)}}{\partial z} \dots \frac{\partial N_n^{(e)}}{\partial z} \end{array} \right] \end{array} \right\} dx dz
\end{aligned} \tag{5.56}$$

Using interpolation functions and Equation (3.41) the arrays of the effective advective-dispersive matrix for each element can be evaluated as

$$\begin{aligned}
\left[\hat{D}^{(e)} \right] = & \frac{\hat{D}_{xx}^{(e)}}{4A^{(e)}} \begin{bmatrix} b_i^2 & b_i b_j & b_i b_k \\ b_j b_i & b_j^2 & b_j b_k \\ b_k b_i & b_k b_j & b_k^2 \end{bmatrix} + \frac{\hat{D}_{zz}^{(e)}}{4A^{(e)}} \begin{bmatrix} c_i^2 & c_i c_j & c_i c_k \\ c_j c_i & c_j^2 & c_j c_k \\ c_k c_i & c_k c_j & c_k^2 \end{bmatrix} + \\ & \frac{\hat{D}_{xz}^{(e)}}{4A^{(e)}} \begin{bmatrix} b_i c_i & b_i c_j & b_i c_k \\ b_j c_i & b_j c_j & b_j c_k \\ b_k c_i & b_k c_j & b_k c_k \end{bmatrix} + \frac{\hat{D}_{zx}^{(e)}}{4A^{(e)}} \begin{bmatrix} c_i b_i & c_i b_j & c_i b_k \\ c_j b_i & c_j b_j & c_j b_k \\ c_k b_i & c_k b_j & c_k b_k \end{bmatrix} + \\ & \frac{q_x^{(e)}}{6} \begin{bmatrix} b_i & b_j & b_k \\ b_i & b_j & b_k \\ b_i & b_j & b_k \end{bmatrix} + \frac{q_z^{(e)}}{6} \begin{bmatrix} c_i & c_j & c_k \\ c_i & c_j & c_k \\ c_i & c_j & c_k \end{bmatrix}
\end{aligned} \tag{5.57}$$

Three-dimensional element matrix

The element effective advective-dispersive matrix for two dimensional problems is written in the expanded form as

$$\begin{aligned}
 [\hat{D}^{(e)}] = & - \iint_{A^{(e)}} \left\{ \begin{array}{c} \frac{\partial N_1^{(e)}}{\partial x} \quad \frac{\partial N_1^{(e)}}{\partial y} \quad \frac{\partial N_1^{(e)}}{\partial z} \\ \vdots \quad \quad \quad \vdots \\ \frac{\partial N_n^{(e)}}{\partial x} \quad \frac{\partial N_n^{(e)}}{\partial y} \quad \frac{\partial N_n^{(e)}}{\partial z} \end{array} \right\} \begin{bmatrix} \hat{D}_{xx}^{(e)} & \hat{D}_{xy}^{(e)} & \hat{D}_{xz}^{(e)} \\ \hat{D}_{yx}^{(e)} & \hat{D}_{yy}^{(e)} & \hat{D}_{yz}^{(e)} \\ \hat{D}_{zx}^{(e)} & \hat{D}_{zy}^{(e)} & \hat{D}_{zz}^{(e)} \end{bmatrix} \left\{ \begin{array}{c} \frac{\partial N_1^{(e)}}{\partial x} \dots \frac{\partial N_n^{(e)}}{\partial x} \\ \frac{\partial N_1^{(e)}}{\partial y} \dots \frac{\partial N_n^{(e)}}{\partial y} \\ \frac{\partial N_1^{(e)}}{\partial z} \dots \frac{\partial N_n^{(e)}}{\partial z} \end{array} \right\} + \\
 & \left. \begin{array}{c} \begin{bmatrix} N_1^{(e)} & N_1^{(e)} & N_1^{(e)} \\ \vdots & \vdots & \vdots \\ N_n^{(e)} & N_n^{(e)} & N_n^{(e)} \end{bmatrix} \begin{bmatrix} \hat{q}_{xx}^{(e)} & 0 & 0 \\ 0 & \hat{q}_{zz}^{(e)} & 0 \\ 0 & 0 & \hat{q}_{xx}^{(e)} \end{bmatrix} \begin{bmatrix} \frac{\partial N_1^{(e)}}{\partial x} \dots \frac{\partial N_n^{(e)}}{\partial x} \\ \frac{\partial N_1^{(e)}}{\partial y} \dots \frac{\partial N_n^{(e)}}{\partial y} \\ \frac{\partial N_1^{(e)}}{\partial z} \dots \frac{\partial N_n^{(e)}}{\partial z} \end{bmatrix} \right\} dx dy dz \quad (5.58)
 \end{aligned}$$

Then, using interpolation functions and Equation (3.42) the arrays of the effective advective-dispersive matrix for each element can be evaluated as

$$\begin{aligned}
\left[\hat{D}^{(e)} \right] = & \frac{\hat{D}_{xx}^{(e)} \theta}{36V^{(e)}} \begin{bmatrix} m_{ji}^2 & m_{ji}m_{jj} & m_{ji}m_{jk} & m_{ji}m_{jm} \\ m_{jj}m_{ji} & m_{jj}^2 & m_{jj}m_{jk} & m_{jj}m_{jm} \\ m_{jk}m_{ji} & m_{jk}m_{jj} & m_{jk}^2 & m_{jk}m_{jm} \\ m_{jm}m_{ji} & m_{jm}m_{jj} & m_{jm}m_{jk} & m_{jm}^2 \end{bmatrix} + \\
& \frac{\hat{D}_{yy}^{(e)} \theta}{36V^{(e)}} \begin{bmatrix} m_{ki}^2 & m_{ki}m_{kj} & m_{ki}m_{kk} & m_{ki}m_{km} \\ m_{kj}m_{ki} & m_{kj}^2 & m_{kj}m_{kk} & m_{kj}m_{km} \\ m_{kk}m_{ki} & m_{kk}m_{kj} & m_{kk}^2 & m_{kk}m_{km} \\ m_{km}m_{ki} & m_{km}m_{kj} & m_{km}m_{kk} & m_{km}^2 \end{bmatrix} + \\
& \frac{\hat{D}_{zz}^{(e)} \theta}{36V^{(e)}} \begin{bmatrix} m_{mi}^2 & m_{mi}m_{mj} & m_{mi}m_{mk} & m_{mi}m_{mm} \\ m_{mj}m_{mi} & m_{mj}^2 & m_{mj}m_{mk} & m_{mj}m_{mm} \\ m_{mk}m_{mi} & m_{mk}m_{mj} & m_{mk}^2 & m_{mk}m_{mm} \\ m_{mm}m_{mi} & m_{mm}m_{mj} & m_{mm}m_{mk} & m_{mm}^2 \end{bmatrix} + \\
& \frac{\hat{D}_{yx}^{(e)}}{36V^{(e)}} \begin{bmatrix} m_{ki}m_{ji} & m_{ki}m_{jj} & m_{ki}m_{jk} & m_{ki}m_{jm} \\ m_{kj}m_{ji} & m_{kj}m_{jj} & m_{kj}m_{jk} & m_{kj}m_{jm} \\ m_{kk}m_{ji} & m_{kk}m_{jj} & m_{kk}m_{jk} & m_{kk}m_{jm} \\ m_{km}m_{ji} & m_{km}m_{jj} & m_{km}m_{jk} & m_{km}m_{jm} \end{bmatrix} + \\
& \frac{\hat{D}_{xy}^{(e)}}{36V^{(e)}} \begin{bmatrix} m_{ji}m_{ki} & m_{ji}m_{kj} & m_{ji}m_{kk} & m_{ji}m_{km} \\ m_{jj}m_{ki} & m_{jj}m_{kj} & m_{jj}m_{kk} & m_{jj}m_{km} \\ m_{jk}m_{ki} & m_{jk}m_{kj} & m_{jk}m_{kk} & m_{jk}m_{km} \\ m_{jm}m_{ki} & m_{jm}m_{kj} & m_{jm}m_{kk} & m_{jm}m_{km} \end{bmatrix} + \\
& \frac{\hat{D}_{yz}^{(e)}}{36V^{(e)}} \begin{bmatrix} m_{ki}m_{mi} & m_{ki}m_{mj} & m_{ki}m_{mk} & m_{ki}m_{mm} \\ m_{kj}m_{mi} & m_{kj}m_{mj} & m_{kj}m_{mk} & m_{kj}m_{mm} \\ m_{kk}m_{mi} & m_{kk}m_{mj} & m_{kk}m_{mk} & m_{kk}m_{mm} \\ m_{km}m_{mi} & m_{km}m_{mj} & m_{km}m_{mk} & m_{km}m_{mm} \end{bmatrix} + \\
& \frac{\hat{D}_{zy}^{(e)}}{36V^{(e)}} \begin{bmatrix} m_{mi}m_{ki} & m_{mi}m_{kj} & m_{mi}m_{kk} & m_{mi}m_{km} \\ m_{mj}m_{ki} & m_{mj}m_{kj} & m_{mj}m_{kk} & m_{mj}m_{km} \\ m_{mk}m_{ki} & m_{mk}m_{kj} & m_{mk}m_{kk} & m_{mk}m_{km} \\ m_{mm}m_{ki} & m_{mm}m_{kj} & m_{mm}m_{kk} & m_{mm}m_{km} \end{bmatrix} + \\
& \frac{\hat{D}_{xz}^{(e)}}{36V^{(e)}} \begin{bmatrix} m_{ji}m_{mi} & m_{ji}m_{mj} & m_{ji}m_{mk} & m_{ji}m_{mm} \\ m_{jj}m_{mi} & m_{jj}m_{mj} & m_{jj}m_{mk} & m_{jj}m_{mm} \\ m_{jk}m_{mi} & m_{jk}m_{mj} & m_{jk}m_{mk} & m_{jk}m_{mm} \\ m_{jm}m_{mi} & m_{jm}m_{mj} & m_{jm}m_{mk} & m_{jm}m_{mm} \end{bmatrix} +
\end{aligned} \tag{5.59}$$

$$\begin{aligned}
& \frac{\hat{D}_{zx}^{(e)}}{36V^{(e)}} \begin{bmatrix} m_{mi}m_{ji} & m_{mi}m_{jj} & m_{mi}m_{jk} & m_{mi}m_{jm} \\ m_{mj}m_{ji} & m_{mj}m_{jj} & m_{mj}m_{jk} & m_{mj}m_{jm} \\ m_{mk}m_{ji} & m_{mk}m_{jj} & m_{mk}m_{jk} & m_{mk}m_{jm} \\ m_{mm}m_{ji} & m_{mm}m_{jj} & m_{mm}m_{jk} & m_{mm}m_{jm} \end{bmatrix} + \\
& \frac{q_x^{(e)}}{24} \begin{bmatrix} m_{ji} & m_{jj} & m_{jk} & m_{jm} \\ m_{ji} & m_{jj} & m_{jk} & m_{jm} \\ m_{ji} & m_{jj} & m_{jk} & m_{jm} \\ m_{ji} & m_{jj} & m_{jk} & m_{jm} \end{bmatrix} + \\
& \frac{q_y^{(e)}}{24} \begin{bmatrix} m_{ki} & m_{kj} & m_{kk} & m_{km} \\ m_{ki} & m_{kj} & m_{kk} & m_{km} \\ m_{ki} & m_{kj} & m_{kk} & m_{km} \\ m_{ki} & m_{kj} & m_{kk} & m_{km} \end{bmatrix} + \\
& \frac{q_z^{(e)}}{24} \begin{bmatrix} m_{mi} & m_{mj} & m_{mk} & m_{mm} \\ m_{mi} & m_{mj} & m_{mk} & m_{mm} \\ m_{mi} & m_{mj} & m_{mk} & m_{mm} \\ m_{mi} & m_{mj} & m_{mk} & m_{mm} \end{bmatrix}
\end{aligned}$$

5.6.3 Global effective characteristics of domain

Summing up the weighted residuals of elements over the domain and minimising it to zero yield

$$\begin{aligned}
& \sum_e \left(- \int_{V^{(e)}} \left\{ \left([N_i^{(e)}] \bar{q}_x^{(e)} \frac{\partial [N_i^{(e)}]}{\partial x} \right) + [N_i^{(e)}] \bar{q}_y^{(e)} \frac{\partial [N_i^{(e)}]}{\partial y} + [N_i^{(e)}] \bar{q}_z^{(e)} \frac{\partial [N_i^{(e)}]}{\partial z} \right. \right. \\
& \quad + \left(\frac{\partial [N_i^{(e)}]}{\partial x} \right) \hat{D}_{xx} \frac{\partial [N_i^{(e)}]}{\partial x} + \frac{\partial [N_i^{(e)}]}{\partial x} \hat{D}_{xy} \frac{\partial [N_i^{(e)}]}{\partial y} + \frac{\partial [N_i^{(e)}]}{\partial x} \hat{D}_{xz} \frac{\partial [N_i^{(e)}]}{\partial z} \\
& \quad + \left(\frac{\partial [N_i^{(e)}]}{\partial y} \right) \hat{D}_{yx} \frac{\partial [N_i^{(e)}]}{\partial x} + \frac{\partial [N_i^{(e)}]}{\partial y} \hat{D}_{yy} \frac{\partial [N_i^{(e)}]}{\partial y} + \frac{\partial [N_i^{(e)}]}{\partial y} \hat{D}_{yz} \frac{\partial [N_i^{(e)}]}{\partial z} \\
& \quad \left. \left. + \frac{\partial [N_i^{(e)}]}{\partial z} \hat{D}_{zx} \frac{\partial [N_i^{(e)}]}{\partial x} + \frac{\partial [N_i^{(e)}]}{\partial z} \hat{D}_{zy} \frac{\partial [N_i^{(e)}]}{\partial y} + \frac{\partial [N_i^{(e)}]}{\partial z} \hat{D}_{zz} \frac{\partial [N_i^{(e)}]}{\partial z} \right\} \{ \bar{c} \} \right) dV \\
& - \{ f_i^{(e)} \} = 0
\end{aligned} \tag{5.60}$$

Equation (5.60) in a matrix form is

$$\sum_e \left[[\hat{D}^{(e)}] \{c_i^{(e)}\} - \{f_i^{(e)}\} \right] = 0 \quad (5.61)$$

Then the general finite element formulation for the solute transport is

$$[\hat{D}] \{\bar{c}\} - \{f\} = \{0\} \quad (5.62)$$

where $[\hat{D}]$ is the global effective advective-dispersive matrix over the problem domain.

5.7 FE formulation for unsteady-state solute transport

The stochastic partial differential equation for unsteady-state solute transport through an unsaturated soil is

$$n \frac{\partial \bar{c}}{\partial t} = - \frac{\partial (\bar{c} q_i)}{\partial x_i} + \frac{\partial}{\partial x_i} \left[(\hat{D}_{ij}) \frac{\partial \bar{c}}{\partial x_j} \right] \quad (5.63)$$

The weighted average of residuals at nodes, produced by substituting the approximated solution into the Equation (5.63), over the solution domain is forced to be zero. Then,

$$\begin{aligned} \int \int \int_{\Omega} -w_i & \left(\frac{\partial (\bar{q}_x \hat{c})}{\partial x} + \frac{\partial (\bar{q}_y \hat{c})}{\partial y} + \frac{\partial (\bar{q}_z \hat{c})}{\partial z} \right. \\ & + \frac{\partial}{\partial x} \left[\hat{D}_{xx} \frac{\partial \hat{c}}{\partial x} + \hat{D}_{xy} \frac{\partial \hat{c}}{\partial y} + \hat{D}_{xz} \frac{\partial \hat{c}}{\partial z} \right] \\ & + \frac{\partial}{\partial y} \left[\hat{D}_{yy} \frac{\partial \hat{c}}{\partial x} + \hat{D}_{yx} \frac{\partial \hat{c}}{\partial y} + \hat{D}_{yz} \frac{\partial \hat{c}}{\partial z} \right] \\ & \left. + \frac{\partial}{\partial z} \left[\hat{D}_{zx} \frac{\partial \hat{c}}{\partial x} + \hat{D}_{zy} \frac{\partial \hat{c}}{\partial y} + \hat{D}_{zz} \frac{\partial \hat{c}}{\partial z} \right] + \frac{n \partial \hat{c}}{\partial t} \right) d\Omega = 0 \end{aligned} \quad (5.64)$$

5.7.1 Element weighted residual for unsteady-state solute transport

The contribution of any element, e , to the residual at node i , to which the element is jointed, is acquired by substituting the approximated solute concentration and other related hydraulic parameters of each element into the Equation (5.64) and using the Galerkin's method, as

$$\begin{aligned}
 R^{(e)} = & - \int_{V^{(e)}} W_i^{(e)} \left\{ - \left(\frac{\partial(\bar{q}_x^{(e)} \hat{c})}{\partial x} + \frac{\partial(\bar{q}_y^{(e)} \hat{c})}{\partial y} + \frac{\partial(\bar{q}_z^{(e)} \hat{c})}{\partial z} \right) \right. \\
 & - \frac{\partial}{\partial x} \left(\hat{D}_{xx}^{(e)} \frac{\partial \hat{c}}{\partial x} + \hat{D}_{xy}^{(e)} \frac{\partial \hat{c}}{\partial y} + \hat{D}_{xz}^{(e)} \frac{\partial \hat{c}}{\partial z} \right) \\
 & - \frac{\partial}{\partial y} \left(\hat{D}_{yx}^{(e)} \frac{\partial \hat{c}}{\partial x} + \hat{D}_{yy}^{(e)} \frac{\partial \hat{c}}{\partial y} + \hat{D}_{yz}^{(e)} \frac{\partial \hat{c}}{\partial z} \right) \\
 & \left. - \frac{\partial}{\partial z} \left(\hat{D}_{zx}^{(e)} \frac{\partial \hat{c}}{\partial x} + \hat{D}_{zy}^{(e)} \frac{\partial \hat{c}}{\partial y} + \hat{D}_{zz}^{(e)} \frac{\partial \hat{c}}{\partial z} \right) - n^{(e)} \left(\frac{\partial(\hat{c})}{\partial t} \right) \right\} dV
 \end{aligned} \tag{5.65}$$

Integrating by parts and applying the Green Theorem yields the residual Equation as

$$\begin{aligned}
 R^{(e)} = & -f_i^{(e)} - \int_{V^{(e)}} \left\{ -N_i^{(e)} \left(\frac{\partial(\bar{q}_x^{(e)} \hat{c})}{\partial x} \right) - N_i^{(e)} \left(\frac{\partial(\bar{q}_y^{(e)} \hat{c})}{\partial y} \right) - N_i^{(e)} \left(\frac{\partial(\bar{q}_z^{(e)} \hat{c})}{\partial z} \right) + \right. \\
 & \hat{D}_{xx}^{(e)} \left(\frac{\partial N_i^{(e)}}{\partial x} \right) \frac{\partial \hat{c}}{\partial x} + \hat{D}_{xy}^{(e)} \left(\frac{\partial N_i^{(e)}}{\partial x} \right) \frac{\partial \hat{c}}{\partial y} + \hat{D}_{xz}^{(e)} \left(\frac{\partial N_i^{(e)}}{\partial x} \right) \frac{\partial \hat{c}}{\partial z} + \\
 & \hat{D}_{yx}^{(e)} \left(\frac{\partial N_i^{(e)}}{\partial y} \right) \frac{\partial \hat{c}}{\partial x} + \hat{D}_{yy}^{(e)} \left(\frac{\partial N_i^{(e)}}{\partial y} \right) \frac{\partial \hat{c}}{\partial y} + \hat{D}_{yz}^{(e)} \left(\frac{\partial N_i^{(e)}}{\partial y} \right) \frac{\partial \hat{c}}{\partial z} + \\
 & \left. \hat{D}_{zx}^{(e)} \left(\frac{\partial N_i^{(e)}}{\partial z} \right) \frac{\partial \hat{c}}{\partial x} + \hat{D}_{zy}^{(e)} \left(\frac{\partial N_i^{(e)}}{\partial z} \right) \frac{\partial \hat{c}}{\partial y} + \hat{D}_{zz}^{(e)} \left(\frac{\partial N_i^{(e)}}{\partial z} \right) \frac{\partial \hat{c}}{\partial z} + \left\{ n^{(e)} \frac{\partial \hat{c}}{\partial t} \right\} dA \right\} dV
 \end{aligned} \tag{5.66}$$

Over each element, the following variables are approximated by polynomial shape functions relating them to their nodal values:

$$\hat{c}^{(e)} = [N_i^{(e)}] \{ \bar{c}_i^{(e)} \} \tag{5.67}$$

$$\frac{\partial \hat{c}^{(e)}}{\partial t} = [N_i^{(e)}] \left\{ \frac{\partial \bar{c}_i^{(e)}}{\partial t} \right\} \quad (5.68)$$

Substituting Equations (5.67) and (5.68) in to Equation (5.66) yields:

$$\begin{aligned} R^{(e)} = - \int_{V^{(e)}} \left\{ \left([N_i^{(e)}] \bar{q}_x^{(e)} \frac{\partial [N_i^{(e)}]}{\partial x} + [N_i^{(e)}] \bar{q}_y^{(e)} \frac{\partial [N_i^{(e)}]}{\partial y} + [N_i^{(e)}] \bar{q}_z^{(e)} \frac{\partial [N_i^{(e)}]}{\partial z} + \right. \right. \\ \left. \left. + \left(\frac{\partial [N_i^{(e)}]}{\partial x} \right) \hat{D}_{xx}^{(e)} \frac{\partial [N_i^{(e)}]}{\partial x} + \left(\frac{\partial [N_i^{(e)}]}{\partial x} \right) \hat{D}_{xy}^{(e)} \frac{\partial [N_i^{(e)}]}{\partial y} + \left(\frac{\partial [N_i^{(e)}]}{\partial x} \right) \hat{D}_{xz}^{(e)} \frac{\partial [N_i^{(e)}]}{\partial z} \right. \right. \\ \left. \left. + \frac{\partial [N_i^{(e)}]}{\partial y} \hat{D}_{yx}^{(e)} \frac{\partial [N_i^{(e)}]}{\partial x} + \left(\frac{\partial [N_i^{(e)}]}{\partial y} \right) \hat{D}_{yy}^{(e)} \frac{\partial [N_i^{(e)}]}{\partial y} + \frac{\partial [N_i^{(e)}]}{\partial y} \hat{D}_{yz}^{(e)} \frac{\partial [N_i^{(e)}]}{\partial z} \right. \right. \\ \left. \left. + \frac{\partial [N_i^{(e)}]}{\partial z} \hat{D}_{zx}^{(e)} \frac{\partial [N_i^{(e)}]}{\partial x} + \frac{\partial [N_i^{(e)}]}{\partial z} \hat{D}_{zy}^{(e)} \frac{\partial [N_i^{(e)}]}{\partial y} + \frac{\partial [N_i^{(e)}]}{\partial z} \hat{D}_{zz}^{(e)} \frac{\partial [N_i^{(e)}]}{\partial z} \right) \{ \bar{c}_i \} \right. \\ \left. + \{ n^{(e)} \} [N_i^{(e)}] \{ \dot{\bar{c}} \} \right\} dV \quad (5.69) \end{aligned}$$

Equation (5.69) is written in a matrix form as

$$\{ R^{(e)} \} = [\hat{P}^{(e)}] \{ \dot{\bar{c}} \} + [\hat{D}^{(e)}] \{ \bar{c} \} - \{ f^{(e)} \} \quad (5.70)$$

where the element effective capacitance matrix $[\hat{P}^{(e)}]$ is:

$$[\hat{P}^{(e)}] = - \int_A [N_i^{(e)}] \{ n^{(e)} \} [N_i^{(e)}] dA \quad (5.71)$$

5.7.2 Determination of element effective capacitance matrix

The element effective capacitance matrix for two dimensional problems is written in the expanded form as

$$[\hat{P}^{(e)}] = \int \int \int_{V^{(e)}} \begin{bmatrix} N_1^{(e)} & N_1^{(e)} \\ \vdots & \vdots \\ N_n^{(e)} & N_n^{(e)} \end{bmatrix} \left[n^{(e)} \right] \begin{bmatrix} N_1^{(e)} \dots N_n^{(e)} \\ N_1^{(e)} \dots N_n^{(e)} \end{bmatrix} dx dy dz \quad (5.72)$$

Using interpolation functions and Equation (3.41) the arrays of the effective capacitance matrix for each element is evaluated as

$$[\hat{P}^{(e)}] = \frac{n^{(e)}A^{(e)}}{12} \begin{bmatrix} 2 & 1 & 1 \\ 1 & 2 & 1 \\ 1 & 1 & 2 \end{bmatrix} \quad (5.73)$$

and with similar procedure the effective capacitance matrix for each tetrahedral element (three-dimensional element) is evaluated as

$$[\hat{P}^{(e)}] = \frac{n^{(e)}V^{(e)}}{20} \begin{bmatrix} 2 & 1 & 1 & 1 \\ 1 & 2 & 1 & 1 \\ 1 & 1 & 2 & 1 \\ 1 & 1 & 1 & 2 \end{bmatrix} \quad (5.74)$$

5.7.3 Global effective characteristics of domain

Summing up the weighted residuals of elements over the domain and minimising it to zero yield

$$\begin{aligned} \sum_e \left(- \int_{V^{(e)}} \left\{ \left[[N_i^{(e)}] \bar{q}_x^{(e)} \frac{\partial [N_i^{(e)}]}{\partial x} \right] + [N_i^{(e)}] \bar{q}_y^{(e)} \frac{\partial [N_i^{(e)}]}{\partial y} + [N_i^{(e)}] \bar{q}_z^{(e)} \frac{\partial [N_i^{(e)}]}{\partial z} \right. \right. \\ + \left(\frac{\partial [N_i^{(e)}]}{\partial x} \right) \hat{D}_{xx} \frac{\partial [N_i^{(e)}]}{\partial x} + \frac{\partial [N_i^{(e)}]}{\partial x} \hat{D}_{xy} \frac{\partial [N_i^{(e)}]}{\partial y} + \frac{\partial [N_i^{(e)}]}{\partial x} \hat{D}_{xz} \frac{\partial [N_i^{(e)}]}{\partial z} \\ + \left(\frac{\partial [N_i^{(e)}]}{\partial y} \right) \hat{D}_{yx} \frac{\partial [N_i^{(e)}]}{\partial x} + \frac{\partial [N_i^{(e)}]}{\partial y} \hat{D}_{yy} \frac{\partial [N_i^{(e)}]}{\partial y} + \frac{\partial [N_i^{(e)}]}{\partial y} \hat{D}_{yz} \frac{\partial [N_i^{(e)}]}{\partial z} \\ \left. \left. + \frac{\partial [N_i^{(e)}]}{\partial z} \hat{D}_{zx} \frac{\partial [N_i^{(e)}]}{\partial x} + \frac{\partial [N_i^{(e)}]}{\partial z} \hat{D}_{zy} \frac{\partial [N_i^{(e)}]}{\partial y} + \frac{\partial [N_i^{(e)}]}{\partial z} \hat{D}_{zz} \frac{\partial [N_i^{(e)}]}{\partial z} \right\} \{ \bar{c} \} \right. \\ \left. + \{ \bar{n}^{(e)} \} [N_i^{(e)}] \{ \dot{\bar{c}}_i \} \right) dV - \{ f_i^{(e)} \} = 0 \end{aligned} \quad (5.75)$$

Equation (5.75) can be written in the matrix form as

$$\sum_e \left[[\hat{P}^{(e)}] \{ \dot{\bar{c}}_i^{(e)} \} + [\hat{D}^{(e)}] \{ \bar{c}_i^{(e)} \} - \{ f_i^{(e)} \} \right] = 0 \quad (5.76)$$

Then the general finite element formulation for the transient solute transport is

$$[\hat{P}]\{\dot{\bar{c}}\} + [\hat{D}]\{\bar{c}\} - \{f\} = \{0\} \quad (5.77)$$

where $[\hat{D}]$ is the global effective advective-dispersive matrix, $[\hat{P}]$ is the global capacitance matrix and $\{f\}$ solute flux vector over the problem domain.

5.8 Finite difference formulation for transient solute transport

5.8.1 Single domain solute transport

Numerical evaluation of transient solute transport equation is completed using time discretisation of effective matrices in time domain. Applying the finite difference approach to Equation (5.77) yields the final form of equation system for evaluation of mean solute concentration in the single domain problem as

$$\left([\hat{P}] + \Delta t [\hat{D}]\right)\{\bar{c}\}_{t+\Delta t} = [\hat{P}]\{\bar{c}\}_t + \Delta t \{f\}_{t+\Delta t} \quad (5.78)$$

5.8.2 Dual domain solute transport

Dual domain solute transport equation is written as

$$\frac{\partial(n_m \bar{c}_m)}{\partial t} + \frac{\partial(n_{im} \bar{c}_{im})}{\partial t} = L(\bar{c}_m) \quad (5.79)$$

$$\frac{\partial(n_{im} c_{im})}{\partial t} = \zeta(c_m - c_{im}) \quad (5.80)$$

where,

$$L(\bar{c}_m) = \frac{\partial}{\partial x_i} \left(D_{ij} \left(\frac{\partial \bar{c}_m}{\partial x_j} \right) \right) - \frac{\partial(\bar{q}_i \bar{c}_m)}{\partial x_i} \quad (5.81)$$

$L(\bar{c}_m)$ is the operator representing the advection, dispersion, and solute sink/source terms in the mobile domain and this term is solved using Finite element method with similar procedure applied for advection, dispersion terms in single domain equation. Applying finite element method to Equations (5.79) and (5.80) yields

$$\left[\hat{P}_m \right] \left\{ \dot{\bar{c}}_m \right\} + \left[\hat{P}_{im} \right] \left\{ \dot{\bar{c}}_{im} \right\} + \left[\hat{D} \right] \left\{ \bar{c}_m \right\} - \left\{ f \right\} = \left\{ 0 \right\} \quad (5.82)$$

$$\left[\hat{P}_{im} \right] \left\{ \dot{\bar{c}}_{im} \right\} = \zeta \left(\left\{ \bar{c}_m \right\} - \left\{ \bar{c}_{im} \right\} \right) \quad (5.83)$$

where,

$$\left[\hat{P}_{im} \right] = \sum_e \left[\hat{P}_{im}^{(e)} \right]; \quad \left[\hat{P}_{im}^{(e)} \right] = \frac{n_{im}^{(e)} V^{(e)}}{20} \begin{bmatrix} 2 & 1 & 1 & 1 \\ 1 & 2 & 1 & 1 \\ 1 & 1 & 2 & 1 \\ 1 & 1 & 1 & 2 \end{bmatrix} \quad (5.84)$$

and

$$\left[\hat{P}_m \right] = \sum_n \left[\hat{P}_m^{(e)} \right]; \quad \left[\hat{P}_m^{(e)} \right] = \frac{n_m^{(e)} V^{(e)}}{20} \begin{bmatrix} 2 & 1 & 1 & 1 \\ 1 & 2 & 1 & 1 \\ 1 & 1 & 2 & 1 \\ 1 & 1 & 1 & 2 \end{bmatrix} \quad (5.85)$$

Substituting Equation (5.83) into Equation (5.82) and rearranging it yields

$$\left[\hat{P}_m \right] \left\{ \dot{\bar{c}}_m \right\} + \left[\hat{D} \right] \left\{ \bar{c}_m \right\} - \left\{ f \right\} - \zeta \left(\left\{ \bar{c}_m \right\} - \left\{ \bar{c}_{im} \right\} \right) = \left\{ 0 \right\} \quad (5.86)$$

Applying the finite difference algorithm to Equation (5.86) yields

$$\left[\hat{P}_m \right] \frac{\left\{ \bar{c}_m \right\}_{t+\Delta t} - \left\{ \bar{c}_m \right\}_t}{\Delta t} = \left[\hat{D} \right] \left\{ \bar{c}_m \right\}_{t+\Delta t} - \left\{ f \right\} - \zeta \left(\left\{ \bar{c}_m \right\}_{t+\Delta t} - \left\{ \bar{c}_{im} \right\}_{t+\Delta t} \right) \quad (5.87)$$

Equation (5.87) contains two primary dependant variables, $c_m^{t+\Delta t}$ and $c_{im}^{t+\Delta t}$, the solute concentration in the mobile and immobile domains respectively. Therefore, one must be expressed in terms of the other. This can be accomplished by applying finite difference algorithm to Equation (5.83).

$$\left[\hat{P}_{im} \right] \frac{\left\{ \bar{c}_{im} \right\}_{t+\Delta t} - \left\{ \bar{c}_{im} \right\}_t}{\Delta t} = \zeta \left(\left\{ \bar{c}_m \right\}_{t+\Delta t} - \left\{ \bar{c}_{im} \right\}_{t+\Delta t} \right) \quad (5.88)$$

Equation (5.88) can be arranged to yield

$$\{\bar{c}_{im}\}_{t+\Delta t} = \frac{\zeta}{\vartheta} \{\bar{c}_m\}_{t+\Delta t} + \frac{[\hat{P}_{im}]}{\Delta t \vartheta} \{\bar{c}_{im}\}_t \quad (5.89)$$

where, $\vartheta = \frac{[\hat{P}_{im}]}{\Delta t} + \zeta$.

Substituting Equation (5.89) into Equation (5.87) yields

$$[\hat{P}_m] \frac{\{\bar{c}_m\}_{t+\Delta t} - \{\bar{c}_m\}_t}{\Delta t} = [\hat{D}] \{\bar{c}_m\}_{t+\Delta t} - \{f\} - \left(\zeta + \frac{\zeta^2}{\vartheta} \right) \{\bar{c}_m\}_{t+\Delta t} + \frac{\zeta [\hat{P}_{im}]}{\Delta t \vartheta} \{\bar{c}_{im}\}_t \quad (5.90)$$

Equations (5.89) and (5.90) represent final solution of solute transport equation in dual domain systems.

5.9 Solution procedure

A computer code was written in Compaq Visual FORTRAN 2000 (© 2000 Compaq Compute Corporation) to solve the equations presented above for evaluation of stochastic properties of water flow and solute transport problems. The solution procedure and the algorithm used in the developed stochastic finite element code are summarized in Figure (5.1).

The first step of the solution procedure involves defining the input data and the geometry of the problem. The expected values are determined using the related equations presented in chapter 4, and consequently, the effective permeability and capacitance matrices for each element are evaluated. They are assembled to create the global matrices. The boundary conditions are implemented and the global system of equations is solved using finite difference scheme in the time domain. The results of H and σ_h^2 are evaluated for each node. The solution procedure for evaluation of H is repeated to satisfy the convergence criteria of the problem. The convergence criteria of the results in this model is satisfied if the difference between two successive iterations at each point of the domain is smaller than 1%. The convergence of mean pressure head is checked and if the nodal values converge, the transport equation can be solved, otherwise, the flow equation is solved. Once the convergence of pressure head for each

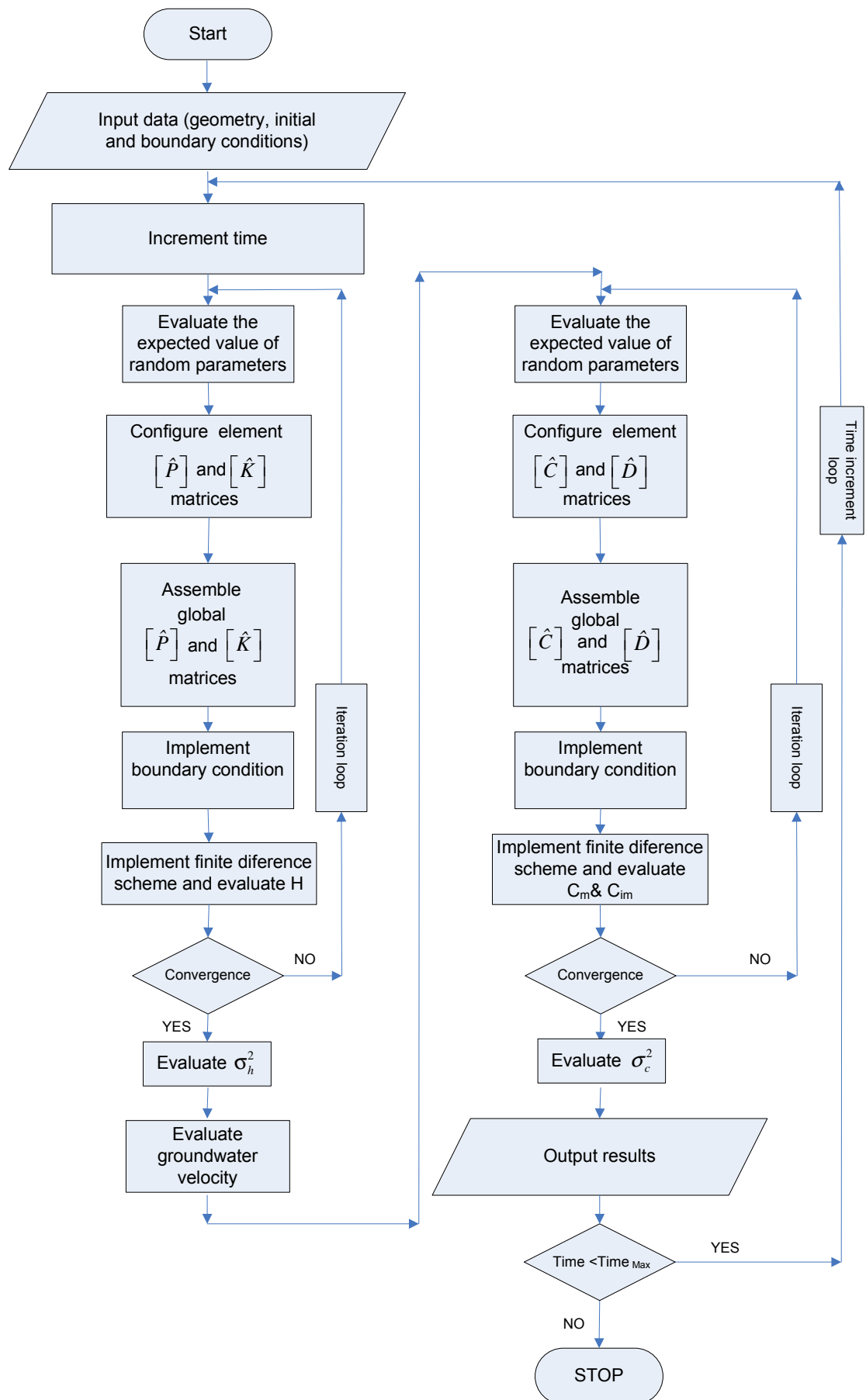


Figure 5.1 General structure of developed model.

node is achieved, then the field water velocity is evaluated and the arrays of macrodispersion coefficient are numerically determined; thereafter the advective-dispersive transport and capacitance matrices are computed. The boundary conditions of transport problems are implemented. The system of equations for transport problems is solved using a finite difference scheme in time domain and mean and variance of solute concentration are evaluated. The solution procedure is repeated for the next time steps up to the total duration of the problem under study.

CHAPTER 6

NUMERICAL EXAMPLES AND CASE STUDIES

6.1 Introduction

Stochastic FE model was used to simulate 7 different scenarios. The first case consists of simulating a one-dimensional transient unsaturated flow through a vertical column of soil. Analytical solution was used to verify the accuracy of the model. The second case consists of simulating a one-dimensional transient unsaturated flow through a layered soil. The results from stochastic FE analysis were compared to deterministic FE results and experimental data. The stochastic FE theory for solute transport was verified in the next case through simulation of a one-dimensional steady-state unsaturated flow and transient contaminant transport. The stochastic FE results were compared to deterministic and Monte Carlo results. In the fourth case, the capability of the developed model for simulation of three-dimensional problems is verified. The ability of the model in considering the effects of immobile water was verified in the fifth case. This case consists of simulation of solute transport in a column of soil with high density of macropores. The results of the developed model were compared with those obtained using an analytical solution and experimental measurements.

Applicability and performance of the developed model for simulation of real problems was verified with simulation of two different case-studies; (i) a steady-state flow and transient solute transport case-study, (ii) a transient flow and contaminant transport case-study. Stochastic and deterministic results were compared to each other. Details of these 7 cases are presented in the following sections.

6.2 Numerical examples

6.2.1 Example 1

This example has been selected to verify the model by comparing the results obtained from the developed model with those obtained from analytical equations presented by Tracy (1995) for 1-D horizontal and vertical unsteady-state groundwater flow in unsaturated soil samples. Effect of gravitational force on seepage potential of groundwater in vertical direction distinguishes horizontal and vertical groundwater flow.

Problem definition for horizontal groundwater flow

The problem, as shown in Figure 6.1, consists of horizontal, unsaturated groundwater seepage in a dry soil sample of length L . The right-hand boundary of the sample is kept as dry as possible, so pressure head is set to residual head. The residual head is the largest (in absolute value) negative pressure head allowed for the soil which is a function of type and properties of soil (Fredlund and Rahardjo 1993). Irrigation is applied to the left-hand side of the soil sample. As a result, water seepage occurs from left to the right through the soil sample. This causes the water pressure head at $x=0$ to gradually increase from a negative value (as the soil is unsaturated) to zero (saturated pressure head). Figure 6.1 (a) and (b) show the geometric dimensions and the element discretisation employed in the solution, respectively. Three-node triangular elements have been used in the discretisation of the area. The FE (finite element) mesh generated for this example consists of 80 triangular elements and 82 nodes, here referred to as mesh A. Also, the example was solved with a finer mesh; 200 triangular elements and 202 nodes, here referred to as mesh B (Figure 6.1 c) to check the accuracy of numerical solution. The simulation results obtained with the finer mesh are very close to those obtained with the previous simulation (Figure 6.2). This proves that the first generated

mesh is an efficient one for this example and the finer mesh does not increase the accuracy of the prediction. The values of the parameters used in the numerical (FE) model and analytical solution are summarized at table 6.1. These values were chosen in order to enable comparison with results from the literature (Tracy, 1995). However, the values of parameters used by Tracy (1995) were not chosen very sensibly. As in the development of the analytical solution it was assumed that the soil sample is homogeneous, in the numerical simulation the variance of soil hydraulic parameters, is set to zero and the example is treated deterministically.

Table 6.1 Value of parameters used in horizontal groundwater flow example.

L	200 m	k_s	10 m day ⁻¹
H_r	-100 m	H_s	0
θ_r	0.15	θ_s	0.45

The parameters presented in the table were defined in chapters 5 and 6.

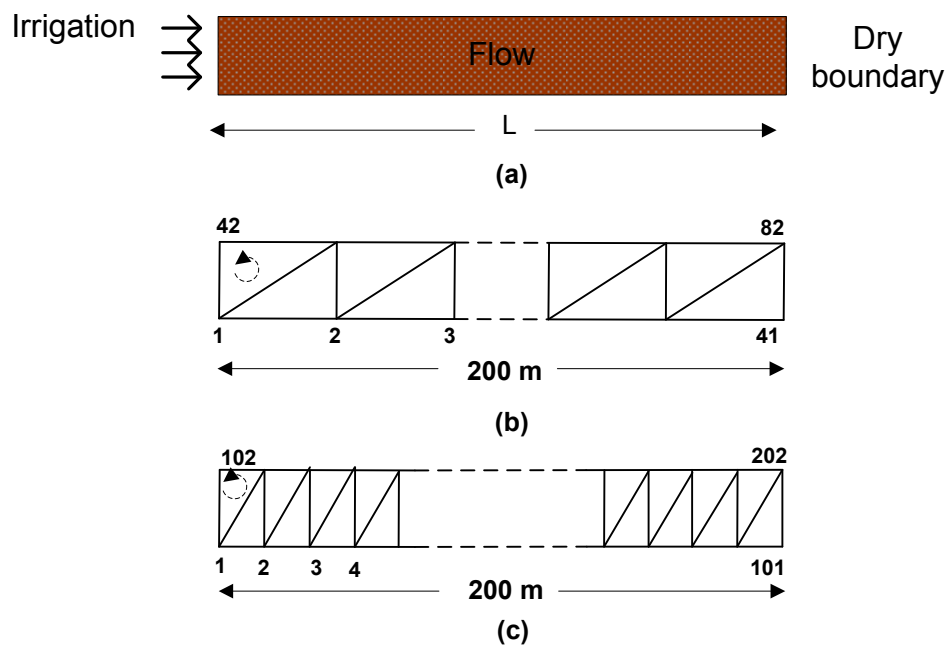


Figure 6.1 (a) 1-D horizontal groundwater seepage with the boundary conditions, (b) Finite element mesh with linear triangle element.

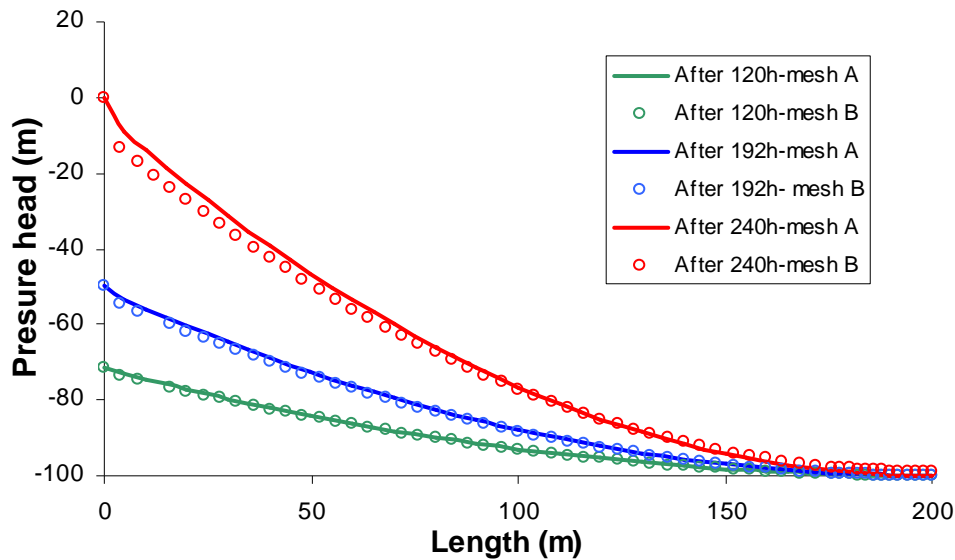


Figure 6.2 Pressure head distribution through the bar for various times (mesh B: symbols, mesh A: solid lines).

Initial conditions

The initial pressure head at each point of the bar is assumed as a function of residual pressure head, length of the bar and distance of the point from the left hand side of the bar (i.e., x) as

$$H_i = H_r \left[1 - \frac{1}{6} \left(\frac{x-L}{L} \right)^2 \right] \quad (6.1)$$

Boundary conditions

The pressure head at the left-hand boundary of the bar (i.e., $x=0$) is calculated as a function of time as

$$H_0 = H_r \left[1 - \frac{1}{6 - \frac{5t}{t_D}} \right] \quad (6.2)$$

where t_D is time duration which is defined as the time that the bar stays totally unsaturated. t_D is calculated as (Tracy 1995)

$$t_D = -\frac{5L^2(\theta_s - \theta_r)}{6H_r k_s} \quad (6.3)$$

At the right-hand boundary that is kept dry the pressure head is equal to residual pressure head, So

$$H_L = H_r \quad (6.4)$$

Analytical solution

The governing differential equation for horizontal water flow in homogeneous unsaturated soil is

$$\frac{\partial}{\partial x} \left(k_s k_r \frac{\partial H}{\partial x} \right) = C \frac{\partial H}{\partial t} \quad (6.5)$$

where, k_r is relative hydraulic conductivity and is calculated as (Tracy 1995)

$$k_r = \frac{H - H_r}{H_s - H_r} \quad (6.6)$$

Tracy (1995) presented an analytical solution for this example using partial differential equation (6.5) and applying initial and boundary conditions presented at equations (6.1), (6.2) and (6.4), as

$$H = -\frac{c}{6} \frac{(x + c_1)^2}{t + c_2} + H_r \quad (6.7)$$

where

$$c_1 = -L \quad (6.8)$$

$$c_2 = \frac{cL^2}{H_r} \quad (6.9)$$

$$c = \frac{\theta_s - \theta_r}{k_s} \quad (6.10)$$

Results

Figure (6.3) illustrates transient pressure head distribution through the bar at various times during the groundwater seepage obtained from numerical and analytical methods. The solid lines represent the numerical solution and the symbols represent the analytical solution. Apart from the right end of the bar which is kept dry, the water pressure head through the bar increases with time. The initial water pressure head at left side of the sample is -83.33 m. As time progresses this value increases and after 10 days (i.e., 240 hours) it reaches to zero (saturated condition).

Transient water content distribution through the bar for various times, are depicted in Figure (6.4). At the beginning, the maximum value of water content is located at the left-hand side of the bar and it is equal to $0.2 \text{ m}^3\text{m}^{-3}$. Minimum value of water content is located on the right end of the sample which is equal to $0.15 \text{ m}^3\text{m}^{-3}$. The results of analytical and numerical models both show that the water content increases with time through the sample. The water content on the left boundary increases to $0.23 \text{ m}^3\text{m}^{-3}$ and $0.3 \text{ m}^3\text{m}^{-3}$ after 5 and 8 days respectively. After 10 days (i.e., 240 hours), the left end of the sample became nearly saturated.

The results presented at Figure (6.3) and (6.4) show good agreement between analytical and numerical results. This proves reliability of developed model for simulation of groundwater seepage through the unsaturated soil.

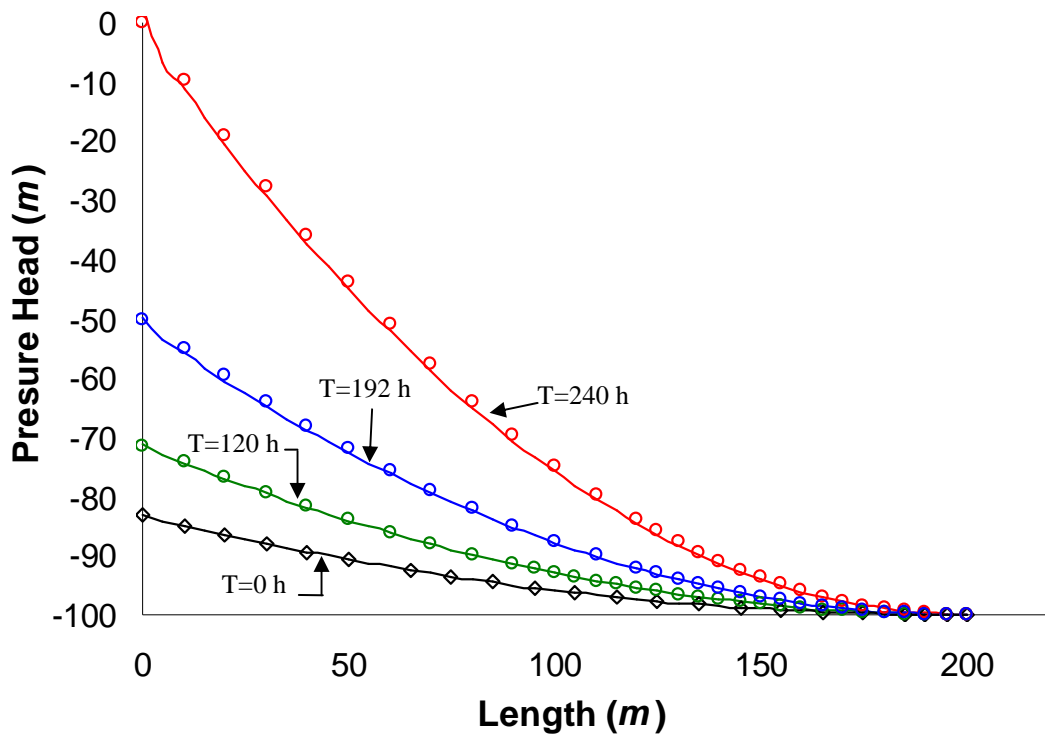


Figure 6.3 Pressure head distribution through the bar for various times (analytical: symbols, numerical: solid lines, t: time).

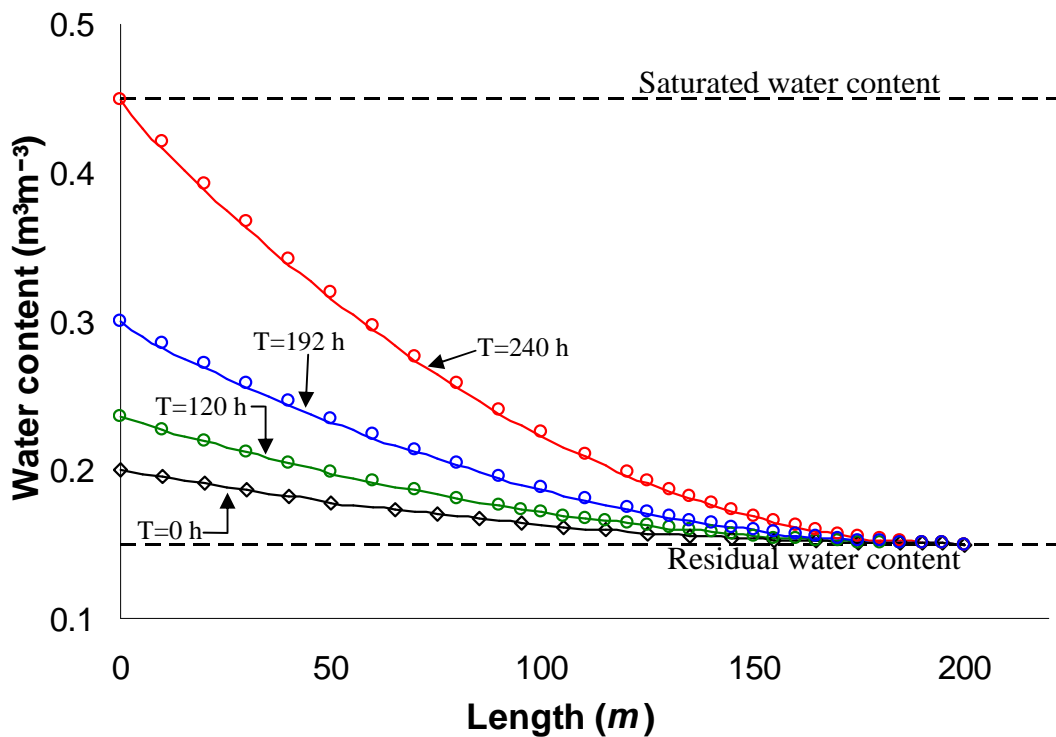


Figure 6.4 Water content distribution through the bar for various times (analytical: symbols, numerical: solid lines, t: time).

Problem definition for vertical flow with gravity

The problem, as shown in Figure 6.4, consists of downward, unsaturated flow in a rather dry soil sample of depth L . The bottom ($z=0$) rests on impervious rock, and the top ($z=L$) is at the ground surface. The impervious rock gives a no-flow boundary condition. Rain at the surface causes the pressure head H_L to increase towards zero. Figure 6.5 (a) and (b) show the geometric dimensions and the element discretisation employed in the solution, respectively. Three-node triangular elements have been used in the discretisation. The FE mesh generated for this example consists of 80 triangular elements and 82 nodes.

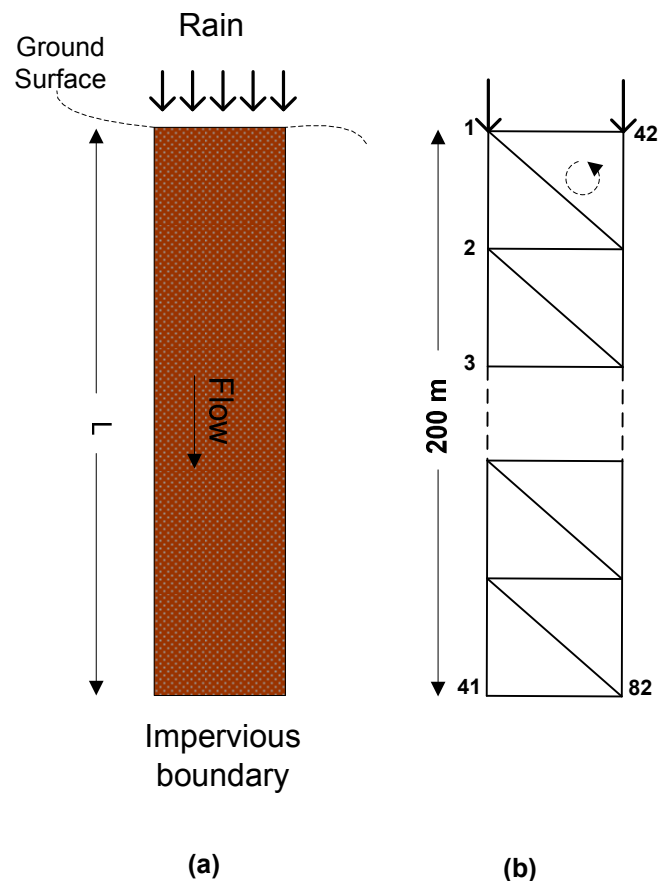


Figure 6.5 (a) 1-D vertical groundwater flow with the boundary conditions, (b) Finite element mesh with linear triangle element.

The values of the parameters used in the numerical (FE) model and analytical solution are summarized at table 6.2. This example is, also, solved deterministically for the same reason for the case of horizontal flow simulation and the variance of soil hydraulic parameters is set to zero.

Table 6.2 Value of parameters for vertical groundwater flow example.

L	200 m	k_s	0.115 m h^{-1}
H_r	-1.50 m	H_s	0
θ_r	$0.15\text{ m}^3\text{ m}^{-3}$	θ_s	$0.45\text{ m}^3\text{ m}^{-3}$
α	5.06 m^{-1}		

Initial conditions

The initial pressure head through the column is calculated as

$$H_I = \frac{1}{\alpha} \ln \left(\exp[\alpha(H_T - z)] + \left\{ \exp(\alpha H_B) - \exp[\alpha(H_T - L)] \right\} \times \frac{\alpha z - 1 + e^{-\alpha z}}{\alpha L - 1 + e^{-\alpha L}} \right) \quad (6.11)$$

where H_T and H_B are mean pressure heads at the top and base of the column, respectively

Boundary conditions

The impervious rock at the base of the column is defined as no flow boundary condition, then

$$\frac{\partial H}{\partial z} = 0 \quad z = 0 \quad (6.12)$$

The pressure head at the top of the column is calculated for various times as

$$H_L = H_T - \frac{1}{\alpha} \ln \left(1 - \left(\frac{\alpha^2}{c} \right) \left\{ \frac{\exp(\alpha H_T) - \exp[\alpha(H_B - L)]}{\alpha L - 1 + e^{-\alpha L}} \right\} t \right) \quad (6.13)$$

and

$$c = \frac{1}{k_s} \left(\frac{\theta_s - \theta_r}{H_s - H_r} \right) \quad (6.14)$$

Analytical solution

The governing equation for groundwater flow in 1-D vertical direction with the gravity term is

$$\frac{\partial}{\partial z} \left[k \left(\frac{\partial H}{\partial z} + 1 \right) \right] = C \frac{\partial H}{\partial t} \quad (6.15)$$

For this case, K is considered as (Tracy 1995)

$$k = k_s e^{\alpha H} \quad (6.16)$$

Tracy (1995) presented an analytical solution for this example using partial differential equation (6.15) with initial and boundary conditions presented as equations (6.12) and (6.13) as

$$H = \frac{1}{\alpha} \ln \left(\frac{\exp[\alpha(H_T - z)] + \left\{ \exp(\alpha H_B) - \exp[\alpha(H_T - L)] \right\} \left(\frac{\alpha z - 1 + e^{-\alpha L}}{\alpha L - 1 + e^{-\alpha L}} \right)}{1 - \left(\frac{\alpha^2}{c} \right) \left\{ \frac{\exp(\alpha H_B) - \exp[\alpha(H_T - L)]}{\alpha L - 1 + e^{-\alpha L}} \right\} t} \right) \quad (6.17)$$

Results

The results obtained from finite element simulation are compared with those obtained from the analytical solution. Figure 6.6 illustrates transient pressure head distribution through the column, at various times during the groundwater seepage obtained from numerical and analytical methods. The solid lines represent the numerical solution and the symbols represent the analytical solution.

Water pressure head through the column increases with time. The initial water pressure head at the top of the column is -50 cm and at the base of the column is -150 cm. Water pressure heads at the top of the column are equal to -40 cm and -29 cm, and at the base are equal to -140 cm and -129cm after 3 and 5 hours, respectively, for both analytical and numerical methods.

After 7.12 hours, water pressure head value at the top reaches zero (saturated condition). At this time, water pressure head at the base for the numerical solution is -96.4 cm. This value is only 3.6% smaller than the analytical one which is equal to -100 cm. This is the largest difference between numerical and analytical solutions which is negligible.

Transient water content distributions through the column for various times, are depicted in Figure (6.7). At the beginning, water contents at the top and base of the column are 0.35 and 0.15, respectively. After 7.12 hours the top became saturated. The maximum value of the water content which is located at the bottom of the sample is equal to $0.26 \text{ cm}^3 \text{ cm}^{-3}$.

Comparison of the results shows that the results obtained using the FEM (finite element model) are in excellent agreement with those obtained from the analytical solution. This shows the potential of the developed finite element model in simulation of vertical groundwater seepage through unsaturated soils.

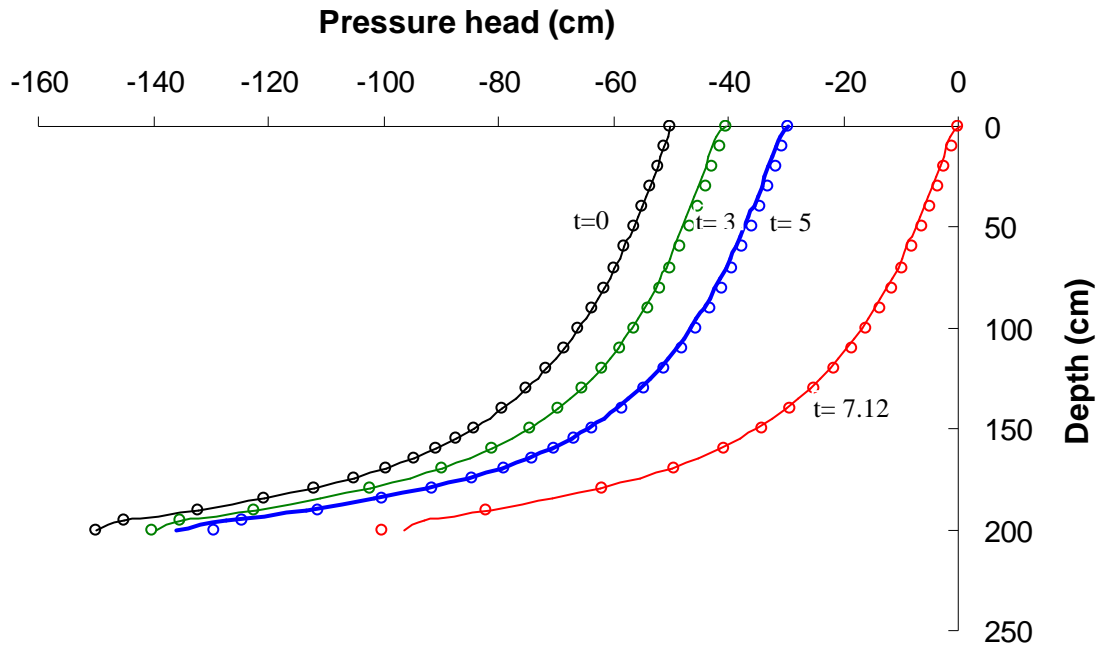


Figure 6.6 Pressure head distribution through the column for various times (symbols: analytical, solid lines: numerical results, t: time (hr)).

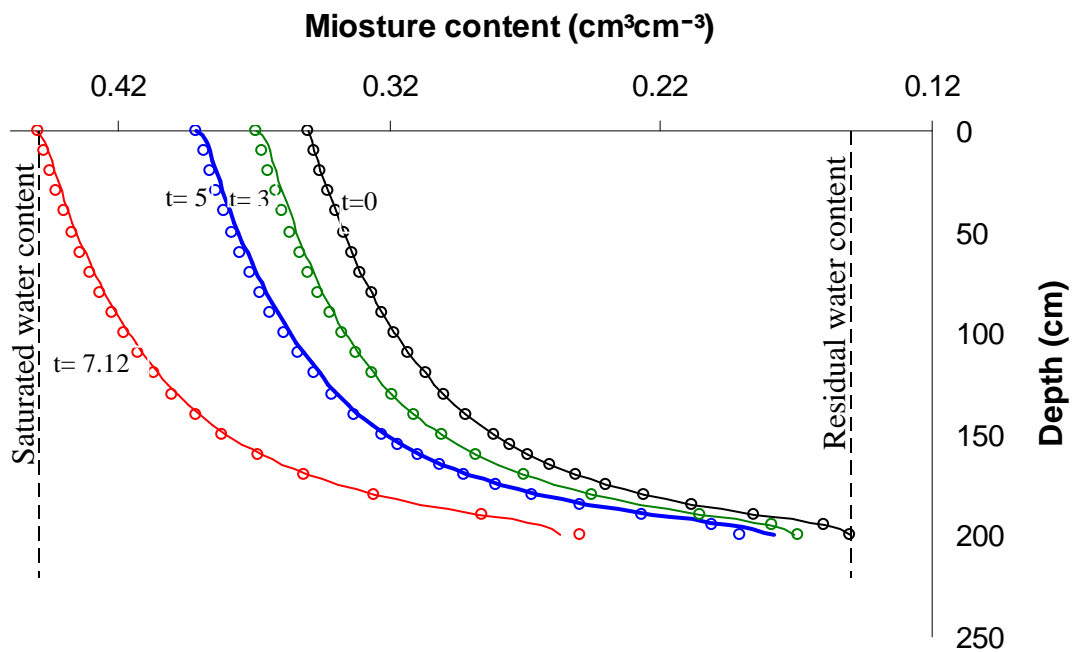


Figure 6.7 Moisture content distribution through the column for various times (symbols: analytical, solid lines: numerical results, t: time (hr)).

6.2.2 Example 2

An example of modelling transient flow in unsaturated soil is chosen in order to validate the developed stochastic finite element model for water flow in heterogeneous layered soil. Field observations show that natural soil formations are often stratified. In this example, STOHYSO is used to simulate a lysimeter test and the results are compared with the actual experimental values (Polmann et al., 1990).

Problem definition

This experiment is usually performed in order to study the effects of heterogeneity (due to layered formation of soil) on water flow. In this particular test the lysimeter was 6 m long with a diameter of 0.95 m, and was filled with alternating 20 cm thick layers of Berino loamy fine sand and Glendale silty loam. The soil was air dried, sieved and packed into the lysimeter at a known density. Two tensiometers were placed into each soil layer, installed through the lysimeter and located at 10 cm apart. An access tube for a neutron probe was installed vertically in the centre of the lysimeter. The irrigation water was applied to the top of the lysimeter. Irrigation was performed by a needle-embedded plate installed just above the soil surface. This plate was rotated at a constant speed to distribute the flux of water uniformly over the surface. Water was added to the lysimeter at a rate of 0.083 cm/hr for 1200 hours. The dimensions of the lysimeter together with the FE mesh and boundary conditions are shown in Figure 6.8. The generated FE mesh for this example consists of 300 triangular elements and 302 nodes.

The values of the parameters used in the example are presented in Table 6.3. Apart from correlation length in vertical direction (i.e., λ) other input parameters were measured experimentally (Polmann et al. 1990). The final value of λ was fine tuned through a trial and error procedure.

Table 6.3 Values of parameters for example problem (Polmann et al., 1990).

parameter	value	parameter	Value
K_s - Glendale silty loam ($cmhr^{-1}$)	0.5436	ψ_r (cm)	-100
α -Glendale silty loam (cm^{-1})	0.0392	ψ_s (cm)	0
K_s - Berino loamy fine sand ($cmhr^{-1}$)	22.536	A (cm^{-1})	0.0628
α - Berino loamy fine sand (cm^{-1})	0.0863	σ_a^2 (cm^{-2})	0.000555
θ_r ($cm^3 cm^{-3}$)	0.03	F	1.25
θ_s ($cm^3 cm^{-3}$)	0.33	σ_f^2	3.47
λ (cm)	10	Δt (hr)	0.1

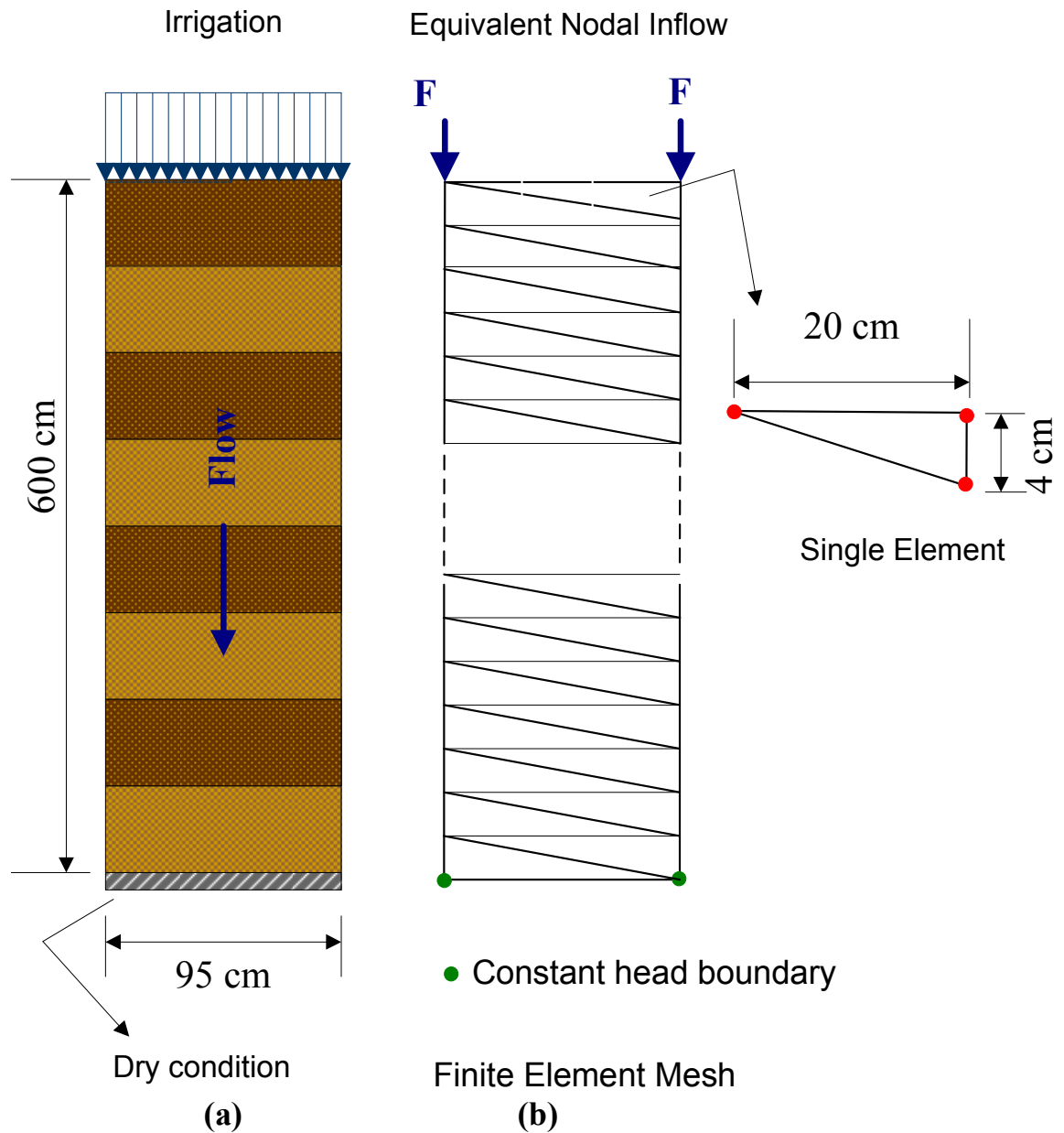


Figure 6.8 (a) Dimensions of the lysimeter used for the experiment and (b) the FE mesh showing boundary conditions.

Initial conditions

Because the soil was dried, the initial capillary tension head through the column is considered equal to the residual capillary tension head and water content is considered equal to the residual water content which is the minimum water that soil can hold at its driest condition.

$$H(z) = -100 \text{ cm}$$

(6.18)

$$\theta(z) = \theta_r \quad (6.19)$$

Boundary conditions

The bottom of the column was kept dry in the experiment; hence, in the model, the capillary tension head is fixed to a constant value equal to the residual capillary tension head.

$$H(z) = -100 \text{ cm} \quad z=L \quad (6.20)$$

A uniformly distributed inflow flux due to irrigation above the column is applied at the top of the column.

$$q(z=0) = 0.083 \text{ cmhr}^{-1} \quad (6.21)$$

and

$$q(z \neq 0) = 0 \quad (6.22)$$

Since in the finite element method, all calculations are done at nodal points, the flux implemented at the top of the column is applied on two top nodal points of the column. The contribution of each node of element from distributed water flux that is applied to a portion of length of that element is determined as (Istock 1989)

$$F_i^{(e)} = q \int_{\Gamma_{bc}} [N_i^{(e)}] d\Gamma_{bc} = q \int_{\Gamma_{bc}} \frac{1}{2A^{(e)}} (a_i + b_i x + c_i y) d\Gamma_{bc} \quad (6.23)$$

$F_i^{(e)}$ is the contribution of node i of element e from the distributed flux; q is the distributed flux over the length of element that is positive for inflow and negative for outflow; Γ_{bc} is the element boundary over which the flux is applied. The rest of the parameters in Equation (6.23) have already been defined in chapter 5.

In summary, the equivalent nodal inflow (i.e, F in Figure 6.8) which is applied along the

upper boundary of the element, is evaluated by substituting the relevant parameters of that element in Equation (6.23).

Results

Figure 6.9 shows the position of the wetting front versus time obtained from (i) the experimental measurements, (ii) the deterministic FE model and (iii) the stochastic FE model between 600 to 1200 hours after the beginning of irrigation. The results obtained from the stochastic FE model are in good agreement with the experimental measurements while those obtained from the deterministic model are considerably ahead of the measured ones. Velocity of wetting front can be used as an index in order to compare the results obtained from the stochastic and deterministic models with the measured results. The slope of the position curve of wetting front versus time represents the velocity of the wetting front. Based on the results presented in Figure 6.9, the velocity of the wetting front for deterministic approach is 34.79% greater than the measured velocity. While the wetting front velocity for the stochastic approach is very close to the experimental one.

The position of the wetting front for the stochastic and deterministic models at different times between 0 and 1200 hours are presented in Figure 6.10. The wetting front moves faster for the deterministic case than for the stochastic case. It can be seen that the difference between the results of the two approaches increases with time.

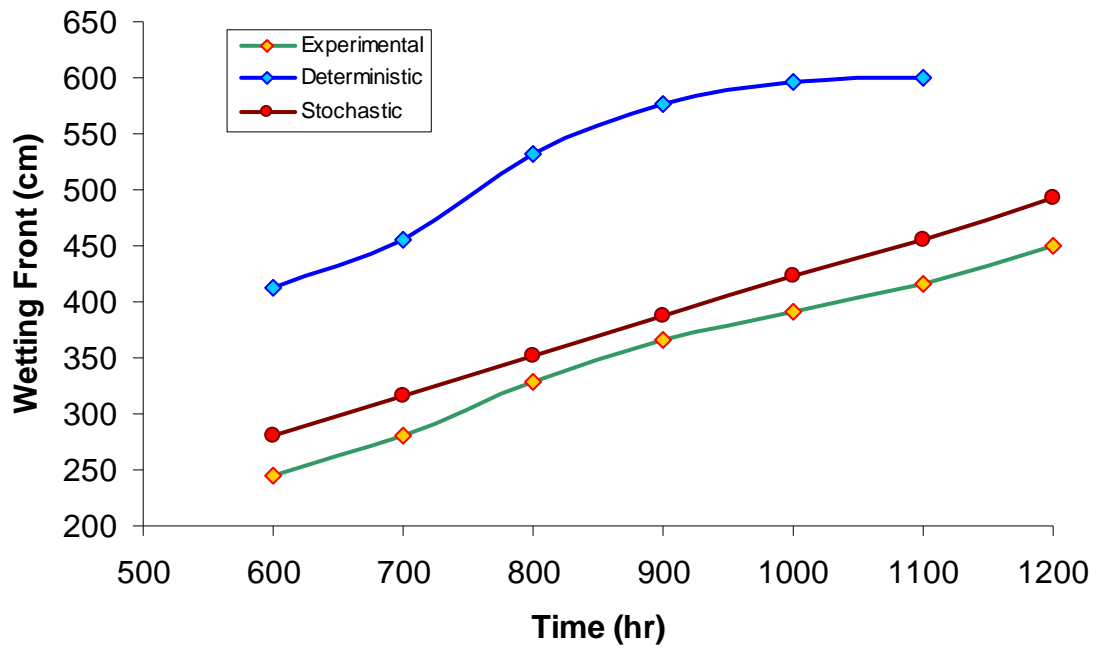


Figure 6.9 Position of wetting front vs. time for Stochastic, deterministic and experimental approaches.

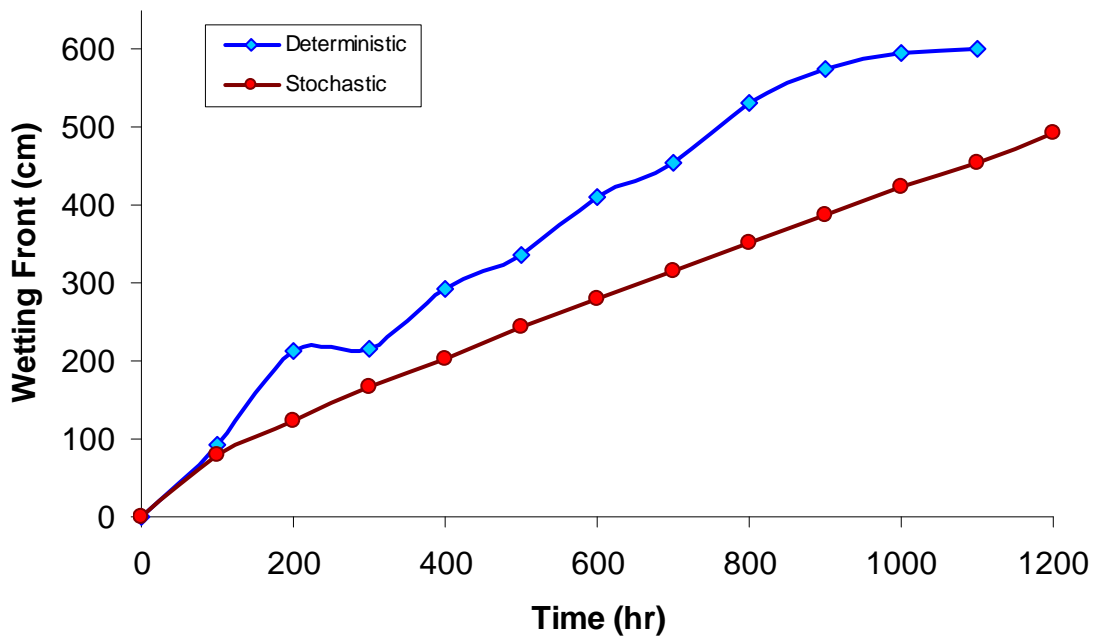


Figure 6.10 Position of wetting front vs. time for Stochastic, deterministic approaches.

The values of measured soil water content at different locations in the lysimeter, and at different times, are compared with the predicted values using the stochastic and deterministic models and the results are presented in Figures 6.11 and 6.12. It can be seen that the stochastic model produced results which are in better agreement with the observed water contents, whereas the deterministic model gave relatively poor predictions. The R^2 values in Figures 6.12 and 6.13 represent the coefficient of precision for the predicted water contents from the stochastic and deterministic approaches. The R^2 factor is evaluated using the following equation.

$$R^2 = \frac{\sum_N (X_m)^2 - \sum_N (X_m - X_p)^2}{\sum_N (X_m)^2} \quad (6.24)$$

where X_m is measured value, X_p is predicted value and N is number of data points.

The R^2 value obtained for the stochastic approach is 0.911, whereas the value of this coefficient for the deterministic approach is 0.611.

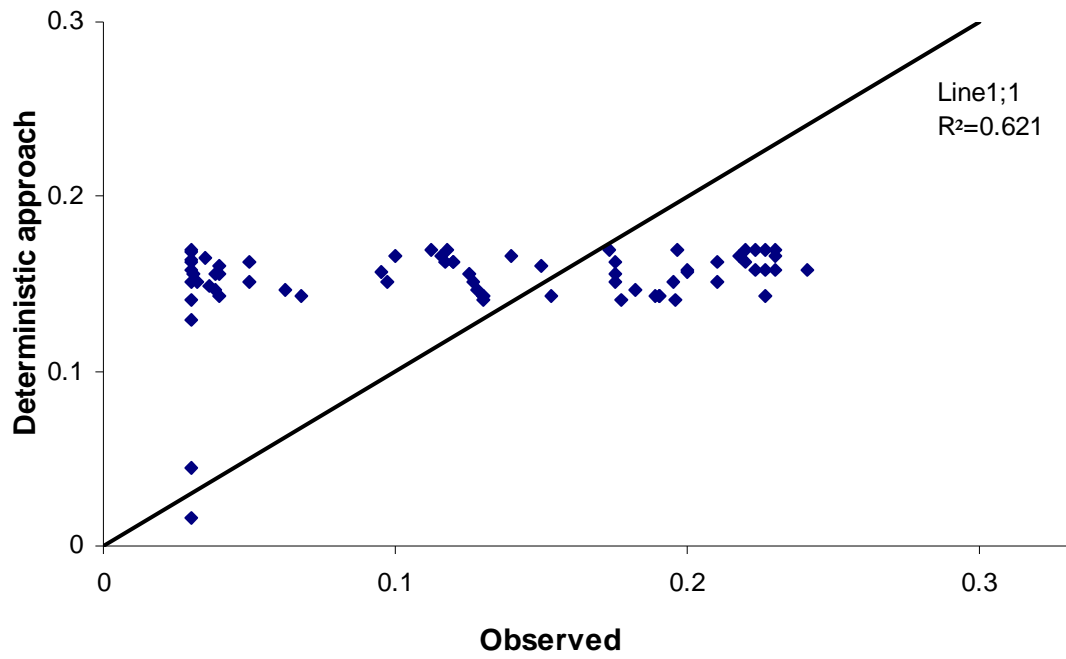


Figure 6.11 Volumetric water content (predicted by deterministic approach vs. the observed values).

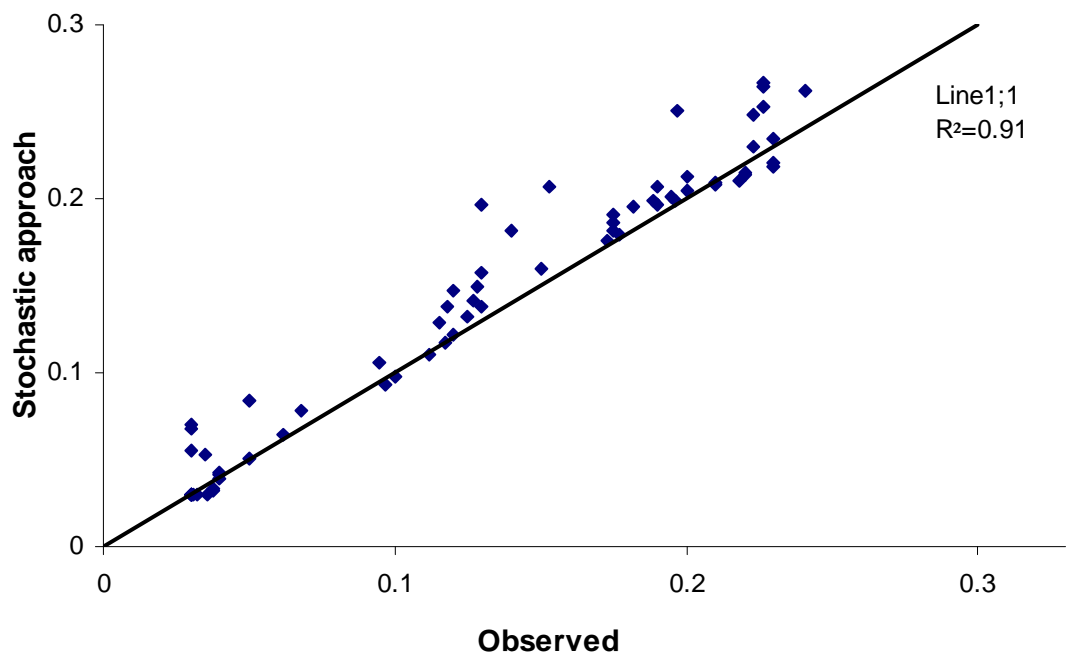


Figure 6.12 Volumetric water content (predicted by stochastic approach vs. observed).

Figure 6.13 shows the pressure head distributions along the depth plotted for every 100 hours during the 1200 hours of the wetting cycle for the deterministic and stochastic models. At $t=0$, the pressure head is -100 cm over the entire domain. After 100 hours of irrigation, the pressure head increases to -63.22 cm for the deterministic approach and to -39.28 cm for the stochastic approach. The position of the wetting front at this time is 92 cm and 80 cm along the depth for the deterministic and stochastic approaches respectively. As time progresses the wetting front moves downwards, and the pressure head and moisture content increase over the entire domain. After 200 hours, the wetting front is located much deeper, at $z=172$ cm, for the deterministic approach while for the stochastic approach it is located at $z=124$ cm. The moisture front continues to move downwards and at $t=500$ hours it is located at $z=412$ cm for the deterministic approach; while, for the stochastic approach it is located at $z=280$ cm. At $t=700$ hours, the position of the wetting front is 456 cm for the deterministic approach while for the stochastic approach it is at $z=316$ cm. Based on the result obtained from the deterministic model, after 900 hours, the wetting front almost reaches to the bottom of the lysimeter and after 1000 hours, the moisture front passes the bottom of the column; whereas, at this time the stochastic approach predicts that the wetting front is located at 492 cm of the depth.

In conclusion, the stochastic approach shows slower movement of the wetting front. Also the values of moisture content and pressure head at the same location, obtained from the stochastic approach, are more than those obtained from the deterministic approach. As a result, with the same input moisture into the lysimeter for both methods, according to the mass conservation law, the water content at the wetted sections is higher in stochastic simulation.

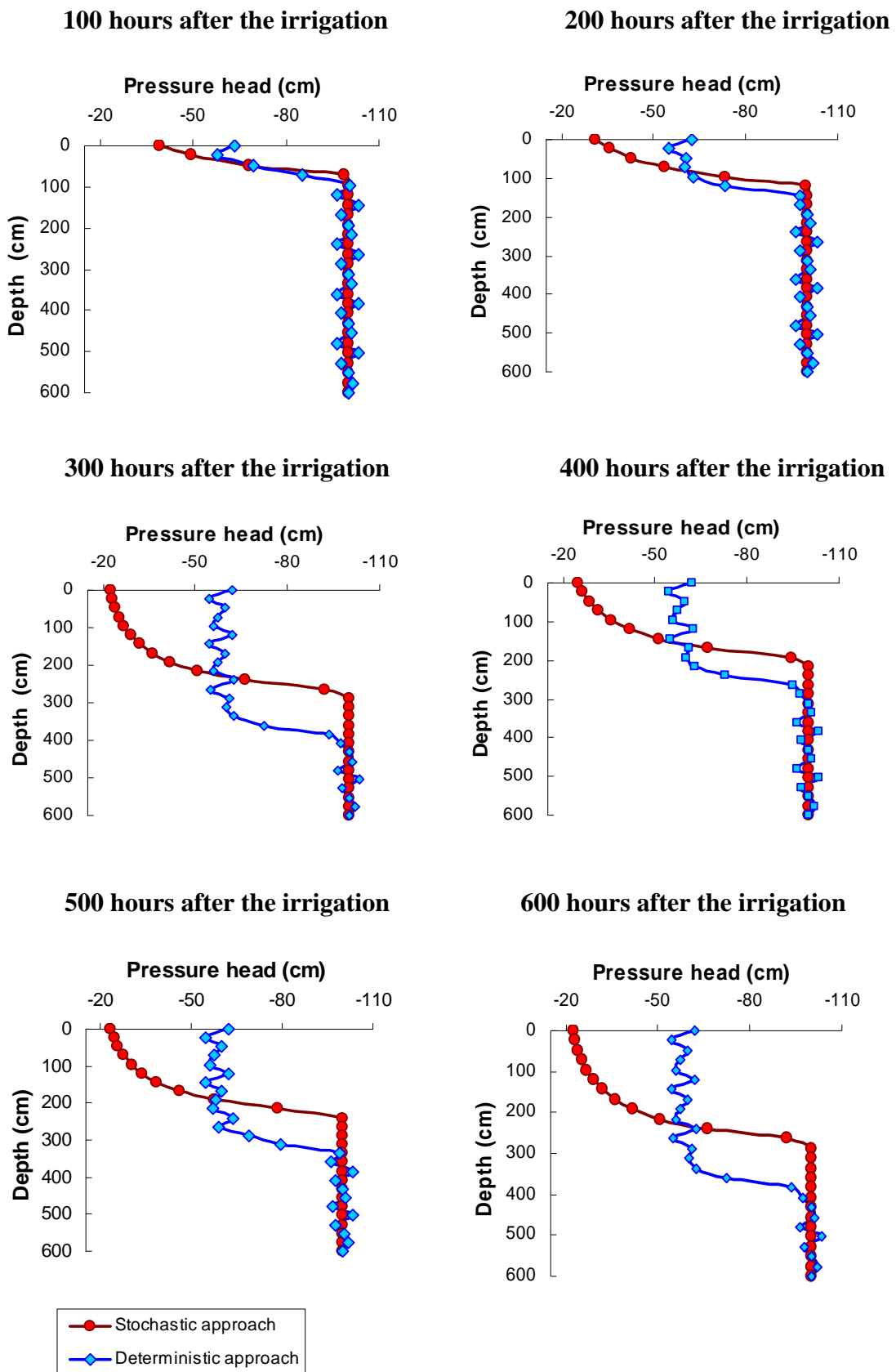
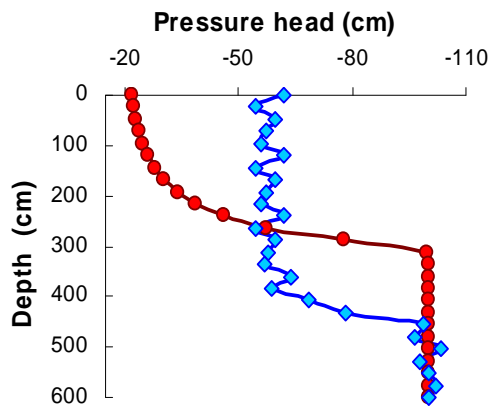
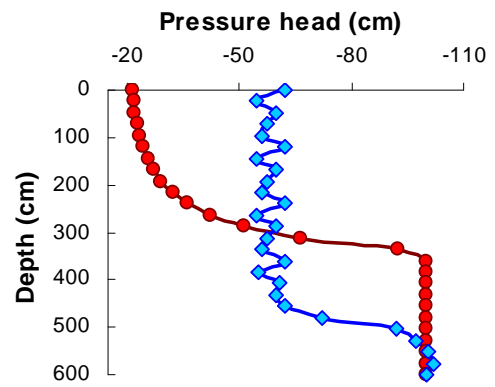


Figure 6.13 Pressure head distribution through the lysimeter for the stochastic and deterministic models (from 100 hrs until 1200 hrs).

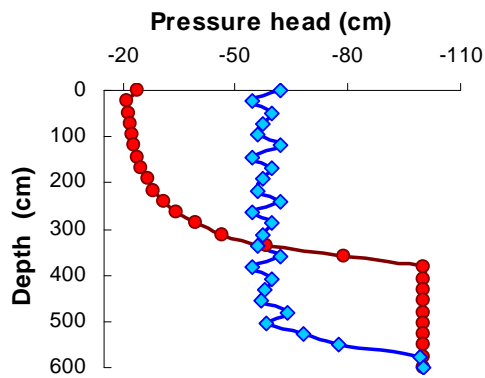
700 hours after the irrigation



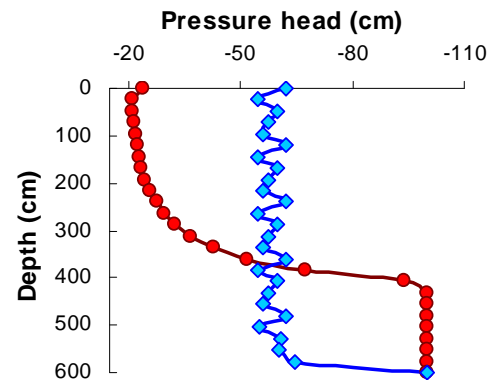
800 hours after the irrigation



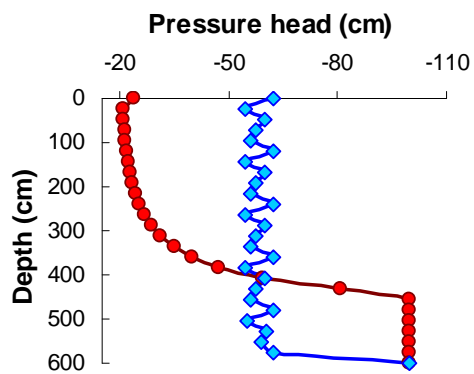
900 hours after the irrigation



1000 hours after the irrigation



1100 hours after the irrigation



1200 hours after the irrigation

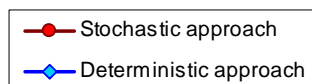
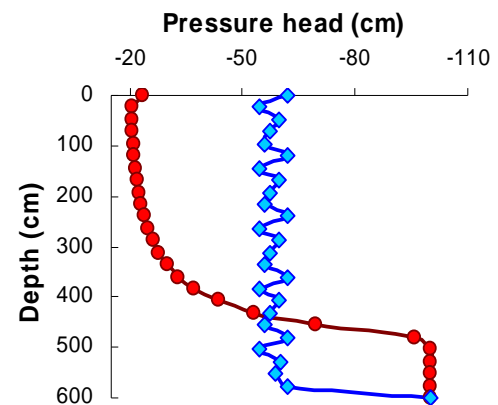


Figure 6.13 (continued).

Figure 6.14 shows the volumetric moisture content distribution along the depth plotted for every 100 hours during the 1200 hours of the irrigation procedure. The linear relationship of Van Genuchten was used to evaluate the water content.

$$\theta = \theta_r + \frac{\theta_s - \theta_r}{H_s - H_r}(H - H_r) \quad (6.25)$$

The maximum value of water content for the stochastic approach is $0.26 \text{ cm}^3/\text{cm}^3$ and for the deterministic approach is $0.15 \text{ cm}^3/\text{cm}^3$; whereas, the maximum value for measured water content is $0.23 \text{ cm}^3/\text{cm}^3$.

The smooth nature of the stochastic solution shows that this is a large-mean solution where small-scale fluctuations within or across the layers are not represented. In the deterministic case, the small scale spatial variations in the hydraulic parameters of the soil are included directly in the numerical description. In the stochastic case, spatial variations, such as layering, are incorporated into the effective parameters that are homogeneous over the entire domain. Hence, the presence of the small-scale fluctuations across the layers is not evident in the stochastic simulation.

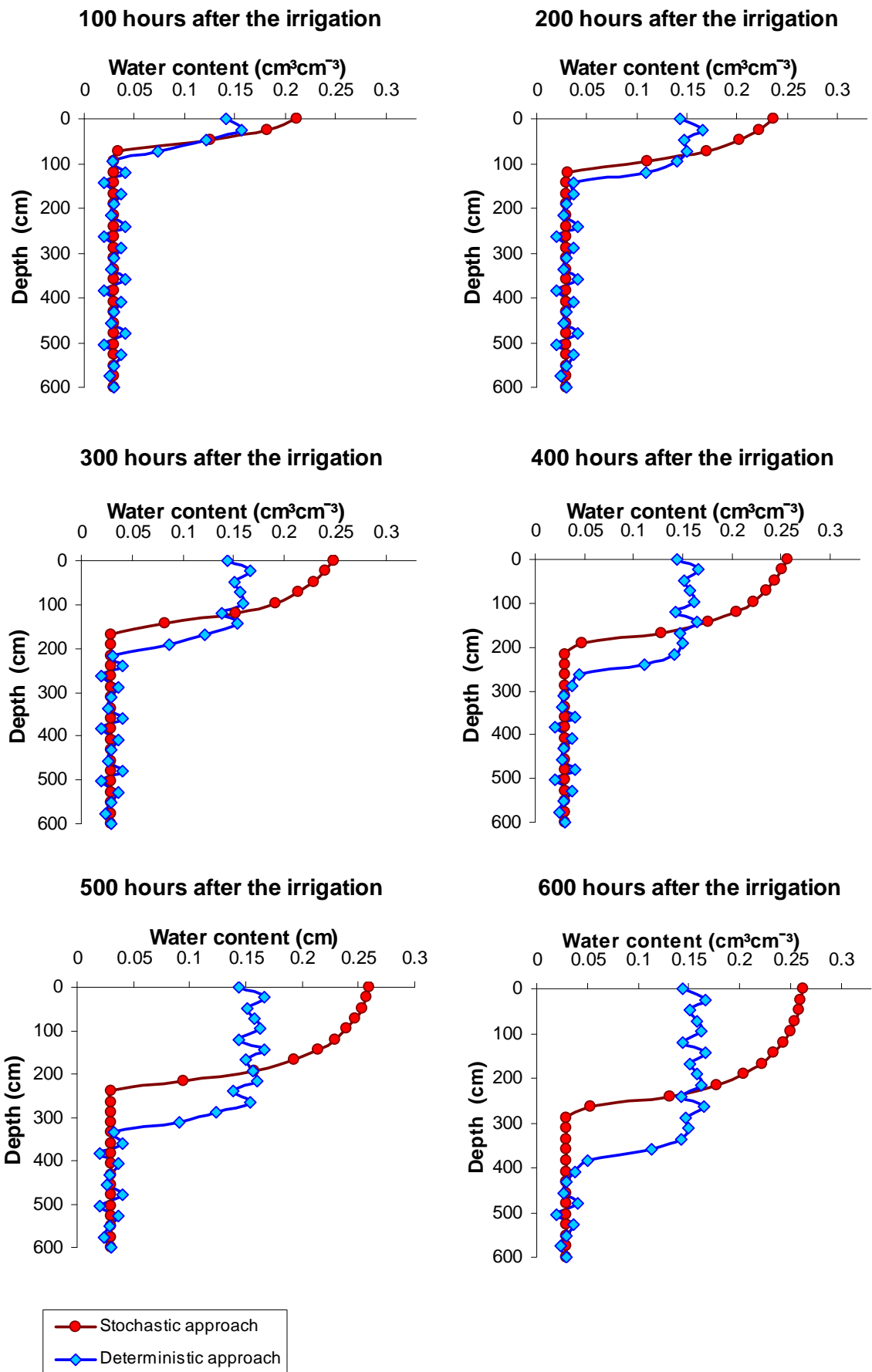


Figure 6.14 Volumetric water content distribution through the lysimeter from stochastic and deterministic approach every 100 hours (from 00 hrs until 1200 hrs).

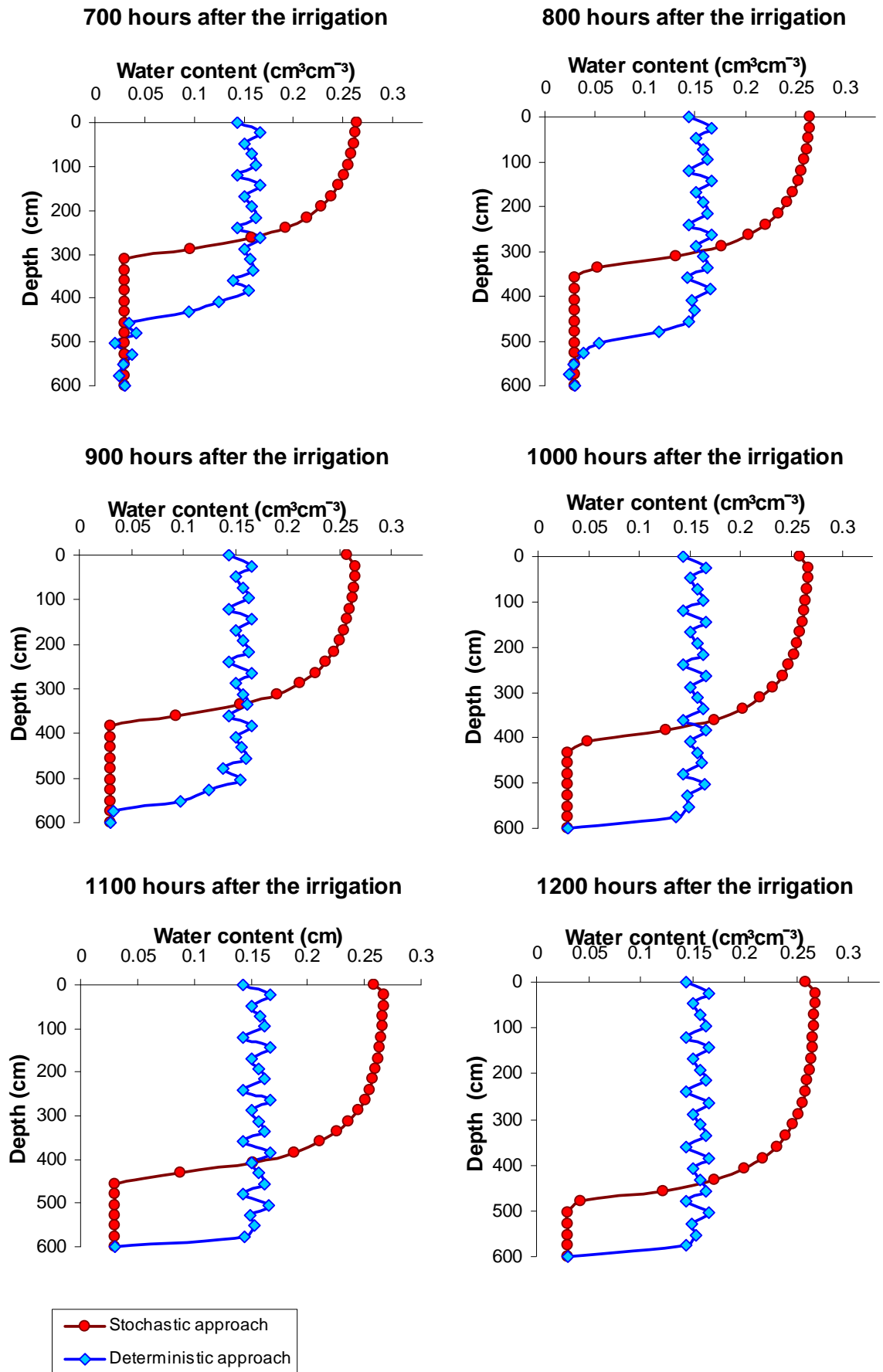


Figure 6.14 (continued).

Figure 6.15 shows the pressure head variance versus depth from the beginning until 1200 hours for every 200 hours. The minimum value of the pressure head variance is about 122 and the maximum value is about 3448. The pressure head variance decreases with time as more amount of water infiltrates into the soil, and increases through the depth. The maximum value of the variance is at the wetting front position. In theory, as the wetting front moves vertically, it encounters a series of soil layers that were previously dry. The dry coarse soil layers generally inhibit vertical flow, and they tend to remain dry, while the fine soil layers are easily wetted. Then, at the wetting front position a relatively large pressure head variance is expected. But, at the other parts of the soil, where water already passed and made them wet, less pressure head variance is expected (Mantoglou and Gelhar, 1987a).

Variance is an index of reliability of the prediction and can be used to estimate a possible range of the out value. A probable interval (mean concentration minus and plus standard deviation) is estimated for the real value of the output. So, having a higher value for the variance, the mean value of the model output can not be a proper estimation of the real value. This implies that the predicted mean values are not as reliable at the points with high variance as they are in the other parts of domain.

In the stochastic model, the output of the problem which is a random variable is described by statistical moments. The possible values of output at each location or time are in a range between mean plus and minus standard deviation rather than an explicit value. Figures 6.16 and 6.17 show mean pressure head distribution minus and plus one standard deviation at 600 hours and 1200 hours after the start of the irrigation. It is clear that standard deviation of pressure head from the mean value increases with decrease in the water pressure head. Comparison of the results presented in Figures 6.16 and 6.17 shows that the standard deviation decreases with time while the mean pressure head increases. So, the mean pressure heads can be predicted more accurately at wetter conditions.

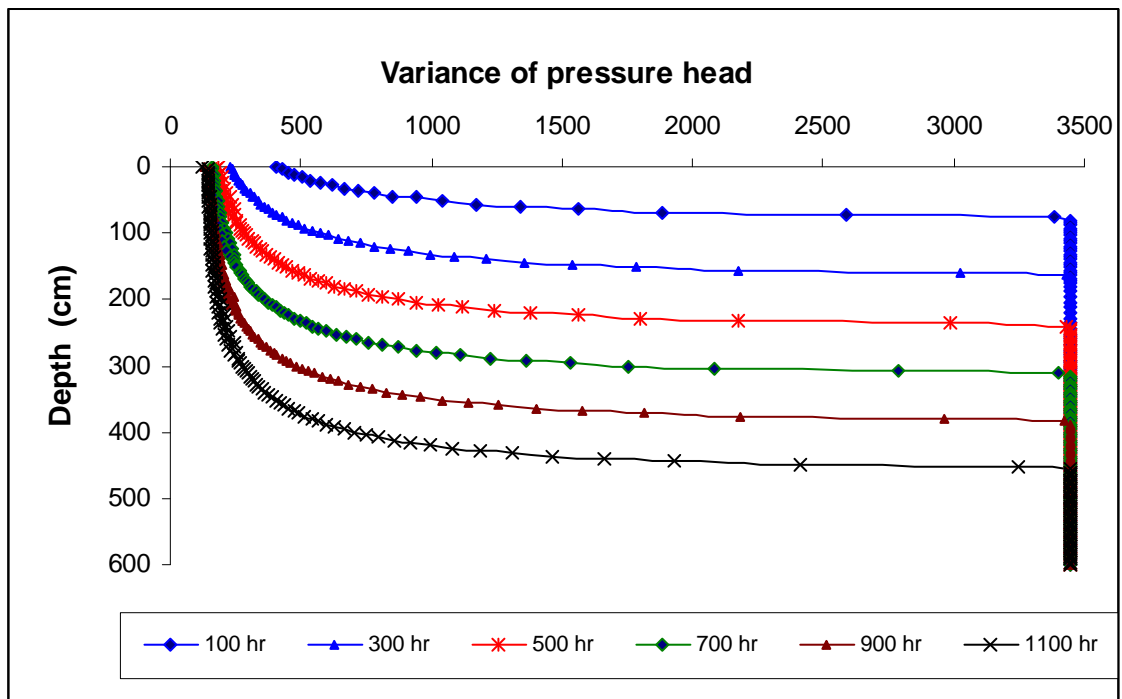


Figure 6.15 Pressure head variance through the lysimeter for various time.

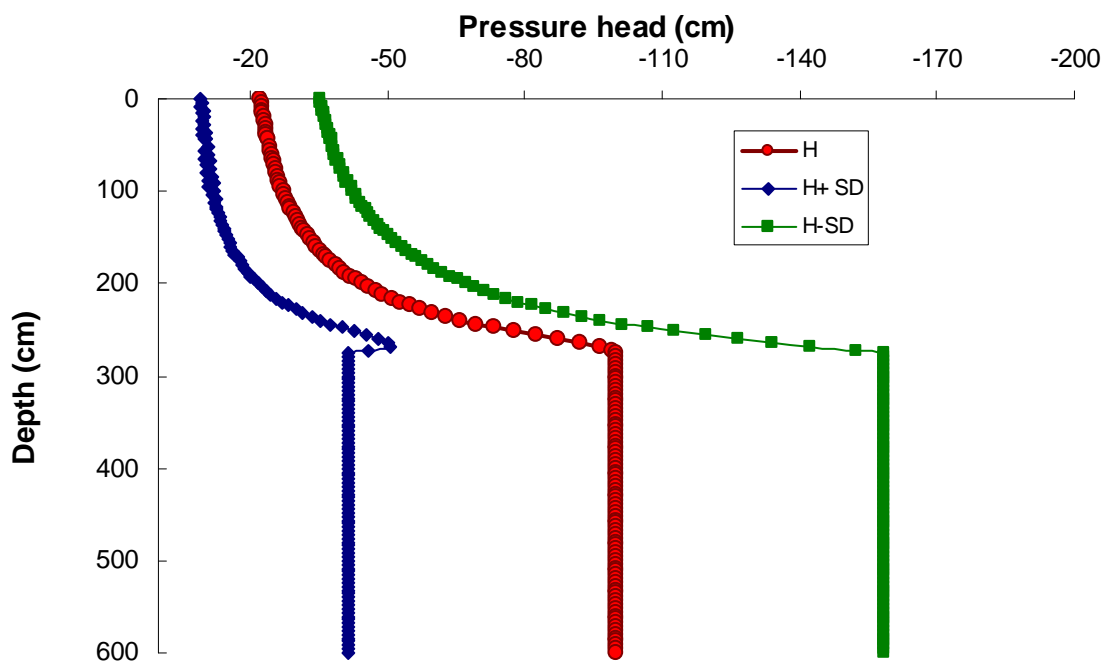


Figure 6.16 Mean pressure head distribution +/- standard deviation vs. depth 600 hours after irrigation (SD: Standard deviation, H : Mean pressure head).

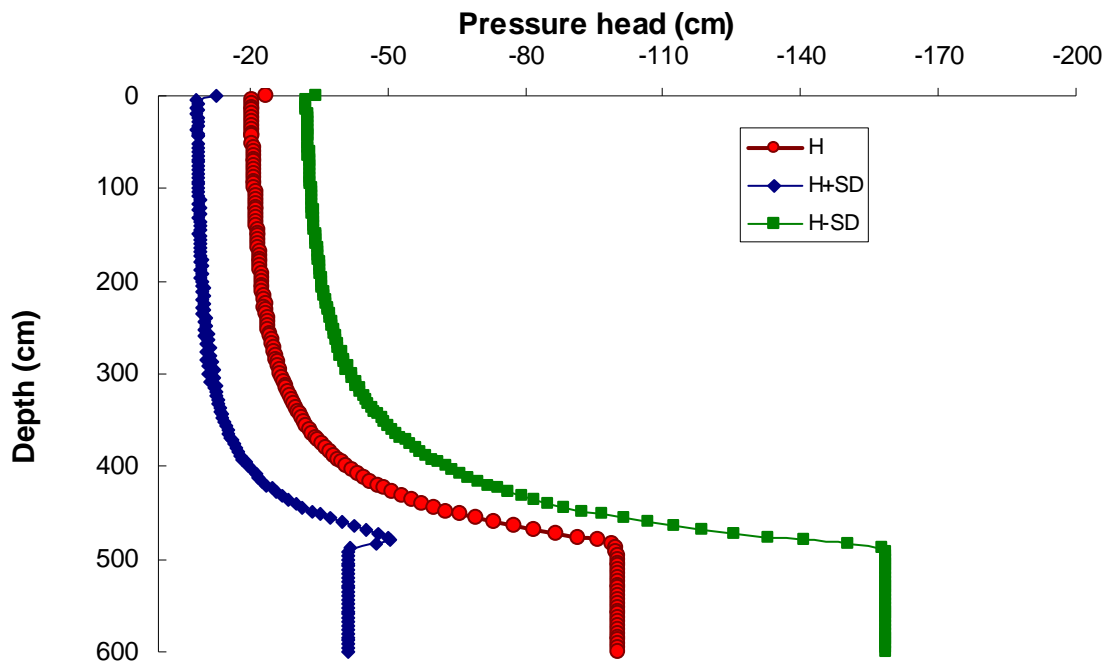


Figure 6.17 Mean pressure head distribution +/- standard deviation vs. depth 1200 hours after irrigation (SD: Standard deviation, H : Mean pressure head).

6.2.3 Example 3

Definition of the example

This example was chosen to validate the model for simulation of solute transport in heterogeneous soil by comparing the result obtained from the stochastic finite element method with those obtained from the Monte Carlo method. The example consists of transient solute transport with steady-state unsaturated flow through a column of soil. A solute with concentration of C_0 equal to 1 kg/m^3 is applied at the surface of the column for 20 days and is leached vertically into the soil column while the concentration at bottom of the column (C_L) is kept at zero. Figures 6.18 (a) and (b) show the geometric dimensions and the element discretisation employed in the solution, respectively. The length of the column is 0.5m and its width is 0.01m but computational domain was extended to 1.5 m in order to semi infinite space. As a result, solute concentration distribution through the column is independent of the type of boundary condition applied to the end of the column. The FE (finite element) mesh generated for this example consists of 150 triangular elements and 152 nodes.

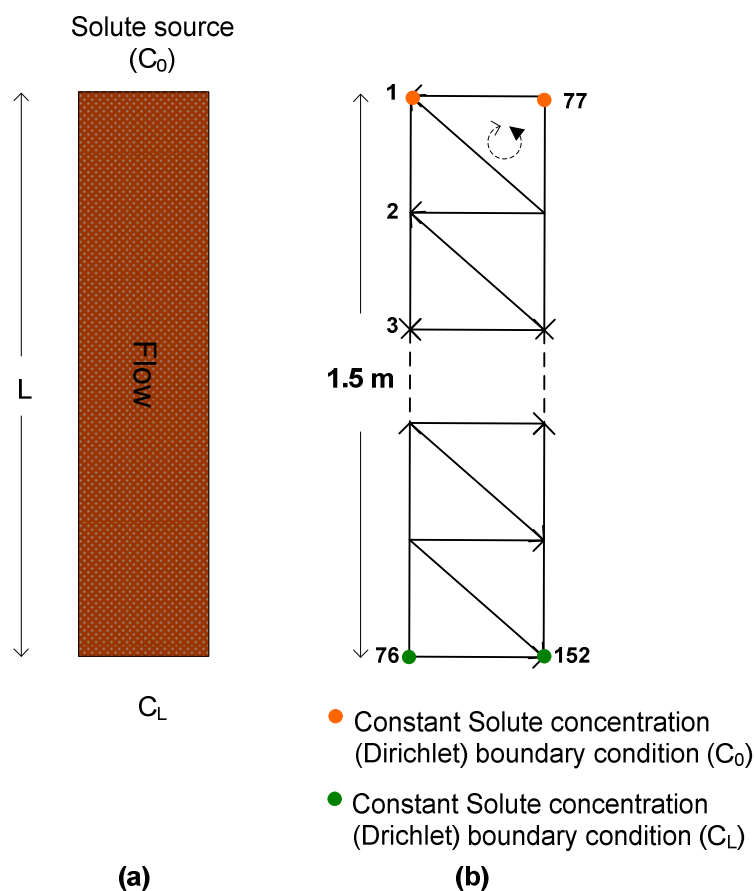


Figure 6.18 (a) Dimensions of the simulated soil column for steady-state flow and solute transport (b) the FE mesh showing boundary conditions.

The input parameter values are the same as those used by Persaud et al. (1985) who solved the same problem using the Monte Carlo method. A constant velocity of water equal to 1.3×10^{-7} m/sec is assumed through the column and the coefficient of diffusion is 3.6×10^{-8} m²/sec in vertical direction of the column. Mean of natural log of saturated hydraulic conductivity is taken as 0.31 with variance equal to 0.2135 and the variance scaling parameter is equal to 1.3 m^{-2} . Values of the parameters used in the model are summarized in Table 6.4.

Table 6.4 Value of parameters for steady-state groundwater flow and solute transport example.

F	0.31	q	$1.32 \times 10^{-7} \text{ m/sec}$
E	$3.6 \times 10^{-8} \text{ m}^2/\text{sec}$	σ_f^2	0.2135
σ_a^2	1.3 m^{-2}	λ	0.25 m

Initial conditions

The initial solute concentration through the domain is as

$$C(z, t) = 0 \quad 0 < z \leq 1.5 \text{ m}, t = 0 \quad (6.26)$$

$$C(z, t) = 1 \text{ kg} / \text{m}^3 \quad z = 0, t = 0 \quad (6.27)$$

Boundary conditions

The boundary conditions implemented to the domain is defined as

$$C(z, t) = 1 \text{ kg} / \text{m}^3 \quad z = 0, 0 \leq t \leq 20 \text{ days} \quad (6.28)$$

$$C(z, t) = 0 \quad z = 0, 20 \text{ days} < t \leq 50 \text{ days} \quad (6.29)$$

$$C(z, t) = 0 \quad z = 1.5 \text{ m} \quad (6.30)$$

Results

Figure 6.19 (a) shows the variation of the mean solute concentration with time at depth of 0.5 m of the column obtained using stochastic finite element model and Monte Carlo method. The mean values obtained from stochastic finite element model are in

agreement with the Monte Carlo results, while the computational time for simulation using stochastic finite element model would be about 200 times less than that of Monte Carlo method for achieving approximately the same results as Monte Carlo analysis involved 200 calls of FE model. This reduction in computational time and costs indicates the advantage of the stochastic finite element method over Monte Carlo method.

Figure 6.19 (b) shows the variance of solute concentration. The variance reaches its maximum after 23 hours and its minimum after 39 hours. The solute concentration distribution along the column presented in Figure 6.19 (c) shows that at time equal to 23 hours the gradient of solute concentration ($\tan \alpha$ in Figure 6.19c) at this depth is maximum and at time 39 hours, it is zero. Time variation of solute concentration distribution along the column can be seen in Figure 6.19 (e). For lower concentration gradients indicating uniform distribution or smooth variation in concentration in the domain, the solute transport occurs with less fluctuation. Therefore, in the region-around the centre of the concentration plume where the plume moves more uniformly a lower value is estimated for the variance. Uncertainty (variance) is higher at higher concentration gradients. This can be seen in the close form equation presented for evaluation of variance of solute concentration which shows the variance is directly proportional to the solute concentration gradient (G_i and G_j). However, the small value estimated for the variance in this example shows that the predicted mean concentrations are reliable.

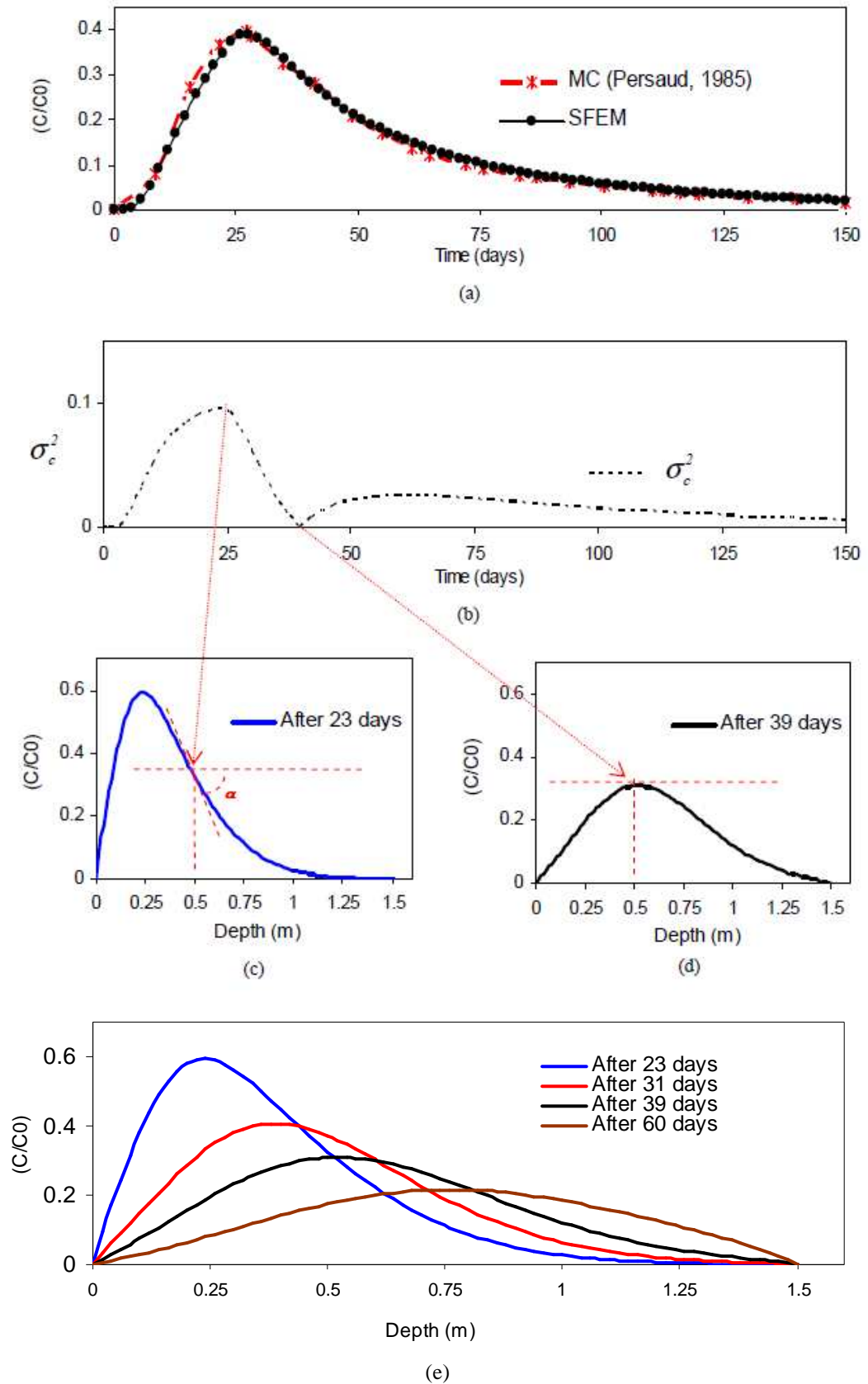


Figure 6.19 (a) Mean solute concentration vs. time obtained from MCM and SFEM, (b) σ_c^2 vs. time, (c) normalized mean solute concentration vs. depth after 23 days, (d) normalized solute concentration vs. depth after 39 days, normalized solute concentration vs. depth for different times.

A sensitivity analysis on the variance of saturated hydraulic conductivity was carried out to show the effects of spatial variability of this parameter on macrodispersion coefficient and solute transport speed. Figure 6.20 shows solute concentration versus time at 0.5 m depth obtained from stochastic finite element model using different values for σ_f . The solute concentration in earlier time of simulation increases because of implementation of solute at the top of the column at first 20 days of the simulation and transport of solute from the upper part of the column to this depth. After some times, concentration starts to decrease in response to change of solute concentration applied to the column surface from 1 kg/m³ to zero. It is shown that in the initial part of the curves when the mean solute concentration increases with time, the concentration increases with increasing σ_f . On the other hand, in the post peak part of the curve, increasing σ_f , causes decrease in concentration. This shows that solute spread faster with increasing σ_f as index of soil heterogeneity.

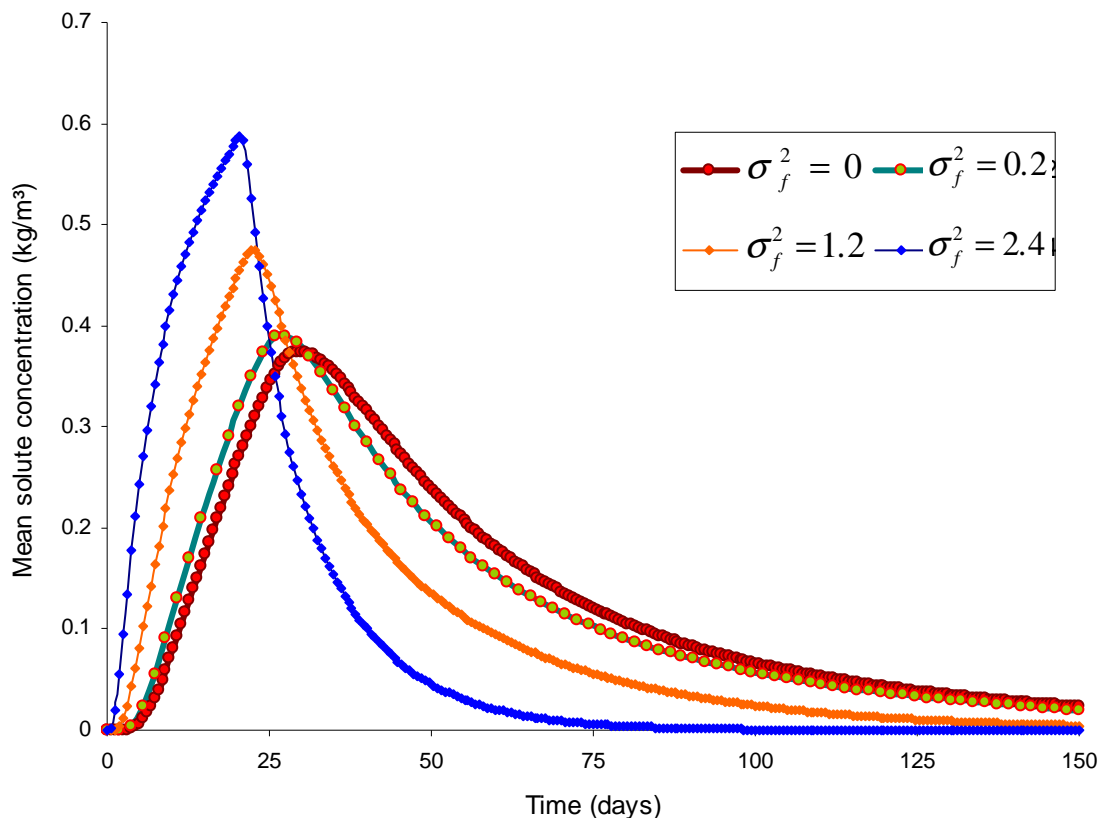


Figure 6.20 Solute concentration vs. time obtained for different values of σ_f .

Figure 6.21 shows the solute concentration distributions vs. depth at 50 days for different values of variance of natural log saturated hydraulic conductivity. It is shown that concentration decreases as the variance increases. This means that solute spreads faster when the soil heterogeneity increases. That is because of the direct relationship between macrodispersivity and the large-scale fluctuations of the water flow.

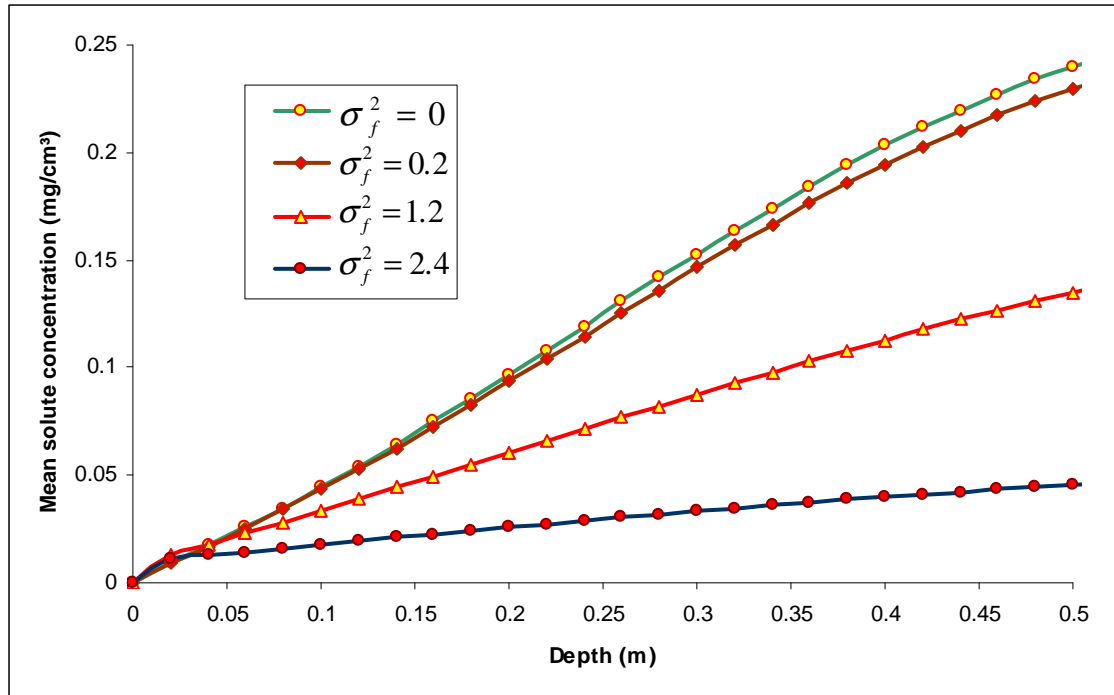
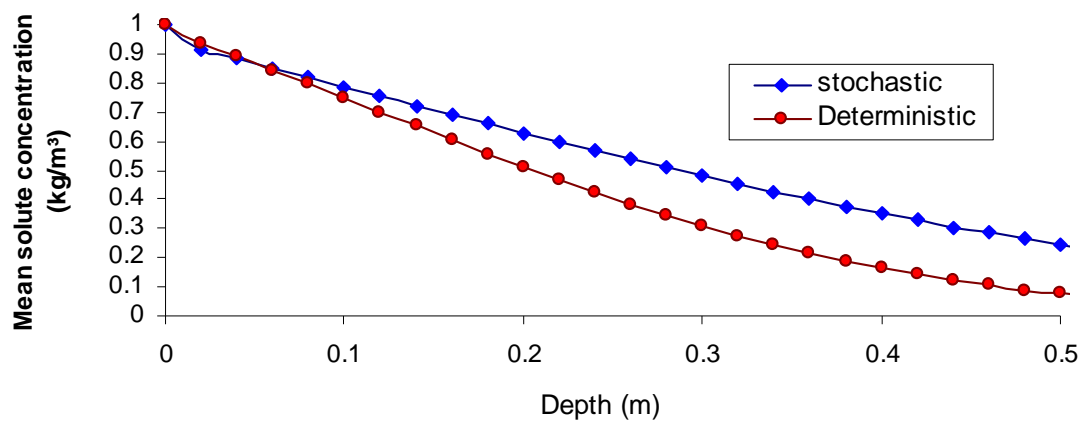


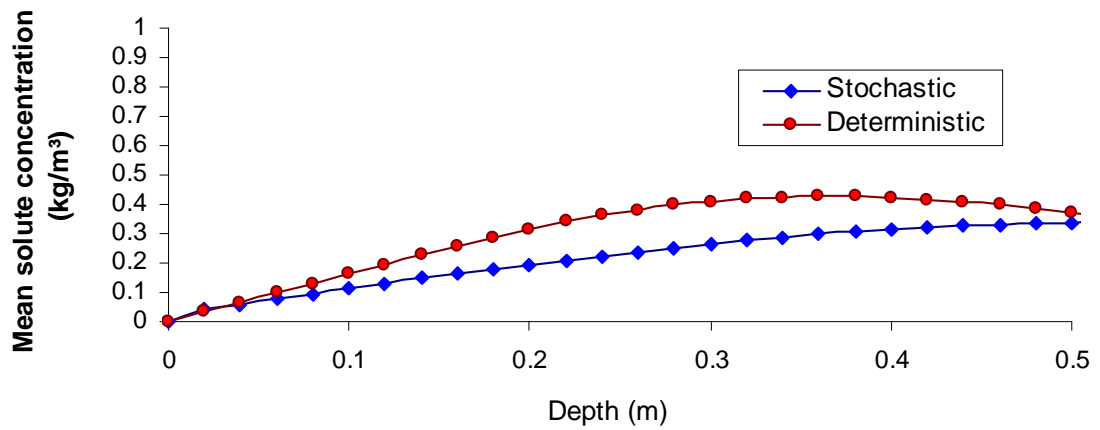
Figure 6.21 Solute concentration vs. depth obtained for different values of σ_f .

In order to highlight the effects of soil heterogeneity on solute transport, the results obtained from the stochastic finite element model using a higher value of σ_f equal to 1.2 were compared with deterministic results. Figure 6.22 shows mean solute concentration versus depth after 10, 30 and 50 days obtained from deterministic and stochastic finite element models. It is shown that solute moves downward with time for both stochastic and deterministic cases, but the deterministic results show slower solute transport than stochastic results. This is because in the deterministic model macrodispersivity which is dispersion due to soil heterogeneity and variability of local velocity is ignored.

(a) After 10 days



(b) After 30 days



(c) After 50 days

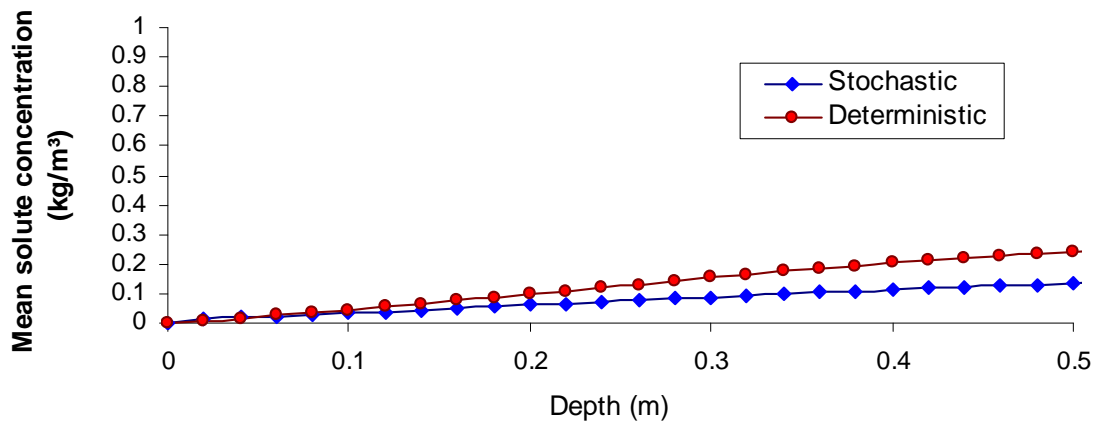


Figure 6.22 Solute concentration vs. depth obtained from the stochastic and deterministic finite element models after a) 10 days, b) 30 days and c) 50 days.

6.2.4 Example 4

This example has been selected to verify the model for simulation of three-dimensional problems. In this section, the analytical solution for a transient solute transport presented by Wexler, (1992) is used to check the accuracy of the developed model. A set of sensitivity analysis is performed.

Problem definition

The problem (Figure 6.23) consists of steady-state flow and transient solute transport in an aquifer of finite width (W) and height (H) with a solute source of finite width and finite height. The aquifer is infinite in x direction and the flow is assumed to be in x direction only with a constant mean velocity. It was assumed that the soil is stratified in x direction. A source of pollution of 1 m width and 1 m height is located at the left boundary of the aquifer. The values used for σ_f^2 and λ_3 are based on measurements of hydraulic conductivity for samples collected from an aquifer in Vancouver, B.C., (Smith 1978 and, Smith and Schwartz 1980) and the values of the other parameters are based on real soil data available in the literature (Polmann, 1990). Values of the parameters used in the model are summarized at Table 6.5.

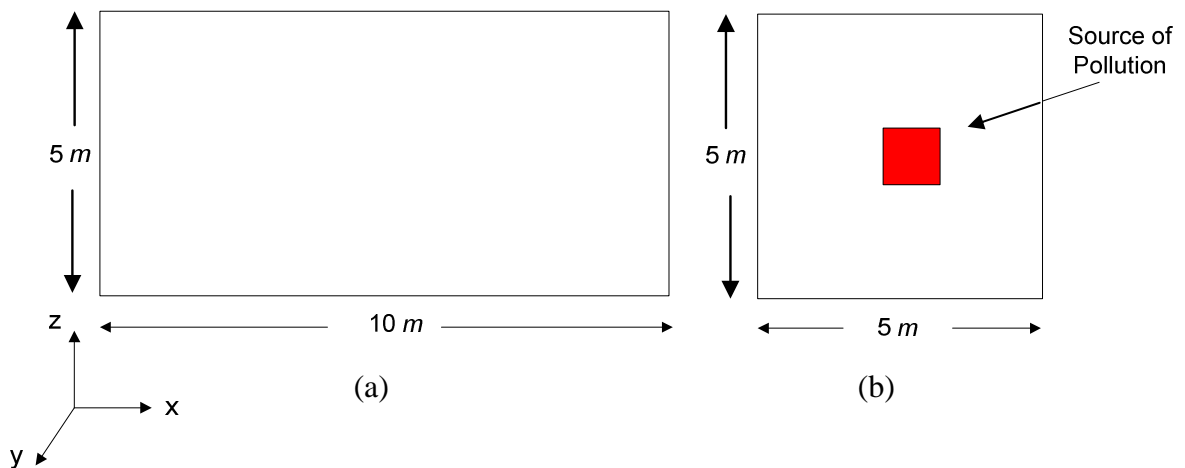


Figure 6.23 Dimensions of the simulated 3D hypothetical solute transport problem. (a) Plan, (b) Cross section.

Table 6.5 Values of parameters used for 3D solute transport example.

F	0.31	W	5m
σ_f^2	0.2	H	5m
σ_a^2	1.3 m^2	Y_1	2 m
λ_1, λ_2	2 m	Y_2	3 m
λ_3	0.38 m	Z_1	2 m
E	$3.6 \times 10^{-8} \text{ m}^2/\text{sec}$	Z_2	3 m
q	$1.32 \times 10^{-7} \text{ m}/\text{sec}$	C_0	100 mg/l

where, Y_1 is y coordinate of lower limit of the source, Y_2 is y coordinate of upper limit of the source, Z_1 is z coordinate of lower limit of the source and Z_2 is z coordinate of upper limit of the source at $x=0$.

Initial conditions

The initial solute concentration at each point of the domain is assumed as

$$C = 0 \quad 0 < x < \infty, \quad 0 < y < W, \text{ and } 0 < z < H, \quad t = 0 \quad (6.31)$$

Boundary conditions

The boundary conditions implemented to the domain are

$$C = C_0 \quad x = 0, Y_1 < y < Y_2 \text{ and } Z_1 < z < Z_2 \quad (6.32)$$

$$C = 0 \quad x = 0 \text{ and } y < Y_1 \text{ or } y > Y_2 \text{ and } z < Z_1 \text{ or } z > Z_2 \quad (6.33)$$

$$\frac{\partial C}{\partial y} = 0 \quad y = 0 \quad (6.34)$$

$$\frac{\partial C}{\partial y} = 0 \quad y = W \quad (6.35)$$

$$\frac{\partial C}{\partial z} = 0 \quad z = 0 \quad (6.36)$$

$$\frac{\partial C}{\partial z} = 0 \quad z = H \quad (6.37)$$

$$\frac{\partial C}{\partial x} = 0 \quad z = \infty \quad (6.38)$$

Analytical solution

Wexler, (1992) presented an analytical solution for this example using the classical partial differential equation for solute transport and applying initial and boundary conditions presented in equations (6.31)-(6.38) as

$$C(x, y, z, t) = C_0 \sum_{m=0}^{\infty} \sum_{n=0}^{\infty} L_{mn} O_m P_n \cos(\zeta z) \cos(\eta y) \cdot \left\{ \exp\left[\frac{x(v-\beta)}{2D_{xx}}\right] \cdot \text{erfc}\left[\frac{x-\beta t}{2\sqrt{D_{xx}t}}\right] + \exp\left[\frac{x(v+\beta)}{2D_{xx}}\right] \cdot \text{erfc}\left[\frac{x+\beta t}{2\sqrt{D_{xx}t}}\right] \right\} \quad (6.39)$$

where

$$L_{mn} = \begin{cases} \frac{1}{2} & m = 0, \text{ and } n = 0 \\ 1 & m = 0, \text{ and } n > 0 \\ 1 & m > 0, \text{ and } n = 0 \\ 2 & m > 0, \text{ and } n > 0 \end{cases} \quad (6.40)$$

$$O_m = \begin{cases} \frac{Z_2 - Z_1}{H} & m = 0 \\ \frac{[\sin(\zeta Z_2) - \sin(\zeta Z_1)]}{m\pi} & m > 0 \end{cases} \quad (6.41)$$

$$P_n = \begin{cases} \frac{Y_2 - Y_1}{W} & n = 0 \\ \frac{[\sin(\eta Y_2) - \sin(\eta Y_1)]}{n\pi} & n > 0 \end{cases} \quad (6.42)$$

$$\zeta = \frac{m\pi}{H} \quad m = 0, 1, 2, 3, \dots \quad (6.43)$$

$$\eta = \frac{n\pi}{W} \quad n = 0, 1, 2, 3, \dots \quad (6.44)$$

$$\beta = \sqrt{v^2 + 4D_{xx}(\eta^2 D_{yy} + \zeta^2 D_{zz} + \lambda)} \quad (6.45)$$

Results

A computer program was developed to compute the analytical solution of this example using Equations (6.39-6.45). The program is written in Maple 11.0. In order to provide better visualization, the results are presented in 1D curves. Figure (6.24) shows solute concentration distribution at $y=2\text{ m}$ and $z=2.5\text{ m}$ after 24, 60 and 120 hours obtained from the analytical solution and the deterministic (variances=zero) finite element method. The solid lines represent the analytical solution and the symbols represent the deterministic solution. The largest difference between the deterministic and analytical solutions is 4.1%, which is negligible and proves the accuracy of the developed model.

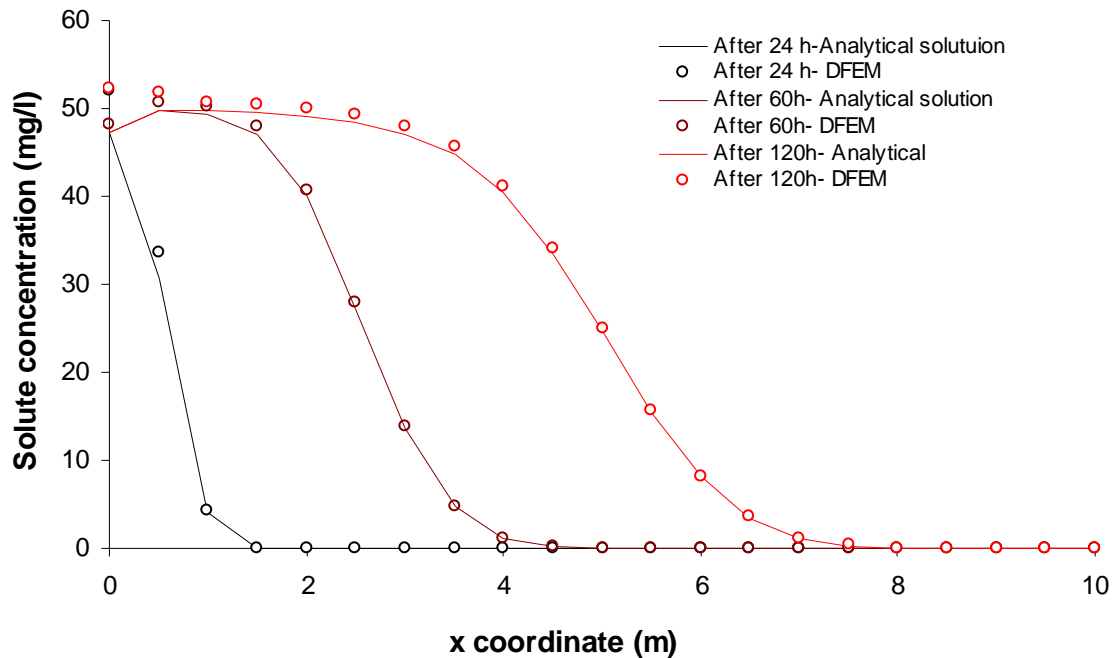


Figure 6.24 Solute concentration vs. x direction obtained from analytical and deterministic finite element methods ($y=2$ and $z=2.5\text{ m}$).

Figure (6.25) and (6.26) show solute concentration distribution at $y=2\text{ m}$ after 12, 60 and 120 hours obtained from the deterministic and stochastic finite element methods, respectively. From the analysis of the results, it was concluded that stochastic FE model predicts a wider contaminant distribution in area. After 12 hours, the contaminant reaches the length of 1.5 m while it reaches to 3 m for the stochastic case. At $t=60$ hours, it reaches 5 m in deterministic case and reaches 7.5 m in stochastic case and after 120 hours reaches to 8.5 m and 10 m for deterministic and stochastic, respectively.

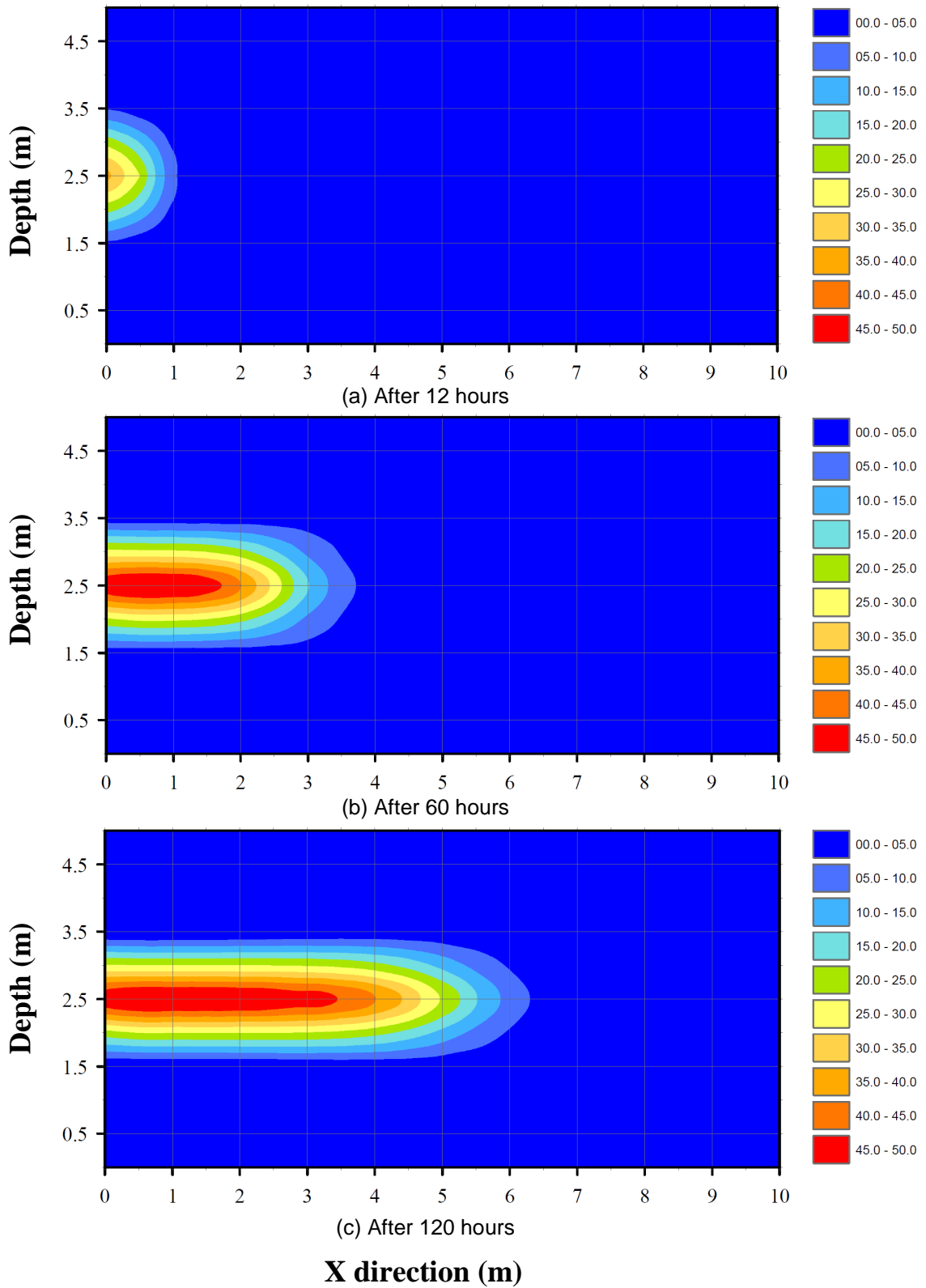


Figure 6.25 Solute concentrations (mg/l) at $y=2$ m obtained from DFE method at different times.

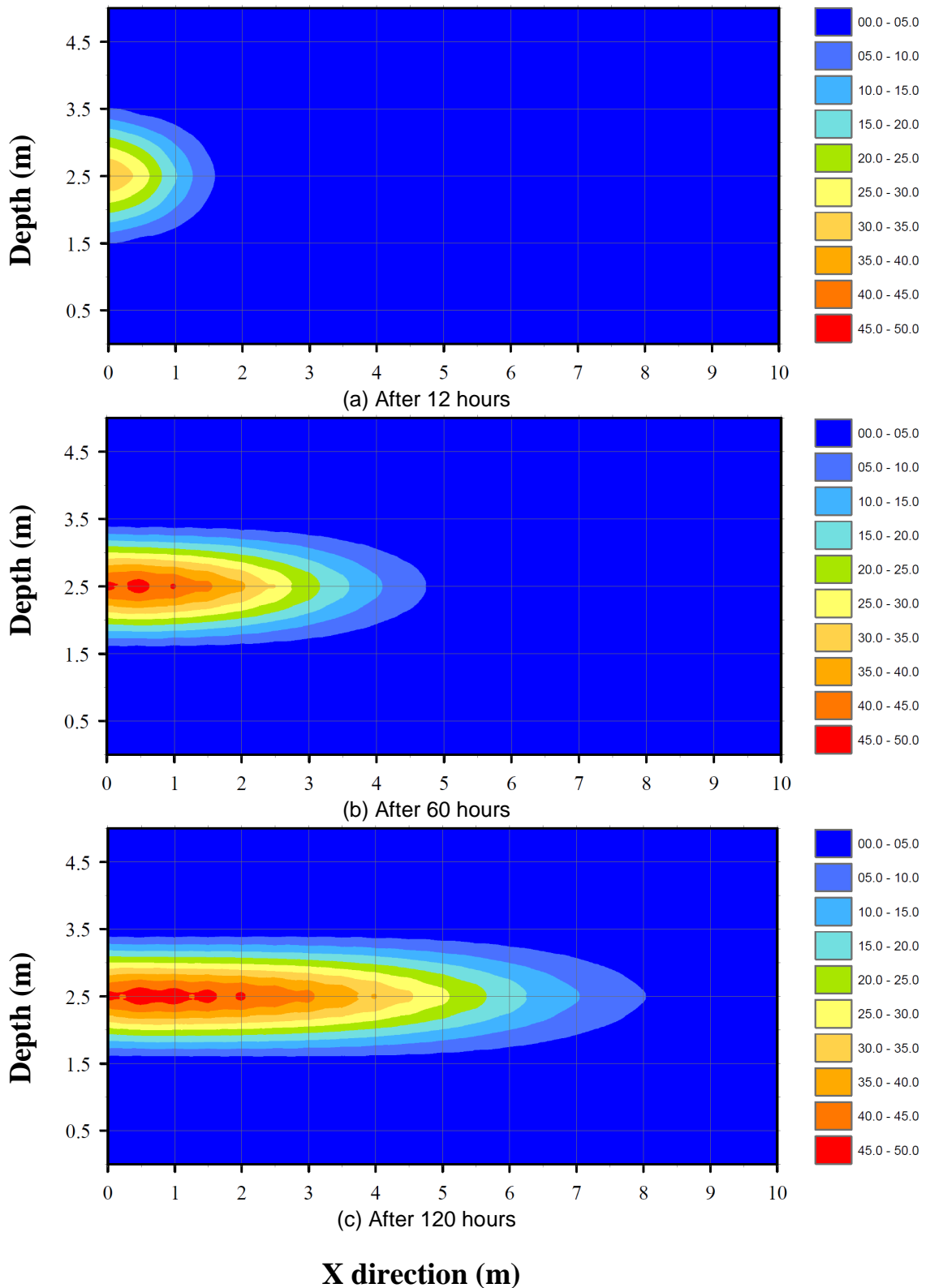


Figure 6.26 Solute concentrations (mg/l) at $y = 2$ m obtained from SFE method $\sigma_f^2 = 0.2$ at different times.

The example was also simulated with σ_f^2 equal to 0.5. Figure (6.27) shows the results of this simulation for $t= 12, 60$ and 120 hours. The difference in dimension of the contaminated plume in direction perpendicular to the stratification (z direction) between results of the stochastic finite element model with $\sigma_f^2 = 0.2$ and the deterministic finite element model is negligible.

Although, this difference increases with increasing σ_f^2 and the stochastic results show a larger contaminated plume in this direction, however this difference is very small in comparison with that in the direction parallel to the mean flow. This is in agreement with the finding of Gelhar and Axness, (1983). They have shown theoretically, using analytical methods, that for the case of stratified soil with mean flow parallel to the direction of stratification (condition assumed for this example), transverse macrodispersion are extremely small and the contribution will be much smaller than the local transverse dispersion.

The stochastic and deterministic results were compared to the analytical results. The deviation in contaminant concentration at $y= 2$ m for the stochastic approach with (a) $\sigma_f^2 = 0$; (b) $\sigma_f^2 = 0.2$; (c) $\sigma_f^2 = 0.5$ and for the deterministic approach is shown in Figure 6.27. The deviation is evaluated as the difference between deterministic analytical and numerical results. The deterministic and analytical results are coincident except for near the source of pollution. The deviation is small. The maximum deviation is 2 mg/l and it decreases with increase in the distance from the source. The deviation between analytical and mean solute concentration increases when σ_f^2 increases. This means that the higher the variability of the soil properties, the higher the difference between deterministic and stochastic results.

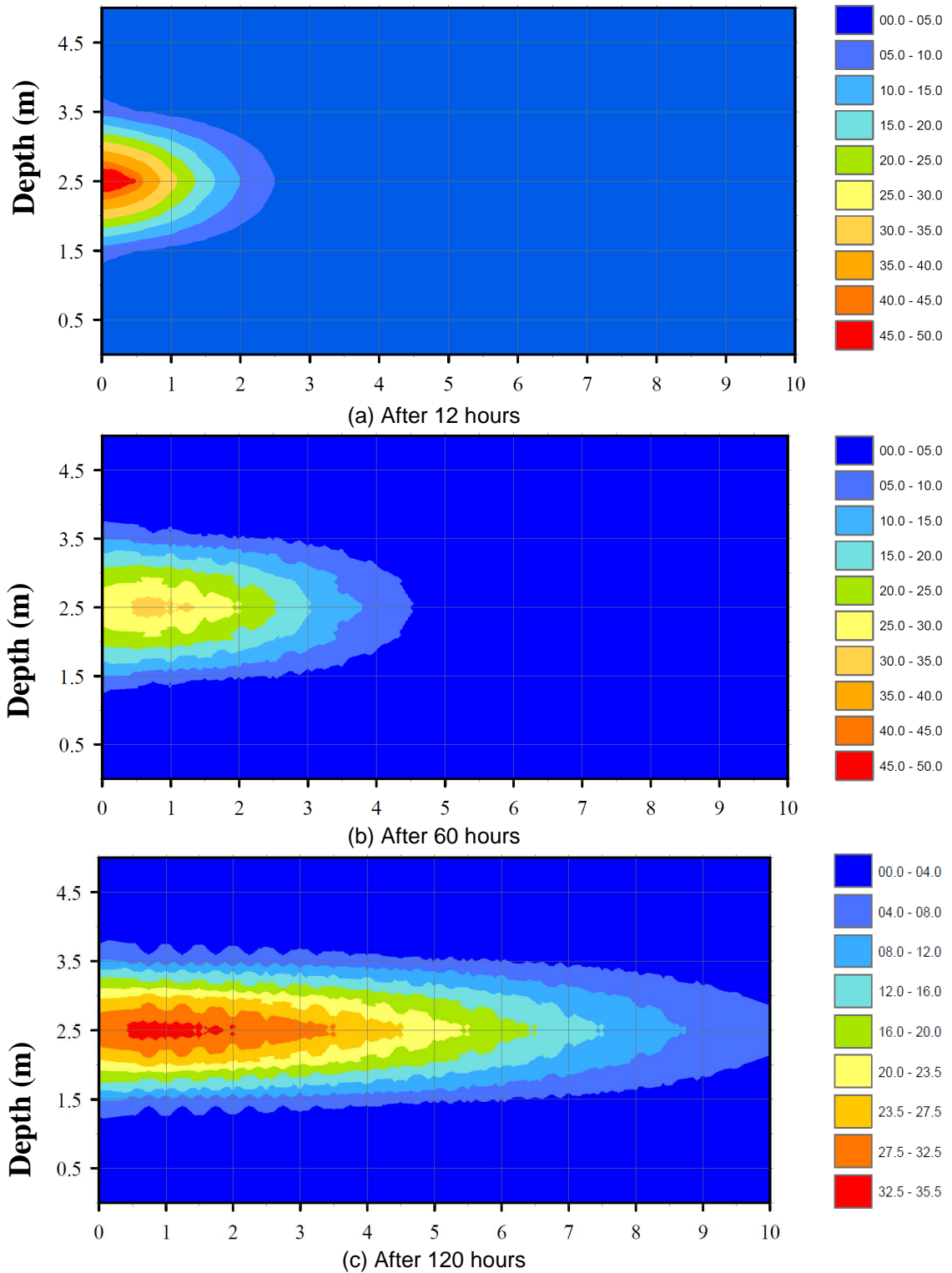


Figure 6.27 Solute concentrations (mg/l) at $y = 2$ m obtained from SFE method $\sigma_f^2 = 0.5$ at different times.

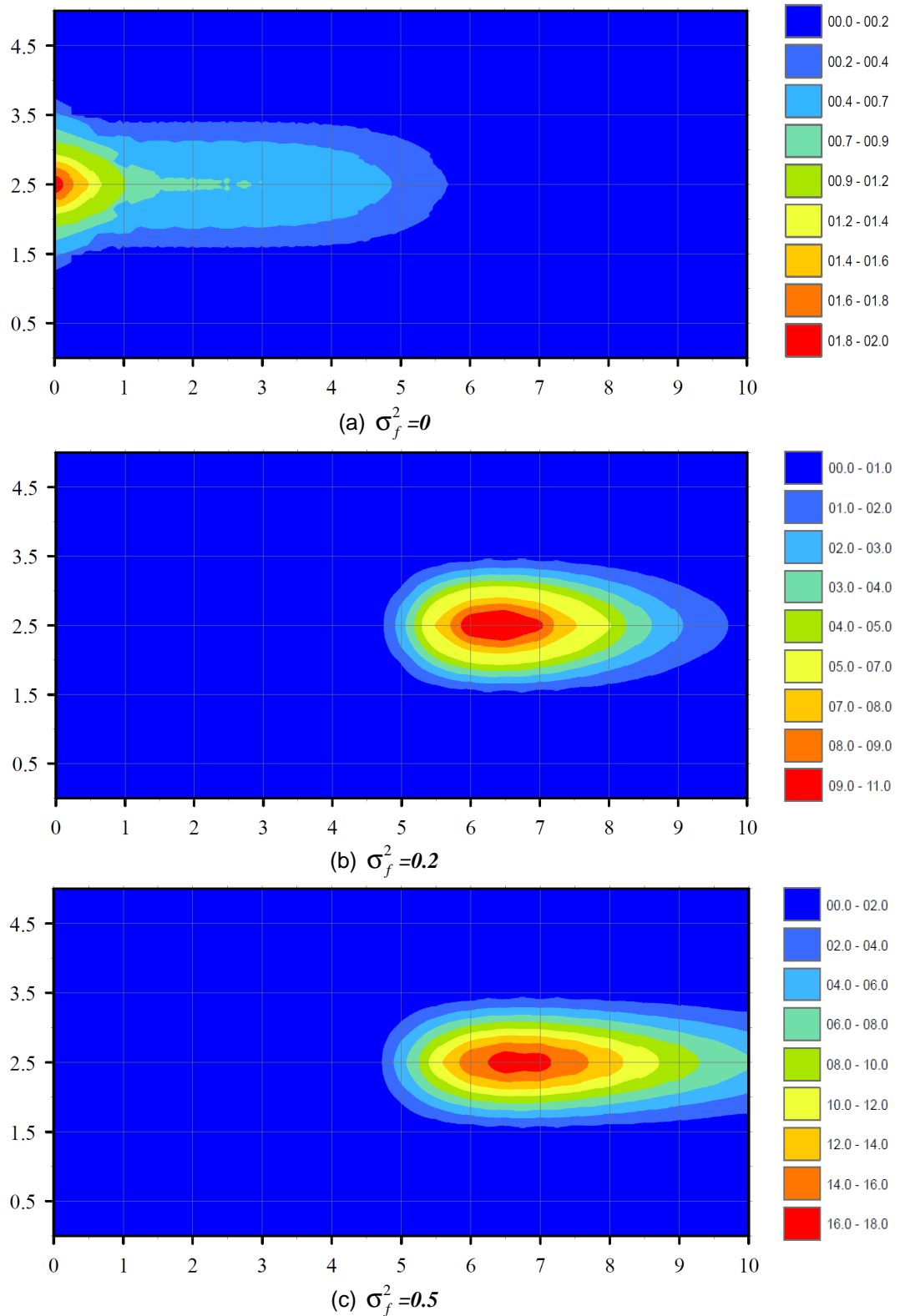


Figure 6.28 Deviation of solute concentration (mg/l) at $y = 2$ m.

In order to study the effects of correlation scale on the solute concentration distribution the problem was simulated for different values of correlation scale. Dimensions of contaminated plume in x,y and z directions for different values of correlation scales are presented in the Table 6.6.

Table 6.6 Contaminated plume dimensions for different value for correlation scale.

Case	Parameter under study	Value (m)	W_c (m)	L_c	H_c (m)
A	λ_1	4	2	8.5	2
B	λ_2	0.5	2	7	2.1
C	λ_3	1	2	7	2.1

where, W_c , L_c and H_c are width, length and height of contaminated plume respectively.

In case A, the value of λ_1 is equal to 4 m. From comparison of the dimensions of contaminated plume with the those of the case with λ_1 equal to 2 m, it is concluded that increase in λ_1 causes a higher amount of solute to disperse in x direction and the dimension of the plume gets longer. However it does not have a significant effect on the dimension in y and z directions. Both reduction of λ_2 from 2 to 0.5 in case C and increase of λ_3 from 0.38 to 1 in case C do not have any significant effects either on the length of plume (i.e. x direction) or the height of plume (i.e. z direction). However, they cause slight increase in the contaminated plume dimension in y direction.

6.2.3 Example 5

This example was chosen to verify the model in considering the effects of immobile water due to the existence of macropores in the domain.

Problem definition

A one-dimensional solute transport experiment conducted by Schoen, et al. (1999) in an undisturbed field lysimeter set up in a site located 40 km northwest of Grenoble, France, is considered to be simulated using the model developed in this study. The lysimeter with 1.2 m^2 surface area and 1.5 m depth (Figure 6.29) was kept under controlled water flux conditions. There was no surface vegetation on the lysimeter during the experiments, and the surface was covered in order to avoid evaporation. The soil was an aggregated sandy and clayey loam. A higher density of macro-pores was observed and the percentage and size of sand gravel and stones increased with increasing depth. A finite element grid consisting of 120 triangular 3-nodes elements is used for the numerical simulation.

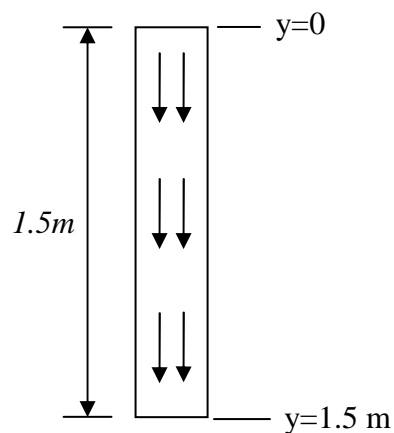


Figure 6.29 Problem definition.

Initial conditions

A zero initial solute concentration is considered through the lysimeter.

$$C(z, t) = 0 \quad 0 < z \leq 1.5 \text{ m}, t = 0 \quad (6.46)$$

Boundary conditions

The following concentration boundary conditions are used:

Lower BC:

$$\partial C(\infty, t) / \partial z = 0 \quad (6.47)$$

Upper BC:

$$C(0, t) = C_0, \quad 0 < t \leq t_0 \quad (6.48)$$

$$C(0, t) = 0, \quad t_0 < t$$

where, t_0 is initial time.

The lysimeter was subjected to two different flow flux conditions using rainfall simulator grid; one with a constant water flux of 1.48 mm/h (experiment A) and another with a constant water flux of 1.05 mm/h (experiment B). Solute pulses as KBr and KCl were applied to the surface of the lysimeter when the flow condition was reached to steady state. Duration (t_0), composition, concentration (C_0) of the pulses and value of the other parameters used in the simulations are reported in Table 1. Numerical simulation of the problem is carried out for four different scenarios assumed for structure and formation of the soil:

- A single domain system having uniform hydraulic properties (SDU); the variance of the hydraulic parameters of the domain and coefficient of solute exchange rate (ζ) between the domains are fixed to zero.
- A dual-domain system with uniform hydraulic properties (DDU); the spatial variability of hydraulic properties of the soil is ignored and the variances of the hydraulic parameters of the domain are fixed to zero.
- A single domain system with spatially variable hydraulic properties (SDV).
- A dual-domain system with spatially variable hydraulic properties (DDV). The variance of saturated hydraulic conductivity equal to 3 and correlation length equal to 10 cm are considered for the DDV in the experiment B.

Table 6.7 Values of input parameters used for simulation of the experiments A and B.

Experiment	θ	t_0 (h)	C_0 (mg/l)	D^* (cm ² /h)	D^{\dagger}	ζ (cm ² /h)	θ_m
A	0.248	75.5	476	3.5	5.3	2×10^{-4}	0.181
B	0.247	112.0	972	5.2	5.2	6×10^{-5}	0.195

D^* =Dispersion coefficient used for the scenarios DDU and DDV,

D^{\dagger} =Dispersion coefficient used for the scenarios CD.

Results

Experiment A

The breakthrough curves (BTCs) presented in the Figure 6.30, shows the numerical results obtained using the SFEM, and the analytical and experimental results presented by Schoen, et al. (1999) for the experiment A, assuming two scenarios SDU and DDU. The result obtained based on the SDU scenario, is in very good agreement with the analytical solution of convective-dispersive (CD) transport equation presented by (Schoen, et al. 1999). However the results are not fitted with experimental measurements. The possible reason for this discrepancy is that the effects of soil heterogeneity and existence of macropores in the domain were not considered in the simulations. As, the results obtained based on DDU Scenario present good agreement with experimental measurements. This result is also in agreement with analytical solution of governing equation of transport in dual-domain system presented by Schoen, et al., (1999). These agreements show the validity of the developed model for simulation of solute transport in dual-domain system and highlight the significant effects of micro-heterogeneity (macro-pores) in the solute fate.

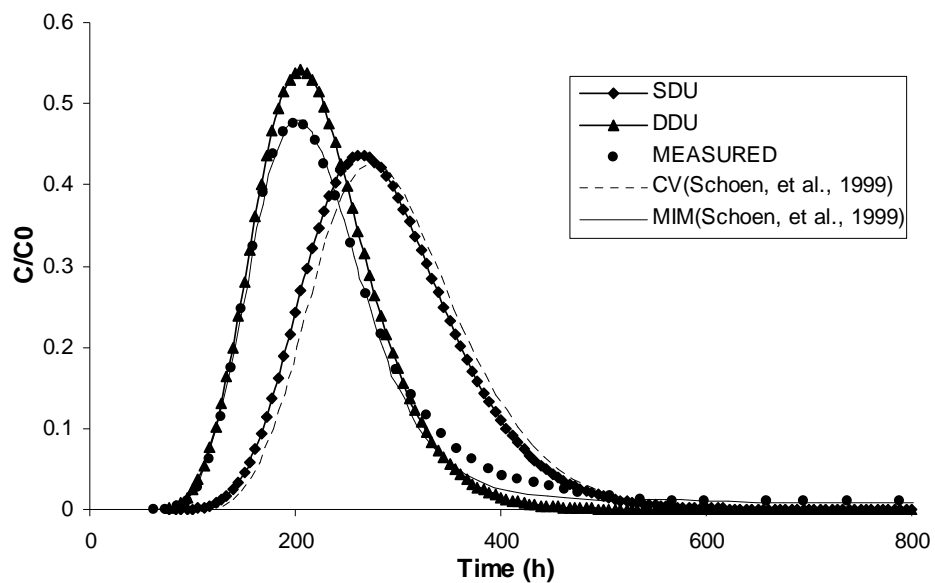


Figure 6.30 Relative solute concentration vs. time.

During transport process, mass is trapped in the top zone of the lysimeter due to its diffusion to immobile water stacked in the macro-pores, so less mass moves downstream. Sensitivity analysis can be utilized to address the effects of soil structural heterogeneity (macro-pores) on solute transport. Figure 6.30 shows the results of a

sensitivity analysis of relative solute concentration distribution along of the lysimeter with respect to ζ . The relation between solute concentration distribution and ζ depends on the sign of temporal variation of concentration ($\Delta C/\Delta t$). To illustrate this relation, solute concentrations at an arbitrarily chosen section (at a depth of 0.4m) of the lysimeter are considered 83 and 139 hours after the start of the solute application (S1 and S2 in Figure 6.31). As shown in the figure, after 83 hours, when the peak of solute concentration has not yet reached this section (S1) and $\Delta C/\Delta t$ is positive in S1, increase in ζ causes decrease in the concentration while after 139 hours, when the concentration peak has passed this section and $\Delta C/\Delta t$ is negative, concentration increases with ζ in this area (see sections S1 and S2, magnified in Figure 6.31).

For lower values of ζ indicating less heterogeneity in the soil structure, the transport regime approaches the behaviour of a single-domain system having a total porosity equal to the mobile porosity of the dual-domain system. Therefore, the plume moves downstream at a faster rate, causing higher relative concentration to appear in the lower zone. When the mass transfer rate coefficient is increased more connection is exchanged between the domains, and the system behaves like a single-domain regime having a porosity approaching the total porosity of the dual-domain system. Thus the plume travels through the domain at a slower rate.

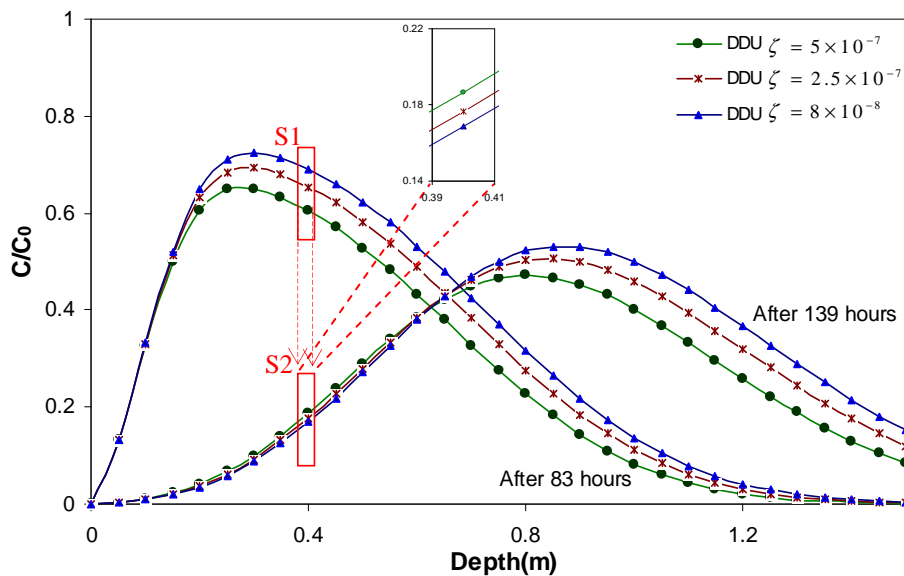


Figure 6.31 Relative solute concentration vs. depth, for different value of ζ after 83 and 139 h.

Experiment B

Figure 6.32 shows the numerical results obtained from the developed model for experiment B, assuming scenarios SDU, DDU, together with experimental measurements presented by Schoen, et al., (1999). In experiment B which was based on stratified formation of soil, the soil in the lysimeter was assumed to consist of 10 layers having constant water content. Water contents and solute concentration were measured by extracting 30 samples in every 10 cm thick layer, (2 samples in each layer). The measured water contents show spatial variability along of lysimeter. Existing oscillations in measured solute concentrations make it difficult to find a simulated profile using a numerical method to fit the measured values. The results obtained with SDU and DDU scenarios do not fit the measured data. The possible reason is that in these scenarios, the effect of the macro-heterogeneity of soil is ignored. A better fit can be observed between the results obtained based on DDV scenario and the experimental data (Figure 6.33). It is noticeable that the results of SDV which only considers the effects of macro-heterogeneity are not in agreement with the measured results as much as those of DDV. This indicates the significance of consideration of both types of heterogeneity.

Although, the mean concentration profile obtained based on DDV does not still cover all the measured data, the measured concentration realization is more or less surrounded by mean concentration plus and minus a standard deviation with a fairly good accuracy. The mean concentration profile shows a better agreement with the measurements at the lower zone of the lysimeter than the upper zone. Discrepancy between the results at the upper area of the lysimeter might be because of the boundary effects in the numerical results, as it is close to source of solute injection. Also, the coefficient of variability of the concentration as index of reliability of results shows higher value at the area close to the source.

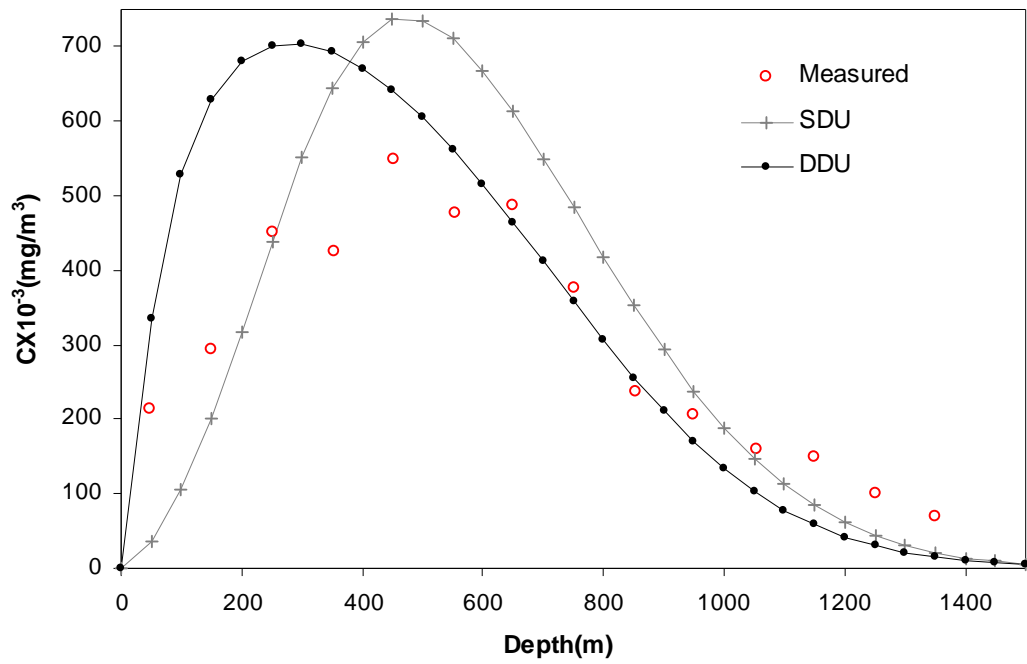


Figure 6.32 Solute concentration vs. depth.

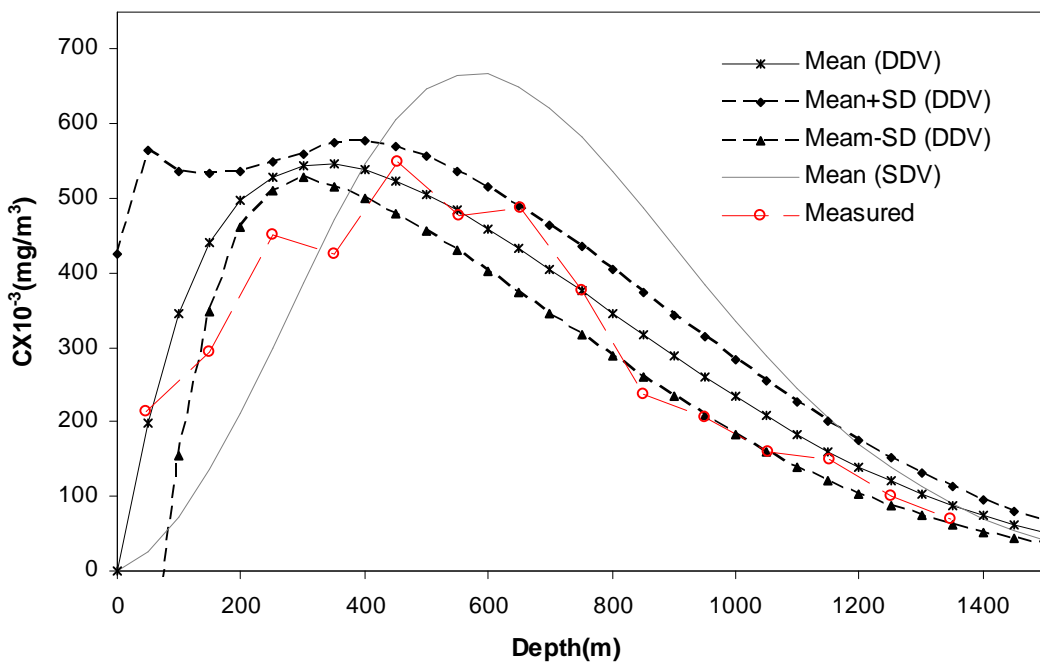


Figure 6.33 Solute concentration vs. depth.

6.3 Case studies

6.3.1 Case-study 1

The developed SFEM is applied to a case study involving transport of a petroleum-based contaminant at a site in south west of England, in order to examine the applicability of the SFEM for simulation of field scale problems.

Site description

The local geology comprises Yeovil Sand beds to 60m depth, with Jurassic limestone immediately to the north. The surface geology of the site includes shallow, fine alluvial deposits containing organic matter, and layers of coarse grained material, probably weathered limestone with limestone fragments. The site is underlain by a major aquifer and is on the boundary of a fluvial floodplain, having an annual flooding risk of 1%. The plot is approximately 20m by 20m and consists of a building formerly used as a shop and office, together with two attached workshops with concrete floors, used for repairs and storage (Figure 6.34). Adjacent to the current office entrance is a store containing two paraffin or light oil tanks, each of 1300 litre capacity. The forecourt is concrete surfaced above the fuel tanks, with a tarmac and gravel access road to the rear. The fuel filling area is directly adjacent to the public pavement and consists of four diesel pumps. Five manhole covers are nearby, two of which provide access to fuel storage tanks, with two adjacent surface drains (Javadi et al., 2008).

Site observation

Numerous inspection covers are present on the site, providing access to fuel tank fillers, pipe manifolds, water supply pipes and two surface drains, with two further drains on the site periphery. Tests carried out by a consulting engineers company, showed that one drain adjacent to the fuel pumps discharges directly into a receptor, which means that any spillages from pump operation has a direct pathway to local surface water. Water present beneath some inspection covers has shown considerable contamination by heavy oils.

Eight monitoring boreholes have been used for the survey as shown in Figure 6.34 to provide comprehensive information about the possible amount of dispersed and

dissolved fuel compounds. Such contaminants can be expected to show greatest mobility and hence potential for migration off-site.

Four monitoring boreholes had previously been installed to three meters depth, adjacent to the storage tanks and pump areas. Four additional boreholes were installed by the consultant in charge of the investigation as close as possible to the site boundaries. The installation points were selected to surround the site as far as practicable, with emphasis on the north and west boundaries, as observations suggest that groundwater is likely to flow in this direction. The new boreholes, *B5 – B7*, were of a similar design to the original, slotted from 1*m* below ground level, and were installed to a depth of 5 *m*. Groundwater in the boreholes was allowed to equilibrate and was sampled four days after installation. Water samples were taken at 0.3 *m* below groundwater surface to exclude floating product, which may be constrained on the site, and to detect dispersed and dissolved fuel components which are more vulnerable to migration with groundwater. The receptor was also sampled upstream and downstream of the site, adjacent to the site boundaries (Javadi et al., 2008).

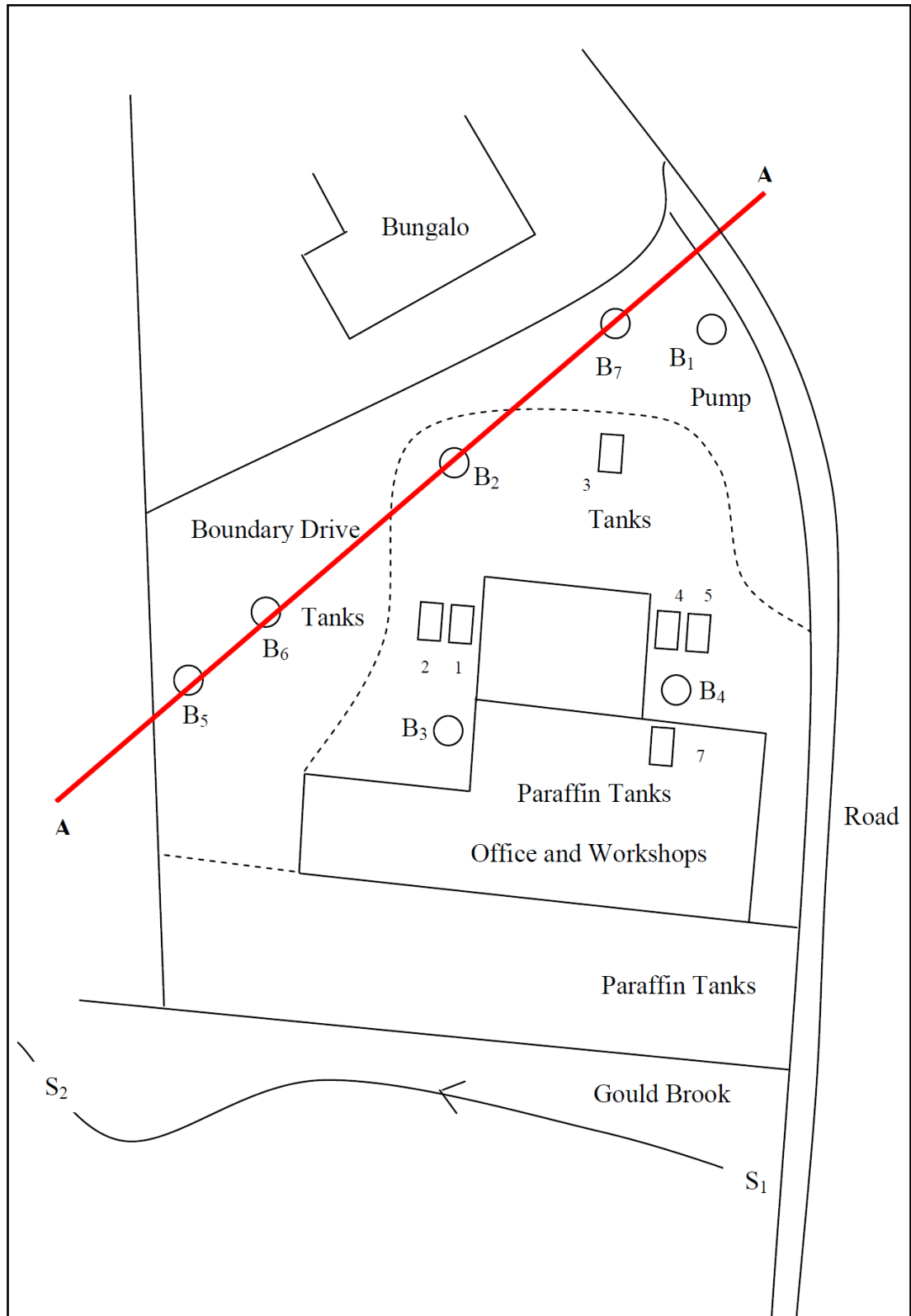


Figure 6.34 Plan of site.

Results

A survey was undertaken initiated in January 2003 in order to assess the extent of contamination throughout the site and general groundwater movement. This survey found hydrocarbon contamination at all sample points within the site and around the periphery as shown in Table 6.8. A section of the site, 40m wide and 10m deep as shown in Figure 6.34 is analyzed using SFEM. The section is divided into 800 three-node triangular elements (Figure 6.35).

Table 6.8 Analysis of contaminants in aquifer (January 2003) (Data provided by Exeter Environmental Services).

Sample ID	Benzene mg/l	Toluene mg/l	Ethyl benzene mg/l	Xylene total isomers mg/l	Total Petroleum Hydrocarbons (TPH) mg/l
B1	<0.1	0.1	3.3	3.4	124
B2	97.5	5.0	61.4	205.7	115034
B3	0.2	0.1	0.9	0.8	141
B4	0.7	0.1	1.1	4.0	141014
B5	0.2	0.2	0.6	0.7	22000
B6	3.6	0.7	1.2	1.5	20100
B7	29.7	0.6	34.6	9.2	2462
B8	0.2	1.1	1.5	2.5	921
Brook upper	0.1	0.1	0.8	0.8	<40
Brook lower	0.1	0.1	0.3	0.4	<40
Dutch Intervention Levels	30	1000	150	70	600

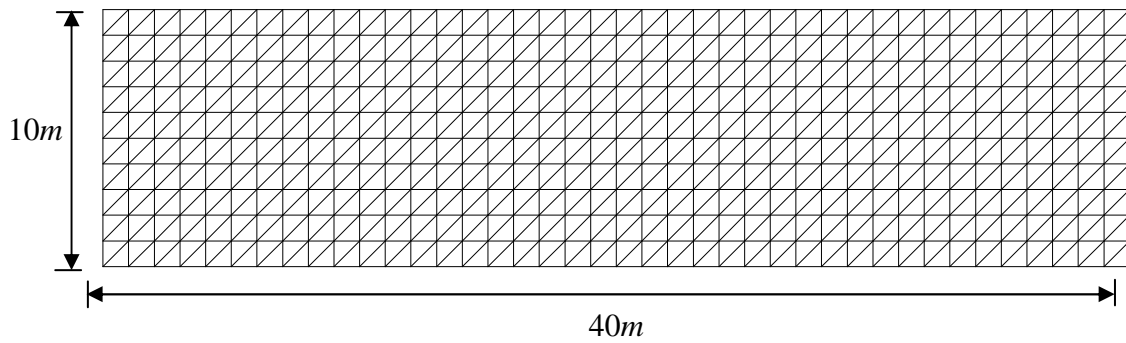


Figure 6.35 Finite element mesh.

The transport of the contaminant by advection, diffusion and dispersion mechanisms is considered. Table 6.9 shows model parameters used in the SFEM. The parameters were measured or estimated as a part of the site investigation. In the model the water velocity v_w was estimated by measurement of the hydraulic gradient of the aquifer. Unfortunately, data describing the spatial variability of soil properties (e.g., lnk_s and c) in real field situations are not sufficient to evaluate all the necessary statistical parameters. The correlation length has been reported between 0.08 to 1.8 m for different types of soils in the literature (Polmann et al., 1990). The correlation lengths of f and c were assumed to be 0.4 m, based on the soil type.

Table. 6.9 Model parameters used in the FEM analysis.

Model parameters	
parameter	value
D_{m_w} : coefficient of water molecular diffusion ($m^2 \cdot sec^{-1}$)	1×10^{-7}
α_{L_w} : longitudinal dispersivity for water phase (m)	0.5
θ : moisture contents (%)	21
ρ_s : density of the solid phase ($Mg \cdot m^{-3}$)	2.69
K_s : saturated permeability (m/s)	1×10^{-5}
T : absolute temperature (K)	293
e_o : initial void ratio	0.713
v_w : water velocity ($m \cdot sec^{-1}$)	2.3×10^{-7}

Figure 6.36 compares the results of the model prediction with the measured values of contaminant concentration recorded in September 2004. The results are plotted for section A-A (Figure 6.37). It is shown that the results of the SFEM are in better agreement with field measurements than the results of the DFEM presented by Javadi et al., (2008). Figure 6.37 shows the contaminant distribution in February and March 2003 obtained from SFEM and DFEM. The results of SFEM show a lower peak concentration in the plume than those of the DFEM. A sensitivity analysis is performed to examine the sensitivity of the model to variations of σ_f^2 . Figure 6.38 shows solute concentration distribution in Sept 2004 for different values of σ_f^2 . It can be seen that this parameter plays a significant role in transport of the contaminant and changes in concentrations with time. Increasing σ_f^2 will increase the amount of contaminant that will spread in the soil matrix due to increase in the random variation of local velocity.

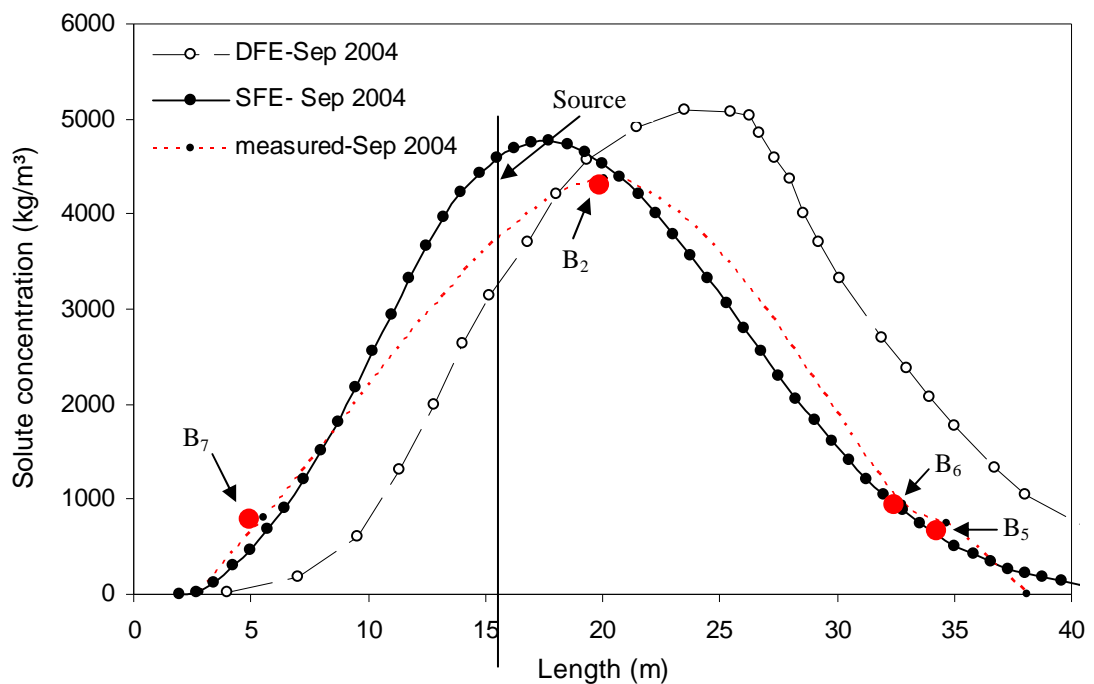


Figure 6.36 Comparison between measured data and the results of SFEM and DFEM.

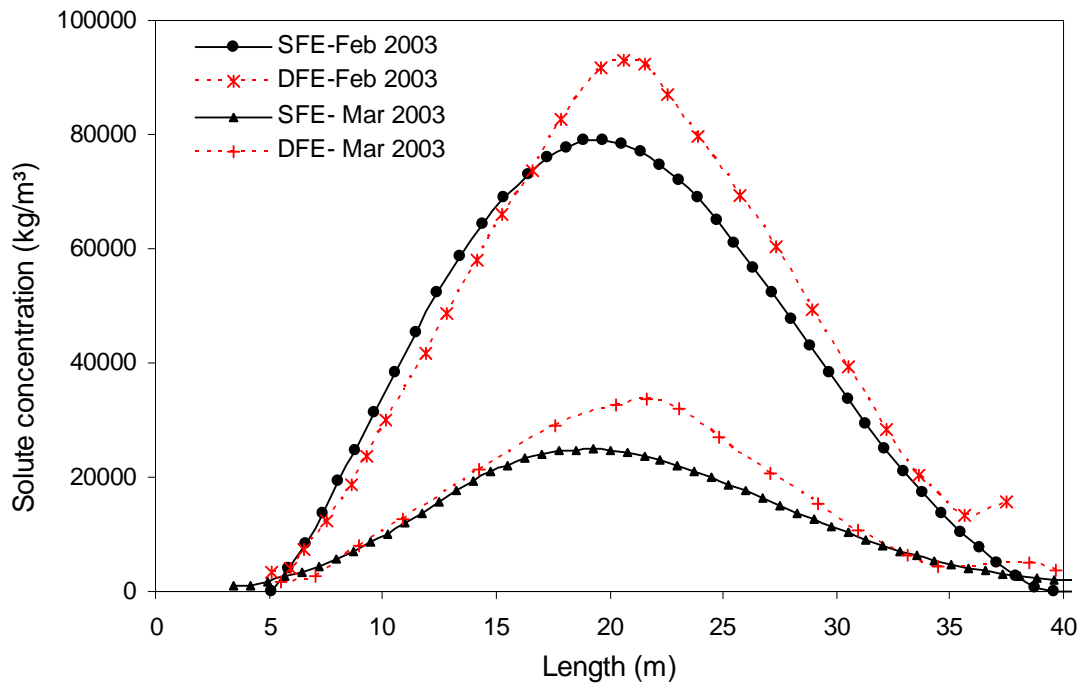


Figure 6.37 Comparison between SFEM and DFEM predictions.

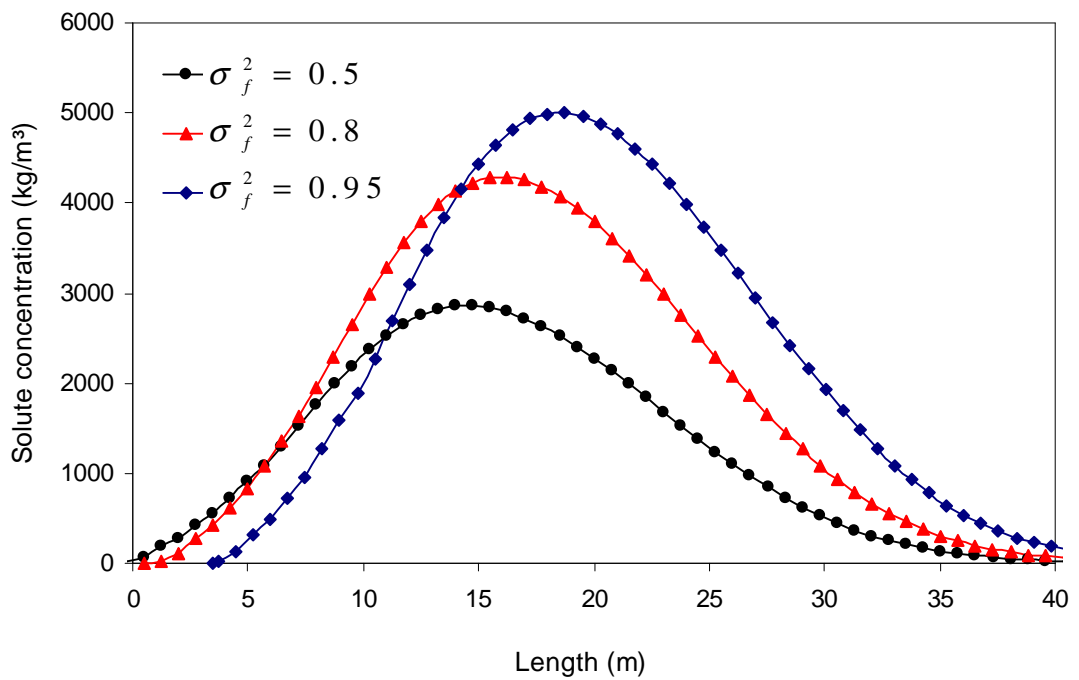


Figure 6.38 Solute concentration vs. length at Sep 2004 obtained for different values

of σ_f^2 .

6.3.2 Case-study 2

A field-scale experiment conducted at the Maricopa Agricultural Center, Phoenix, Arizona, USA. (Abbasi et al., 2003a,b), was simulated by the developed stochastic finite element model to show applicability of the model for field scale problems. This experiment was conducted to investigate the distribution of soil moisture and solute concentration in soil profile below agricultural irrigation furrows. The soil of the field site is bare sandy loam. The experiment was carried out on 115 m long furrows under free-draining (FD) condition, spaced 1 m apart (Figure 6.39). The experiment was run with two irrigation events 10 days apart; the first irrigation lasted 275 min and the second irrigation 140 min. Two sets of neutron probe access tubes were installed at $x = 5$ and 110 m along the monitored furrow. Hereafter we refer to these locations as the inlet and outlet sites, respectively. In addition to initial readings before the irrigation, water contents were recorded 6 and 12 h after each irrigation and then daily.

Soil samples for investigation of gravimetric soil water content and bromide concentration, were collected from one side of the monitored furrows at three different locations top, side, and bottom of the furrows (e.g. at locations 1, 2 and 3 in Figure 6.40), in a cross-section perpendicular to the furrow axis at similar depths as they used for the neutron probe measurements. Water flow depths in the furrows were taken at the inlet and outlet sites every few minutes and these measurements served as the upper boundaries for the numerical calculations.

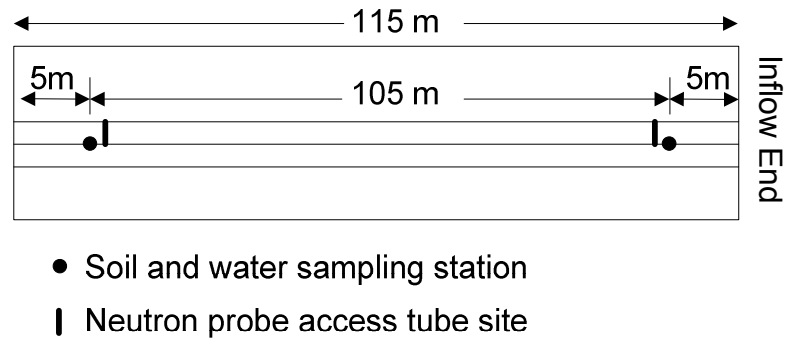


Figure 6.39 Plan view of the furrow irrigation field experiments, not to scale, (Abbasi, et al., 2004).

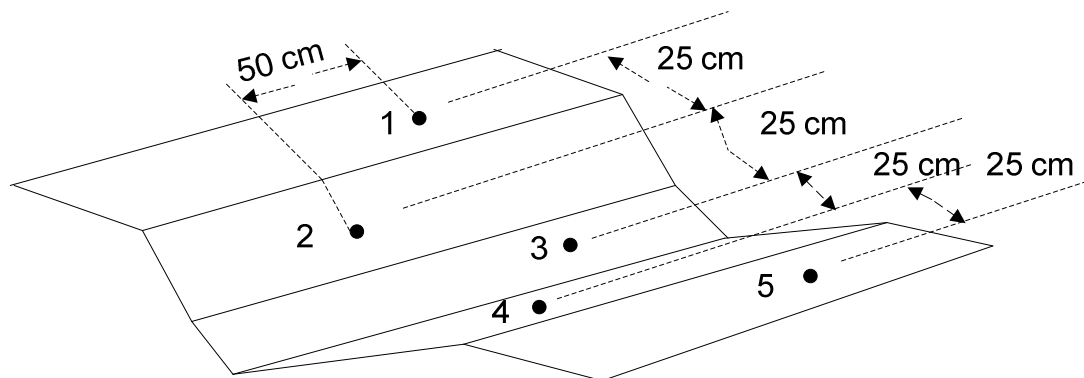


Figure 6.40 Position of neuron probe access tubes at different locations in the furrow cross-section. Numbers relate to access tubes installed in two different rows; the first row includes tubes 2 and 4 along the sides and the second row includes tubes 1, 3 and 5 (Abbasi, et al., 2004).

The values of scaling parameter A , saturated and residual soil water contents (θ_s and θ_r) are considered equal to 0.055 1/m, 0.411 and 0.106 based on laboratory analyses of soil water content data obtained from 38 undisturbed soil samples. Measured soil water

retention parameters showed considerable spatial variability in the soil hydraulic properties at the field site. The FE (finite element) mesh generated for this example consists of 1288 triangular elements and 702 nodes. The parameters used in the stochastic finite element model and HYDROUS2-D (Šimunek, 1999) are summarized in Table 6.10. Different values combination of variances of stochastic parameters and the vertical correlation length were used to simulate the experiment and the best fit was achieved with assuming σ_f^2 and σ_a^2 equal to 0.6 and 0.02 1/m², respectively.

Table.6.10 Parameter values used for the numerical simulations.

	Site	K_s (m/s)	θ_s	λ (m)	α_L (m)	α_T (m)
<i>Simultaneously optimization</i>	<i>Inlet</i>	1.39×10^{-5}	0.411		0.222	0.044
	<i>Outlet</i>	1.59×10^{-5}	0.411		0.091	0.0001
<i>Two-step optimization</i>	<i>Inlet</i>	7.6×10^{-6}	0.301		0.2005	0.0434
	<i>Outlet</i>	1.78×10^{-5}	0.387		0.0174	0.0004
<i>Stochastic finite element</i>	<i>Inlet</i>	1.5×10^{-5}	0.411	0.2	0.22	0.044
	<i>Outlet</i>	1.5×10^{-5}	0.411	0.2	0.22	0.044

The values of the parameters used in the HYDROUS2-D model were inversely estimated by Abbasi et al. (2004) using an optimization method in combination with the HYDRUS-2D numerical code using two optimization approaches;

- Simultaneously optimization approach; in this approach the saturated hydraulic conductivity K_s and the convective dispersive solute transport parameters were estimated simultaneously using a optimization method (Abbasi et al., 2004).
- Two-step optimization approach; in this approach; the saturated soil water content, the parameter n in van Genuchten's soil hydraulic property model, and the saturated hydraulic conductivity K_s as the most sensitive soil hydraulic parameters (Abbasi et al., 2003b) were estimated, followed by estimation of transport parameters (Abbasi et al., 2004).

Initial conditions

Measured soil water contents before the experiments were used as initial conditions within the flow domain and initial Bromide concentration was assumed zero through the entire domain.

$$C(x, z, t) = 0 \quad t = 0 \quad (6.49)$$

Boundary conditions

Time-space dependent flow depths (surface ponding, $h(x,t)$ in Figure 6.41) were specified as the upper boundary condition in the furrow during irrigation. A free-drainage condition for water was applied to the lower boundary of the domain (Figure 6.42). No-flux boundary conditions were applied to both sides of the flow domain. Bromide in the form of CaBr_2 was injected at a constant rate equal to 6.3 g Br l^{-1} during the entire irrigation. A Cauchy (solute flux) boundary condition was used for the upper boundary of the domain for solute transport.

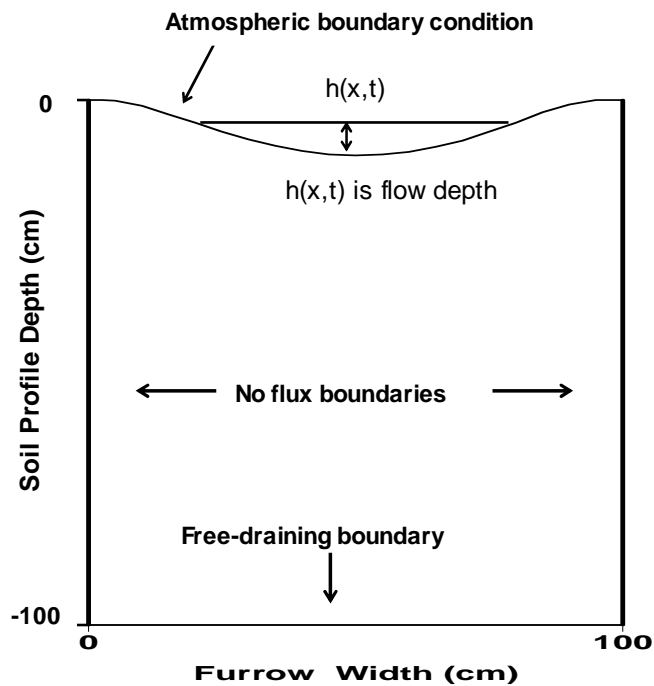


Figure 6.41 Water boundary conditions used for numerical modelling.

Result

Measured and predicted (using the stochastic finite element model developed in this study and HYDROUS2-D model soil water contents at the inlet and outlet sites of the experiment are presented in Figure 6.41. The results are given by means of 1D curves to

provide a better visual comparison between the measured and calculated distributions. The results are given at two different times (12 h and five days after the start of irrigation, being representatives of relatively wet and dry conditions) and for three different locations in the furrow cross-section (bottom, side and top of the furrow) up to a depth of 100 cm below the ground surface. The results are plotted versus depth (instead of versus lateral distance) since considerably more data were available versus depth. The black solid and dashed lines show simulation results obtained by HYDRUS-2D in combination with simultaneous and two-step optimization approaches, respectively (Abbasi et al., 2004). The solid red lines show the results obtained using the stochastic finite element model. From comparison of the results, it is concluded that stochastic finite element method produced better agreement with the observed water contents than HYDROUS2-D. HYDROUS2-D is a deterministic numerical code and effects of spatial variability of soil hydraulic parameters are not considered in this model. Saturated hydraulic conductivity used in this model was obtained by inverse estimation using two different simultaneous and two-step optimization approaches and different values were found for each inlet and outlet sections of the problem that shows spatial variability of the hydraulic parameters of domain. However in the stochastic finite element model spatial variability of these parameters is considered; and this could be the possible reason for agreement of its results with measured ones.

Other advantage of the developed stochastic finite element model over the HYDROUS-2D or similar deterministic models are its capability for considering the effects of large-scale hysteresis. The large-scale hysteresis is referred to as hysteresis due to spatial variability of large scale parameters (Mantoglou and Gelhar, 1987). The effective parameters (i.e., effective hydraulic conductivity, effective moisture capacity) are functions of time history of mean capillary pressure head. It is generally accepted that the hysteresis often occurs in field-scale problems and it may have played a major role in this problem. The results obtained for the inlet site show (Figure 6.42) that after 12 hour and 5 days from the start of irrigation when soil is in wetting and drying conditions respectively, stochastic model predicts less amount of water content along the soil profile than the deterministic model. It is expected that water moves slower at early time when soil is still dry and in wetting condition due to the effects of large-scale hysteresis. So, less amount of water infiltrates into the soil profile. While after 5 days that the soil is in drying condition, a faster drainage of water from the bottom of the furrow is

expected. So less amount of water predicts in using the model that considers the hysteresis than the other one.

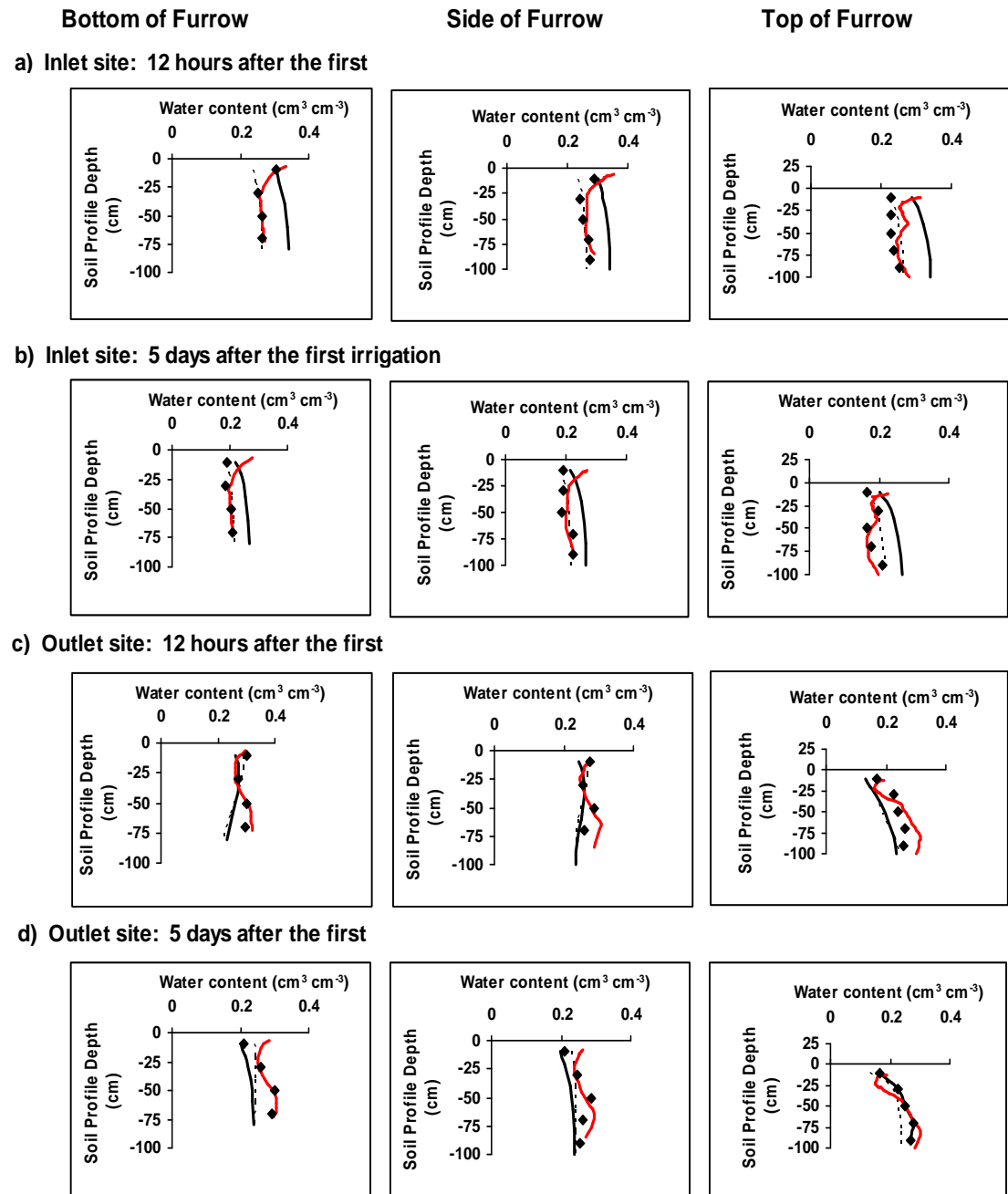


Figure 6.42 Measured and predicted (using stochastic finite element and HYDRUS2-D models) soil water contents for the inlet and outlet sites (measured: symbols, simultaneous: solid black lines, two-step: dashed lines, stochastic finite element: solid red lines).

In the case of outlet section, the results show that the hysteresis does not play significant role in water content distribution. This is because at the times under study of water movement, the soil profile in this site is not in neither wetting nor drying conditions. The initial measured water content showed that at this section of furrow, soil profile was

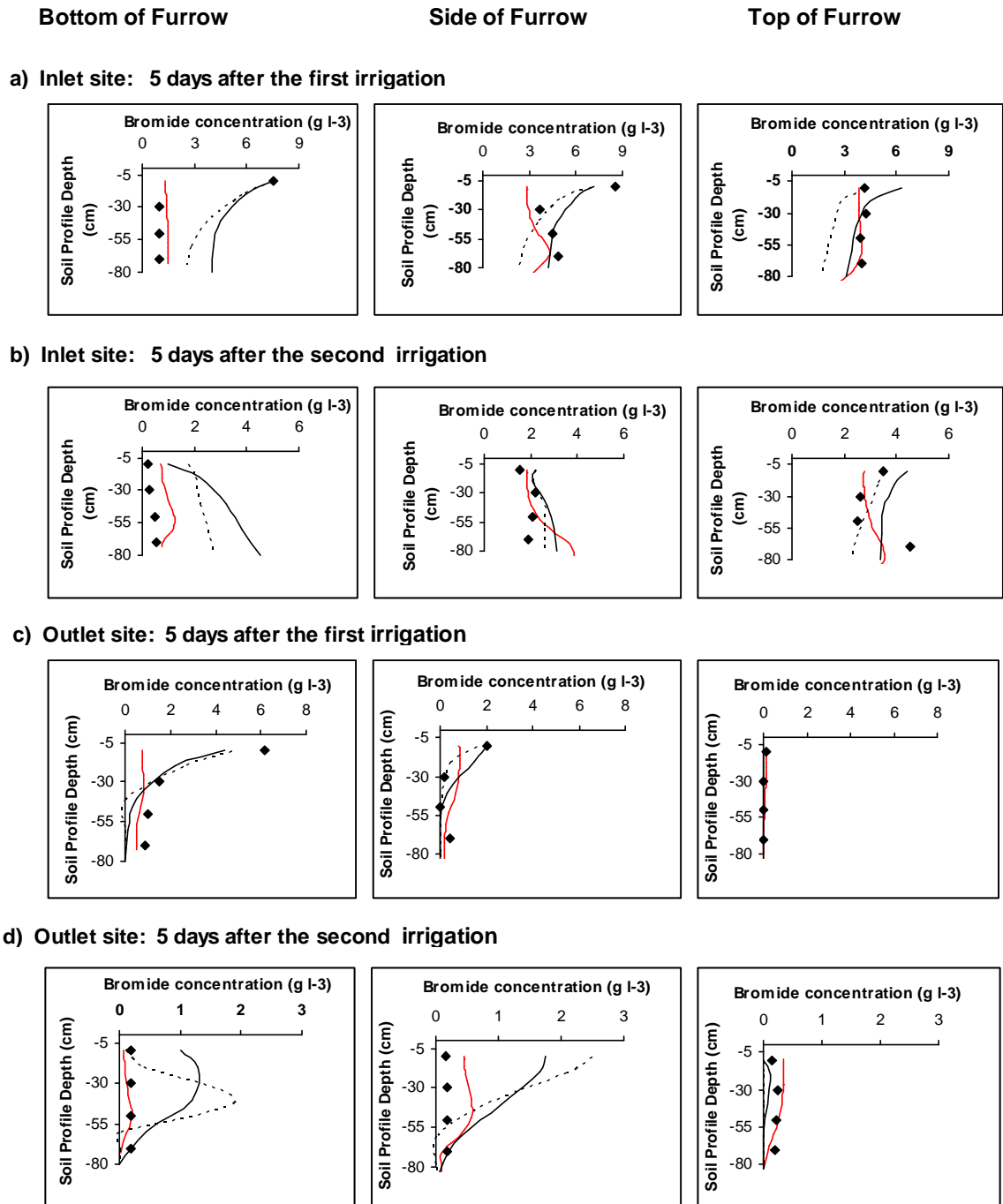


Figure 6.43 Measured and predicted (using stochastic finite element and HYDRUS2-D models) bromide concentration for the inlet and outlet sites (measured: symbols, simultaneous: solid black lines, two-step: dashed lines, stochastic finite element: solid red lines).

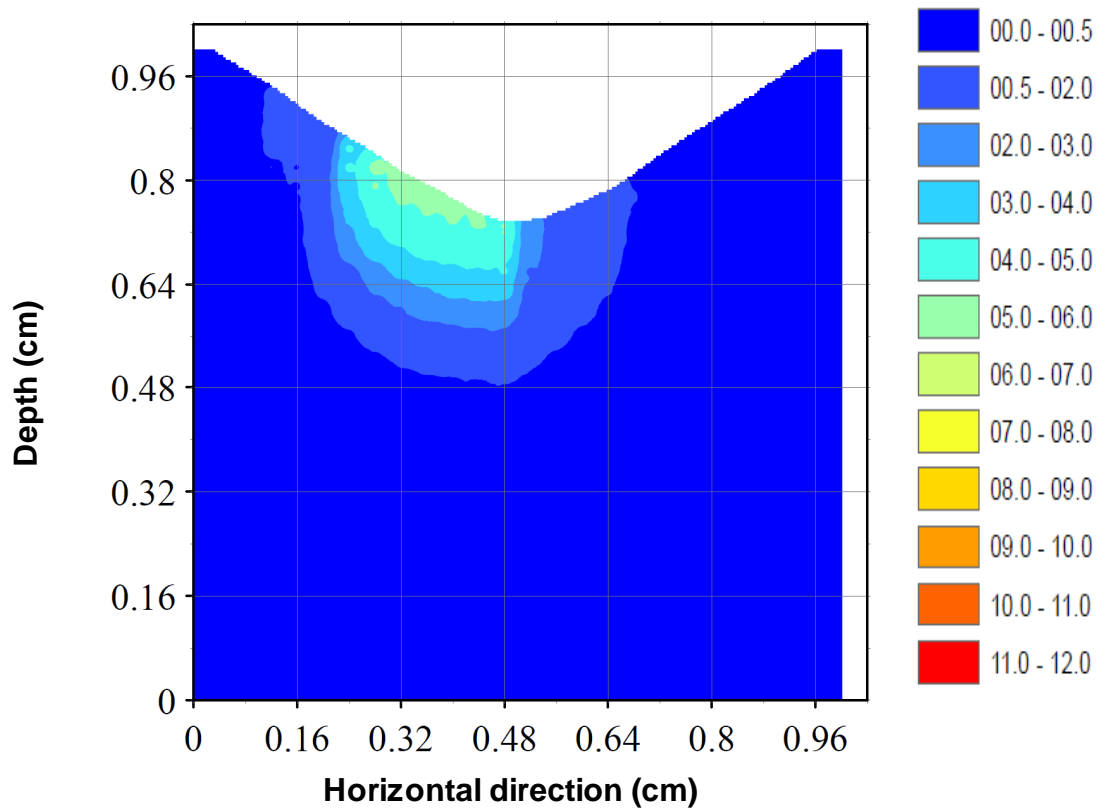
already wet. So, after 12 hours, the surface water infiltrates into a wet soil. Also, after 5 days the profile does not reach to drying condition because of the late arrival of surface water to this site as the outlet site is located 105m far from the irrigation place (see Figure 6.39). The results presented in Figure (6.42) show that the stochastic model predicts a slower water movement and consequently higher amount of water content

through the soil profile than the deterministic one due to considering the effects of soil heterogeneity.

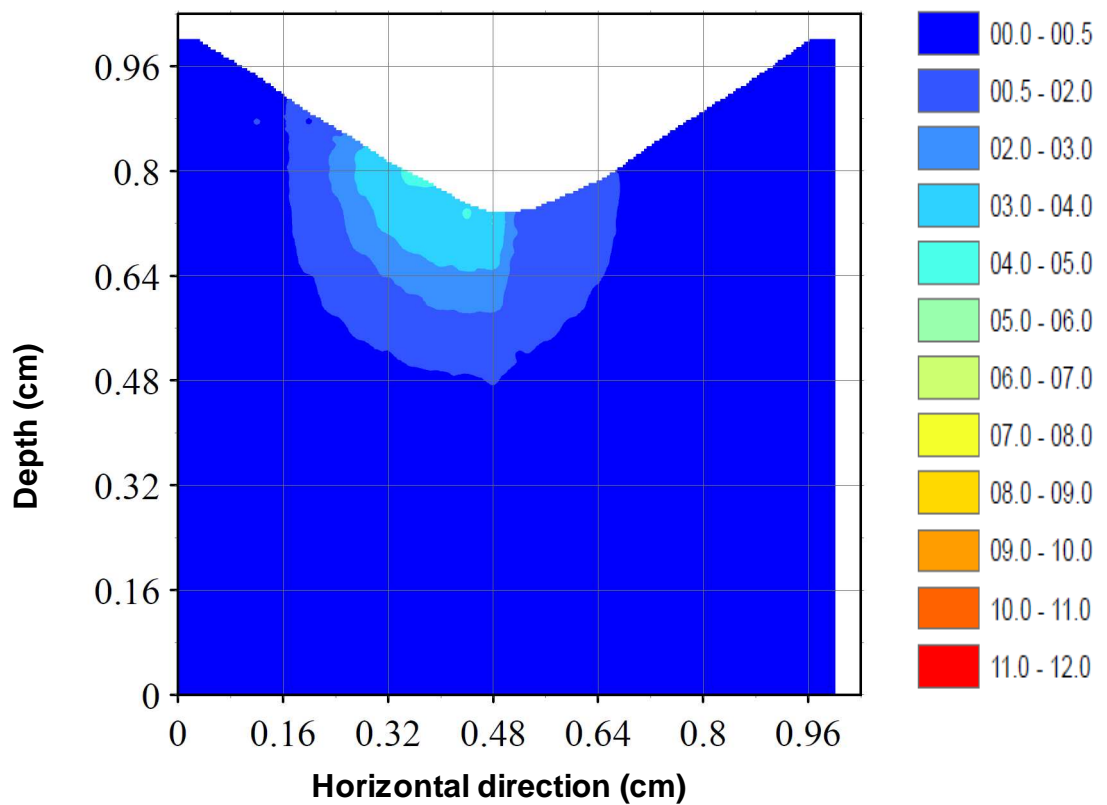
The measured and predicted Br concentrations at the inlet and outlet sites of the experiment are presented in Figure 6.43. The results are given at two different times (five days after the start of each of the first and the second irrigations) and for three different locations in the furrow cross-section (bottom, side and top of the furrow). The black solid and dashed lines show simulation results obtained by HYDRUS-2D in combination with simultaneous and two-step optimization approaches, respectively (Abbasi et al., 2004). The solid red lines show results obtained using stochastic finite element model. From comparison of the results, it is concluded that stochastic finite element method produced better agreement with the observed water contents, than HYDRUS-2D.

Comparison of both solute concentration profiles obtained by SFEM and DFEM is difficult because it is impossible to detect if the differences in the two profiles are due to the different flow fields and or due to the different approaches used to solve the contaminant transport equation. In order to study the effect of the inclusion of the macrodispersion as a transport mechanism, the transient unsaturated flow equation was solved using a stochastic approach and the transport equation was solved twice; first time using a deterministic approach for the transport part and the second time using a stochastic approach. The Figures 6.44, 6.45 and 6.46 show mean solute concentration through the domain after 2 hours, 2 days and 5 days after the start of first irrigation.

The stochastic results show lower value of bromide concentration at the area close to the surface of the furrow than the deterministic results. Deterministic model overestimates solute concentration around of the solute source. This means that the effect of including the variability of the properties of the soil into the transport equation is to increase the lateral and longitudinal spreading of the contaminant. So, greater amount of solute disperses through the domain and it is distributed at larger area. This can be seen in the Figures 6.44 and 6.45 for example; the area with concentration between 2-3 mg/l is larger for the stochastic case in comparison with the deterministic one. Deterministic approaches predict slower movement of the solute in both directions than the stochastic approach.



(a)



(b)

Figure 6.44 Solute concentration (mg/l) after 2 hours from the start of the first irrigation using (a) deterministic (b) stochastic method.

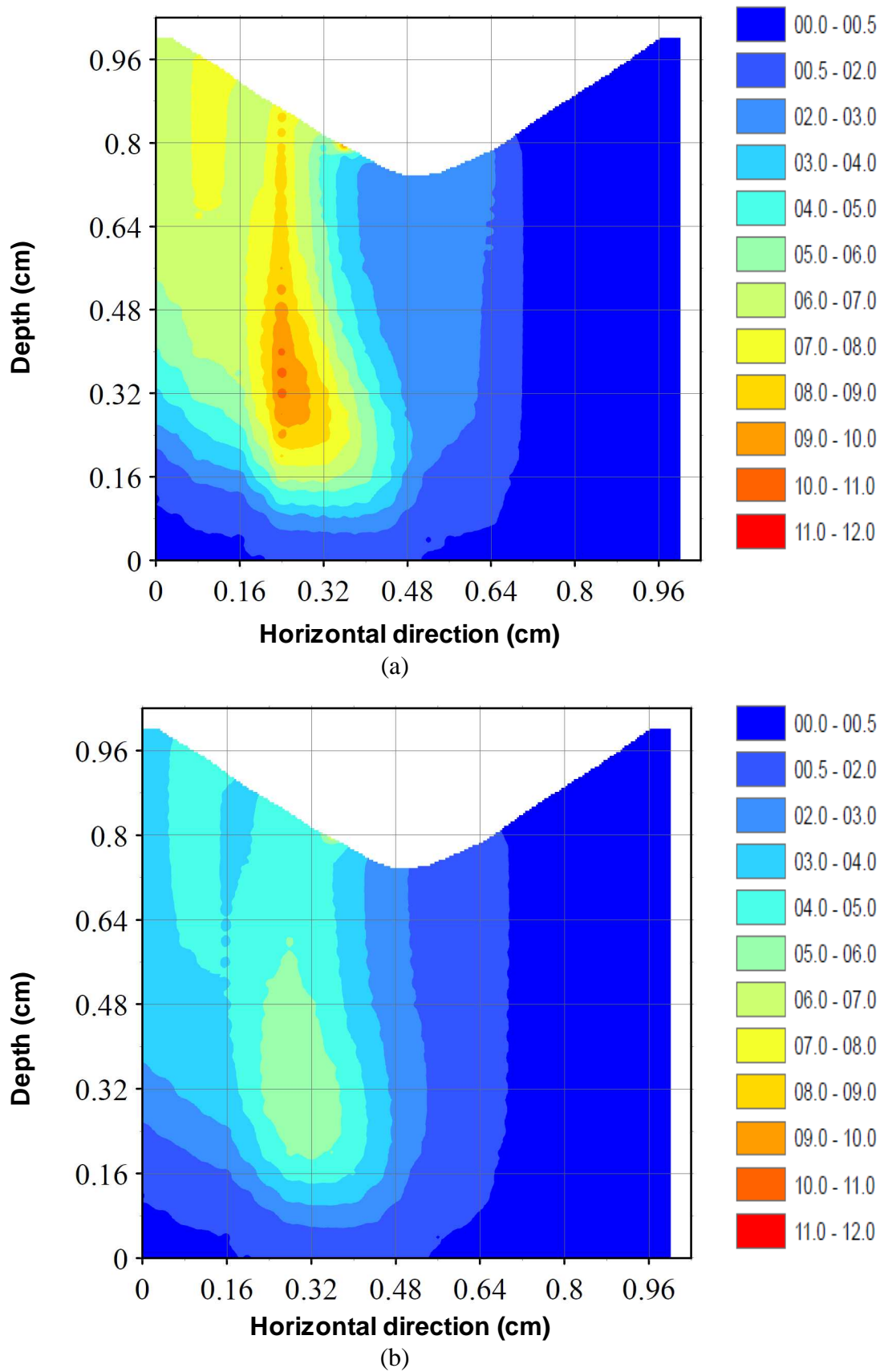
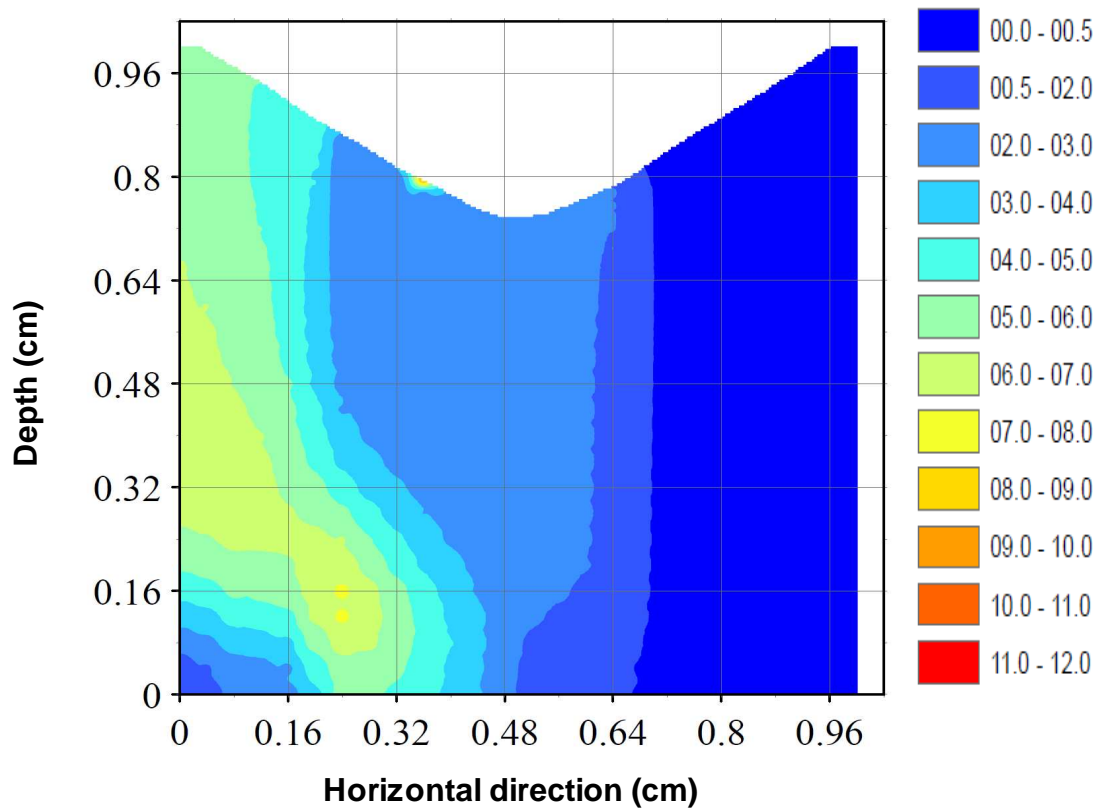
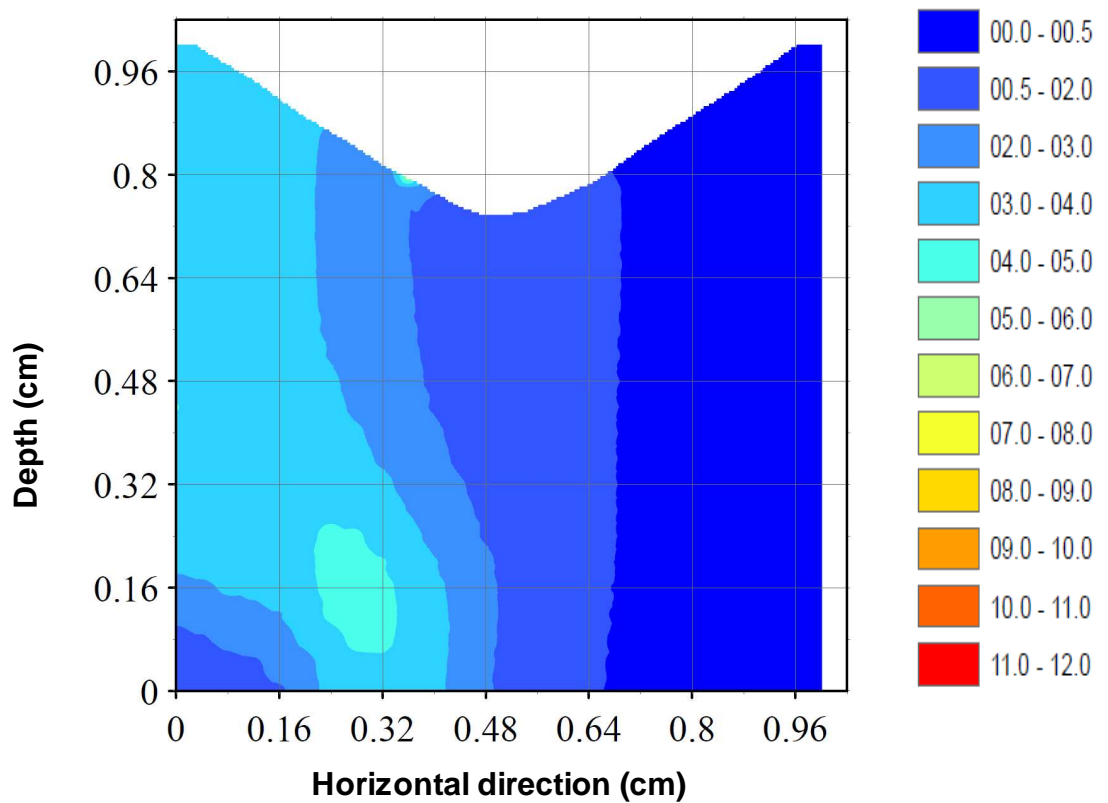


Figure 6.45 Solute concentration (mg/l) after 2 days from the start of the first irrigation using (a) deterministic (b) stochastic method.



(a)



(b)

Figure 6.46 Solute concentrations (mg/l) after 5 days from the start of the first irrigation using (a) deterministic (b) stochastic method.

Higher amount of dispersion resulting from the stochastic method is mathematically referred to as the macrodispersion coefficient which is added to the local dispersion. Since the total dispersion coefficient in the SFEM is greater than the local dispersion coefficient, a wider area leached by solute is predicted.

Figure 6.47 shows the variance of bromide concentration. The variance is higher along the border of the contaminant plume but, the coefficient of variation is low. This means that the uncertainty on the predicted bromide concentration is higher along the borders of the contaminant plume compared to other regions of the domain, but the predicted values are still reliable since the coefficient of variation is low.

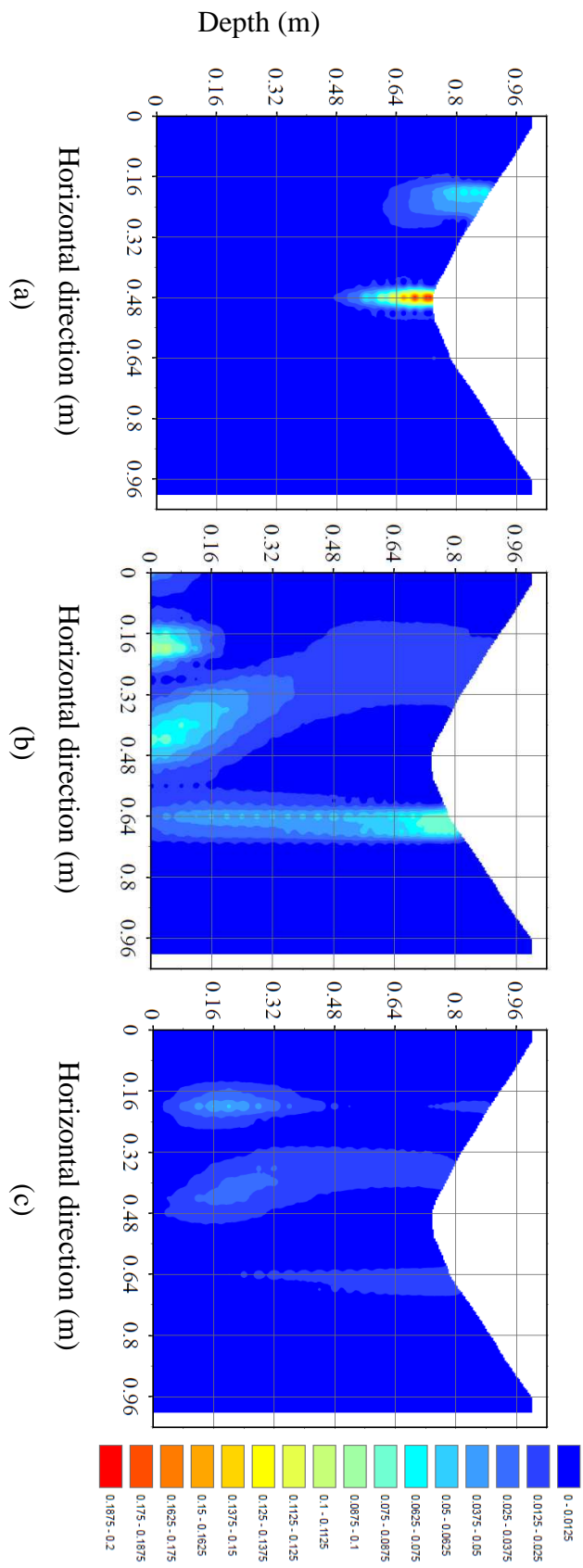


Figure 6.47 Bromide concentration ($\times 10^{-3} \text{ mg/l}$) at (a) $t=2$ hours, (b) 2 days and (c) 5 days after the start of first irrigation.

CHAPTER 7

CONCLUSIONS AND RECOMMENDATIONS

7.1 Concluding remarks

In this study, a stochastic FE based model was developed for simulation of water flow and contaminant transport in unsaturated soils. The stochastic spectral method was implemented in the governing equations for water flow (Richard' equation) and convective-dispersive solute transport to incorporate the spatial variability of hydraulic properties of soil and to reduce the uncertainty in prediction of contaminant fate and transport. The procedure of the stochastic methodology was explained.

Two stochastic differential equations for mean flow and contaminant transport and a set of mathematical algebraic equations for evaluation of important parameters such as effective hydraulic conductivity, the variance of capillary tension head and solute concentration were presented. Stochastic governing equations obtained for the mean flow and solute transport were solved using the FE method in space domain and a FD scheme in time domain. Mean and variance of saturated hydraulic conductivity (k_s), scaling parameter (α) and correlation scale of these random parameters are the inputs of the model and can be provided by site investigation and statistical analysis of data

obtained from the region under study. The variance of capillary tension head and solute concentration are indicators of reliability of the model.

The developed model was verified for both flow and transport problems through comparison of the results obtained using stochastic FE model with analytical, deterministic and Monte Carlo simulations, as well as experimental results. From this comparison, it can be concluded that the stochastic based model performs better than the deterministic one. Also, the developed model is more efficient than Monte Carlo method in terms of computational time and efforts.

A lysimeter experiment conducted at NSMU College Ranch near Las Cruces was simulated numerically using both stochastic and deterministic FE methods. The stochastic approach which includes the variability of the soil properties in the formulation predicts a slower movement of the wetting front in the vertical direction. The stochastic and deterministic results were compared to the field-measured values. The results predicted by the stochastic finite element theory presented in this work are in good agreement with the experimental values.

A one-dimensional transient contaminant transport with steady-state flow was simulated. The mean solute concentration profiles were compared to Monte Carlo simulations. The great advantage of the stochastic FE method over the Monte Carlo method is the tremendous saving in the computational costs. In this example, 200 Monte Carlo simulations were necessary to obtain basically the same results using stochastic finite element approach. Then, the capability of the developed model in simulation of three-dimensional non-isotropic statistical problems was tested with simulation of one hypothetical example and comparison of the results with analytical solutions.

The model was used to simulate transport of non-reactive solute in an undisturbed lysimeter during steady-state water flux. Numerical simulation of the problem was carried out for four different scenarios assumed for the structure and formation of the soil: a single domain having uniform hydraulic properties (SDU), a dual-domain system with uniform hydraulic properties (DDU), a single domain with spatially variable hydraulic properties (SDV) and a dual-domain system with spatially variable hydraulic properties (DDV). The numerical results were compared with experimental measured data. The results obtained based on SDU were not in agreement with the measured data.

The dual domain system method (i.e., DDU) yielded satisfactory results but higher accuracy was achieved using the DDV scenario. Analysis of the results shows that the incorporation of both types of micro- and macro- heterogeneity in the simulation models can greatly improve the accuracy of the predictions. So, combination of dual domain approach with stochastic approach provides an effective approach to predict solute transport problems in naturally heterogeneous soil with higher accuracy.

Two field-scale transport problems were simulated using the developed stochastic FE model. The results were compared to those obtained using deterministic models from the literature and experimental measurement. The results of these case-studies proved the capability of the model for simulation of large-scale problems.

From the results of this study following conclusion can be drawn:

- Stochastic finite element methodology is an efficient method to incorporate the small-scale variability of the soil properties into large-scale models for water flow and solute transport in unsaturated soil. The variances of the capillary tension head and solute concentration are provided as results along with the predictions for the mean capillary tension head and mean solute concentration values.
- An interesting feature of developed model is that only limited number of stochastic properties (e.g., mean, variance, correlation scale) of soil hydraulic parameters is required to evaluate the output of the model. Mean and variance of saturated hydraulic conductivity (k_s), scaling parameter (α), specific moisture capacity (C) and correlation scale of random parameters are the inputs of the model and can be provided by site investigation and statistical analysis of field-observed values obtained from the region under study.
- The numerical results presented in this study, show that the stochastic finite element approach is a very attractive alternative to Monte Carlo approaches in terms of time and computational cost. Because of reliance of the Monte Carlo approaches on repeated computation of random numbers, which can be a very time consuming procedure, they are not efficient techniques. While only one call of stochastic finite element model is required to simulate problems and achieve

virtually the same result as Monte Carlo one.

- The developed model prevail over the Monte Carlo approaches in terms of providing physical and conceptual understanding of the effects of soil heterogeneity on transport mechanisms, which is necessary for planning appropriate and efficient remediation techniques. This is achieved with implementation of a set of closed form equations built up using the spectral analytical method, into the developed model. These equations clearly present the relationship between stochastic properties of hydraulic parameters of soil and outputs of the model. However, Monte Carlo approaches do not provide conceptual understanding of the random process because of statistical nature of these approaches.
- A set of sensitivity analysis performed on the saturated hydraulic conductivity as index of soil heterogeneity and correlation scale of random parameters. The higher value of saturated hydraulic conductivity causes slower movement of wetting front and an enhancement of solute spreading in the soil. Also, it is concluded that the higher the correlation length results in higher effects of soil heterogeneity on the water flow and solute transport processes.
- The developed model also is capable to consider the effects of micro-heterogeneity of soil and presence of macro pores in simulation of solute transport. The field soils exhibit two different types of spatial heterogeneity including micro- and macro- heterogeneity which often coexist. Simulation of in situ problems with high density of macropores in soil structure, the effects of both types of heterogeneity must be considered. The developed model is capable to consider the potential impacts of both micro-and macro-heterogeneity, through implementation of SFE method on the mathematical model of contaminant transport in a dual-domain system.
- The model is capable of evaluating the variance of concentration as an index of reliability of the model output. This makes it possible to estimate a probable interval (mean concentration minus and plus standard deviation) for the range of oscillation of possible realizations of contaminant distribution.

7.2 Recommendations for further work

The numerical study that has been discussed in this work, shows great influence of the uncertainty in the structure and formation of the soil on contaminant transport problems and stochastic FE methodology provides an efficient and reliable way for reduction and quantification of uncertainties in modelling and prediction of contaminant transport. The benefits of the stochastic FE methodology used for the development the model can be the motivation for more work in this area. The recommendations for the future work presented here are aimed at promoting to make the best use of the developed model and to develop a more comprehensive model covering wider range of physical and chemical transport mechanisms. A list of further research needs arising out of this study are listed in the following

- Soil heterogeneity has influence on the rate of chemical reaction and chemical reactions play significant role in contaminant fate which has not been considered in this work. The approach developed in this study can be extended to model the transport of reactive contaminant.
- Accuracy of the developed model is dependent on the choice of the proper values for the stochastic hydrologic parameters of the site under consideration. So, it is important to develop and test accurate methods for determining the stochastic parameters of the soil such as mean, variance and correlation lengths.
- One of the most challenging issues facing environmental researchers is finding a timely and cost effective remediation approach for contaminated soil and groundwater. The model can be integrated with optimization softwares and decision support systems to find the best remediation techniques for sustainable management of contaminated land.

References

- Ababou, R., (1988). "Three-dimensional flow in random porous media.", Ph.D. thesis, Department of Civil Engineering., MIT, Cambridge, Mass.
- Ababou, R. and L. W. Gelhar (1988). "A high resolution finite difference simulator for 3D unsaturated flow in heterogeneous media.", In: Computational Methods in Water Resources. Volume I. (Ed: Celia, M.), Elsevier, New York, 173-178.
- Abbasi, F., Feyen, J., Roth, R. L., Sheedy, M. and Van Genuchten, M. Th. (2003a). "Water flow and solute transport in furrow irrigated fields.", *Irrigation Science*, 22 (2), 57-65.
- Abbasi, F., Šimunek, J., van Genuchten, M. Th., Feyen, J., Adamsen, F. J., Hunsaker, D. J. Strelkoff, T. S. and Shouse, P. (2003b). "Overland water flow and solute transport: model development and field data analysis.", *Journal of Irrigation Drainage Engineering*, 129 (2), 71-81.
- Abbasi, F., Feyen, J. and van Genuchten, M. Th., (2004). "Two-dimensional simulation of water flow and solute transport below furrow: model calibration and validation.", *Journal of Hydrology*. 290 (2), 63-79.
- Abdou, H.M. and Flury, M (2004). "Simulation of water flow and solute transport in free-drainage lysimeters and field soils with heterogeneous structures.", *European Journal of Soil Science*, 55, 229–241.

- Aguirre, C.G. and Haghghi, K. (2002). "Stochastic finite element analysis of transient unsaturated flow in porous media.", *American Society of Agricultural Engineers*, 41 (1), 163-173.
- Aguirre, C.G. and Haghghi, K. (2003). "Stochastic modelling of transient contaminant transport.", *Journal of Hydrology*, 276, 224-239.
- Ahuja, L.R. and Lehman, O.R. (1983). "The extent and nature of rainfall-soil interaction in the release of soluble chemicals to runoff.", *Journal of Environmental Quality*, 12, 34-40.
- AL-Najjar, M. (2006). "Finite element modelling of contaminant transport in unsaturated soils.", PhD dissertation, University of Exeter, Exeter, UK.
- Anderson, J. and Shapiro, A.M. (1983). "Stochastic analysis of one-dimensional steady state unsaturated flow: A comparison of Monte Carlo and perturbation methods.", *Water Resources Research*. 19(1), 121-133.
- Arsene, C. (2000). "Migration behaviour of ^3H ^{14}C and ^{241}AM in unsaturated soils.", *Proceeding of the International Conference Nuclear Energy in Central Europe*, Bled, Slovenia.
- Awadallah S.A. and Abu-Ghararah, Z.H. (1997). "Contaminant transport through initially dry soil.", *Water, Air and Soil Pollution*, 100, 107-118.
- Bachmat, Y. (1967). "On the similitude of dispersion phenomena in homogeneous and isotropic porous media.", *Water Resources Research*, 3 (4), 1079-1083.
- Bakr, A. (1976). "Effects of spatial variability of hydraulic conductivity on groundwater flow.", PhD dissertation, N. M. Inst. of Mine. and Technol., Socorro.
- Bakr, A., Gelhar, L.W., Gutjahr, A.L. and Mac Millan, J.R. (1978). "Stochastic analysis of spatial variability in subsurface flows 1. Comparison of one and three dimensional flows.", *Water Resources Research*. 14 (2), 263-271.
- Barry, D. A., Parlange, Y. and Sivaplan, M. (1993). "A class of exact solutions for Richards' equation.", *Journal of Hydrology*, 142, 29-46.
- Baveye, P. and Valocchi, A. (1989). "an evaluation of mathematical models of the transport of biologically reacting solutes in saturated soils and aquifers.", *Water Resources Research*, 25 (6), 1414-1421.
- Bear, J. (1961). "On the tensor form of dispersion in porous media.", *Journal of Geophysical Research*, 66, 4, 1185-1197.
- Bear, J. (1972). "Dynamic of Fluids in Porous Media.", American Elsevier, New York, USA.
- Bear, J., Tassang, C.F. and Marsily, G.D. (1993). "Flow and contaminant Transport in Fractured Rock.", Academic Press, Inc., San Diego, California, USA.

- Benson, D.A., Huntly, D. and Johnson, P.C. (1993). "Modelling vapour extraction and general transport in the presence of NAPL mixtures and nonideal conditions.", *Groundwater*, 31 (3), 437-445.
- Binning, P.J. (1994). "Modelling unsaturated zone flow and contaminant transport in the air and water phases.", PhD dissertation, Princeton University, New Jersey, USA.
- Bouma, J., (1981). "Soil morphology and preferential flow along macropores.", *Agricultural Water Management*, 3, 235-250.
- Bouma, J., (1991). "Influence of soil macroporosity on environmental quality.", *Advances in Agronomy*, 46, 1-37.
- Bouwer, E.J. and McCarty, P.L. (1984). "Modelling of trace organics biotransformation in the subsurface.", *Groundwater*, 22, 433-440.
- Brooks, R.H. and Corey, A.T. (1964). "Hydraulic properties of porous media." Hydrology Paper No. 3, Civil Engineering Department, Colorado State University, Fort Collins, Colorado, USA.
- Brooks, A.N. and Hughes, T.J.R (1982). "Streamline upwind/petrov-Galerkin Formulations for convection dominated Flows with Particular Emphasis on the Incompressible navier-stokes equation.", *Computer Methods in Applied Mechanics and Engineering*, 32, 199-256.
- Bruggeman, A.C., Mostaghimi, S. and Brannan K. M. (1999). "A stochastic model for solute transport in macroporous soils.", *Transactions of the ASAE*, 42 (6), 1743-1752.
- Brusseau, M.L., Max, Q.H., Wang, J.M. and Maier, R.M. (1999). "Biodegradation during contaminant transport in porous media. 2. The influence of physicochemical factors.", *Environmental Science and Technology*, 33, 96-103.
- Brutsaert, W. (1976). "The concise formulation of diffusive sorption of water in a dry soil.", *Water Resources Research*, 12, 1118-1124.
- Buckingham, E. (1907). "Studies on the movement of soil moisture.", USDA Bureau of Soils. Bulletin No. 38, pp 64.
- Burr, D.T., Sudicky, E.A. and Naff, R.L. (1994). "Nonreactive and reactive solute transport in three-dimensional heterogeneous porous media: Mean displacement, plume spreading, and uncertainty. " *Water Resources Research*. 30, 791-815
- Butters, G., Jury, W. A. and Ernst, F. F. (1989). "Field scale transport of bromide in an unsaturated soil 1. Experimental methodology and results.", *Water Resources Research*, 25 (7), 1575-1581.
- Chandrupatla, T.R. and Belegundu, A.D. (1991). "Introduction to Finite Elements in Engineering.", Prentice-Hall, Englewood Cliffs, New Jersey.

- Chang, C.M. and Kemblowski, M.W. (1994). "Unsaturated flows in soils with self-similar hydraulic conductivity distribution.", *Stochastic Hydrology and Hydraulics*, 8, 281-300.
- Characklis, W.G. (1990). "Energetics and stoichiometry,.", In: *Biofilms*, (Eds: characklis, W.G. and Kevin, C.M.), Wiley Interscienc, 93-130.
- Chaudhuri, A. and Sekhar, S. (2005). "Analytical solution for macrodispersion in a 3D heterogeneous porous medium with random hydraulic conductivity and dispersivity.", *Transport in Porous Media*, 58, 217-241.
- Chen, X. (1994) "1-Finite element transport modelling of biodegradable contaminant in heterogeneous porous media and 2-Geostatistical methods for the study of pressure compartments: A case study in the Highlight oil field, Powder River Basin, Wyoming.", PhD dissertation, University of Wyoming, Wyoming, USA.
- Cheung, Y.K., Lo, S.H. and Leung, A.Y.T. (1996). *Finite Element Implementation*, Blackwell Science, Oxford.
- Childs, E.C. and Collis-George, G.N. (1950). "The permeability of porous Materials.", *Proceedings of the Royal Society of London, Series A, Mathematical and Physical Sciences*. 201, 392-405.
- Childs, E.C. (1969). "An introduction to physical basis of soil water phenomena.", Wiley Interscience, London. UK.
- Clement, T. P., Sun, Y., Hooker, B. S. and Petersen, J. N. (1998). "Modeling multi-species reactive transport in groundwater aquifers.", *Spring, Groundwater Monitoring and Remediation*, 18(2),79–92.
- Clement, T.P., Hooker, B.S. and Skeen, R.S. (1996). "Numerical modelling of biologically reactive transport near nutrient injection well.", *Journal of Environmental Engineering*, 122 (9), 833–839.
- Celia, M.A., Bouloutas, E.T. and Zarba, R.L. (1990). "A general mass-conservative numerical solution for the unsaturated flow equation.", *Water Resources Research*, 26 (7), 1483-1496.
- Clifton, P.M. and Neuman, S.P. (1982). "Effects of kriging and inverse modeling on conditional simulation of the Avra Valley aquifer in southern Arizona.", *Water Resources Research*, 18, 1215-1234.
- Coppola A., Basile, A., Comegna, A. and Lamaddalena, N. (2009). " Monte Carlo analysis of field water flow comparing uni- and bimodal effective hydraulic parameters for structured .", *journal of Contaminant Hydrology*, 104, 153-165.
- Culver, T.B., Shoemaker, C. A. and Lion, L.W. (1991). "Impact of vapour sorption on the subsurface transport of volatile organic compounds: A numerical model and analysis.", *Water Resources Research*, 27 (9), 2259-2270.

-
- Connel, L.D. (1995). "An analysis of perturbation based methods for the treatment of parameter uncertainty in numerical groundwater models.", *Transport in Porous Media*, 21, 225-240.
- Dagan, G. (1979). "Models of groundwater flow in statistically homogeneous porous formations.", *Water Resources Research*, 15 (1), 47-63.
- Dagan, G. (1988). "Time-Dependent macrodispersion for solute transport in anisotropic heterogeneous aquifer.", *Water Resources Research*, 24 (9), 1491-1500.
- Dagan, G. (1982). "Stochastic modelling of groundwater flow by unconditional and conditional probabilities 2. The solute transport.", *Water Resources Research*, 18 (4), 835-848.
- Dagan, G. (1984). "Solute transport in heterogeneous porous formation.", *Journal of Fluid Mechanics*, 145, 151-177.
- Dagan, G. (1990). "Transport in heterogeneous porous formations: spatial moment, ergodicity, and effective dispersion.", *Water Resources Research*, 26 (6), 1281-1290.
- Darcy, H. (1856). "Les Fontaines Publiques de la Ville de Dijon.", In: *The theory of groundwater motion and related papers*. Hurbbert, (Ed: Hafner, M.K., 1969) Pub. Co., New York.
- Daryl, L.L. (2002). *Finite Element Method*, Wadsworth Group, Brooks Cole.
- Davis, M.W. (1987). "Production of conditional simulations via the LU triangular decomposition of the covariance matrix.", *Mathematical Geology*, 19(2), 91-98.
- Dawson, C. (1998). "Analysis of an upwind-mixed finite element method for nonlinear contaminant transport equations.", *Society for Industrial and Applied Mathematics*, 35 (5), 1709-1724.
- Day, P.R. (1956). "Dispersion of a moving salt-water boundary advancing through a saturated sand. Transactions, American Geophysical Union.", 37, 595-601.
- De Josselin de Jong, G. (1958). "Longitudinal and transverse diffusion in granular deposits." *Transactions, American Geophysical Union*, 39, 67-74.
- Delhomme, J.P. (1979). "Spatial variability and uncertainty in groundwater flow parameters: a geostatistical approach.", *Water Resources Research*, 15, 269-280.
- Engesgaard, P. and Kip, K.L. (1992). "A geochemical model for redox-controlled movement of mineral fronts in ground-water flow systems: A case of nitrate removal by oxidation of pyrite.", *Water Resources Research*, 28 (10), 2829-2843.
- Fredlund, D. and Rahardjo, H. (1993). *Soil Mechanics for Unsaturated Soils*., John-Wiley & Sons, New York, USA.

- Fu, J. and Gómez-Hernández J. (2008). "Uncertainty assessment and data worth in groundwater flow and mass transport modeling using a blocking Markov chain Monte Carlo method", *Journal of Hydrology*, 364, 328-341.
- Fu, J. and Gómez-Hernández J. (2009). "A blocking Markov chain Monte Carlo method for inverse stochastic hydrogeological.", *Mathematical Geosciences*, 41, 105–128.
- Gao, H., Vesovic, V., Butler A. and Wheater, H. (2001). "Chemically reactive multi-component transport simulation in soil and groundwater: 2. Model demonstration.", *Environmental Geology*, 41, 280-284.
- Gardner, W.R. (1958). "Some steady state solutions of the unsaturated moisture flow equation with application to evaporation from a water table.", *Soil Science*, 85 (4), 228-232.
- Gee, G.W., Kincaid, C.T. Lenhard, R.J. and Simmons, C.S. (1991). "Recent studies of flow and transport in the vadose zone.", *Reviews of Geophysics*, Supplement, 227-239.
- Gelhar, L.W. and Axness, C.L. (1983). "Three-dimensional stochastic analysis of macrodispersion in aquifers.", *Water Resources Research*, 19 (1), 161-180.
- Gelhar, L.W. (1993). "Stochastic Subsurface Hydrology.", Prentice Hall, Englewood Cliffs, New Jersey.
- Gelhar, L.W. (1986). "Stochastic subsurface hydrology from theory to applications.", *Water Resources Research*, 22 (9), 135S-145S.
- Gerke, H.H., van Genuchten, M.Th., (1993a). "A dual-porosity model for simulating the preferential movement of water and solutes in structured porous media.", *Water Resources Research*, 29 (2), 305-319.
- Gerke, H.H., van Genuchten, M.Th., (1993b). "Evaluation of a firstorder water transfer term for variably saturated dual-porosity models.", *Water Resources Research*, 29 (4), 1225–1238.
- Gerke, H.H., van Genuchten, M.T., (1996). "Macroscopic representation of structural geometry for simulating water and solute movement in dual-porosity media.", *Advances in Water Resources*, 19 (6), 343–357.
- Gillham, R.W. and Cherry, J.H. (1982). "Contaminant migration in saturated unconsolidated geologic deposits.", *Geological Society of America Special Paper*, 31-61.
- Gotovac, H., Cvetković, V. and Andricević, R. (2009). "Adaptive Fup multi-resolution approach to flow and advective transport in highly heterogeneous porous media: Methodology, accuracy and convergence.", *Advances in Water Resources*, 32, 885-905.

- Gottardi, G. and Venutelli, M. (1993). "RICHARDS: Computer model for the numerical simulation of one-dimensional infiltration into unsaturated soil.", *Computers and Geosciences*, 19 (9), 1239-1266
- Govindaraju, R.S., Kavvas, M.L., Jones, S.E. and Rolston, D.E. (1996). "Use of Green-Ampt model for analyzing one-dimensional convective transport in unsaturated soils.", *Journal of Hydrology*, 178, 337– 385.
- Gunduz, O. (2004). "Coupled flow and contaminant transport modelling in large watersheds.", Ph.D. Dissertation, Georgia Institute and Technology, Atlanta, Georgia, USA.
- Harter, T. and Yeh, T.C.J. (1998). "Flow in unsaturated random porous media, nonlinear numerical analysis, and comparison to analytic models.", *Advances in Water Resources*, 22 (3), 257-272.
- Hassan, A.E., Cushman, J.H., Delleur, J.W., (1998a). "A Monte Carlo assessment of Eulerian flow and transport perturbation models.", *Water Resources Research*, 34 (5), 1143–1163.
- Hassan, A.E., Cushman, J.H., Delleur, J.W., (1998b). "Significance of porosity variability to transport in heterogeneous porous media.", *Water Resources Research*, 34 (9), 2249–2259.
- Hills, R.G., Porro, I., Hudson, D.B. and Wierenga, P.J. (1989). "Modelling one-dimensional infiltration into very dry soils 1. Model development and evaluation.", *Water Resources Research*, 25 (6), 1259-1269.
- Hong, L.D., Akiyama J. and Ura, M. (1994). "Efficient mass-conservative numerical solution for the two-dimensional unsaturated flow equation.", *Journal of Hydroscience and Hydraulic Engineering*, 11 (2), 1-18.
- Huang, K., Mohanty B.P. and Van Genuchten, M.T. (1996). "A new convergence criterion for the modified Picard iteration method to solve the variably saturated flow equation.", *Journal of Hydrology*, 260, 69-91.
- Huang, W.E., Oswald, S.E., Lerner, D.N., Smith, C.C and Zheng, C. (2003). "Dissolved oxygen imaging in a porous medium to investigate biodegradation in a plume with limited electron acceptor supply.", *Environmental Science and Technology*, 37 (9), 1905–1911.
- Huebner, K.H., Dewhirst, D.L., Smith, D.E. and Byrom, T.G. (2001). "The Finite Element Method for Engineers.", John Wiley and Sons, New York.
- Hutton, D.V. (2004). "Fundamentals of Finite Element Analysis.", McGraw-Hill Companies, Inc., New York, USA.
- Islas, A.L. and Illangasekare, T.H. (1992). "Solute Transport Under a Constant Infiltration Rate. 1 – Analytical Solutions.", In: *Abstracts of Annual American Geophysical Union, Hydrology Days*, (Ed: Morel-Seytoux, H. J.), 57 Selby Lane, Atherton, California, USA.

- Istock, J. (1989). "Groundwater Modelling by the Finite Element Method. American Geophysical Union," Water Resources Monograph, Washington, DC., USA.
- Jarvis, N.J., Jansson, P-E., Dik, P.E., Messing, I., (1991a). "Modelling water and solute transport in macroporous soil. I. Model description and sensitivity analysis.", *Journal of Soil Science*, 42, 59–70.
- Jarvis, N.J., Jansson, P-E., Dik, P.E., Messing, I., (1991b). "Modelling water and solute transport in macroporous soil. 11. Chloride breakthrough under non-steady.", *Journal of Soil Science*, 42, 71–81.
- Javadi, A.A., AL-Najjar, M.M. and Elkassas, A.S.I. (2006). "Numerical modeling of contaminant transport in unsaturated soil.", *Proceeding of the 5th International Congress on Environmental Geotechnics*. Cardiff, U.K., 1177-1184.
- Javadi, A.A. and AL-Najjar, M.M and Evans, B. (2008). "Finite element modelling of contaminant transport through soils, A case study.", *Journal of Geotechnical and Geoenvironmental Engineering*, 134 (2), 214-230.
- Javadi, A.A. and AL-Najjar, M.M. (2007). "Finite element modelling of contaminant transport in soils including the effect of chemical reactions.", *Journal of Hazardous Materials*. 143, 690-701.
- Johnson, R.L. and Perrott, M. (1991) "Gasoline vapor transport through a high-water-content soil.", *Journal of Contaminant Hydrology*, 8, 317-334.
- Jury, W.A., Spencer, W.F. and Farmer, W.J. (1983). "Behaviour assessment model for trace organics in soil: 1. Model description.", *Journal of Environmental Quality*, 12 (4), 558-564.
- Kabala, Z.J. and Sposito, G. (1991). "A stochastic model of reactive solute transport with time-varying velocity in a heterogeneous aquifer.", *Water Resources Research*, 27, 341-350.
- Kacur, J., Bratislava, Roger Van Keer, R. and Gent, (2003). "Contaminant transport with adsorption in dual-well flow.", *Applications of Matyematics*, 48 (5), 525-536.
- Kapoor, V. and Gelhar, L.W. (1994a). "Transport in three-dimensionally heterogeneous aquifers 1. Dynamics of concentration fluctuations.", *Water Resources Research*, 30 (6), 1775-1788.
- Kapoor, V. and Gelhar, L.W. (1994b). "Transport in three-dimensionally heterogeneous aquifers 2. Predictions and observations of concentration fluctuations.", *Water Resources Research*, 30 (6), 1789-1801.
- Karkuri, H.M. and Molenkamp, F. (1997). "Analysis of advection dispersion of pollutant transport through a layered porous media.", *Proceeding of the International Conference on Geoenvironmental Engineering*, Cardiff University, Wales, UK., 193-198.

- Kemblowski, M.W., Chang, C.M. and Kamil, I., (1997). "A mean-behaviour model of aerobic biodegradation in heterogeneous formation.", *Stochastic Hydrology and Hydraulics*, 11(3), 255–266.
- Kengni, L., Vachaud, G., Thony, J.L., Laty, R., Garino, B., Casabianca, H., Jame, P., Viscogliosi, R., (1994). "Field measurements of water and nitrogen losses under irrigated maize.", *Journal of Hydrology*, 162, 23–46.
- Kindred, J.S. and Celia, M.A., (1989). "Contaminant transport and biodegradation. 2. Conceptual model and test simulations.", *Water Resources Research*, 25 (6), 1149–1159.
- Klaus, J.B. (1996). "Finite Element Procedures.", Prentice-Hall, Upper Saddle River, New Jersey.
- Kohn, J., Santos, J.E. and Kruse, E.E. (1998). "A TVD method for contaminant transport in porous media.", *Computational Mechanics*, 1-8.
- Kuechler, R. and Noack, K. (2002). "Transport of reacting solutes through the unsaturated zone.", *Transport in Porous Media*, 49, 361-375.
- Lessoff, S.C. and Indelman, P. (2004). "Analytical model of solute transport by unsteady unsaturated gravitational infiltration.", *Journal of Contaminant Hydrology*, 72, 85-107.
- Liang, X., Xu, F., Lin, B., Fan Su, Schramm, K. and Kettrup, A. (2002). "Retention behavior of hydrophobic organic chemicals as a function of temperature in soil leaching column chromatography.", *Geosphere*, 49, 569-474.
- Liedl, R. (1994). "A conceptual perturbation model of water movement in stochastically heterogeneous soils.", *Advances in Water Resources*, 17, 171-179.
- Li, X., Cescotto, S. and Thomas, H.R. (1999). "Finite element method for contaminant transport in unsaturated soils.", *Journal of Hydrologic Engineering*, 4 (3), 265-274.
- Lumley, J.L. and Panofsky, H.A. (1964). "The structure of atmospheric turbulence.", Wiley Interscience, New York.
- Lu, T.X., Biggar, J.W. and Nielsen, D.R. (1994). "Water movement in glass bead porous media 2. Experiments of infiltration and finger flow.", *Water Resources Research*, 30 (12), 3283-3290.
- McGrail, B.P. (2001). "Inverse reactive transport simulator (INVERTS): an inverse model for contaminant transport with nonlinear adsorption and source terms.", *Environmental Modelling and Software*, 16, 711-723.
- MacKay, D.J.C. (1998) "Introduction to monte carlo methods.", In: *Learning in graphical models*, (Ed: Jordan, M.I.), Kluwer academic publishers, Netherlands, 174-204.

- MacQuarrie, K.T.B., Sudicky, E.A. and Frind, E.O. (1990). "Simulation of biodegradable organic contaminants in groundwater, 1. Numerical formulation in principle directions.", *Water Resources Research*, 26 (2), 207-222.
- Mantoglou, A. (1984). "Large-scale models of transient unsaturated flow and contaminant transport using stochastic methods.", PhD thesis, MIT, Cambridge, USA.
- Mantoglou, A. and Gelhar, L.W. (1985). "Large-scale models of transient unsaturated flow and contaminant transport using stochastic methods.", *Ralph M. Parsons Laboratory Hydrology And Water Resource Systems*, Report No. 299.
- Mantoglou, A. and Gelhar, L.W. (1987a). "Stochastic modelling of large-scale transient unsaturated flow systems.", *Water Resources Research*, 23 (1), 37-46.
- Mantoglou, A. and Gelhar, L.W. (1987b). "Capillary tension head variance, mean soil moisture content, and effective specific soil moisture capacity of transient unsaturated flow in stratified soils.", *Water Resources Research*, 23 (1), 7-56.
- Mantoglou, A. and Gelhar, L.W. (1987c). "Effective hydraulic conductivities of transient unsaturated flow in stratified soils.", *Water Resources Research*, 23 (1), 57-67.
- Mantoglou, A. and Wilson, J.L. (1982). "The turning bands method for simulation of random fields using line generation by a spectral method.", *Water Resources Research*, 18, 1379-1394.
- Marshall, J.D., Shimada, B.W. and Jaffe, P.R. (2000). "Effect of temporal variability in infiltration on contaminant transport in the unsaturated zone.", *Journal of Contaminant Hydrology*, 46, 151-161.
- Matheron, G. (1973). "The intrinsic random functions and their applications.", *Advances in Applied Probability*, 5, 439-468.
- Mendoza, C.A. and Frind, E.O. (1990). "Advective dispersive transport of dense organic vapours in the unsaturated zone 1. model development.", *Water Resources Research*, 26 (3), 379-387.
- Miller C.T., Williams, G.A., Kelley, C.T. & Tocci, M.D. (1998). "Robust solution of Richards' equation for non-uniform porous media.", *Water Resources Research*, 34 (10), 2599-2610.
- Milly, P.C. (1988). "Advances in Modelling of Water in the unsaturated zone.", D. Reidel Publishing Company, Dordrecht, Holland
- Miralles-Wilhelm, F. and Gelhar, L. (1996). "Stochastic analysis of sorption macrokinetics in heterogeneous aquifers.", *Water Resources Research*. 32 (6), 1541-1549.
- Miralles-Wilhelm, F., Gelhar, L. and Kapoor, V. (1997). "Stochastic analysis of oxygen-limited biodegradation in three-dimensionally heterogeneous aquifers.", *Water Resources Research*. 33 (6), 1251-1263.

- Miralles-Wilhelm, F., Gelhar, L. and Kapoor, V. (2000). "Stochastic analysis of oxygen-limited biodegradation in heterogeneous aquifers with transient microbial dynamics.", *Journal of Contaminant Hydrology*, 42(1), 69-97.
- Molz, F.J., Widowson, M.A. and Benefield, L.D. (1986). "Simulation of microbial growth dynamics coupled to nutrient and oxygen transport in porous media.", *Water Resources research*, 22 (8), 1207-1216.
- Mousavi Nezhad, M.M. and Javadi, A.A. (2010). "Modelling of Solute Transport in Soils Considering the Effect of Biodegradation and Microbial Growth.", In: *Modelling of Pollutants in Complex Environmental Systems*, (Ed: Hanrahan, G.), Volume II, ILM Publications, UK.
- Mualem, Y. (1976). "A new model for predicting the hydraulic conductivity of unsaturated porous media.", *Water Resources Research*, 12 (3), 513-522.
- Nazaroff, W. W. and Alvarez-Cohen, L. (2001). "Environmental Engineering Science.", John Wiley & Sons, Inc. USA.
- Neylon, K.J. (1994). "Non-symmetric Methods in the Modelling of Contaminant Transport in Porous Media.", Ph.D. Dissertation, University of Reading, Reading, U.K.
- Nwaogazie, I.L. (1986). "Groundwater recharge estimate by numerical modelling; a case study.", *Aqua*, 2, 77-80.
- Owen, D.R.J. and Hinton, E. (1980). "Finite Elements in Plasticity: Theory and Practice.", Pineridge Press, Swansea.
- Pan, L., Warrick, A.W. and Wierenga, P.J. (1996). "Finite element methods for modelling water flow in variably saturated porous media: Numerical oscillation and mass-distributed schemes.", *Water Resources Research*, 32 (6), 1883-1889.
- Pan, L. and Wierenga, P.J. (1997). "Improving numerical modelling of two dimensional water flow in variably saturated, heterogeneous porous media.", *Soil Science Society of America Journal*, 61 (2), 335-346.
- Persaud, N. Giraldez, J.V. and Chang, A.C. (1985). "Monte Carlo simulation of noninteracting solute transport in a spatially heterogeneous soil.", *Soil Science society America Journal*, 49, 562-568.
- Philip, J.R., Knight, J.H. (1991). "Redistribution from plane, line, and point sources.", *Irrigation Science*, 12, 169– 180.
- Philip, J.R. (1992). "Exact solutions for redistribution by nonlinear convection-diffusion.", *Journal of the Australian Mathematical Society, (Series B), Applied Mathematics*, 33, 363– 383.
- Polmann, D.J. (1990). "Application of stochastic methods to transient flow and transport in heterogeneous unsaturated soils.", PhD thesis, MIT.

- Polmann, D., McLaughlin, D., Luis, S., Gelhar, L. W. and Ababou, R. (1991). "Stochastic modelling of large-scale flow in heterogeneous unsaturated soils.", *Water Resources Research*, 27 (7), 1447-1458.
- Priestley, M. B. (1981). "Spectral analysis and time series.", Volume I, Universal Series, Academic Press, New York.
- Prommer, H., Barry, D.A., Davis, G.B. (1999). "A one-dimensional reactive multi-component transport model for biodegradation of petroleum hydrocarbons in groundwater.", *Environmental Modelling and Software*, 14, 213–223.
- Rathfelder, K. and Abriola, L. M. (1994). "Mass-conservative numerical solutions of the head-based Richards' equation.", *Water Resources Research*, 30 (9), 2579-2586.
- Remesikova, M. (2005). "Numerical solution of contaminant transport problems with non-equilibrium adsorption in 2D.", *Proceeding of the ALGORITMY Conference*, Slovak University, Slovak, 159-166.
- Rifai, M.N.E., Kaufman, W.J. and Todd, D.K. (1956). "Dispersion Phenomena in Laminar Flow Through Porous Media.", University of California Institute of Engineering, Research Series, No. 2.
- Rittmann, B.E., McCarty, P.L. and Roberts, P.V. (1980). "Trace-organics biodegradation in aquifer recharge.", *Groundwater*, 18, 236-243.
- Romano, N., Brunone B. and Santini, A. (1998). "Numerical analysis of one-dimensional unsaturated flow in layered soils.", *Advances in Water Resources*, 21, 315-324.
- Rosenbloom, J., Mock, P. Lawson, P. Brown, J. Turin, H.J. (1993). "Application of VLEACH to vadose zone transport of VOCs at an Arizona Superfund site.", *Groundwater Monitoring and Remediation*, 13 (3), 159- 169.
- Rubin, J. (1983). "Transport reacting solutes in porous media; relation between mathematical nature of problem formulation and chemical nature of reactions.", *Water Resources Research*. 19 (5), 1231–1252.
- Rubin, J. and James, R.V. (1973). "Dispersion affected transport of reacting solutes in saturated porous media-Galerkin method applied to equilibrium controlled exchange in unidirectional steady water flow.", *Water Resources Research*, 9 (5), 1332–1356.
- Russo, D. (1993). "Stochastic modelling of macrodispersion for solute transport in a heterogeneous unsaturated porous media.", *Water Resources Research*, 29 (2), 383-397.
- Russo, D., Zaidel, J. and Laufer, A. (1994). "Stochastic analysis of solute transport in partially saturated heterogeneous soil 1. Numerical experiments.", *Water Resources Research*, 30 (3), 769-779.

- Russo, D. (1995a). "On the velocity covariance and transport modelling in heterogeneous anisotropic porous formations 2. Unsaturated flow.", *Water Resources Research*, 31 (1), 139-145.
- Russo, D. (1995b). "Stochastic analysis of the velocity covariance and the displacement covariance tensors in partially saturated heterogeneous anisotropic porous formations.", *Water Resources Research*, 31 (7), 1647-1658.
- Saffman, P.G. (1959). "A theory of dispersion in a porous medium.", *Journal of fluid mechanics*, 6, 321-349.
- Sander, G.C. and Braddock, R.D. (2005). "Analytical solutions to the transient, unsaturated transport of water and contaminants through horizontal porous media.", *Advances in Water Resources*, 28, 1102-1111.
- Sander, G.C., Parlange, J. and Hogarth, W.L. (1988). "Air and water flow, I. Horizontal flow with an arbitrary flux boundary condition.", *Journal of Hydrology*, 99, 215-223.
- Saxena, R.K., Jarvis, N.J. and Bergstrom, L. (1994). "Interpreting non-steady state tracer breakthrough experiments in sand and clay soils using a dual-porosity model.", *Journal of Hydrology*, 162, 279-298.
- Schoen, R. Gaudet, J.P. Elrick, D.E. (1999). "Modelling of solute transport in a large undisturbed lysimeter, during steady-state water flux.", *Journal of Hydrology*, 215, 82-93.
- Shinozuka, M. (1972). "Monte Carlo solution of structural dynamics.", *Computers and Structures*, 2, 855-874.
- Shoemaker, A.C., Culver, T.B., Lion, L.W. and Peterson, M.G. (1990). "Analytical models of the impact of two-phase sorption on the subsurface transport of volatile chemicals.", *Water Resources Research*, 26 (4), 745-758.
- Šimunek, J. & van Genuchten, M.T. (1994). "The CHAIN_2D Code for Simulating the Two-dimensional Movement of Water, Heat, and Multiple Solutes in Variably-saturated Porous Media.", Research Report No 136, US Salinity Laboratory, US Department of Agriculture, Riverside, CA.
- Sisson, J.B., Ferguson, A.H., Van Genuchten, M. (1980). "Simple method for predicting drainage of field plots.", *Soil Science Society of America Journal*, 44, 1147-1152.
- Sleep, B.E. and Sykes, J.F. (1993). "Compositional simulation of groundwater contamination by organic compounds.1. Model development and verification.", *Water Resources Research*, 29 (6), 1697-1708.
- Smiles, D.E., Philip, J.R., Knight, J.H. and Elrick, D.E. (1978). "Standard Methods for the Examination of Water and Wastewater.", *Soil Science Society of America Journal*, 42, 229, 15th edn, Washington, D.C., USA., American Public Health Association, (1980).

- Smith, D.W., Rowe, R.K and Booker, J.R. (1992). "Contaminant transport and non-equilibrium sorption.", Numerical Models in Geomechanics, 1, 509-517.
- Smith, G.N. and Smith I.G.N. (1998). "Elements of Soil Mechanics.", Blackwell Publishing, UK.
- Smith, L. (1978). "Stochastic analysis steady-state groundwater flow in a bounded domain.", PhD, University of British Columbia, Vancouver.
- Smith, L., and Schwartz, W. (1980). "Mass transport, 1, A stochastic analysis of macroscopic dispersion.", Water Resources research, 16 (2), 303-313.
- Schoen, R., Gaudet, J. P. and Elrick, D. E. (1999). "Modelling of solute transport in a large undisturbed lysimeter, during steady-state water flux.", Journal of Hydrology, 215, 82-93.
- Stagnitti, F., Li, L., Barry, A., Allinson, G., Parlange, J.Y., Steenhuis, T. and Lakshmanan, E. (2001). "Modelling solute transport in structured soils: performance evaluation of the ADR and TRM models.", Mathematical and Computer Modelling Journal. 34, 433-440.
- Stasa, F.L. (1985). Applied Finite Element Analysis for Engineers, The Dryden Press, New York.
- Sundicky, E. A. (1986). "A natural gradient experiment on solute transport in a sand aquifer: spatial variability of hydraulic conductivity and its role in the dispersion process.", Water Resources Research. 22 (13), 2069-2082.
- Sun, Y., Petersen, J. N., Bear, J., Clement, T.P. and Hooker, B.S. (1999). "Modeling microbial transport and biodegradation in a dual-porosity system.", Transport in Porous Media, 35, 49-65.
- Snyder, I.K. and Woolhiser, D.A. (1985). "Effect of infiltration on chemical transport into overland flow.", Transactions of the American Society of Agricultural Engineers, 28, 1450-1457.
- Thomas, H.R., Alonso, E.E. and Gens, A. (1995). "Modelling thermo/hydraulic/mechanical processes in the containment of nuclear waste.", Proceedings of the 1st International Conference on Unsaturated Soils, Paris, France, 2, 1135-1141.
- Thomas, H.R. and Ferguson, W.J.(1999). "A fully coupled heat and mass transfer model incorporating contaminant gas transfer in an unsaturated porous medium.", Computers and Geotechnics, 24, 65-87.
- Thomas, H.R. and He, Y. (1997). "A coupled heat – moisture transfer theory for deformable unsaturated soil and its algorithmic implementation.", International Journal for Numerical methods in Engineering, 40, 3421-3441.
- Tocci, M.D., Kelley, C.T. and Miller, C.T. (1997). "Accurate and economical solution of the pressure-head form of Richards' equation by the method of lines.", Advances in Water Resources, 20 (1), 1-14.

- Tracy, F.T. (1995). "1-D, 2-D and 3-D analytical solutions of unsaturated flow in groundwater.", *Journal of Hydrology*. 170, 199-214.
- Vanderborght, J. Gonzalez, C., Vanclooster, M., Mallants, D. and Feyen, J. (1997). "Effects of soil type and water flux on solute transport.", *Soil Science Society of America*. 61, 372-389.
- Van Dam, J.C. and Feddes, R.A. (2000). "Numerical simulation of infiltration, evaporation and shallow groundwater levels with the Richards' equation.", *Journal of Hydrology*, 233, 72-85.
- Van Kooten, J.J.A. (1994). "Groundwater contaminant transport including adsorption and first order decay.", *Stochastic Hydrology and Hydraulics*, 8, 185-205.
- Van Genuchten, M.T. (1980). "A closed-form equation for predicting the hydraulic conductivity of unsaturated soils.", *Soil Science Society of America Journal*, 44, 892-898.
- Vomvoris, E. and Gelhar, L. (1990). "Stochastic analysis of the concentration variability in a three-dimensional heterogeneous aquifer.", *Water Resources Research*, 26 (10), 2591-2602.
- Vogel, T., Gerke, H.H., Zhang, R. and Van Genuchten, M.Th. (2000). "Modelling flow and transport in a two-dimensional dual-permeability system with spatially variable hydraulic properties.", *Journal of Hydrology*. 238, 78-89.
- Walter, A.L., Frind, E.O., Blowes, D.W., Ptacek, C.J. and Molson, J.W. (1994). "Modelling of multicomponent reactive transport in groundwater 1. Model development and evaluation.", *Water Resources Research*, 30, 3137-3148.
- Wang, K. Zhang, R. and Yasuda, H. (2006). "Characterizing heterogeneity of soil water flow by dye infiltration experiments.", *Journal of Hydrology*, 328, 559- 571.
- Warrick, A.W., Lomen, D.O. and Islas, A. (1990). "An analytical solution to Richards, equation for a draining soil profile.", *Water Resources Research*. 26, 253- 258.
- Watson, K.K. and Jones, M.J. (1981). "Estimation of hydrodynamic dispersion in a fine sand using a approximate analytical solution.", *Australian Journal of Soil Research*, 19, 265-273.
- Weeks, E.P., Douglas E.E., and Glenn M.T. (1982). "Use of atmospheric fluorocarbons F-11 and F-12 to determine the diffusion parameters of the unsaturated zone in the southern high plains of Texas.", *Water Resources Research*, 18 (5), 1365-1378.
- Wexler, E.J. (1992). "Analytical solutions for one-, two-, and three-dimensional solute transport in ground-water systems with uniform flow.", In: *Techniques of Water-Resources Investigations of the United States Geological Survey*, chapter B7, USGS.

- Wildenschild, D., Jensen, K. H. Villholth, K. and Illangasekare, T. H. (1994). "A laboratory analysis of the effect of macropores on solute transport.", *Ground Water*, 32 (3), 381-389.
- Williams, G.A. and Miller, C.T. (1999). "An evaluation of temporally adaptive transformation approaches for solving Richards' equation.", *Advances in Water Resources*, 22 (8), 831-840.
- Williams, G.A., Miller C.T. and Kelley, C.T. (2000). "Transformation approaches for simulating flow in variably saturated porous media.", *Water Resources Research*, 36 (4), 923-934.
- White, R. E. (1985). "Influence of macropores on the transport of dissolved and suspended matter through soil.", *Advances in Soil Science*, 3, 95-121.
- Xin, J. and Zhang, D (1998). "Stochastic analysis of biodegradation fronts in one-dimensional heterogeneous porous media.", *Advances in Water Resources*, 22(2), 103-116.
- Yang, R.N., Mohamed, A. M.O. and Warkentin, B.P. (1996). "Stochastic analysis of adsorbing solute transport in two-dimensional unsaturated soils principles of contaminant transport in soils.", *Water Resources Research*, 32(9), 2747-2756.
- Yeh, T.C.J., Gelhar, L.W. and Gutjahr, A.L. (1985a). "Stochastic analysis of unsaturated flow in heterogeneous soils 1. Statistically isotropic media.", *Water Resources Research*, 21 (4), 447-456.
- Yeh, T.C.J., Gelhar, L.W. and Gutjahr, A.L. (1985b). "Stochastic analysis of unsaturated flow in heterogeneous soils 2. Statistically anisotropic media with variable α .", *Water Resources Research*, 21 (4), 457-464.
- Yeh, T.C.J., Gelhar, L.W. and Gutjahr, A.L. (1985c). "Stochastic analysis of unsaturated flow in heterogeneous soils 3. Observations and applications.", *Water Resources Research*, 21 (4), 465-471.
- Yeh, T.C.J., Srivastava, R., Guzman, A. and Harter, T. (1993). "A numerical model for water flow and chemical transport in variably saturated porous media.", *Groundwater*, 31 (4), 634-644.
- Yeh, T.C.J. (1992). "Stochastic modelling of groundwater flow and solute transport in aquifers.", *Hydrological Processes*, 6, 369-395.
- Yong, R.N., Mohamed, A.M.O and Warkentin, B.P. (1992). "Principles of Contaminant Transport in Soils.", Elsevier Science, Amsterdam, The Netherlands.
- Zhang, X., Bengough, A.G., Crawford J. W. and Young, I. M. (2002). "Efficient methods for solving water flow in variably saturated soils under prescribed flux infiltration.", *Journal of Hydrology*, 260, 75-87.
- Zhang, Z. and Brusseau, M. L. (2004). "Nonideal Transport of Reactive Contaminants in Heterogeneous Porous Media: Distributed-Domain model Incorporating

- immiscible-Liquid Dissolution and Rate-Limited Sorption/Desorption.", *Journal of Contaminant Hydrology*, 74, 83-103.
- Zhang, X. and Ewen, J. (2000). "Efficient method for simulating gravity-dominated water flow in unsaturated soils.", *Water Resources Research*, 36 (9), 2777- 2780.
- Zheng, C. and Bennett, G.D. (2002). " Applied contaminant transport modeling.", John Wiley and Sons, Inc., New York.
- Zysset, A., Stauffer, F. and Dracos, T. (1994). "Modelling of reactive groundwater transport governed by biodegradation.", *Water Resources Research*, 30, 2423–2434.